



Industria Textilă

ISSN 1222-5347

2/2023

ISI rated journal, included in the ISI Master Journal List of the Institute of Science Information, Philadelphia, USA, starting with vol. 58, no. 1/2007, with impact factor 0.828 and AIS 0.070 in 2021.

The journal is indexed by CrossRef, starting with no. 1/2017 having the title DOI: <https://doi.org/10.35530/IT>.

Edited in 6 issues per year, indexed and abstracted in: Science Citation Index Expanded (SCIE), Materials Science Citation Index®, Journal Citation Reports/Science Edition, World Textile Abstracts, Chemical Abstracts, VINITI, Scopus, Toga FIZ teknik, EBSCO, ProQuest Central, Crossref
Edited with the Romanian Ministry of Research, Innovation and Digitalization support

EDITORIAL BOARD:

Dr. Eng. ALEXANDRA-GABRIELA ENE
GENERAL MANAGER

National R&D Institute for Textiles and Leather,
Bucharest, Romania

Dr. Eng. SABINA OLARU
CS I, EDITOR IN CHIEF

National R&D Institute for Textiles and Leather,
Bucharest, Romania

Dr. Eng. EMILIA VISILEANU
CS I, HONORIFIC EDITOR

National R&D Institute for Textiles and Leather,
Bucharest, Romania

Prof. XIANYI ZENG
Ecole Nationale Supérieure des Arts et Industries
Textiles (ENSAIT), France

Prof. Dr. Eng. LUIS ALMEIDA
University of Minho, Portugal

Prof. Dr. STJEPANOVIĆ ZORAN
University of Maribor, Faculty of Mechanical
Engineering, Department of Textile Materials
and Design, Maribor, Slovenia

Lec. ALEXANDRA DE RAEVE
University College Ghent, Fashion, Textile and Wood
Technology Department, Belgium

Prof. LUBOS HES
PhD, MSc, BSc, Department of Textile Evaluation,
Technical University of Liberec, Czech Republic

Prof. Dr. Eng. ERHAN ÖNER
Marmara University, Turkey

Prof. SYED ABDUL REHMAN KHAN
PhD, CSCP, CISCOM, Xuzhou University
of Technology, China

Assistant Prof. Dr. HUIPU GAO
Textile Development and Marketing,
Fashion Institute of Technology, New York, USA

Prof. Dr. S. MUGE YUKSELOGLU
Marmara University, Turkey

Dr. MAZARI ADNAN
ASSISTANT PROFESSOR
Department of Textile Clothing, Faculty of Textile
Engineering, Technical University of Liberec
Czech Republic

Dr. AMINODDIN HAJI
PhD, MSc, BSc, Textile Chemistry and Fiber Science
ASSISTANT PROFESSOR
Textile Engineering Department Yazd University,
Yazd, Iran

Prof. Dr. Eng. CARMEN LOGHIN
VICE-RECTOR
Faculty of Industrial Design and Business
Management, Technical University "Gh. Asachi",
Iași, Romania

Associate Prof. HONG YAN
College of Textile and Clothing Engineering,
Soochow University, China

Associate Prof. Dr. Eng. MARIANA URSACHE
Faculty of Industrial Design and
Business Management, Technical University
"Gh. Asachi", Iași, Romania

Prof. Dr. GELU ONOSE
CS I, "Carol Davila" University of Medicine
and Pharmacy, Bucharest, Romania

Prof. Dr. DOINA I. POPESCU
The Bucharest University of Economic Studies,
Bucharest, Romania

Prof. Dr. MARGARETA STELEA FLORESCU
The Bucharest University of Economic Studies,
Bucharest, Romania

DUNJA ŠAJN GORJANC, KLARA KOSTAJNŠEK

Permeability properties of dry-laid mechanical bonded nonwovens for filter 133-142

GULSEREN KARABAY, MUHAMMET BURAK KILIC, KAZIM SARICOBAN, GİZEM KARAKAN GÜNAYDIN

Forecasting of Turkey's apparel exports using artificial neural network autoregressive models 143-153

LILIANA INDRIE, ZLATIN ZLATEV, JULIETA ILIEVA, IOAN PAVEL OANA
An algorithm for the analysis of static hanging drape 154-162

M. FATHU NISHA, L. MALLIGA, S. MANTHANDI PERIANNASAMY, J. JOHN BENNET, S. AMALORPAVA MARY RAJEE

Smart fabric inspection using Mimosa pudica plant 163-168

FEYZA AKARSLAN KODALOĞLU, NACIYE SÜNDÜZ OĞUZ
Investigation of radiation shielding, antibacterial and some properties
of nanosilver applied and coated woven fabrics 169-174

ARI ALI, BAYRAM ALI, KARAHAN MEHMET, KARAGÖZ SEÇGİN
Evaluation of the mechanical properties of chopped carbon fibre reinforced
polypropylene, polyethylene, polyamide 6, and polyamide 12 composites 175-183

ÖZKAN HACIOĞULLARI SELCEN, BABAARSLAN OSMAN
An investigation on non-flammability properties of polypropylene knitted fabrics 184-191

SADIA AZIZ, MUHAMMAD ABDULLAH KHAN NIAZI, USMAN GHANI, SAMRA KIRAN, MISBAH NOOR
Effect of trade barriers on export performance during COVID-19 pandemic:
a comparative study among South Asian textile industries 192-202

NACIYE SÜNDÜZ OĞUZ, FEYZA AKARSLAN KODALOĞLU
Gamma-rays shielding and antibacterial properties of coated fabrics 203-208

ZHAO SHENGYING, ZHONG MINGJUN, LU XIANGYUAN
The optimal factoring type with partial credit guarantee in the textile
industry: disclosed or undisclosed 209-216

MARIAN CATALIN GROSU, ION RAZVAN RADULESCU, EMILIA VISILEANU, RAZVAN SCARLAT
The design of experiments in the field of technical textiles as an educational
module 217-222

FANGTAO RUAN, QINGYONG YANG, BOBO ZHAO, XINYU XIE, LI YANG, ZHENZHEN XU
Tensile and impact properties of chopped carbon fibre reinforced
thermoplastics with multiple recycle and regenerate 223-229

MUDDASSAR SARFRAZ, MUHAMMAD IBRAHIM ABDULLAH, NAJAF MUMTAZ, SYED IBN-UL-HASSAN, ILKNUR OZTURK
The effect of entrepreneurs' personality on entrepreneurial marketing
in textile sector: the mediating role of self-efficacy 230-237

KEPULAJE ABHAYA KUMAR, PRAKASH PINTO, CRISTI SPULBAR, RAMONA BIRAU, IQBAL THONSE HAWALDAR, SAMARTHA VISHAL, IULIANA CARMEN BĂRBĂCIORU
ARIMA model to forecast the RSS-1 rubber price in India: A case study for textile
industry 238-245

EMILIA VISILEANU, ALEXANDRA ENE, CARMEN MIHAI, ALINA VLADU
Textile structures for the treatment of burn wounds – characterization of elastic
and antibacterial properties 246-255

Scientific reviewers for the papers published in this number:

- PDr. Eva Bou-Belda*, Universitat Politècnica de València, Textile and Paper Engineering, Spain
Prof. Dr. Erhan Öner, Marmara University, Faculty of Technology, Department of Textile Engineering, Turkey
Prof. Dr. Savas Vasilius, TEI Pireius, Greece
Prof. Dr. Olabiyisi Stephen Olatunde, Ladoko Akintola University of Technology, Faculty of Engineering & Technology, Computer Science & Engineering, Nigeria
Prof. Dr. Kösekahyaoğlu Levent, Sülyeman Demirel University, Department of Economics, Turkey
Prof. Rodica Harpa, "Gheorghe Asachi" Technical University of Iasi, Faculty of Industrial Design and Business Management, Romania
B.E., M.E., PhD Benson Edwin Raj, College of Applied Sciences, Department of Information Technology, Oman
Prof. Dr. Mirela Blaga, "Gheorghe Asachi" Technical University of Iasi, Romania
Prof. Dr. Üçgöl İbrahim, Sülyeman Demirel University Department of Textile Engineering, Textile Engineering Department, Turkey
Prof. Zhang Guanyu, Nantong University, School of Textile and Garment, China
Dr. Ramona Birau, Constantin Brancusi University of Targu Jiu, Faculty of Education Science, Law and Public Administration, Romania
Dr. Gizem Karakan Günaydin, Pamukkale University Buldan Vocational School, Department of Fashion and Design, Turkey
Dr. Savin Dorin Ionesi, "Gheorghe Asachi" Technical University of Iasi-Romania, Faculty of Industrial Design and Business Management, Romania
Dr. Kaplan Burçin, Istanbul Aydin University, Department of International Trade and Finance, Turkey
Prof. Dr. Aleksandar Vujović, University of Montenegro, Montenegro
Prof. Dr. Doba Kadem Fusun, Çukurova University, Department of Textile Engineering, Turkey
Prof. Dr. Demboski Goran, Saint Cyril and Methodius University in Skopje, Faculty of Technology and Metallurgy, Department of Textile Engineering, Macedonia
Prof. Dr. Larisa Ivaşcu, Politehnica University of Timisoara, Romania
Dr. Akcagun Engin, Mimar Sinan University, Turkey
Prof. Dr. Li Hui, Hohai University, China
Prof. Dr. Erkan Birol, Iskenderun Technical University, Department of Economics, Turkey
Prof. Dr. Hawaldar Iqbal, Kingdom University, College of Business Administration, Department of Accounting & Finance, Bahrain
Dr. Çağlar Sivri, Bahçeşehir University, Turkey
Dr. Umair Muhammad, National Textile University, Pakistan
Dr. Jatin Trivedi, National Institute of Securities Markets, India
Prof. Dr. Pasayev Nazim, Erciyes University, Turkey
Dr. Irina Cherunova, Don State Technical University, Department of Design and Technology, Russia
Dr. Akçali Kadri, Bartın University, Turkey
Prof. Wang Wenqin, Nanchang University, School of Advanced Manufacturing, China
Prof. Dr. Ozturk Ilhan, Cag University, Turkey
Dr. Naeem Muhammad Zahid, Dokuz Eylül University Izmir, Turkey

EDITORIAL STAFF

- General Manager:** Dr. Eng. Alexandra-Gabriela Ene
Editor-in-chief: Dr. Eng. Sabina Olaru
Onorific editor: Dr. Eng. Emilia Visileanu
Graphic designer: Florin Prisecaru
Translator: Cătălina Costea
Site administrator: Constantin Dragomir
e-mail: industriatextila@incdtp.ro

INDUSTRIA TEXTILA journal, edited by INCOTP BUCHAREST, implements and respects Regulation 2016/679/EU on the protection of individuals with regard to the processing of personal data and on the free movement of such data ("RGPD"). For information, please visit the Personal Data Processing Protection Policy link or e-mail to DPO rpd@incdtp.ro

Aknowledged in Romania, in the Engineering sciences domain, by the National Council of the Scientific Research from the Higher Education (CNCSIS), in group A
Journal edited in collaboration with **Editura AGIR**, 118 Calea Victoriei, sector 1, Bucharest, tel./fax: 021-316.89.92; 021-316.89.93; e-mail: editura@agir.ro, www.edituraagir.ro



This work is licensed under a Creative Commons Attribution 4.0 International Licence. Articles are free to use, with proper attribution, in educational and other non-commercial settings.

Permeability properties of dry-laid mechanical bonded nonwovens for filter

DOI: 10.35530/IT.074.02.202190

DUNJA ŠAJN GORJANC

KLARA KOSTAJNŠEK

ABSTRACT – REZUMAT

Permeability properties of dry-laid mechanical bonded nonwovens for filter

The present study aimed to investigate the permeability of dry-laid, mechanically bonded nonwoven fabrics for filters of five different samples. Various permeability properties were investigated in the experimental part, such as water vapour permeability, air permeability, thermal conductivity, porosity parameters, and surface openness, which affect the permeability properties. The results of the study and statistical confirmation showed that the nonwoven structure has a great influence on filtration performance.

It was found that the sample with the largest mass and thickness had the optimal filtration properties, as it had the smallest open area and thus the lowest water vapour permeability, average air permeability, and highest thermal conductivity.

Statistical analysis confirmed that water vapour permeability correlates strongly with fibre diameter and bubble point, air permeability correlates strongly with thickness and mass, and thermal conductivity correlates strongly with fibre diameter, thickness, and mass of the nonwovens studied.

Keywords: nonwovens, water vapour permeability, air permeability, thermal conductivity, porosity parameters, surface openness

Proprietăți de permeabilitate ale neșesutelor obținute prin consolidare uscată mecanică pentru realizarea filtrelor

Scopul prezentului studiu a fost de a investiga permeabilitatea neșesutelor obținute prin consolidare uscată mecanică, pentru realizarea a cinci probe diferite de filtre. În partea experimentală, au fost investigate proprietățile de permeabilitate, cum ar fi: permeabilitatea la vapori de apă, permeabilitatea la aer, conductivitatea termică, cât și porozitatea și structura suprafeței, care afectează permeabilitatea. Rezultatele studiului și confirmării statistice au arătat că structura neșesută are o mare influență asupra performanței de filtrare.

S-a constatat că proba cu valorile cele mai ridicate ale masei și grosimii a avut proprietăți optime de filtrare, întrucât avea cea mai mică zonă deschisă și astfel cea mai scăzută permeabilitate la vapori de apă și permeabilitate medie la aer, precum și cea mai mare conductivitate termică.

Analiza statistică a confirmat că permeabilitatea la vapori de apă se corelează cu diametrul fibrei și punctul de barbotare, permeabilitatea la aer se corelează cu grosimea și masa, iar conductivitatea termică se corelează cu diametrul fibrei, grosimea și masa materialelor neșesute studiate.

Cuvinte-cheie: neșesute, permeabilitate la vapori de apă, permeabilitate la aer, conductivitate termică, parametri de porozitate, structura suprafeței

INTRODUCTION

Nonwovens belong to the group of unconventional textiles. Nonwovens are produced directly from fibres or continuous filaments. The term nonwovens are often used as a general description for textiles made by a process other than weaving and knitting, or more generally for textiles other than traditional textiles, paper rods, or plastic films. They are used in medicine, hygiene products, construction, household products, as various fillers, and for various types of filters. Nonwovens are innovative, versatile and indispensable. Nowadays it is impossible to live without them [1–4]. According to EDANA [5], around 2,774 million tons of nonwovens were produced in the EU in 2018. The production growth was 4.8% compared to 2017, and the estimated total turnover of the European nonwovens industry is around 8852 million euros [1–6].

In 2018, the main market segments in terms of volume for nonwovens roll goods, were hygiene (27.9%), wipes for personal care (12.8%), construction (9.6%), automotive (6.5%) civil engineering (5.6%), filtration (3.6%), food & beverage (3.0%). In volumes, total nonwoven exports from EU28 countries to the rest of the world increased by only 3.8% in 2018, amounting to 386,563 tons (as compared to 372,297 tons in 2017) for a value of € 1,849 million (a +2.1% increase in value) [6, 7].

The study aimed to investigate the permeability or filtration capacity of dry-laid mechanically bonded nonwovens for filters and to find out and prove which of them is most suitable for filters.

The EDANA definition of filtration is that filtration is a mechanism or device to separate one substance from another. Filtration can be used to separate impurities from a liquid or to separate valuable substances such as minerals, chemicals, or food in a

process operation. Separations can be broadly classified into six categories: Solid-Gas Separations; Solid-Liquid Separations, Solid-Solid Separations; Liquid-Liquid Separations; Gas-Liquid Separations; and Gas-Gas Separations [5]. Nonwovens are ideal for filtration because they can be modified and engineered to meet demanding specifications and complex regulatory requirements. This is the reason why they have displaced many traditional materials and have become the medium of choice in filtration [2].

Apart from the above facts, many researchers are investigating the filtration performance of dry-laid nonwovens. Roy and Ishtiaque study the optimum design of a filter media by tuning the structure of the needle-punched nonwoven fabric. They also deal with the influence of carding parameters on nonwovens as filter media [8]. Some authors explore the filtration performance of mono-, bi- and multicomponent nonwoven air filter media [9]. In addition to the technological parameters, the authors also address the structural parameters of nonwoven media for filters, such as fibre diameter, fibre combinations, and solids volume fraction, which have a significant effect on the air filtration properties of nonwoven media [10].

In their research, Sakthivel et al. investigate the air permeability, mechanical properties, pore size distribution and filtration efficiency of different nonwovens made from recycled fibres [11]. Some authors also focused their research on composite nonwovens in filters and their application [12].

In the first section – the theoretical part – the production process and the main definition of nonwoven filters and porosity are presented. The studied samples (five dry-laid, needle-bonded nonwovens), methods, image analysis and statistical evaluation are presented in the Materials and Methods section. The Results and Discussion and Conclusions sections present the main findings on the influence of fibre diameter, mass and thickness, mean pore diameter, and openness of the surface of the nonwovens to filters on their permeability properties.

Statistical analysis confirmed that water vapour permeability is strongly correlated with fibre diameter and bubble point. Air permeability correlates strongly with thickness and mass, and thermal conductivity correlates strongly with fibre diameter, thickness and mass of the nonwovens studied.

THEORETICAL PART

Nonwoven filters

A nonwoven filter is a porous fabric consisting of a random arrangement of fibres or filaments, the specific function of which is to filter and/or separate phases and components of fluid being transported through the medium or to support the medium performing the separation. The fabric is a web-like structure manufactured in a length long enough to be wound into rolls. Although the random fibre structure is the backbone of the nonwoven fabric, it may contain other components that are part of the forming

process, including (but not limited to) particulate fillers (clays, calcium, adsorptive powders, etc.), sizing agents, wet strength agents, antimicrobial additives, plasticizers, dyes and pigments, softeners, and wetting agents.

The definition implies that the fibres and filaments are bonded together in some form or fashion. The formed fabric may be consolidated during its manufacture. Nonwoven fabrics may also be consolidated by a mechanical bonding process of the nonwoven former, either in-line or offline with the production process. The mechanical bonding process may include any of the following methods: Fibre entanglement by needling, hydroentanglement or stitch bonding, water-based latex treatment, solvent-based resin treatment, and thermal bonding. As long as the fabric is a random fibre structure to be used for filtration and/or separation, the specific bonding process is not critical to the definition. The fabric may be subjected to other chemical and mechanical treatments to improve its properties. Examples include coatings and finishes, flame retardants, antimicrobials, water repellents, dyes, and plasticizers. It may also be subjected to downstream mechanical processing, such as creping, corrugating, embossing, slitting and wrapping, folding, pouching, filming, dyeing, and die-cutting, which are required for the final application as a filter and/or separator [1–3, 5, 9–17]. The filter media is responsible for the rapid and effective formation of a cake and can make a significant contribution to the success of filtration. At the beginning of a filtration process, the filter media retains the particles. Later, the particles are retained by the filter cake itself, while the filter medium serves as a carrier for the cake. The filter media affects the filtrate flow, the initial filter resistance, and the clarity of the filtrate in each filtration cycle. At the end of a cycle, the filter media also affects cake release. Cycle time depends on the type of sludge and the concentration of sludge added. In general, the higher the sludge concentration, the shorter the cycle time [18].

Different natural and manmade fibres are used in filter fabric manufacturing. In most cases, polyester filter fabrics are popular today due to their good resistance to chemicals and ease of availability.

Compared with woven fabric structures, nonwoven fabric structures have more voids; because of this, they are considered to be porous media, which contain a relatively high volume of air and very complex pore structure due to the random arrangement of fibres in the fabric [19].

There is a wide range of needle punch nonwoven filter media with different basis weights used in industrial and residential filtration. Das et al. [7] conducted a comparative study between thermally-bonded and needled nonwovens. They found that needled nonwovens performed better in terms of filtration efficiency and pressure drop. They concluded that needled nonwoven is a better filter media than thermally bonded nonwoven. Kothari et al. [20] carried out a work on the effect of processing parameters on the physical properties of needle-punched nonwoven

Table 1

THE BASIC PROPERTIES OF THE SAMPLES ANALYZED					
Samples	Chemical composition	Length of fibres (mm)	Diameter of fibres (μm)	Thickness (mm)	Mass (g/m^2)
A	50% PET + 50% bico PET fibres (PET-core/PET-sheath)	60	13.830	0.9491	192.50
B			15.654	1.1104	240.00
C			17.851	0.6183	121.50
D			16.663	0.8325	213.00
E			13.799	0.9877	208.00

fabric by changing the machine variables. They concluded that needled nonwoven fabrics have better abrasion-resistant properties and finer fibrous nonwoven fabrics have lower air permeability. They also found that nonwovens have a higher breaking load in the machine direction than in the cross direction and that increasing the punching density reduces the air permeability [21].

Carding and needle punching parameters influence the structure of the nonwoven filters, hence compromising the effectiveness of filtration efficiency of filter media [18–21].

Porosity

The internal geometric structure (voids of different shapes and sizes inside the product) is a condition for the permeability properties of the nonwoven. If these cavities are interconnected from one side of the product to the other, we are dealing with an air and liquid-permeable body. The hollow internal structure of the product is the porosity (the proportion of the volume of the voids in the total volume of the nonwovens). The voids inside are called pores. From a practical point of view, the pores between the fibres in the fibre are of particular interest. The fibre has such a shape that the pores here have no walls from the beginning to the end of the product, and the shape of the pores is arbitrary. In the case of the fibre, a specific internal surface area is used as an indicator to describe the internal structure. A larger specific surface area per unit volume indicates a less permeable nonwoven structure with smaller pores, which is favourable for both the adsorption and filtration of individual particles. The specific surface area is most influenced by the diameter of the fibres and the shape of the cross-section, and to a lesser extent by their length [2, 6–7, 10].

Porosity is the ratio of the volume of air in the fabric to the total volume of the fabric, expressed as a percentage. This is a calculated value based on the specific volume of the constituent fibres and the volume of the fabric from the measured values of width, length, and thickness of the fabric [2, 14, 16].

EXPERIMENTAL PART

Materials and technological parameters

With the presented research, the five dry-laid, needle-bonded nonwovens were analysed. The basic

Table 2

TECHNOLOGICAL PARAMETERS IN THE PRODUCTION PROCESS OF THE SAMPLES ANALYZED			
Samples	Web bonding technique	The intensity of needling ($\text{stitches}/\text{cm}^2$)	The number of plies on a cross lapper
A	Needling	230–300	16
B		500–600	30
C		230–300	14
D		230–300	24
E		230–300	24

properties of the samples analysed are shown in table 1. The samples were produced on the manufacturer Laroche's process line, which includes a roller carding machine, a pre-needling machine and two needling components. The line also includes a horizontal cross-lapper. The number of needles on the needle board is 8000 needles per meter and the width of the needle board is 200 cm. The needles (manufacturer Groz-Beckert) have a reduced blade with a three-lobed shape and regular teeth. The technological parameters of the tested samples are listed in table 2.

Figure 1 shows images of specimens of different magnifications taken under different microscopes, namely a stereomicroscope 65.560 NOVEX (Euromex – Holland) with a digital camera CMEX 5000 and a magnification of 6.5 (the zoom was 0.65 and 4.5) and a handheld digital microscope (Dino-Lite basic capture, which allows you to take the picture at 50 to a maximum of 250 \times magnification).

Methods

Air permeability

The air permeability of nonwovens indicates the amount of air that will pass through a given surface of the specimen at a chosen pressure at a given time. This is the amount of air, measured in cubic meters (m^3), that passes through 1 m^2 of textile in one minute at a pressure of $p = 20 \text{ mm H}_2\text{O}$ ($p = 196.2 \text{ Pa}$). By measuring air permeability, the influence of various factors can be determined: Raw materials, textile construction, finishing processes, etc.

Measurements were made according to ISO 9237 [22] on the air permeability tester (MESDAN S. p. A.,

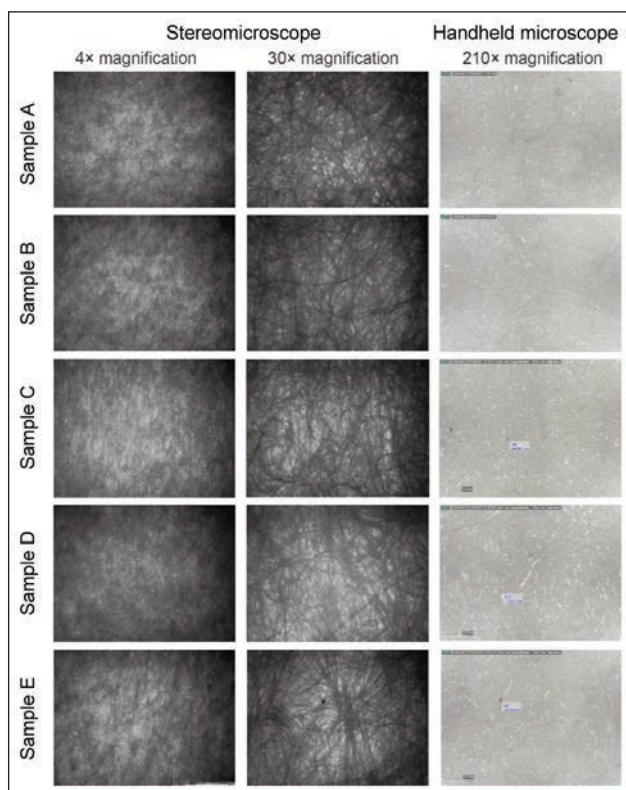


Fig. 1. Visually displayed images in the light transmission function under different magnification

Puegnago del Garda, Italy). For the air permeability measurements, ten test specimens of approx. 15 × 20 cm were cut per sample.

Water vapour permeability

The measurements were carried out according to the ASTM E96:E96M standard [23]. Two test specimens were prepared for each sample. We placed the sample in the metal lid with an opening of 3 cm in diameter and covered the glass container with it and fixed it with a metal holder.

The prepared dishes with lids were weighed on a precision balance and then left at room conditions for one hour before being placed in the chamber for 24 hours. The conditions in the chamber are as follows: humidity 55% and temperature 23°C.

The water vapour permeability, WVT was calculated with equation 1:

$$WVT = \frac{\Delta m}{s \times t} \quad (1)$$

where WVT is water vapour permeability ($\text{g}/\text{m}^2\text{h}$), Δm – the difference in the mass of the water cup with water and sample immediately and after 24 hours (g), S is the surface of the lid open (m^2), and t is time (h) [23–26].

Thermal conductivity

The thermal conductivity of the samples was measured using the comparative method, like DIN 52612-2 [23]. The measurement of thermal conductivity is based on the transport of heat flow from a warmer to a colder region, from the bottom of the apparatus to the top. Both blocks and three measuring plates are connected to the temperature-measuring device

(ALMEMO 2590, Ahlborn Mess, Holzkirchen, Germany). The whole system is insulated [27–29].

The thermal conductivity was calculated with equation 2:

$$\lambda_x = \lambda_n \times \frac{d_x}{d_n} \times \frac{T_4 - T_3}{T_3 - T_2} \quad (2)$$

where λ_x represents the thermal conductivity of the samples (W/mK), λ_n – thermal conductivity of a reference glass sample ($\lambda_n = 1.0319 \text{ W}/\text{mK}$), d_x – thickness of the sample (mm), d_n – thickness of reference glass sample ($d_n = 4 \text{ mm}$).

Porosity

The size and distribution of the pores between the fibres were determined using the Jakšić [29, 30] air flow method also called the fluid flow methods where the changes in the flow are measured concerning the opening of the pores under increasing pressure drop. This involves measuring the volumetric flow of air through a given area of dry sample on a rotameter at different pressure differentials. The sample is then immersed in a liquid of known density and surface tension. When it is completely wetted, it is inserted into the measuring head of the rotameter, slowly increasing the pressure difference until the first air bubble appears. The difference is read, and the hydraulic diameter of the largest pore is calculated. The pressure is then increased, and the pressure value is read at preselected volume flows. The measurement is finished when the volume is squeezed out of even the smallest pores. With the mentioned method we can get a distribution of the minimal diameter of the pore channels in the samples and the highest pore diameter [30–33]. For the study and analysis of some parameters of nonwoven porosity, we have used the bubble point and mean pore diameter from the above method.

Image analysis

Image analysis stands for computer-aided processing and is an important tool for process control. It is based on the transmission of visible light through the material. For image analysis, we mostly use the ImageJ program nowadays. ImageJ is a free Java-based image processing and analysis software. It consists of a program window that contains various tool collections. For example, tools for lines, markers, magnifications, colour changes, etc. are available. One can measure distances and angles, create histograms, allows automatic thresholding, displays results in tables, and provides graphs [34, 35]. The program supports 8-bit, 16-bit, 32-bit grayscale, 8-bit and RGB colour images. With the program, we can change the colours to black and white or grey.

We took the images of the nonwoven fabric samples using a stereo microscope (65.560 NOVEX (Euromex – Holland) under 30× magnification and transformed the image into binary form by thresholding with default settings and evaluated the openness of the surface.

Statistical analysis

The correlation between the independent factors (diameter of fibres, the thickness of nonwoven, mass, porosity) and the dependent factors (air permeability, water vapour permeability, and thermal conductivity) is determined using a correlation matrix.

Also, multiple regression is used as an extension of simple linear regression. It is used when we want to predict the value of one variable based on the value of two or more other variables. The variable we want to predict is called the dependent variable (air permeability, water vapour permeability, and thermal conductivity). The variables we use to predict the value of the dependent variable are called independent variables (diameter of fibres, the thickness of nonwoven, mass, porosity factors). Regression analysis uses a selected estimation method, a dependent variable, and one or more explanatory variables to create an equation that estimates values for the dependent variable. The regression model includes outcomes, such as R^2 and p-values, that provide information about how well the model estimates the dependent variable. The correlation matrix and multiple regression were also created using the program Statgraphics [31, 35].

RESULTS AND DISCUSSION

The results of air permeability and water vapour permeability are shown in figure 2 and thermal conductivity is shown in figure 3. Results of porosity parameters are presented in figure 4 and visually displayed image processing of samples with the program ImageJ in figure 5.

Figure 5 shows the preparation of captured photographs of samples for image analysis using the ImageJ program.

Sample D has the lowest air permeability, a thickness greater than 0.83 mm, a surface mass of 213 g/m², a maximum pore diameter of 95 μm, and the second lowest open area of 3.10%. Sample C has the highest air permeability, with a large variation compared to the other samples. It also has the lowest thickness, mass, and fibre diameter (17.85 μm), one of the largest pore diameters of 104 μm, and the second largest open area 4.2%, which affects the maximum

air permeability of sample C. The air permeability of samples A, B, and E range from 526.5 m³/m²/min to 676.75 m³/m²/min. Samples A, B, and E have fibre diameters of about 13 μm to 15 μm and thicknesses of 0.9 mm to 1.1 mm. Besides the fibre diameter, which is about 17 μm for samples C and D, the thickness and mass are the most important parameters for air permeability and filtration properties, less so the fibre diameter and average pore diameter. The air

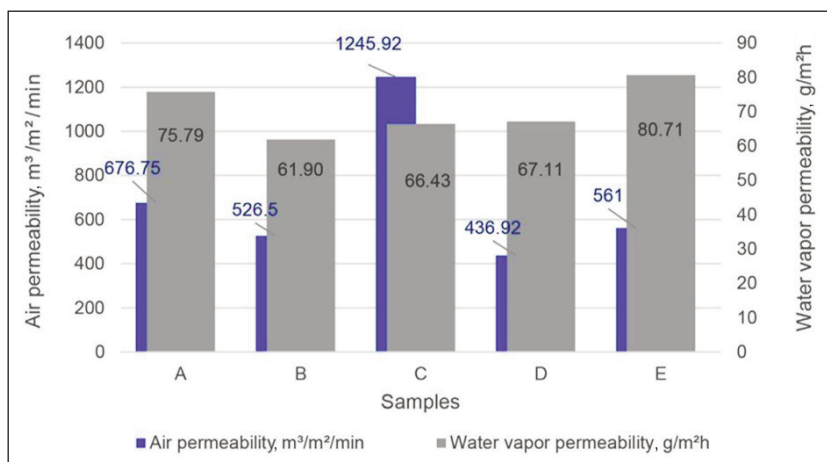


Fig. 2. Air and water vapour permeability values of samples

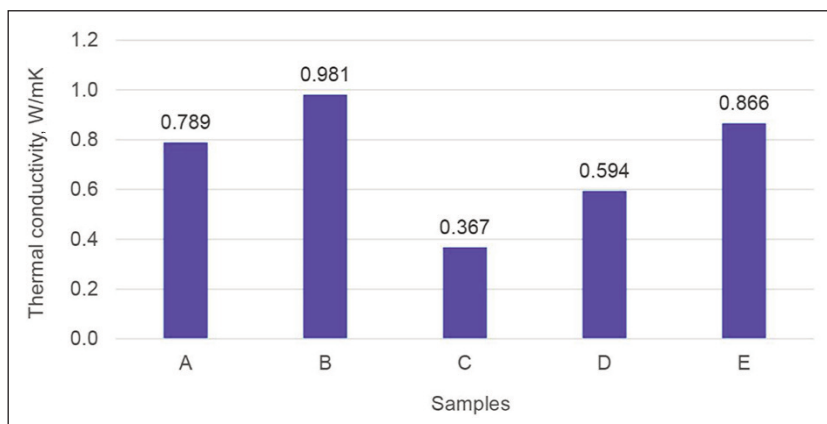


Fig. 3. Thermal conductivity values of samples

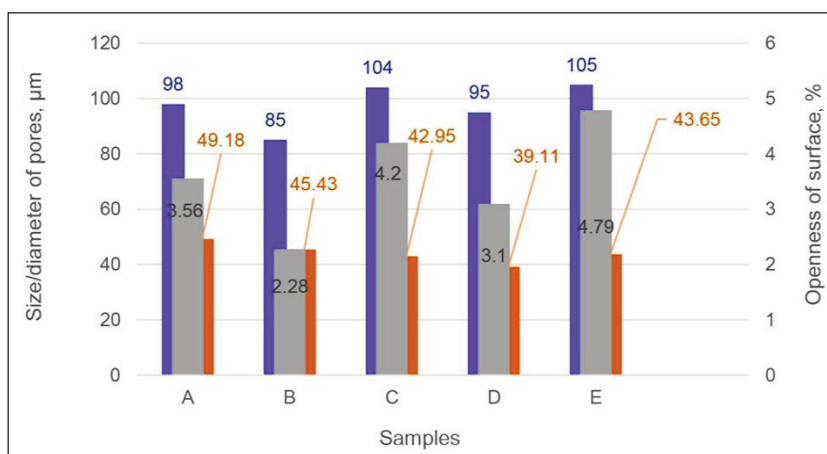


Fig. 4. Porosity parameters of the samples

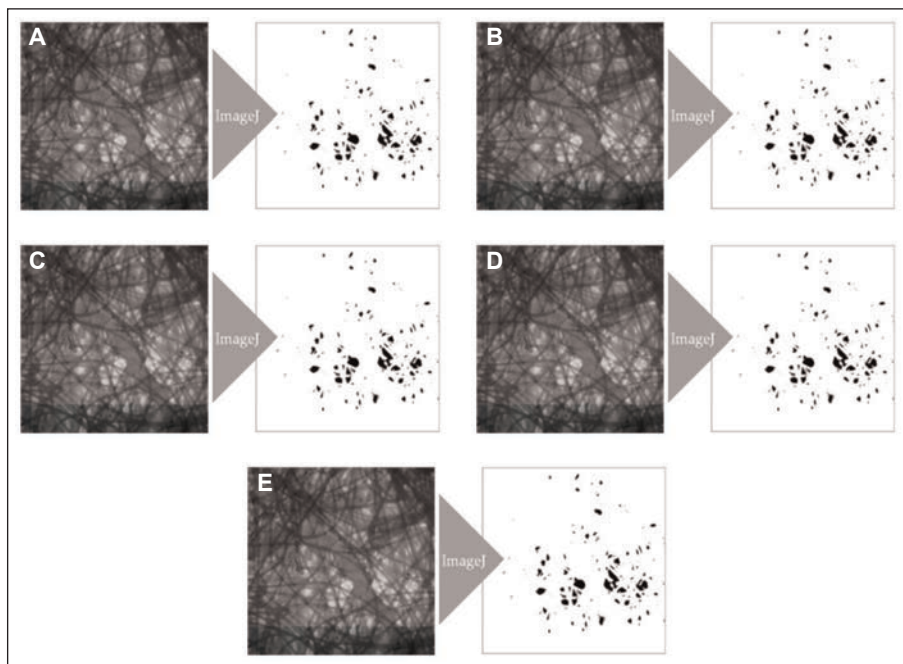


Fig. 5. Visually displayed image processing of samples with the program ImageJ

permeability of the studied samples correlates strongly with the thickness and mass of the studied nonwovens, while the correlation between the air permeability and the diameter of the fibres and the bubble point is moderate.

The lowest thermal conductivity of sample C compared to the other studied samples could be due to the maximum fibre diameter, even considering the open area and the maximum pore diameter. Sample B is the sample with the largest thickness and mass and has the highest thermal conductivity, the lowest water vapour permeability, and the second lowest air permeability. It also contains the smallest pore diameter of 85 μm and the smallest open area of 2.3% (figures 4 and 5), which justifies the results. We assume that the maximum value of thermal conductivity of sample B is influenced by the diameter of the fibres and the average pore diameter (45.43 μm), which is very high compared to the other samples. Sample E has the second largest thickness (more than 0.83 mm), a mass of 208 g/m^2 , the highest water vapour permeability, a maximum pore diameter of 105 μm and a maximum open area of 4.8% (figures 4 and 5), and the lowest fibre diameter (13.799 μm). A much higher water vapour permeability has samples A and E compared to the other samples. The reason for this is probably the smaller diameter of the fibres (about 13.8 μm) and the higher bubble formation point than the other samples studied. The samples with smaller fibre diameter and higher average pore diameter (from 43 to 49 μm) let through a larger amount of water vapour in the environment. The openness of the surface of the studied nonwovens depends on the method of nonwoven bonding, the length of the fibres, the diameter of the fibres, and the orientation of the fibres in the nonwoven web. The samples were bonded using a mechanical bonding

method – the needle bonding method. Sample E is followed by sample A, which has a water vapour transmission rate of 75.79 $\text{g}/\text{m}^2\text{h}$. Sample A has a slightly higher fibre diameter (i.e., 18.83 μm) and a maximum pore diameter (49.18 μm). The highest pore diameter (bubble point) ranges from about 105 to 85 μm (figure 4). There is a high correlation between the values of the measurements of the highest pore diameter and the open area (the correlation coefficient is 0.97). Sample A has the smallest mass (192.5 g/m^2), the third largest thickness (0.9491 mm), and the second largest air and water vapour permeability. There

were large differences in thermal conductivity between the tested samples, on average the differences in thermal conductivity between samples A, B, C, D and E are about 34%. A very low thermal conductivity has the studied samples C, and D compared to the other samples (less than 0.6 W/mK). The reason for this is probably the higher diameter of the fibres (about 17 μm) and the smaller average pore diameter (about 41 μm). The latter probably affects a large air content in the pores and thus a lower thermal conductivity.

Statistical analysis

Statistical analysis of air permeability results

Statistical analysis shows that the air permeability strongly correlates with the thickness and mass of the nonwovens analysed, while the correlation between air permeability and the diameter of fibres and bubble point is moderate ($R^2=0.51$). The analysis also shows a very weak correlation between air permeability and openness of the surface (figure 6). The correlation matrix shows a strong negative correlation between thickness, mass and air permeability and a moderate positive correlation between the diameter of fibres and air permeability. Multiple regression is used to predict air permeability based on the thickness, mass, and diameter of fibres (table 3).

Statistical analysis of water vapour permeability results

Statistical analysis shows that the water vapour permeability (WVT) strongly correlates with the diameter of fibres and bubble point of the nonwovens analysed, while the correlation between WVT and the openness of the surface is moderate ($R^2=0.50$). The analysis also shows a very weak correlation between water vapour permeability and mean pore diameter

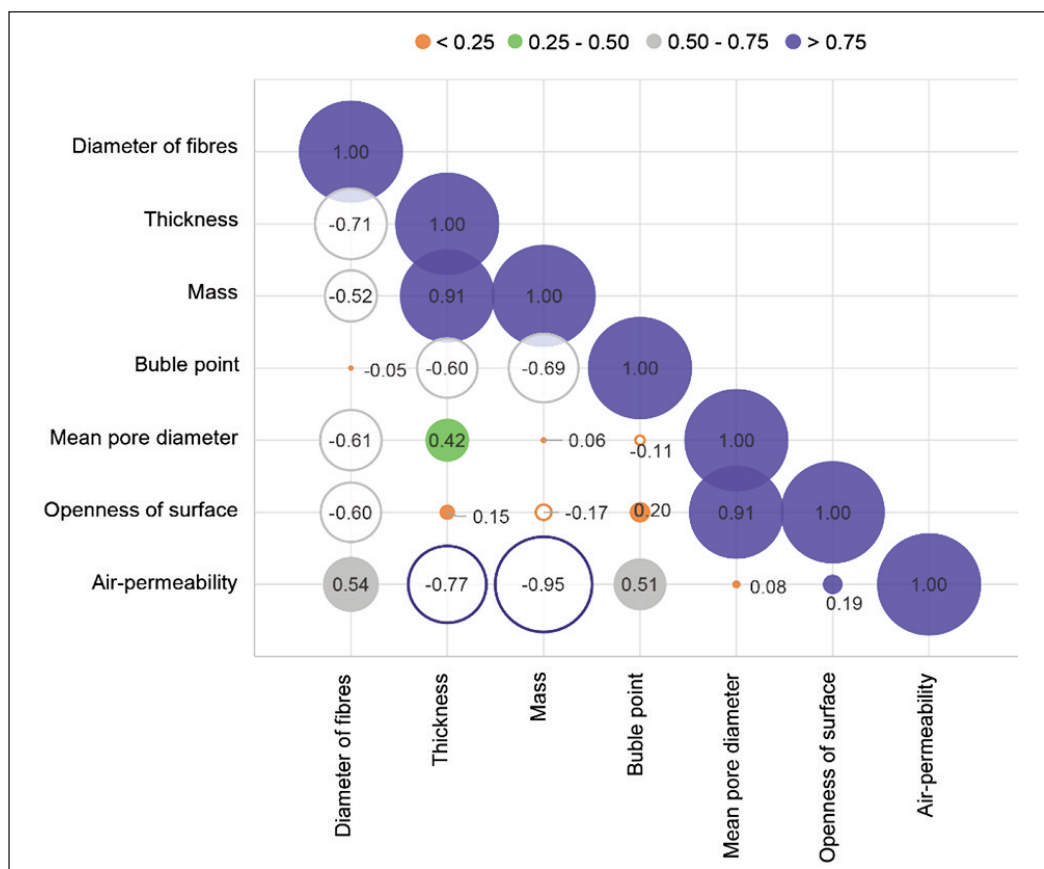


Fig. 6. Correlation analysis between the diameter of fibres, thickness, mass of the sample, bubble point, mean pore diameter, the openness of surface and air-permeability

Table 3

SUMMARY OUTPUT OF MULTIPLE REGRESSION ANALYSIS TO PREDICT AIR-PERMEABILITY						
Regression Statistics		Coefficients	Standard Error	t Stat	P-value	
Multiple R	0.999987	Intercept	305.006	32.87719	9.277131	0.068358543
R Square	0.999974	Diameter of fibres, DF	73.53688	1.470254	50.01645	0.012726512
Adjusted R Square	0.999896	Thickness, T	1752.929	28.28009	61.98457	0.010269727
Standard Error	3.294982	Mass, M	-11.9831	0.096744	-123.865	0.005139531
Observations	5					
Equation to predict air-permeability: $y = 305 + 73.54 DF + 1752.93 T - 11.98 M$						

(figure 7). The correlation matrix shows a strong negative correlation between the diameter of fibres and water vapour permeability and strong positive correlation between bubble point and water vapour permeability and a moderate positive correlation between thickness, mean pore diameter, the openness of surface and water vapour permeability. Multiple regression is used to predict water vapour permeability based on the diameter of fibres, bubble point and openness of the surface (table 4).

Statistical analysis of thermal conductivity results

Statistical analysis shows that the thermal conductivity strongly correlates with the diameter of fibres, thickness and mass of the nonwovens analysed, while the correlation between thermal conductivity,

bubble point and mean pore diameter and openness of surface is moderate ($R^2=0.50$). The analysis also shows a very weak correlation between thermal conductivity and the openness of the surface (figure 8). The correlation matrix shows a strong negative correlation between the diameter of fibres and thermal conductivity and strong positive correlation between mass and thickness and thermal conductivity and a moderate positive correlation between mean pore diameter and thermal conductivity. Further correlation results show a moderate negative correlation between bubble point and thermal conductivity. Multiple regression is used to predict thermal conductivity based on the diameter of fibres, thickness, and mass (table 5).

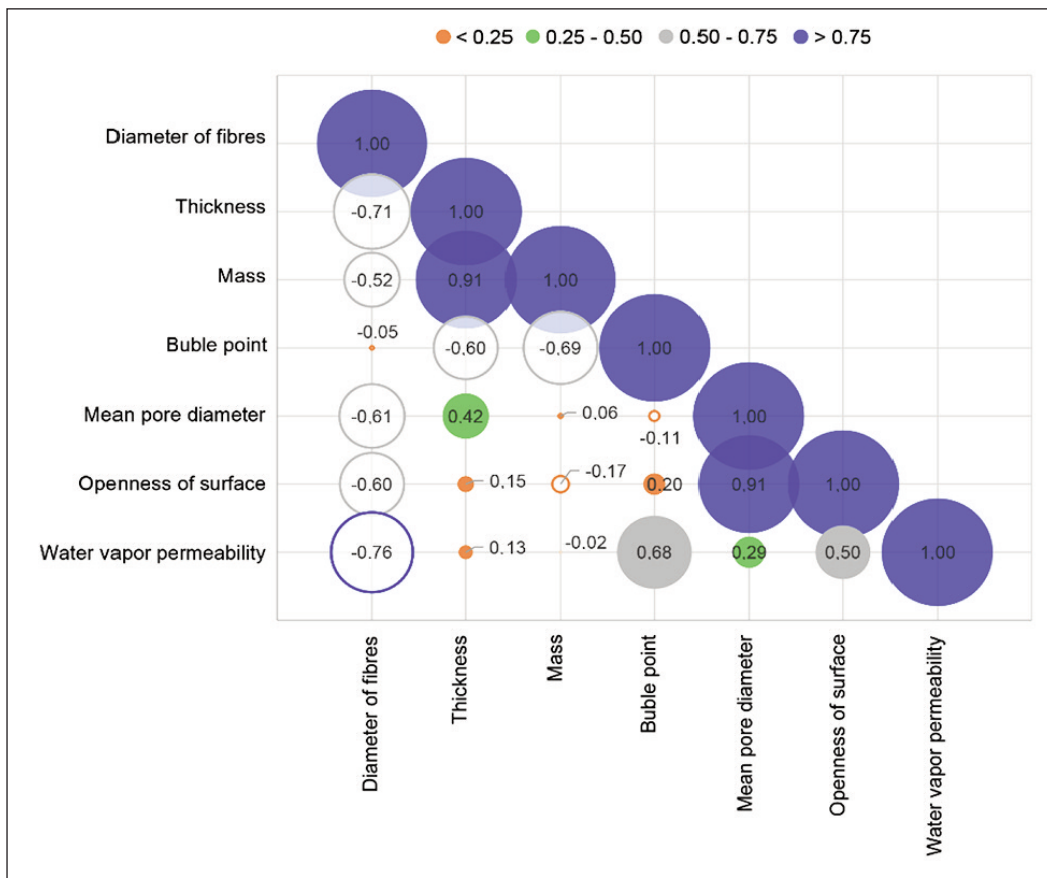


Fig. 7. Correlation analysis between the diameter of fibres, thickness, mass of the sample, bubble point, mean pore diameter, the openness of surface and water vapour permeability

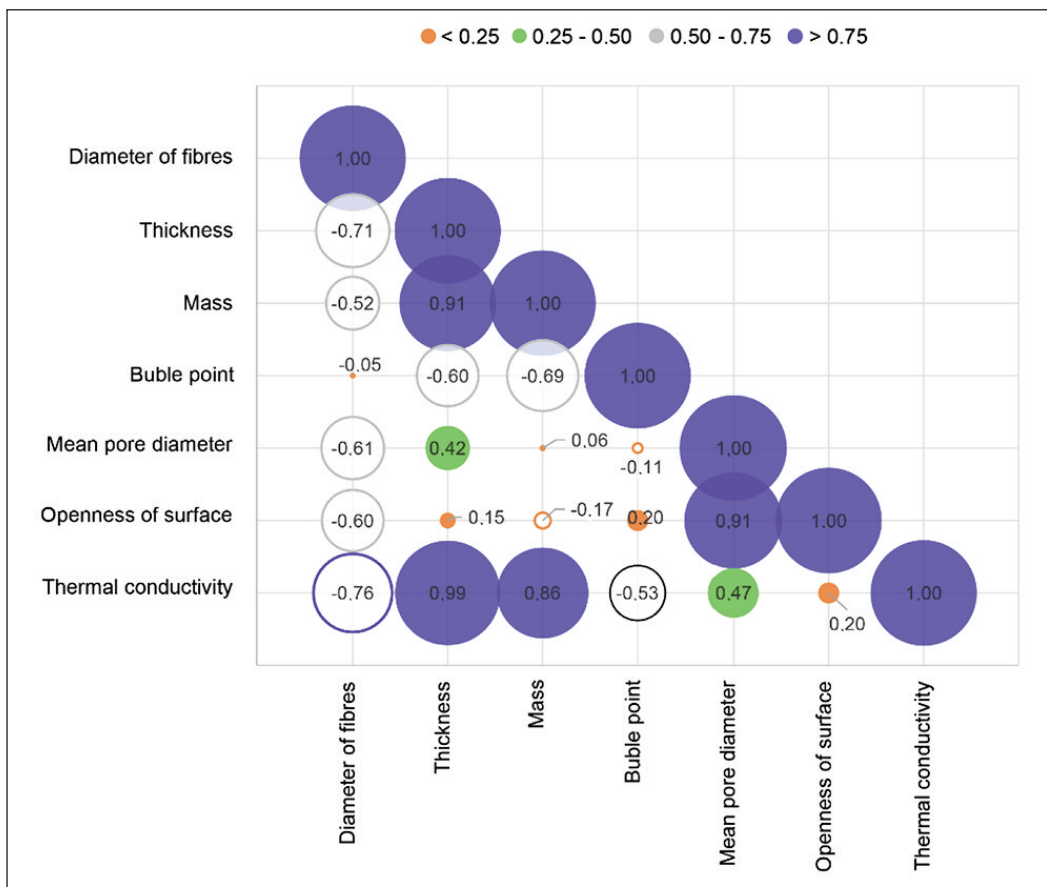


Fig. 8. Correlation analysis between the diameter of fibres, thickness, mass of the sample, bubble point, mean pore diameter, the openness of surface and thermal conductivity

Table 4

SUMMARY OUTPUT OF MULTIPLE REGRESSION ANALYSIS TO PREDICT WATER VAPOUR PERMEABILITY						
Regression Statistics			Coefficients	Standard Error	t Stat	P-value
Multiple R	0.999987	Intercept	65.58951	13.91829	4.712470342	0.068358543
R Square	0.999974	Diameter of fibres, DF	-3.37638	0.540569	-6.245970607	0.012726512
Adjusted R Square	0.999896	Thickness, T	0.625584	0.097055	6.445682981	0.010269727
Standard Error	3.294982	Mass, M	-0.39745	0.486244	-0.81739309	0.005139531
Observations	5					
Equation to predict water vapour permeability: $y = 65.59 - 3.38DF + 0.62BP - 0.39OS$						

Table 5

SUMMARY OUTPUT OF MULTIPLE REGRESSION ANALYSIS TO PREDICT THERMAL CONDUCTIVITY						
Regression Statistics			Coefficients	Standard Error	t Stat	P-value
Multiple R	0.998622	Intercept	-0.29131	0.253641	-1.148524823	0.456061177
R Square	0.997247	Diameter of fibres, DF	-0.00711	0.011343	-0.627019826	0.643460806
Adjusted R Square	0.988986	Thickness, T	1.45515	0.218176	6.669630504	0.094744783
Standard Error	0.02542	Mass, M	-0.00096	0.000746	-1.289535549	0.41991791
Observations	5					
Equation to predict thermal conductivity: $y = -0.29 - 0.0071DF + 1.45T - 0.00096M$						

CONCLUSIONS

The present study focused on permeability (filtration) properties of dry laid (carded) and needle-bonded nonwoven fabrics made of 50% PET + 50% bico PET fibres intended for filters. From the statistical analysis, we can conclude that the air permeability is strongly correlated with the thickness and mass of the nonwovens studied. Besides fibre diameter, which is about 17 μm , thickness and mass are the most important parameters for air permeability and filtration properties, less so fibre diameter and average pore diameter. The water vapour transmission rate (WVT) correlates strongly with the fibre diameter and bubble point of the nonwovens studied. Sample B showed the lowest water vapour permeability and sample E the highest. A much higher water vapour permeability has the samples that have a lower diameter of the fibres (about 13.8 μm) and a higher bubble point (about 105 μm). The thermal conductivity correlates strongly with the diameter of the fibres, the thickness and the mass of the studied nonwovens.

We assume that the maximum value of thermal conductivity is influenced by the diameter of the fibres and the average pore diameter (45.43 μm), which is very high compared to the other analysed samples. The samples have lower thermal conductivity due to the higher diameter of the fibres (about 17 μm) and the smaller mean pore diameter (about 41 μm). The latter probably leads to high air content in the pores and thus to lower thermal conductivity.

The results of the experimental part and statistical analysis confirmed that the sample with a fibre diameter of 15.65 μm , mass of 240 g/m^2 and thickness of 1.11 mm has the optimal filtration properties, the lowest surface openness and consequently the lowest water vapour permeability and average air permeability, and the highest thermal conductivity.

Statistical analysis confirmed that water vapour permeability correlates strongly with fibre diameter and bubble point. Air permeability correlates strongly with thickness and mass, and thermal conductivity correlates strongly with fibre diameter, thickness and mass of the nonwovens studied.

REFERENCES

- [1] Russel, S.J., *Handbook of nonwovens*, Cambridge: Woodhead Publishing Limited, 2007, 16–240
- [2] Hutten, I.M., *Handbook of Nonwoven Filter Media*, Boston: Elsevier, 2007, 4–247
- [3] Kellie, G., *Advances in Technical Nonwovens*, Cambridge: Woodhead Publishing Limited, 2016, 273–303
- [4] Chapman, R., *Applications of Nonwovens in Technical Textiles*, Cambridge: Woodhead Publishing Limited, Cambridge, 2010, 16–240, 3–44
- [5] Lee Joo, H., Cassill, N., *Analysis of World Nonwovens Market*, In: Journal of Textile and Apparel, Technology and Management, 2006, 5, 3, 1–19
- [6] Mao, N., *Nonwoven fabric filters*, Cambridge: Woodhead Publishing Series in Textile, 2017, 133–171

- [7] Das, D., Das, S., Ishtiaque, S.M., *Optimal Design of Nonwoven Air Filter Media: Effect of Fibre Shape*, In: *Fibres and Polymers*, 2014, 15, 1456–1461
- [8] Roy, R., Ishtiaque, S.M., *Optimal Design of a Filter Media by Tuning the Structure of Needle Punched Nonwoven: Influence of Carding Parameters*, In: *Fibres and Polymers*, 2020, 21, 2125–2137
- [9] Kumar, A., Das, D., *A comparative study on filtration performance of mono-, bi-, and multi-constituent nonwoven air filter media*, In: *The Journal of The Textile Institute*, 2018, 109, 11, 1521–1527
- [10] Payen, J., Vroman, P., Lewandowski, M., Perwuelz, A., Callé-Chazelet, S., Thomas, D., *Influence of fibre diameter, fibre combinations and solid volume fraction on air filtration properties in nonwovens*, In: *Textile Research Journal*, 2012, 82, 19, 1948–1959
- [11] Sakthivel, S., Ezhil Anban, J.J., Ramachandran, T., *Development of Needle-Punched Nonwoven Fabrics from Reclaimed Fibres for Air Filtration Applications*, In: *Journal of Engineered Fibres and Fabrics*, 2014, 9, 1, 149–154
- [12] Mukhopadhyay, A., *Composite nonwovens in filters: applications*, In: Das, N., Pourdeyhimi, B. (Ed.). *Composite Nonwoven Materials*, Cambridge: Woodhead Publishing, 2014, 164–210
- [13] *Nonwovens markets, facts and figures: Edana*, Available at: <https://www.edana.org/> [Accessed on February 12th, 2020]
- [14] Tokarska, M., *Analysis of impact air-permeability of fabrics*, In: *Fibres and Textiles in Eastern Europe*, 2008, 16, 1, 76–80
- [15] Subramaniam, V., Madhusoothanan, M., Debnath, C.R., *Air Permeability of Blended Nonwoven Fabrics*, In: *Textile Research Journal*, 1988, 58, 11, 677–678
- [16] Dent, R.W., *The Air-permeability of Non-woven Fabrics*, In: *The Journal of The Textile Institute*, 2008, 67, 6, 220–224
- [17] Zhu, G., Kremenakova, D., Wang, Y., Militky, J., *Air permeability of polyester nonwoven fabrics*, In: *Autex Research Journal*, 2015, 15, 1, 8–12
- [18] Thilagavathi, G., Muthukumar, N., Neelakrishnan, S., Egappan, R.S., *Development of polyester needle-punched nonwoven fabrics for filter press applications*, In: *Journal of Industrial Textiles*, 2019, 48, 10, 1566–1579, <https://doi.org/10.1177/1528083718769929>
- [19] Kumar Chauhan, V., Pratap Singh, J., Debnath, S., *Virgin and recycled polyester filter media: effect of coating, calender roller pressure and roller temperature on dust filtration*, In: *Journal of the Textile Institute*, 2021, 1–8
- [20] Kothari, V.K., Das, A., Sarkar, A., *Effect of processing parameters on properties of layered composite needle-punched nonwoven air filters*, In: *Indian J. Fibre Text. Res.*, 2007, 32, 2, 196–201
- [21] Roy, R., Chatterjee, S., *Development of a Multi-component Air Filter by Incorporating the Density Gradient Structure in Needle Punched Nonwoven*, In: *Fibres and Polymers*, 2018, 19, 12, 2597–2603
- [22] ISO 9237. *Textiles – determination of the permeability of fabric to air*, 1995, 5
- [23] ASTM E96:E96M. *Standard Test Methods for Water Vapour Transmission of Materials*, 2016, 8
- [24] Watkins, D.A., Slater, K., *The moisture-vapour permeability of textile fabrics*, In: *Journal of The Textile Institute*, 1981, 72, 1, 11–18
- [25] McCullough, E.A., Kwon, M., Shim, H., *A comparison of standard methods for measuring water vapour permeability of fabrics*, *Measurement Science and Technology*, 2003, 14, 8, 1402–1408
- [26] Danych, R., Wiecek, B., Kowalski, K., *Air and Water Vapour Permeability in Double-Layered Knitted Fabrics with Different Raw Materials*, In: *Fibres & Textiles in Eastern Europe*, 2006, 14, 3, 77–80
- [27] DIN 52612-2. *Testing of thermal insulating materials; determination of thermal conductivity by means of the guarded hot plate apparatus; conversion of the measured values for building applications*, 1984, 6
- [28] Šajn Gorjanc, D., Dimitrovski, K., Bizjak, M., *Thermal and water vapour resistance of the elastic and conventional cotton fabrics*, In: *Textile Research Journal*, 2012, 14, 82, 1498–1506
- [29] Matusiak, M., *Investigation of the Thermal Insulation Properties of Multilayer Textiles*, In: *Fibres & Textiles in Eastern Europe*, 2006, 14, 5, 98–102
- [30] Jakšič, D., Jakšič, N., *The porosity of masks used in medicine*, *Tekstilec*, 2004, 47, 9–12
- [31] Jakšič, D., Jakšič, N., *Assessment of Porosity of Flat Textile Fabrics*, In: *Textile Research Journal*, 2007, 77, 2, 105–110
- [32] Ogulata, R.T., Serin, M., *Investigation of Porosity and Air-permeability Values of plain knitted fabrics*, In: *Fibres and Textiles in Eastern Europe*, 2010, 18, 5, 71–75
- [33] Kostajnshek, K., Zupin, Ž., Hladnik, A., Dimitrovski, K., *Optical Assessment of Porosity Parameters in Transparent Woven Fabrics*, In: *Polymers*, 2021, 13, 3, 408, <https://doi.org/10.3390/polym13030408>
- [34] Schneider, C.A., Rasband, W.S., Eliceiri, K.W., *NIH Image to ImageJ: 25 years of image analysis*, In: *Nature Methods*, 2012, 9, 671–675
- [35] Devore, J., *Probability and Statistics for Engineering and the Sciences*, 8th ed., Boston: Richard Stratton, 2012, 154–196

Authors:

DUNJA ŠAJN GORJANC, KLARA KOSTAJNŠEK

University of Ljubljana, Faculty for Natural Sciences and Engineering, Department of Textiles,
Graphic Arts and Design, Aškerčeva 12, 1000 Ljubljana, Slovenia

Corresponding author:

DUNJA ŠAJN GORJANC
e-mail: dunja.sajn@ntf.uni-lj.si

Forecasting of Turkey's apparel exports using artificial neural network autoregressive models

DOI: 10.35530/IT.074.02.202265

GULSEREN KARABAY
MUHAMMET BURAK KILIC

KAZIM SARICOBAN
GİZEM KARAKAN GÜNAYDIN

ABSTRACT – REZUMAT

Forecasting of Turkey's apparel exports using artificial neural network autoregressive models

Foreign trade is significant for open economies and has a critical place in the development of national economies in a globally competitive environment. Export has a key role as an important component in foreign trade transactions. In this study, Turkey's exports of HS-61 "Apparel and clothing accessories knitted or crocheted" and HS-62 "Apparel and clothing accessories not knitted or crocheted" products were examined. Turkey's exports of these HS codes to seven countries, which are mostly exported, EU27, OECD and the world were estimated for 2020–2025 using artificial neural networks (ANNs). The model was validated by measuring forecast errors (RMSE, MAE, and MAPE) to ensure that the model can recreate satisfactory results. The results reveal that the ANNs predicted the exports to the selected countries accurately. According to the findings from the NNAR (1,1) model, Turkey's exports of HS-61 coded products to Italy, the UK, France and EU-27 are expected to increase year-on-year from 2020 to 2025, while exports to the USA, Netherlands and Spain are expected to decrease. Exports from Turkey to Germany, the world and the OECD are projected to decrease first and then increase. In the NNAR (2,2) model, Turkey's exports to Italy, the UK and France are expected to increase year on year, while exports to other countries are generally estimated to decrease first and then increase. In the estimation made for the HS-62 product group with NNAR (1,1) model, it is predicted that TURKEY's exports to Italy, the USA, the UK, France and Spain will increase year by year from 2020 to 2025. It is estimated that TURKEY's exports to the Netherlands, Germany, World, OECD and EU-27 will decrease year by year in the same period. In the NNAR (2,2) model, it is predicted that TURKEY's exports to UK, France and Spain will increase year by year, while exports to EU-27, OECD and World will decrease. However, TURKEY's HS-62 exports to Italy, the USA, the Netherlands and Germany are expected to follow a fluctuating course.

Keywords: apparel industry, ready-made clothing sector, export, forecasting, artificial neural networks (ANNs)

Proгноза экспортurilor de îmbrăcăminte din Turcia folosind modele autoregresive ale rețelei neuronale artificiale

Comerțul exterior este semnificativ pentru economiile deschise și are un loc deosebit de important în dezvoltarea economiilor naționale într-un mediu competitiv la nivel global. Exportul are un rol cheie, ca o componentă importantă în tranzacțiile de comerț exterior. În acest studiu, au fost analizate exporturile Turciei de produse HS-61 „îmbrăcăminte și accesorii de îmbrăcăminte tricotate sau croșetate” și HS-62 „îmbrăcăminte și accesorii de îmbrăcăminte netricotate sau croșetate”. Exporturile Turciei privind aceste coduri HS în șapte țări în care sunt în mare parte exportate, UE27, OCDE și global au fost estimate pentru perioada 2020–2025 folosind rețele neuronale artificiale (ANN). Modelul a fost validat prin măsurarea erorilor de prognoză (RMSE, MAE și MAPE) pentru a se asigura că modelul poate recrea rezultate satisfăcătoare. Rezultatele arată că ANN-urile au preconizat cu exactitate exporturile către țările selectate. Conform constatărilor modelului NNAR (1,1), exporturile Turciei de produse codificate HS-61 către Italia, Marea Britanie, Franța și UE-27 sunt de așteptat să crească de la an la an, din 2020 până în 2025, în timp ce exporturile către SUA, Olanda și Spania sunt de așteptat să scadă. Se estimează că exporturile Turciei către Germania, global și OCDE inițial vor scădea și apoi vor crește. În modelul NNAR (2,2), exporturile Turciei către Italia, Marea Britanie și Franța sunt de așteptat să crească de la an la an, în timp ce exporturile către alte țări sunt, în general, estimate inițial să scadă și apoi să crească. În estimarea făcută pentru grupa de produse HS-62 cu modelul NNAR (1,1), se preconizează că exporturile Turciei către Italia, SUA, Marea Britanie, Franța și Spania vor crește de la an la an, din 2020 până în 2025. Se estimează că exporturile Turciei către Olanda, Germania, global, OCDE și UE-27 vor scădea de la an la an în aceeași perioadă. În modelul NNAR (2,2), se preconizează că exporturile Turciei către Marea Britanie, Franța și Spania vor crește de la an la an, în timp ce exporturile către UE-27, OCDE și global vor scădea. Cu toate acestea, exporturile de HS-62 ale Turciei către Italia, SUA, Olanda și Germania sunt de așteptat să urmeze un curs fluctuant.

Cuvinte-cheie: industria de îmbrăcăminte, sectorul îmbrăcămintei de serie, export, prognoză, rețele neuronale artificiale (ANN)

INTRODUCTION

In Turkey, the textile and clothing industry started to grow rapidly with the export-oriented development policy that was put into practice in 1980 and invest-

ments in the sector have increased since then. Today, the textile and clothing industry is one of the most important industries in terms of macro-economic magnitudes such as gross domestic product, share

in the manufacturing industry and industrial production, export, net foreign exchange inflow to the economy, employment, and investment [1]. In 2020, Turkey's ready-to-wear and apparel export share became 10.1% of total exports. 70.9% of sectoral exports were to the European Union countries. 11.8 billion dollars in exports were made to the top ten countries from Turkey to which the most ready-to-wear and apparel exports were made. The share of these ten countries in sectoral exports of 17.1 billion dollars was 68.6% [2]. The graphic of exports of HS-61 and HS-62 coded products to the examined seven countries, and to the groups are given in figures 1 and 2.

Foreign trade is crucial for open economies and plays a key role in the development of national economies in a globally competitive environment. Export is the most important component in foreign trade transactions as it has a driving force among

economic growth, foreign exchange and capital input [3]. Economic growth is the increase in production capacity that causes an increment in income level and the output of a country. "Export-Oriented Growth Hypothesis" suggests that increases in exports will contribute to economic growth. According to this view, an increase in export affects economic growth by implying efficiency of resource allocation, economies of scale, productivity, increasing technological innovations, capital formation and employment [4]. From a micro perspective, if the effects of exports to companies are considered; the exporting firms can allocate the resources efficiently, full of their capacity, take the advantage of economical scale and increase their technological innovation provoked by the competition [5]. Therefore, finding an appropriate strategy and plan to get a smooth flow of international trade between countries is significant. To achieve this, forecasting the export and import of goods is the

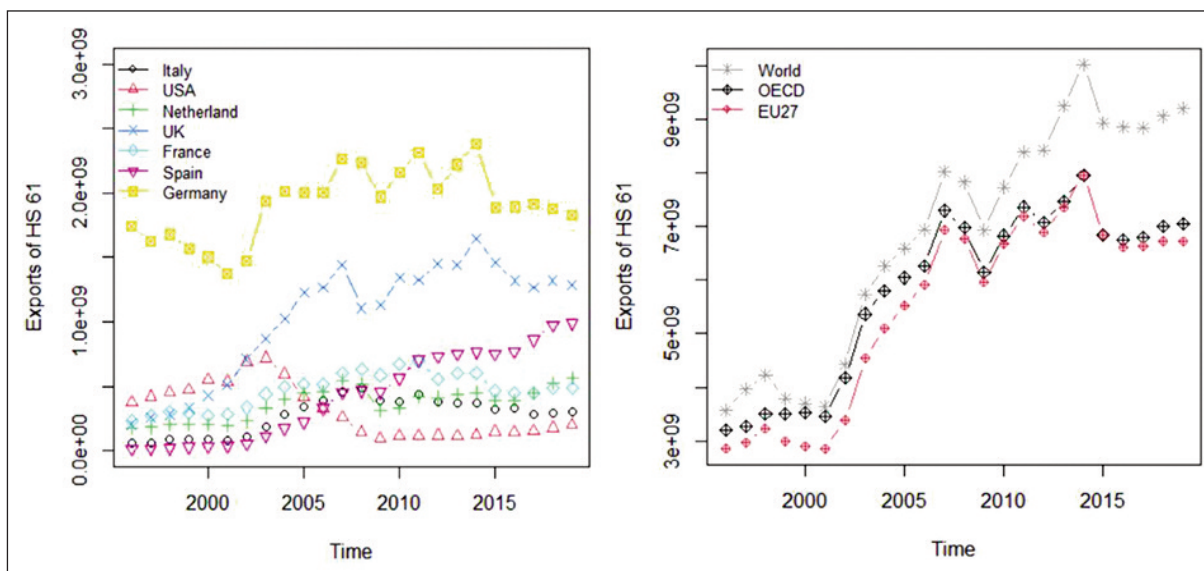


Fig. 1. Exports of HS-61

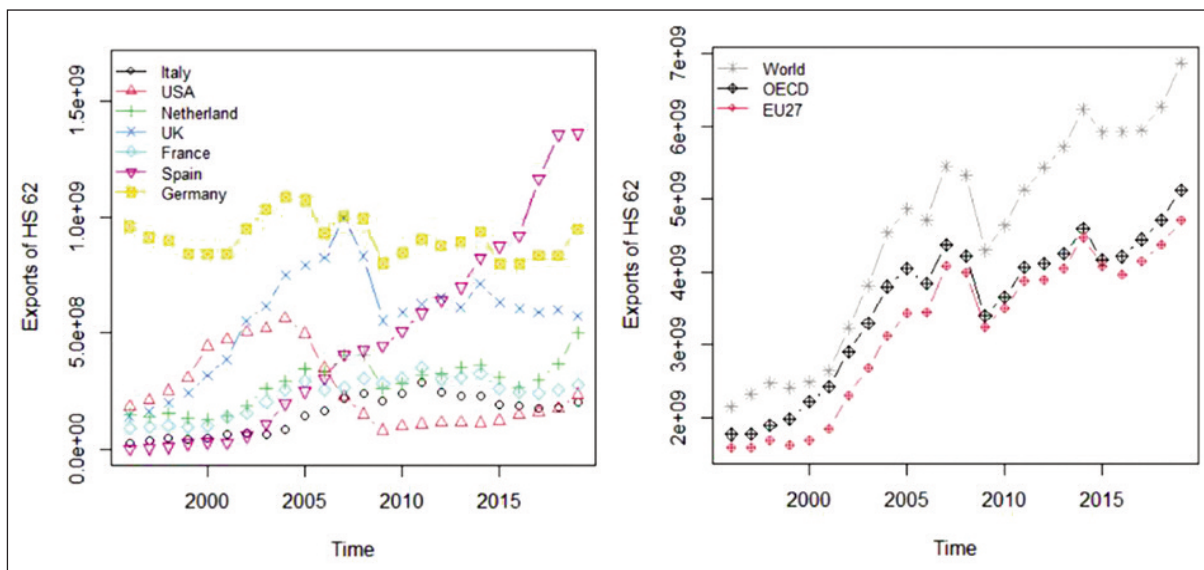


Fig. 2. Exports of HS-62

key point [6]. Particularly, examining trends of export and import is vital for developing countries. Proper estimation and forecasts create a clearer picture in the minds of decision-makers of nations, managers of companies and every individual and provide insight into the future. Thus, it can be possible to assess the situation, define policies, and measure the impact of potential decisions [7, 8]. For this reason, prediction takes the attention of the researchers. There are sectoral studies, in which estimates are made regarding the economical topics of countries and the activities of companies by using different techniques, in the literature.

Many studies predicted the sales of fashion manufacturers in the literature [9–13]. In all these studies, it was emphasized the need to plan properly and thus use the resources effectively, reduce costs, and the importance of correct investment decisions. Again, for fashion production, there are some studies were conducted to estimate the trend of colours [14, 15]. There are several studies on forecasting the exports of some countries' textile and apparel industries.

Quanping and Xiaoyi proposed a hybrid model, that is composed of the GM (1,1) grey forecasting model and EMD method, to forecast the time series of textile export having seasonality characteristics for the period 2003–2011. The forecasting findings were better than the results of the direction prediction method [16].

Ozbek et al. forecasted the export of denim trousers in Turkey by using ANN and the autoregressive-integrated model of moving averages. The results revealed that the ANN model provides more accurate forecasting than the ARIMA model [17].

Xia et al. predicted the next 3–5 years of apparel export in China by using GM (1,1) model. The model was verified with the data from 1999 to 2008. According to the results, forecasting accuracy was better and China's garment exports had the momentum of instant growth from 2011 to 2013 [18].

Xia et al. used the Holt model to predict textile and garment export using data from 1992 to 2008. The result showed that the Holt model has a high prediction accuracy. They forecasted 2009–2010 exports to contribute by providing a series of adjustments of policies, and strategies for the relevant departments [19, 20].

Lu predicted the US total export of textile and apparel for the next ten years by using data from 1984 to 2014 via regression model and ARIMA model [21].

Ghosh studied the estimation of India's cotton export by using 63 monthly observations. The ARIMA model's results would be helpful for trade organizations to evaluate the volatility of the market structure. However, the study was limited to suggesting any policy because of the scarcity of secondary data sets [21].

In all these studies, export volumes were predicted with sufficient accuracy. The apparel industry is a driving force for the Turkish economy and it could not be met in a recent paper that forecasts the Turkish apparel export volume. Forecasting the export may

contribute to the tracking of the development and change of the sector yearly. It can give an idea about the short- and long-term development trend of the sector. At the same time, the future of the export relationship with the top countries is also important. In this study, Turkey's apparel exports for 2020–2025 were estimated based on these countries. This research used the ANNs method for forecasting with time-series data.

MATERIAL AND METHOD

Neural network model for forecasting

Artificial neural networks (ANNs) are based on a mathematical model of the brain. ANNs are focused on non-linear relationships between the response variables and their predictors. In recent years, there has been increasing interest in the use of ANNs for forecasting and modelling [22]. Neural networks are used for complex non-linear forecasting. With time series data, lagged values of the time series can be used as inputs to a neural network, just as we used lagged values in a linear autoregression model. We call this a neural network autoregression or NNAR model [23]. (NNAR) forecasting model, which is relatively new to the Neural Network (NN) model and can be used in open-source software programs. Although artificial neural networks vary according to the applied network model, they have some advantages and disadvantages. Some of these advantages are [24]:

- The network can be trained again and again for system-appropriate solutions.
- They have learning abilities and learn with different learning algorithms.
- They can work with incomplete information.

The constraint arising from the disadvantage of the model is determining the appropriate network structure for the problem.

With all these advantages, the NNAR model was preferred because it provides flexibility in model assumptions compared to classical time series models.

This paper considers a neural network autoregression model (NNAR) with time series data for forecasting the export of “HS 61-apparel and clothing accessories knitted or crocheted” and “HS 62-apparel and clothing accessories not knitted or crocheted”. This model uses inputs as lagged values of time-series data in a neural network model. Here, we consider a feed-forward network with one hidden layer and use the notation NNAR(p, k), p indicates lagged inputs, and k indicates nodes in the hidden layer. An example of the architecture of ANNs is shown in figure 3. In this example, the number of input variables is four and the number of nodes in one hidden layer is two.

To fit NNAR(p, k) model, we use the nnetar function in the forecast package of R [26]. In this paper, we consider NNAR(1,1) and NNAR(2,2) models to forecast the exporting of textiles in Turkey.

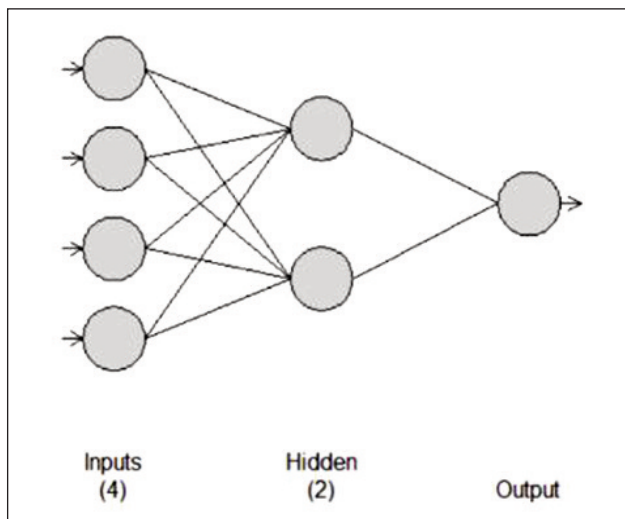


Fig. 3. The architecture of artificial neural network adopted from the nnet package of R [25]

Performance criteria

This paper compares forecast errors for NNAR(1,1) and NNAR(2,2) models. A forecast error is a difference between an observed value and its forecast. This forecast error can be represented as follows:

$$e_{T+h} = y_{T+h} - \hat{y}_{T+h} \quad (1)$$

where $\{y_1, \dots, y_T\}$ is the training dataset and $\{y_{T+1}, y_{T+2}, \dots\}$ is the test dataset [23]. Therefore, we use accuracy measures as root mean square error (RMSE), mean absolute error (MAE) and mean absolute percentage error (MAPE). The formulation of the accuracy measures is as follows:

$$RMSE = \sqrt{\frac{1}{T} \sum_{t=1}^T (e_t)^2} = \sqrt{\text{mean}(e_t^2)} \quad (2)$$

$$MAE = \frac{1}{T} \sum_{t=1}^T |e_t| = \text{mean}|e_t| \quad (3)$$

$$MAPE = \frac{1}{T} \sum_{t=1}^T |p_t|, \quad p_t = \frac{100 e_t}{y_t} \quad (4)$$

Here, residuals are computed on the training dataset while forecast errors are computed on the test dataset. In our study, we separate the available data into training and test data when selecting models. The training dataset is used to estimate the parameters of the NNAR models, and the test dataset is used to evaluate model accuracy. Therefore, the first 20 observations (1996–2015) are used for training dataset, and the last 4 observations (2016–2019) are used for testing the dataset. The lower values of RMSE, MAE and MAPE show the best model. The accuracy values for the MAPE criterion proposed by Lewis (1982) are given in table 1 [27].

RESULTS AND DISCUSSION

The results of training and testing, which are applied to the previous export series for the estimation of the HS-61 “Apparel and clothing accessories knitted or crocheted” coded product exports to selected countries and country groups of Turkey, are given in table 2. The training phase shows the prediction results for the observed dataset. According to the training results, it was seen that the Neural Networks NNAR(2,2) model performed better than the NNAR(1,1) model. To the MAPE value in the training results, only Italy and Spain have “Good accuracy” value, while the USA and other countries have “High accuracy” value. When the training results are examined in general, it is possible to say that NNAR(2,2) models have a better fit than NNAR(1,1) models.

After getting well-matched training results, the testing phase was started. The testing phase shows the estimation results for the unobserved data set. According to the results obtained for France, Italy and the OECD, the NNAR(2,2) models performed better than the NNAR(1,1) models. At the same time, France, Italy and the OECD showed “High accuracy” compliance concerning the MAPE value. For the USA and other countries, NNAR(1,1) test results have shown a better fit than NNAR(2,2). In comparison with MAPE values the USA, Netherlands and Spain have a “Good accuracy” and United Kingdom, Germany, World and EU27 have a “High accuracy”. Examining the MAPE value, only the NNAR(2,2) models of USA and Spain have achieved a “Reasonable accuracy” fit, while all the remaining models have “High accuracy and Good accuracy” values. In short, the models showed a good fit in making export estimations with respect to the Training and Testing results.

After the training and testing models display a good fit to data, Turkey’s export forecasts for the HS-61 “Apparel and clothing accessories knitted or crocheted” product group to the relevant countries and country groups were given in table 3. To make a comparison with the export values of 2020 and to evaluate and control the estimation results obtained, the export estimation results for 2020 are shown in table 3. To make a comparison with the export values of 2020 and to evaluate and control the estimation results got, the export estimation results for 2020 are shown in table 3. Besides, the export values realized in 2019 and the percentage change in exports for both years compared to the previous year are given in the table. The export values used in the table and comments should be read as x\$ 1,000.

The NNAR(2,2) model (\$307,696) gave the forecast for exports to Italy for 2020 within the confidence interval and closer to the realized export value

Table 1

A SCALE OF JUDGMENT OF FORECAST ACCURACY				
MAPE	<=10%	(10%–20%)	(20%–50%)	>=50%
Forecasting ability	High accuracy	Good accuracy	Reasonable accuracy	Inaccurate

COMPARISON RESULTS OF NNAR (1,1) AND NNAR (2,2) FOR HS-61 "APPAREL AND CLOTHING ACCESSORIES KNITTED OR CROCHETED"							
Countries	Model	Training			Testing		
		RMSE	MAE	MAPE	RMSE	MAE	MAPE
Italy	NNAR (1,1)	34561788	28094843	13.20726	66989953	65084375	21.95834
	NNAR (2,2)	30584223	23934885	10.28835	23735012	23519739	7.890762
USA	NNAR (1,1)	64995608	42922670	12.26851	64995608	42922670	12.26851
	NNAR (2,2)	26825831	17659415	5.634005	53694313	53694190	28.64933
Netherlands	NNAR (1,1)	49411481	34890101	10.2399	81774733	71238761	13.34776
	NNAR (2,2)	36034654	24713257	6.913815	89189675	87754150	16.1407
UK	NNAR (1,1)	101956949	68602875	6.633984	73228347	65207657	5.0993
	NNAR (2,2)	77826093	43559928	4.184797	120561423	120100428	9.236127
France	NNAR (1,1)	52165809	41449828	8.816093	48031741	44717312	9.581438
	NNAR (2,2)	43455567	28226764	5.917141	10270473	10250020	2.106736
Spain	NNAR (1,1)	36465447	25247525	15.89645	130919556	127981287	13.46383
	NNAR (2,2)	26111836	19319768	10.46842	201166543	201165241	20.45058
Germany	NNAR (1,1)	156207617	132275343	6.957124	70186797	62392473	3.313713
	NNAR (2,2)	100504414	85791475	4.325895	87100889	83528573	4.521137
World	NNAR (1,1)	563002541	457193094	7.425661	171159222	146826891	1.610776
	NNAR (2,2)	502806270	415876872	6.474047	241429258	241174166	2.643452
OECD	NNAR (1,1)	426658400	364794364	6.442591	92400011	66027316	0.9659175
	NNAR (2,2)	383944262	293484819	5.119292	51908276	51865762	0.738888
EU27	NNAR (1,1)	442942343	364391623	7.227593	180883660	176453982	2.642234
	NNAR (2,2)	377189581	273724951	5.250368	258784934	258594128	3.847987

(\$267,913). Here, the 11% decrease in exports in 2020 should also be taken into account. In both models, HS-61 exports from Turkey to Italy are expected to increase gradually until 2025. For Turkey's exports to the USA, the estimated value (\$181,480) by the NNAR (2,2) model is quite close to the actual value (\$185,085). Despite the 12% increase in exports in 2019, it is possible to say that the estimation result is quite consistent, considering the 7% decrease in exports in 2020. While the 2021 forecast was \$135,952 in the NNAR (1.1) model, it was estimated to decrease gradually to \$132,561 in 2025. In the NNAR (2,2) model, it is predicted that it will decrease to \$125,795 in 2022, but will be worth \$133,843 by 2025.

Both models have estimated close to the value (\$528,322) realized in Turkey's HS-61 exports to the Netherlands in 2020. However, in the NNAR (1,1) model, it is expected that exports will decline to \$460,400 in 2025. In the NNAR (2,2) model, it is predicted that there will be sharp decreases in 2021 and 2022 and there will be an increase after 2023 and an export level of \$477,055 in 2025.

For the United Kingdom, the NNAR (1.1) model estimated a value closer to the actual value than the NNAR (2,2) model. In both models, Turkey's HS-61 exports to the UK are predicted to increase steadily until 2025. Turkey's HS-61 exports to France

decreased by 13% in 2020. Considering this situation, when the export value realized in 2020 is examined, it is seen that the estimation of the NNAR (2,2) model gives a closer result. In both models, Turkey's HS-61 exports to France are projected to increase slightly but steadily until 2025.

According to the forecast results for Spain, in 2020 both models produced results close to the realized value. However, in the NNAR (1,1) model, Turkey's HS-61 exports to Spain are predicted to decline slightly but gradually until 2025, while in the NNAR (2,2) model it is predicted to increase and fall later in 2021.

In the estimation of Turkey's HS-61 products exports to Germany, it is seen that the models gave close results to the realized value for 2020. However, in both models, there is an expectation of a decrease in exports until 2024. In 2025, while exports remain unchanged in the NNAR (1,1) model, an increase in exports is predicted in the NNAR (2,2) model.

When the estimations for Turkey's exports of HS-61 products to the world are examined, the NNAR (1,1) model gives a closer prediction of the real value for 2020, while this model predicts that exports will decrease until 2025. The NNAR (2,2) model, on the other hand, predicts that exports will increase again after a decline until 2023. When the results for the OECD are examined, it is possible to say that both models make close predictions for 2020. The NNAR (1,1) model predicts that Turkey's exports to

FORECASTING RESULTS OF NNAR (1,1) AND NNAR (2,2) FOR HS-61 "APPAREL AND CLOTHING ACCESSORIES KNITTED OR CROCHETED"									
Countries	Actual export (x\$1,000) and rate of change (%)*		Model	Forecasting results (x\$1,000)					
	2019	2020		2020	2021	2022	2023	2024	2025
Italy	301,937 (3)	267,913 (-11)	NNAR (1,1)	333,784	355,258	368,267	375,605	379,571	381,665
			NNAR (2,2)	307,696	310,848	312,485	313,329	313,767	313,998
USA	198,884 (12)	185,085 (-7)	NNAR (1,1)	150,562	135,952	133,134	132,654	132,574	132,561
			NNAR (2,2)	181,480	133,758	125,795	130,948	134,097	133,843
Netherlands	560,044 (7)	528,322 (-6)	NNAR (1,1)	481,363	466,381	462,189	460,918	460,523	460,400
			NNAR (2,2)	478,524	351,162	326,567	406,922	440,691	477,055
UK	1,284,497 (-3)	1,244,106 (-3)	NNAR (1,1)	1,328,640	1,347,005	1,354,165	1,356,883	1,357,904	1,358,287
			NNAR (2,2)	1,370,003	1,387,173	1,405,886	1,411,119	1,413,427	1,414,186
France	487,451 (0,4)	423,052 (-13)	NNAR (1,1)	518,623	543,585	560,912	571,567	577,580	580,797
			NNAR (2,2)	490,396	491,835	492,973	493,899	494,783	495,692
Spain	991,243 (2)	960,789 (-3)	NNAR (1,1)	988,560	986,679	985,358	984,429	983,775	983,314
			NNAR (2,2)	999,153	1,001,290	1,000,199	998,103	996,324	995,325
Germany	1,831,716 (-2)	1,733,117 (-5)	NNAR (1,1)	1,706,148	1,596,249	1,589,874	1,589,806	1,589,805	1,589,805
			NNAR (2,2)	1,754,138	1,651,575	1,592,173	1,560,993	1,559,441	1,560,801
World	9,200,636 (2)	8,387,723 (-9)	NNAR (1,1)	9,099,272	9,043,049	9,011,190	8,992,921	8,982,375	8,976,263
			NNAR (2,2)	9,129,243	9,071,424	9,052,013	9,050,847	9,053,317	9,054,846
OECD	7,039,566 (1)	6,645,923 (-6)	NNAR (1,1)	7,025,330	7,020,554	7,018,942	7,018,398	7,018,213	7,018,151
			NNAR (2,2)	7,044,887	7,045,462	7,045,511	7,045,514	7,045,514	7,045,514
EU27	6,716,491 (-0,1)	6,353,381 (-5)	NNAR (1,1)	6,825,027	6,869,651	6,887,236	6,894,047	6,896,667	6,897,672
			NNAR (2,2)	6,866,084	6,895,301	6,873,494	6,864,694	6,866,943	6,868,852

Note: * Export data taken from UN Comtrade (2021) database [28]. The authors calculated the change in exports.

the OECD will decrease slightly until 2025, while the NNAR(2,2) model predicts that it will increase slightly until 2023 and then remain stable. For EU-27, there is an expectation of an increase until 2025 in the NNAR(1,1) model, and a fluctuating course in close values after the increase in the NNAR(2,2) model in 2021.

In figure 4, the observed values and fitted results for Turkey's HS-61 exports to the world are given to show the fit of neural networks models for forecasting. The title of "HS Code 61" reflects the real values of Turkey's exports of the HS-61 product group to the world. The "Fitted data" title shows the fitted values of the NNAR(1,1) and NNAR(2,2) models. As can be seen here, HS Code 61 observed values are compatible with fitted data. In other words, neural networks models performed well in forecasting and export forecasts were made according to this fit.

It is seen in table 3 that Turkey's HS-61 exports to countries in 2020 declined. The decreasing trend in exports is under the influence of many factors. We can list the two most important reasons as follows. The first is the depreciation of the Turkish lira against foreign currencies, especially in 2019 and 2020. The second is that the COVID-19 pandemic conditions have had a negative impact on global trade. Inevitably, both situations will affect Turkey's exports

in 2020. However, in the export estimation made under these conditions, it is very important that the export values realized in 2020 yielded results close to the estimated values. For example, while exports to the USA decreased by 7% in 2020, the actual export value was \$185,085 and the NNAR(2,2) model estimated it at \$181,480.

For the estimation of Turkey's HS-62 "Apparel and clothing accessories not knitted or crocheted" exports to selected countries and country groups, the results of the training and testing processes applied to Turkey's past export series to these countries and country groups are given in table 4.

According to the training results, it was seen that the NNAR(2,2) model achieved a better fit than the NNAR(1,1) model for all countries. Regarding the MAPE value in the training results, only Spain has the value of "Good accuracy", while all other countries have the value of "High accuracy". This shows that both models have achieved good performance.

After the training results achieved a good fit, the testing phase was started. Based on the findings, the NNAR(2,2) model for the United Kingdom and France, and the NNAR(1,1) model for other countries and country groups performed better and got a good fit with the series. According to the MAPE value, Italy, the USA, Netherlands, Spain and OECD showed

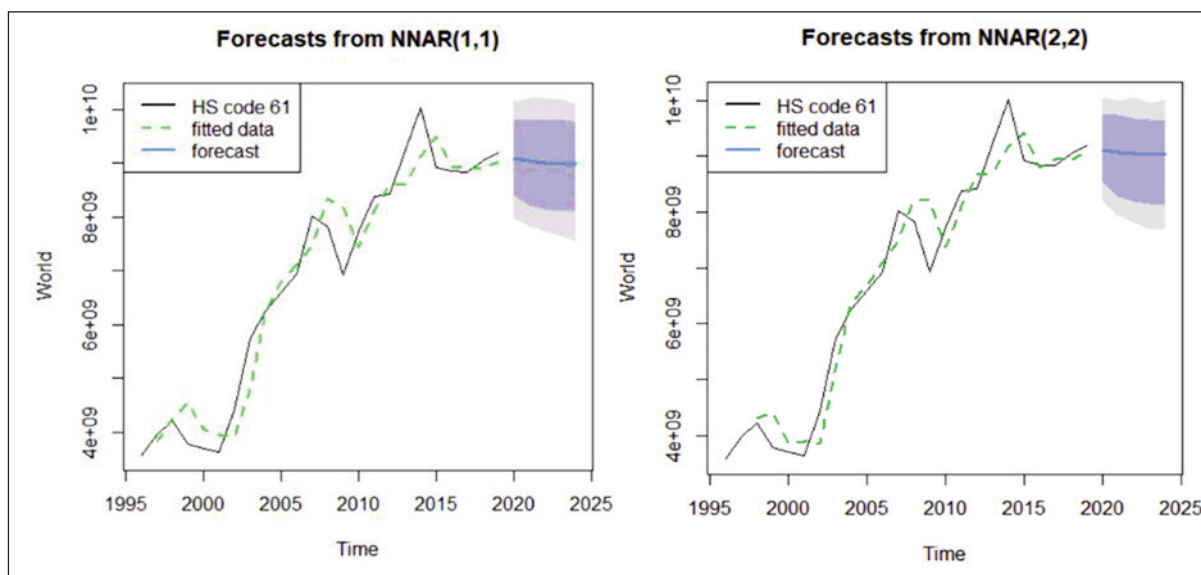


Fig. 4. Turkey's HS61 coded product export estimation to the world

Table 4

COMPARISON RESULTS OF NNAR (1,1) AND NNAR (2,2) FOR HS-62 "APPAREL AND CLOTHING ACCESSORIES NOT KNITTED OR CROCHETED"							
Countries	Model	Training			Testing		
		RMSE	MAE	MAPE	RMSE	MAE	MAPE
Italy	NNAR (1,1)	20429519	15296331	11.83968	31189243	28683437	15.78400
	NNAR (2,2)	17250409	11545844	9.087663	32061554	30295198	16.09653
USA	NNAR (1,1)	63440814	46588829	20.1182	37340604	29414934	13.9548
	NNAR (2,2)	17379058	12875438	6.044775	54573686	48775284	22.42279
Netherlands	NNAR (1,1)	35075527	28182295	11.19503	93447043	69688198	15.43911
	NNAR (2,2)	27006315	21028065	8.110915	104761611	90301734	19.3544
UK	NNAR (1,1)	84453272	56282812	8.808795	73035142	71691724	12.24422
	NNAR (2,2)	49350975	39183677	6.237545	56785809	53877665	9.255832
France	NNAR (1,1)	22204518	16865527	7.328232	30955714	27496546	10.97946
	NNAR (2,2)	21705080	15851835	6.850044	23194277	21879605	8.324111
Spain	NNAR (1,1)	28862211	22610032	37.10514	184219414	178629790	13.99512
	NNAR (2,2)	21310488	18173609	15.10049	330335814	329393168	24.28814
Germany	NNAR (1,1)	69039535	55848010	6.106877	52226114	49237465	5.55239
	NNAR (2,2)	35029667	28133448	3.173606	59740375	58569034	6.517465
World	NNAR (1,1)	356872566	250654180	5.906928	710185379	629096431	9.615673
	NNAR (2,2)	292905104	221547369	5.068071	738219648	704930863	10.59872
OECD	NNAR (1,1)	233166527	150590086	4.255936	652398425	601130786	12.35826
	NNAR (2,2)	135643361	77608831	2.015422	1138142056	1013274516	20.18734
EU27	NNAR (1,1)	240862319	153833335	4.950147	450925793	412278679	9.160216
	NNAR (2,2)	202477535	139782051	4.482708	733533035	668668926	14.50173

"Good accuracy", while other countries showed a "High accuracy" fit. This displays that both models perform well to estimate Turkey's exports to selected countries.

Turkey's export values of HS-62 "Apparel and clothing accessories not knitted or crocheted" product group to the selected countries and country groups in 2019 and 2020 and its export's rate of change and HS-62 export forecast results from 2020 to 2025 are

presented in table 5. As mentioned before, the real export values of 2020 have been tested for control. Thus, it is possible to compare the actual value in 2020 with the forecast results. In addition, exports in 2019 and the rate of change in exports compared to the previous year are also given in the table to monitor the course of exports better.

From the prediction results got, it is seen that Turkey's exports to Italy in 2020 in the HS-62 code

FORECASTING RESULTS OF NNAR (1,1) AND NNAR (2,2) FOR HS-62 "APPAREL AND CLOTHING ACCESSORIES NOT KNITTED OR CROCHETED"									
Countries	Actual export (x\$1,000) and rate of change (%)*		Model	Forecasting results (x\$1,000)					
	2019	2020		2020	2021	2022	2023	2024	2025
Italy	203,660 (12)	219,032 (8)	NNAR (1,1)	214,602	220,455	223,360	224,745	225,394	225,694
			NNAR (2,2)	225,051	231,799	229,305	227,296	226,329	225,936
USA	237,088 (36)	362,858 (53)	NNAR (1,1)	252,377	268,344	284,808	301,514	318,145	334,339
			NNAR (2,2)	355,807	459,335	503,091	517,175	515,917	508,676
Netherlands	500,040 (35)	619,928 (24)	NNAR (1,1)	375,975	363,103	359,932	359,059	358,812	358,741
			NNAR (2,2)	529,979	301,369	273,852	312,166	361,253	384,176
UK	573,419 (-4)	522,809 (-8)	NNAR (1,1)	620,786	654,320	676,411	690,243	698,620	703,588
			NNAR (2,2)	585,335	609,558	630,003	643,369	654,871	6,656,044
France	279,242 (9)	247,780 (-11)	NNAR (1,1)	287,073	289,992	291,016	291,367	291,487	291,528
			NNAR (2,2)	296,290	300,922	302,866	303,404	303,614	303,676
Spain	1,359,057 (0,4)	1,046,576 (-23)	NNAR (1,1)	1,421,826	1,463,700	1,489,919	1,505,650	1,514,841	1,520,124
			NNAR (2,2)	1,399,310	1,404,960	1,408,297	1,409,049	1,409,350	1,409,433
Germany	948,116 (14)	960,744 (1)	NNAR (1,1)	926,371	913,353	905,862	901,655	899,325	898,045
			NNAR (2,2)	1,023,649	1,033,922	901,067	887,999	868,142	873,015
World	6,871,159 (10)	6,600,585 (-4)	NNAR (1,1)	6,607,516	6,448,785	6,348,756	6,283,965	6,241,268	6,212,815
			NNAR (2,2)	6,878,794	6,877,840	6,875,970	6,874,545	6,873,621	6,873,051
OECD	5,128,781 (9)	5,073,618 (-1)	NNAR (1,1)	4,674,967	4,511,734	4,441,274	4,408,714	4,393,212	4,385,728
			NNAR (2,2)	7,011,919	9,664,157	9,917,357	9,907,495	9,904,198	9,904,075
EU27	4,706,070 (8)	4,533,935 (-4)	NNAR (1,1)	4,350,902	4,223,962	4,170,932	4,147,462	4,136,818	4,131,938
			NNAR (2,2)	4,483,861	4,323,926	4,237,345	4,192,936	4,170,274	4,158,637

Note: * Export data taken from UN Comtrade (2021) database [28]. The authors calculated the change in exports.

(\$219,032) are very close to the forecast produced by the NNAR (1,1) model. Turkey's HS-62 exports to Italy tend to increase by 2025. In exports to the USA (\$362,858), it is seen that the NNAR (2,2) model gave results close to the actual export value. Considering that Turkey's HS-62 exports to the USA increased by 36% in 2019 and by approximately 53% in 2020, it is possible to say that the NNAR (2,2) model made a very accurate estimation. It is predicted that Turkey's exports to the USA will increase by 2023 and will begin to decrease in 2024.

The NNAR (2,2) model gave the closest estimate of Turkey's exports to the Netherlands. Increasing Turkey's exports to the Netherlands at high rates and growing decreasingly, may affect the forecast results. According to the NNAR (2,2) model, a decrease in exports to the Netherlands in 2021 and 2022, and then an increase is forecasted. Turkey's HS-62 exports to the UK decreased by 4% and 8% in 2019 and 2020, respectively. When the estimation results are examined, it is seen that the NNAR (2,2) model gave a closer result to the exports realized in 2020. In general, there is an expectation of an increase in HS-62 exports to the UK until 2025.

While the exports to France under the code HS-62 increased by 9% in 2019 compared to the previous year, they decreased by 11% in 2020. Considering

the estimation results in this fluctuating course, it is seen that the NNAR (1,1) model's estimation is close to the actual export. There is an expectation of an increase, albeit slowly, until 2025. While there was a 0.4% increase in Turkey's HS-62 exports to Spain in 2019, there was a 23% decrease in 2020. After almost zero growth in exports in 2019, with the sudden decrease in 2020, the forecast result is close to the 2019 value, but it is far away from the 2020 value. An increase in exports is expected in the coming years.

In Turkey's estimation of HS-62 exports to Germany for 2020, NNAR (1,1) model's result was close to the value realized. Considering that, the export increase in 2019 was 14% and in 2020 was 1%, it is possible to conclude that there was a fluctuating course in the real export values. Therefore, it can be said that the forecast value is quite accurate.

When Turkey's HS-62 exports to country groups and the world are evaluated, it is seen that the NNAR (2,2) model for EU-27 and NNAR (1,1) model for the OECD and the World give results close to the realized values. Although Turkey's HS-62 exports, especially to the world, increased by 10% in 2019 and decreased by 4% in 2020, it is an important result that the 2020 forecast was realized very close to the real value. However, it is estimated that Turkey's

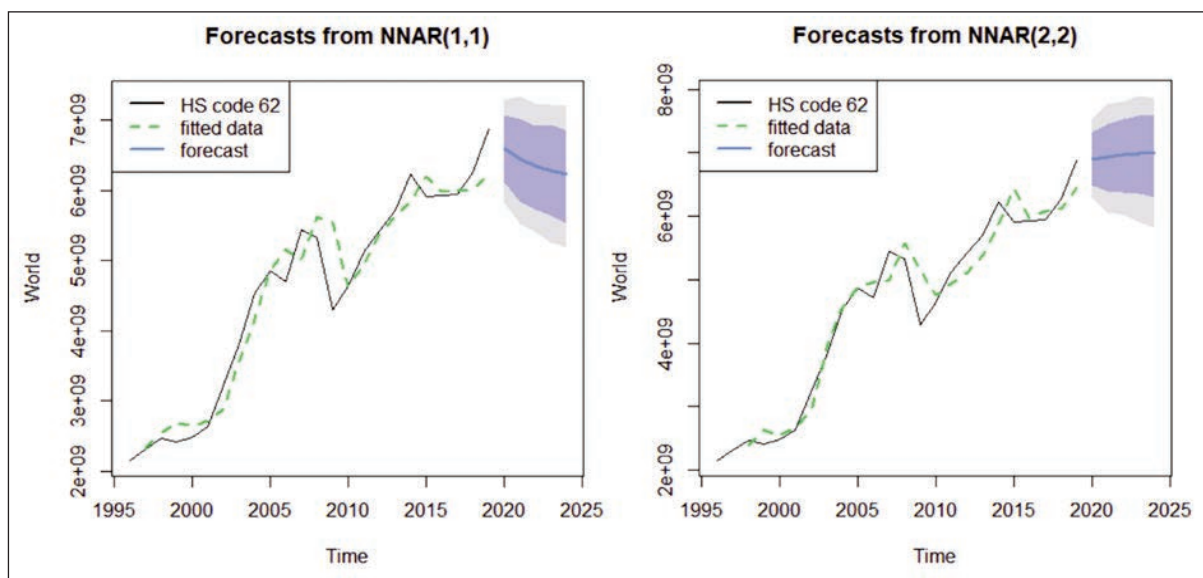


Fig. 5. HS-62 coded export forecast of Turkey to the world

HS-62 exports to the world will decrease gradually by 2025. Similar expectations are available for OECD and EU-27.

In figure 5, to see how Neural Networks models fit for forecasting, the fit status of the models for Turkey's HS-62 exports to the World yearly is shown. The title "HS Code 62" shows the real (observed) value of Turkey's export of HS-62 to the world. The title "Fitted data" shows the fitted values of the NNAR (1,1) and NNAR (2,2) prediction models. As seen here, the HS Code 62 observed values are consistent with the fitted values. In other words, Neural Networks models performed well in forecasting and export forecasts were made according to this fit.

In summary, compared with the 2020 realized values, it seems that in general, the estimates for HS-61 and HS-62 are within the confidence interval. However, in some cases, differences between the real and estimated values have been seen to open up. It has been said before that the reasons for this are the depreciation of TL against foreign currencies (the rise in the exchange rate) and the negative conditions created by the COVID-19 pandemic. Here, the declines in Turkey's HS-62 exports in 2020, excluding Italy, the USA and Netherlands, are noteworthy again. Both the depreciation of the TL and the impact of the pandemic conditions have affected Turkey's exports in 2020. However, in the export estimation made under these conditions, it was observed that the export values realized in 2020 gave results close to the estimation values. For example, while Turkey's HS-62 exports to France decreased by 11% in 2020, the NNAR (1,1) model estimated value (\$287,073) is close to the actual value (\$247,780). Again, Turkey's exports of the same product group to the USA increased by 53% and the estimated value was quite close to the actual export.

Here, besides the COVID-19 pandemic conditions, the depreciation of the domestic currency against foreign currencies in Turkey, especially in 2019 and

2020, is an issue that needs to be considered. Although there is a prevailing view in the economics literature that the depreciation of the domestic currency will increase exports [29], there are also studies suggesting that exchange rate volatility reduces exports [30–32]. This situation arises economically due to low short-term elasticity. It takes time for producers and consumers to adapt to this new situation. Producers may not increase their production capacity in a short time against the increasing demand or they may not make a new agreement since their commercial relations are based on contracts. In addition, exporters may delay their sales by anticipating that the exchange rates will rise even more. It is also difficult for consumers to change their tastes and habits in a short time [29, 33]. Many reasons like this may not increase or even decrease exports the first time when the local currency depreciates. Here, too, there may be a similar situation in Turkey's 2020 exports of both HS-61 and HS-62 product groups. However, after the harmonization process of producers and consumers, exports will continue in their normal course.

CONCLUSION

In this study, Turkey's exports to the countries and country groups to which it exports the most in the codes HS-61 "Apparel and clothing accessories knitted or crocheted" and HS-62 "Apparel and clothing accessories not knitted or crocheted" were discussed. Using the export data to these countries for 1996–2019, the 2020–2025 export values of Turkey in both product groups were estimated with Neural Networks models. Both HS-61 and HS-62 training and testing results have "Good accuracy" and "High accuracy" values according to MAPE value. In other words, it has been seen that Neural Networks models provide good results in estimating Turkey's apparel export values.

If we evaluate the findings for the HS-61 and HS-62 product groups separately, the estimation results for Turkey's exports to selected countries in the HS-61 product group can be summarized as follows; in the NNAR(1,1) model, Turkey's exports of HS-61 products to Italy, UK, France and EU-27 are expected to increase year-on-year from 2020 to 2025, while exports to USA, Netherlands and Spain are expected to decrease. However, first, a decrease and then an increase is foreseen in Turkey's exports to Germany, the World and the OECD. In the NNAR(2,2) model, while there is an expectation of an increase in Turkey's exports to Italy, the UK and France from year to year, it is estimated that exports to other countries first decrease and then increase.

The export forecast of Turkey's HS-62 product group to selected countries is as follows: In the NNAR(1,1) model, Turkey's exports to Italy, the USA, the UK, France and Spain are predicted to increase from year to year from 2020 to 2025. In the same period, Turkey's exports to the Netherlands, Germany, World, OECD and EU-27 are expected to decrease year by year. In the NNAR(2,2) model, while there is an expectation of an increase in exports to the UK, France and Spain from year to year, the opposite is expected in exports to EU-27, OECD and the World.

However, a fluctuating course is expected in exports to Italy, the USA, the Netherlands and Germany.

It is expected that this study will contribute to future studies on forecasting the export of apparel and other industries. However, since forecasting is a concept related to the unseen and uncertain future, it also brings some limitations. There may be deviations from the estimation in case of situations such as shocks to be experienced in supply and demand, volatility in exchange rates, and economic and political instability. In this study, Turkey's exchange rate increases, especially in the last period, caused fluctuations in exports. In the economic literature, it is expected that exports will increase with the increase in exchange rates. However, exports may not increase or even decrease in the short run [30–32]. This is a concept related to the elasticities of supply and demand. If elasticities are low in the short run, exports do not increase, but on the contrary decrease (30). Factors caused this situation such as commercial agreements, the insufficient scale of production or the inability to change the tastes and preferences of the consumer in the short term. In future studies, new model trials can be made that consider such constraints.

REFERENCES

- [1] *Ready-to-wear Country Report*, Ministry of Commerce, General Directorate of Export, 2018
- [2] *Apparel and Apparel Industry Country Export Evaluation*, IHKIB, January-December 2020
- [3] Yaman Selçi, B., Akgul, Y., *Analysis on the estimation of Turkey's Export Values with Artificial Neural Networks*, In: Journal of Quantitative Sciences, 2020, 2, 2, 29–42
- [4] Todaro, M.P., *Economic Development*, (7th edition): Addison-Wesley Publications, 2000
- [5] Awokuse, T.O., *Causality between exports, imports, and economic growth: Evidence from transition economies*, In: Economics Letters, 2007, 94, 3, 389–395
- [6] Tran, T.T., *Applying Grey System Theory to Forecast the Total Value of Imports and Exports of Top Traded Commodities in Taiwan*, In: International Journal of Analysis and Applications, 2019, 17, 2, 282–230
- [7] Carnot, N., Koen, V., Tissot, B., *Economic Forecasting: Palgrave Macmillan UK*, 2005
- [8] Sadullojevich, K.I., Jobir Ugli, A.I., *Estimating and Forecasting Trends of Global Export and Import of Goods in International Markets*, In: İqtisodiyot va Innovatsion Texnologiyalar Ilmiy Elektron Jurnalı, 2020, 2, 2, 229–236
- [9] Huang, H., Liu, Q., *An Intelligent Retail Forecasting System for New Clothing Products Considering Stock-out*, In: Fibres & Textiles in Eastern Europe, 2017, 25, 121, 10–16
- [10] Loureiro, A.L.D., Miguéisa, V.L., Silva, L.F., *Exploring the use of deep neural networks for sales forecasting in fashion retail*, In: Decision Support Systems, 2018, 114, 81–93
- [11] Xia, M., Wong, W.K., *A seasonal discrete grey forecasting model for fashion retailing*, In: Knowledge-Based Systems, 2014, 57, 119–126
- [12] Ren, S., Chan, H.L., Ram, P., *A Comparative Study on Fashion Demand Forecasting Models with Multiple Sources of Uncertainty*, In: Ann. Oper. Res, 2017, 257, 335–355
- [13] Choi, T.M., Hui, C.L., Liu, N., Ng, S.F., Yu, Y., *Fast fashion sales forecasting with limited data and time*, In: Decision Support Systems, 2014, 59, 84–92
- [14] Lin, J.J., Sun, P.T., Chen, J.J.R., Wang, L.J., Kuo, H.C., Kuo, W.G., *Applying gray model to predicting trend of textile fashion colors*, In: The Journal of the Textile Institute, 2010, 101, 4, 360–368
- [15] Choi, T.M., Hui, C.L., Ng, S.F., Yu, Y., *Color Trend Forecasting of Fashionable Products with Very Few Historical Data*, In: IEEE Transactions on Systems, Man, and Cybernetics, Part C (Applications and Reviews), 2012, 42, 6, 1003–1010
- [16] Quanping, H., Xiaoyi, Y., *Base a EMD-Grey Model for Textile Export Time Series Prediction*, In: International Journal of Database Theory and Application, 2013, 6, 6, 29–38
- [17] Özbek, A., Akalın, M., Topuz, V., Sennaroğlu, B., *Prediction of Turkey's Denim Trousers Export Using Artificial Neural Networks and the Autoregressive Integrated Moving Average Model*, In: Fibres & Textiles In Eastern Europe, 2011, 19, 3, 10–16

- [18] Xia, L., Kong, F., Liu, Y., *Applying GM(1,1) model in China's apparel export Forecasting*, In: Fourth International Symposium on Computational Intelligence and Design, Hangzhou, China, 2011, 245–247
- [19] Xia, L., Yaomei, G., Weiwei, S., *Forecast to Textile and Garment Exports Based on Holt Model*, In: International Conference of Information Science and Management Engineering, Shaanxi, China, 2010, 274–277
- [20] Jinzhao, L., *Forecasting of US Total Textiles and Apparel Export to the World in Next 10 Years (2015–2025)*, In: JTATM, 2015, 9, 2, 1–8
- [21] Ghosh, S., *Forecasting Cotton Exports in India using the ARIMA model*, In: Amity Journal of Economics, 2017, 2, 2, 36–52
- [22] Co, H.C., Boosarawongse, R., *Forecasting Thailand's rice export: Statistical techniques vs. artificial neural networks*, In: Computers & Industrial Engineering, 2007, 53, 610–627
- [23] Hyndman, R.J., Athanasopoulos, G., *Forecasting: Principles and Practice: Otexts*, 2nd Edition, 2018
- [24] Yavuz, S., Deveci, M., *The Effect of Statistical Normalization Techniques on the Performance of the Artificial Neural Network*, In: Erciyes Üniversitesi İktisadi ve İdari Bilimler Fakültesi Dergisi, 2012, 40, 167–187
- [25] Kourentzes, N., *nnfor: Time Series Forecasting with Neural Networks 2017*, R package version 0.9. 6.
- [26] Hyndman, R.J., Athanasopoulos, G., Bergmeir, C., Caceres, G., Chhay, L., O'Hara-Wild, M., Wang, E., *Package 'forecast'*, 2020, Available at: <https://cran.r-project.org/web/packages/forecast/forecast> [Accessed on March 2022]
- [27] Lewis, C.D., *Industrial and Business Forecasting Methods: A Practical Guide to Exponential Smoothing and Curve Fitting*, London: Butterworth Scientific, 1982
- [28] UN Comtrade, *UN comtrade database*, 2021, Available at: <https://unstats.un.org/unsd/comtrade/maintenance.html> [[Accessed on July 21, 2021]
- [29] Seyidođlu, H., *International Economics, Theory, Policy and Practices*, Güzem Can Publications, 16th Edition, İstanbul, 2017
- [30] Vieira, F.V., MacDonald, R., *Exchange rate volatility and exports: a panel data analysis*, In: Journal of Economic Studies, 2016, 43, 2, 203–221
- [31] Choudhry, T., *Exchange rate volatility and the United States exports: Evidence from Canada and Japan*, In: Journal of the Japanese and International Economies, 2005, 19, 1, 51–71
- [32] Bahmani-Oskooee, M., Harvey, H., Hegerty, S.W., *Exchange-rate volatility and commodity trade between the USA and Indonesia*, In: New Zealand Economic Papers, 2015, 49, 1, 78–102
- [33] Karluk, R., *International Economics, Theory-Policy*, Beta Publications, 9th Edition, İstanbul, 2013

Authors:

GULSEREN KARABAY¹, MUHAMMET BURAK KILIC², KAZIM SARICOBAN³, GİZEM KARAKAN GÜNAYDIN⁴

¹Dokuz Eylul University Department of Textile Engineering,
Tinaztepe Campus, Buca, İzmir, Turkey
e-mail: gulseren.karabay@deu.edu.tr

²Burdur Mehmet Akif Ersoy University, Department of Business Administration,
İstiklal Campus, 15030 Burdur, Turkey
e-mail: mburak@mehmetakif.edu.tr

³Burdur Mehmet Akif Ersoy University, Department of Economics,
İstiklal Campus, 15030 Burdur, Turkey
e-mail: ksaricoban@mehmetakif.edu.tr

⁴Pamukkale University, Buldan Vocational School, Fashion&Amp; Design Programme,
20400, Buldan, Denizli, Turkey

Corresponding author:

GİZEM KARAKAN GÜNAYDIN
e-mail: ggunaydin@pau.edu.tr

An algorithm for the analysis of static hanging drape

DOI: 10.35530/IT.074.02.202247

LILIANA INDRIE
ZLATIN ZLATEV

JULIETA ILIEVA
IOAN PAVEL OANA

ABSTRACT – REZUMAT

An algorithm for the analysis of static hanging drape

In this paper, an analysis of drape characteristics of textile waste derived from their 2D colour digital images was made. There have been proposed algorithms and procedures for obtaining 3D shapes of real drape. The description of the drape characteristics of fabrics was made by a total of 17 features. The advantages of the proposed methods and tools are that they don't need complicated calculation methods or a lot of time to measure and obtain a three-dimensional model. A predictive model was created from the obtained data for automated prediction of the drape coefficient of textile waste. The proposed methods and procedures can be applied in the analysis of fabric drape on video files obtained after exposure of the textile fabrics at different airflow rates.

Keywords: textile waste, drape characteristics, algorithms, 3D shapes

Un algoritm pentru analiza drapajului static

În această lucrare, au fost analizate caracteristicile de drapaj ale deșeurilor textile, derivate din imaginile digitale color 2D ale acestora. Au fost propuși algoritmi și proceduri pentru obținerea de forme 3D ale drapajului real. Descrierea caracteristicilor de drapaj ale materialelor a fost realizată prin 17 caracteristici. Avantajele metodelor și instrumentelor propuse sunt acelea că nu necesită proceduri complexe de calcul și un timp îndelungat pentru măsurarea și obținerea unui model tridimensional. Din datele obținute a fost creat un model predictiv pentru preconizarea automată a coeficientului de drapaj al deșeurilor textile. Metodele și procedurile propuse pot fi aplicate pe fișiere video în analiza drapajelor pe fișiere video obținute după expunerea țesăturilor textile la diferite debite de aer.

Cuvinte-cheie: deșeuri textile, caracteristici de drapaj, algoritmi, forme 3D

INTRODUCTION

A major problem in the fashion and textile industries is reducing the cost of developing textile garments. The preliminary analysis of textile fabrics through simulation is a way to reduce this type of cost. For such a simulation analysis of the properties of the textile fabric to be sufficiently effective, it is necessary to know its density, extensibility, resistance to bending, and type of textile materials used. In other words, the physical and mechanical characteristics of the textile fabric must be largely known [1–3]. Classical methods for the analysis of the characteristics of textile fabrics are accurate, reliable, and similar, but require particular laboratory conditions, chemical reagents, and qualified specialists. The duration of the analyses, and their labour intensity, make them ineffective in the express determination of the fabric properties. The methods of visual evaluation of the properties of textile fabrics are also subjective and depend on the experience and qualification of the evaluator.

An important feature of textile fabrics is their drape. It is related to how the textile fabric falls, folds, and thus shapes the final look of interior elements, clothing,

curtains, upholstery, tablecloths, napkins, blankets, and fashion accessories.

To determine the draping of textile fabrics, the most common methods used in practice are hanging drape, Cusick's drape, and modified Cusick's drape [4, 5]. According to Davis et al. [6], and also Ju et al. [7] the benefit of using a hanging drape is that it is suitable for determining certain physical properties, such as the degree of bending of the fabric.

In addition to the classical method for the analysis of the drapability of textile fabrics, using a round sample, some methods use samples with a rectangular shape [7].

According to Bhat et al. [6] and Bi et al. [8], the simulation analysis of rectangular drape is a complex task because it requires knowledge of many factors that affect the formation of drape. The authors propose an algorithm that can be used to determine the drape characteristics in dynamic mode, based on video file data. The results are compared with those obtained for real clothes such as dresses and skirts. Bouman et al. [9], expand the scope of this type of research by offering a method for analysing hanging drape based on video file data. The study was performed by determining the influence of airflow rate on the properties of textile fabric. The authors give a

comparison of the outcomes produced by their system and those obtained by specialists in the field of textile production.

According to Yang et al. [10] and Maqsood et al. [11], the methods for analysing hanging drape on video clips have the main disadvantage that they require the use of markers, as well as the use of complex algorithms and procedures to determine the characteristics of the drape. In most cases, the research is limited to a specific type of textile fabric. The reported results are more often obtained under specific conditions of video recording, which are difficult to apply to fabrics that the authors did not use. One solution to this problem is to use methods such as neural networks. Duan et al. [12], point out that the physical similarity network (PhySNet), shared with the Bayesian optimization procedure, can determine the drape characteristics, with an accuracy of 34% for textile fabrics and 68% for clothing. The analysis is done after the application of various air movements around textile fabrics and clothing.

According to Rasheed et al. [13], in the analysis of video files of fabrics, it is necessary to take into account their mechanical properties. This thesis has also been confirmed by Santesteban et al. [14], for clothing, with the authors proposing a new self-learning algorithm suitable for this purpose.

It should be summed up based on the examination of the available literary sources that in the simulation analysis of hanging drape, a method of extracting data from video clips is more often used. Because the video file can be divided into individual frames of which it consists, each frame can be considered a static image, the processing of data from this video file is based on the differences between the individual frames. In the analysis of these images, it is necessary to take into account the mechanical characteristics of the textile fabric. It is also necessary to offer algorithms and procedures, as well as predictive models that provide sufficient accuracy of the analysis, without requiring complex and powerful computational tools, requiring long analysis time, and high cost.

In the textile industry, waste is generated mainly during the tailoring stage. Incineration and landfilling should be the last method used for the management of textile waste, after reuse and recycling. One solution to reduce the negative impact on the environment would be to move to a circular textile production and consumption system [15–18]. The circular design of textiles is a significant measure to improve the durability and recyclability of the products and to guarantee the take-up of secondary raw materials in new products.

The paper aimed to obtain 3D shapes from 2D images of fabric drape resulting from textile waste. There were proposed methods and tools for obtaining 3D shapes of hanging drape.

From the textile waste resulting from production, fabric samples with a size of 30×30 cm were prepared. Depending on the percentage of cotton contained,

they were divided into three classes. A total of 90 samples were analysed.

To obtain colour digital images, a distance of 50 cm from the camera to the sample was fixed. From the obtained data, a predictive model was created for the automatic prediction of the drape coefficient of some fabrics resulting from textile waste.

MATERIAL AND METHODS

From the textile waste resulting from production, fabric samples with a size of 30×30 cm were prepared. Depending on the percentage of cotton contained, they were divided into three classes.

Table 1 shows data on the textile fabric samples used.

By using the Cusick method, the drape coefficient (DC) was determined according to the method presented in [19–20].

The thickness of the fabric (B , mm) was determined with a micrometre Carbon Fibre Composites Digital Thickness Caliper Micrometre Gauge (Shenzhen Ruize Technology Co., Ltd., Shenzhen, PR China), with a range of 12.7 mm, resolution of 0.01 mm and accuracy 0.1 mm.

The textile fabrics' weight (GSM , g/m²) was determined with a scale Pocket Scale MH-200 (ZheZhong Weighing Apparatus Factory), the maximum determined the mass of 200 g, with a resolution of 0.02 g, according to the following formula:

$$GSM = \frac{10000 W_s}{A_s}, \text{ g/m}^2 \quad (1)$$

where W_s is the mass of the measured sample, g; A_s – area of the sample in cm².

Table 1

DATA ON THE TEXTILE FABRICS USED			
Class \ Parameter	C1	C2	C3
Cotton (%)	100	74.15±15.56	0
Polyester (%)	0	17.85±14.23	66.85±15.9
Elastane (%)	0	8.17±9.09	0
Polyamide (%)	0	0	33.15±15.9

During the preparatory measurements, 3 samples of each type were measured. The scaling factor, the appropriate image capturing distance of the objects and the direction of the stage lighting were determined. Measurements and analyses were made after measuring 30 samples of each type of fabric. A total of 90 samples were analysed. 50% of the data was used to create the algorithms and procedures, and the remaining 50% of them were for their test validation.

Figure 1 shows the experimental configuration used to obtain digital colour images of the drape. As can be seen in the figure on a fixed support (1) is placed the measured sample (2) which is fixed with clips (3). A video camera Rapoo XW180 (4) (Rapoo Europe BV,

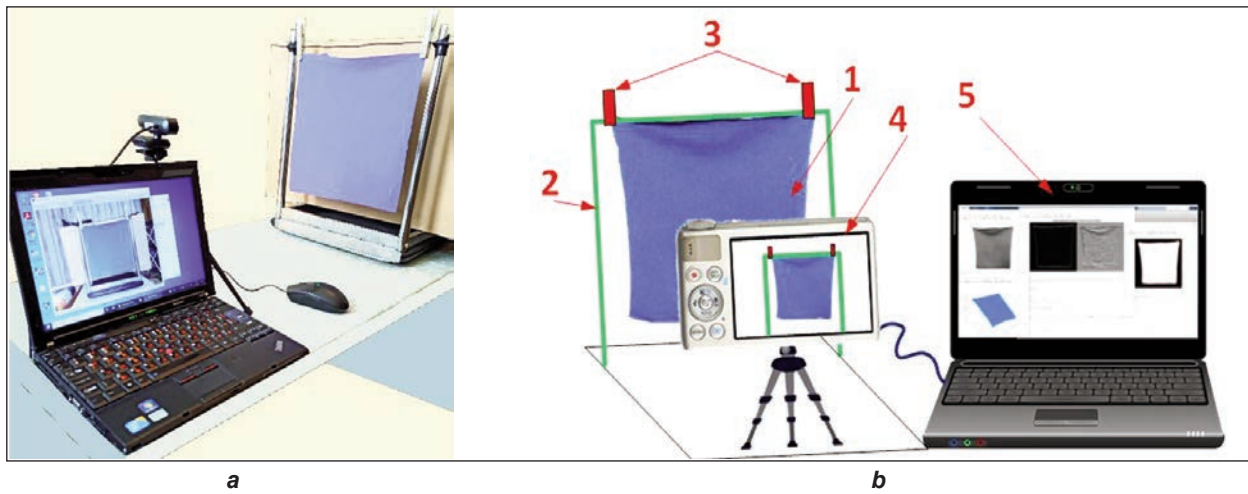


Fig. 1. Experimental set-up for obtaining drape images: a – general view; b – principle schematic

GX Bergschenhoek, The Netherlands) was used for recording. The camera has been connected via the USB interface to a personal computer (5) that receives, processes, and analyses drape images. To obtain colour digital images, a distance of 50 cm from the camera to the sample was fixed. The algorithms and procedures in the present work were created using utilizing the Matlab programming language 2017a (The MathWorks Inc., Natick, MA, USA). The characteristics describing the drape were calculated according to the mathematical equations derived by Sanad et al. [19] and Alikhanov et al. [21]. The area ratio (KA) is determined by the percentage of the area of the textile fabric before placing the test bench and the area after the appearance of the drape. It is determined by the following mathematical dependence:

$$KA = \frac{A_{fs}}{A_d} \quad (2)$$

where A_{fs} is the area of the textile fabric after draping; A_d – the area of the sample.

Circularity (C): this is a descriptor of the complexity of the form and its sharpness:

$$C = \frac{4\pi A_{fs}}{P_{fs}^2} \quad (3)$$

where A_{fs} is the area of the drape; P_{fs} – drape perimeter.

K is the coefficient that describes the object's form. It is a relationship between the drape shape and its dimensions.

$$K = \frac{P_{fs}^2}{A_{fs}} \quad (4)$$

where A_{fs} is the area of the drape; P_{fs} – drape's perimeter.

Eccentricity (E): illustrates how the drape's shape deviates from an ideal circle:

$$E = \frac{D_{fs}}{d_{fs}} \quad (5)$$

where d_{fs} is the major axis of the drape; D_{fs} – drape's small axis.

AR -Coefficient of the minimum rectangle that reveals how close the object (drape) is to its minimum rectangle.

$$A_{mr} = d_{fs} D_{fs}; \quad AR = \frac{A_{fs}}{A_{mr}} \quad (6)$$

where A_{mr} is area of the minimum rectangle outlined around the drape; D_{fs} – large axis of the drape; d_{fs} – small axis of the drape.

Calculation of moment of inertia (Area moment of inertia, m^4) was used to determine changes in drape. The moment of inertia (I) is a characteristic that describes the ability of a textile fabric to withstand bending. This factor is determined by the vertical or horizontal axis of the sample. The centre of the sample or its lower-left corner can be taken as the origin of the coordinate system.

Figure 2 shows the two options for determining the moment of inertia of a textile fabric, with a different origin in the coordinate system.

The variables used to calculate the moments of inertia include the thickness of the textile fabric (B), and its height (H). There were calculated the following parameters: the moment of inertia along the x (I_x) axis; a moment of inertia along the y (I_y) axis; the moment of inertia on both axes (I_{xy}); drape moment of inertia (I_D). In the case of the variant with the origin of the coordinate system in the left corner of the textile fabric, the moment of inertia along section A-A (I_{AA}) was also determined.

The moments of inertia in the case of the variant with the origin of the coordinate system – the centre of the textile fabric and those with the beginning of the lower-left corner were determined by the following mathematical dependences [6]:

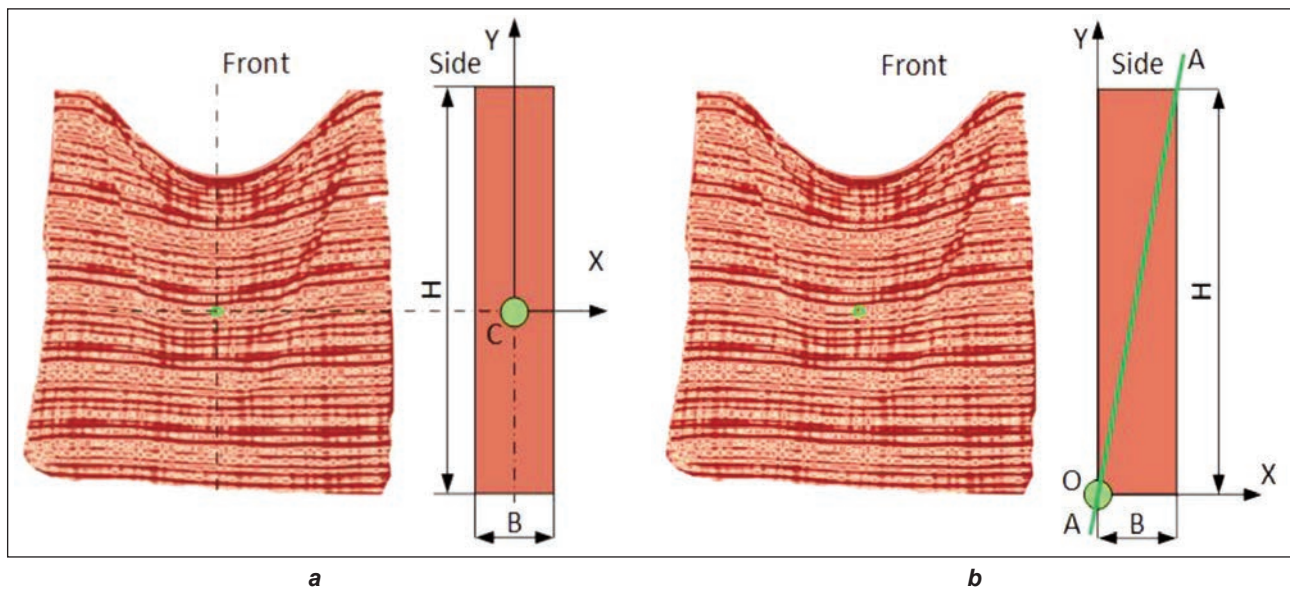


Fig. 2. Variants for determining the moment of inertia of textile fabric, with different origins of the coordinate system: a – centre of fabric; b – left corner

Centre of fabric

$$I_{x1} = \frac{BH^3}{12} \quad (7)$$

$$I_{y1} = \frac{B^3H}{12} \quad (8)$$

$$I_{xy1} = 0 \quad (9)$$

$$I_{D1} = \frac{BH}{12} (B^2 + H^2) \quad (10)$$

$$I_{AA2} = \frac{B^3H^3}{6(B^2 + H^2)} \quad (15)$$

Left corner

$$I_{x2} = \frac{BH^3}{12} \quad (11)$$

$$I_{y2} = \frac{B^3H}{12} \quad (12)$$

$$I_{xy2} = \frac{B^2H^2}{4} \quad (13)$$

$$I_{D2} = \frac{BH}{3} (B^2 + H^2) \quad (14)$$

There were developed algorithms to determine the drape characteristics. The first algorithm serves to determine the drape characteristics, and the second for its three-dimensional visualization. Drape was scaled using the scale parameter, expressed as pixels per millimetre (pix/mm).

The algorithm for determining the drape characteristics is presented in figure 3: Stage 1. Load the original RGB image; Stage 2. Convert to grey levels with

rgb2gray function; Stage 3. Define the contour of the drape in the image; Stage 4. Calculation of the drape coefficients according to the mathematical formulas is presented above.

The algorithm for three-dimensional visualization of the drape is shown in figure 4: Stage 1. Load the original RGB image; Stage 2. Convert to grey levels; Stage 3. Defines the gradient of the image with the *imgradientxy* and *imgradient* functions; Stage 4. Find the coordinates of the pixels that have a gradient higher than 1. Calculate the coordinates of the 3D graphics of the drape. The pixels of the drape in the image are detected by $[x, y] = \text{find}(L=1)$. The gradient of these pixels is determined by $z = \text{find}(Gmag>5)$. Prediction of drape coefficient (DC). According to Hunter et al. [5], the draping coefficient can be predicted by the degree to which the textile fabric is folded (R_B), the mass of the fabric (W), the moment of inertia (I_D), and the coefficient of stretching (Y).

$$DC = f(R_B, W, I_D, Y) \quad (16)$$

To select the informative features describing the drape characteristics of textiles waste, as well as the reduction of their number, methods of continuous improvement of the meaning of the features were used: ReliefF, FSNCA and SFCPP [21]. Features

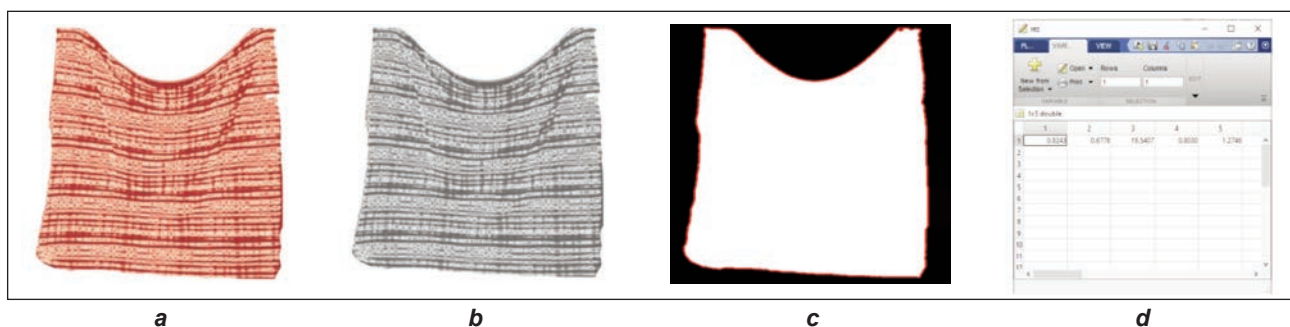


Fig. 3. Algorithm for determining the drape characteristics: a – Stage 1; b – Stage 2; c – Stage 3; d – Stage 4

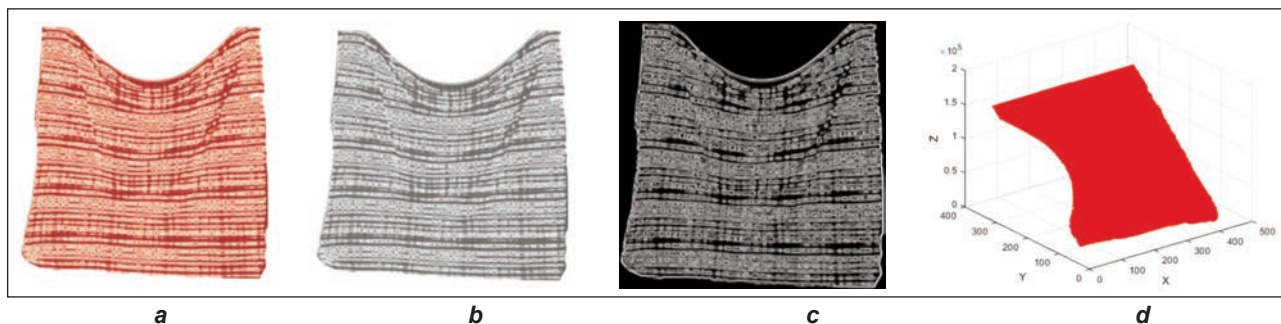


Fig. 4. Algorithm for 3D visualization of drape: *a* – Stage 1; *b* – Stage 2; *c* – Stage 3; *d* – Stage 4

with weights greater than 0,6 were selected as informative. A vector of features was created from them, through which the drape coefficient (*DC*) is predicted after reducing its data volume.

The data in the resulting vector of traits are reduced by the methods of latent variables and principal components [22–24]. A second-order model was used. It describes the relationship between reduced data from drape characteristics and *DC*. In general, the model has the form:

$$z = f(x,y)$$

$$z = b_0 + b_1x + b_2y + b_3x^2 + b_4xy + b_5y^2 \quad (17)$$

where "b" is the coefficients of the model; "x" and "y" are the independent variables; "z" is the dependent variable. Depending on the p-value, the non-informative coefficients are removed from the regression model. The accuracy of these models was assessed

by the criteria: coefficient of determination (R^2); F-criterion; Standard error (SE); p-value. The differences between the actual measured values and those of the model are estimated by the residuals.

The softwares used for obtaining and processing data are Matlab 2017b (The MathWorks Inc., Natick, MA, USA) and Statistica 12 (TIBCO Software Inc., Palo Alto, CA, USA).

All data were analysed with a significance level of 0.05.

RESULTS AND DISCUSSION

As a result of the measurements and calculations, the values of the characteristics of the drape were determined. They are presented in table 2 by standard deviation and their mean.

The results of the selection of informative features that describe the drape are shown in figure 5. It can

Table 2

OBTAINED DATA FOR THREE CLASSES OF TEXTILE FABRICS				
Parameter	Class	C1	C2	C3
	DC		33.64±6.88	28.52±9.1
GSM (g/m ²)		139.29±25.18	182.74±19.21	194.18±14.74
B (mm)		0.36±0.1	0.51±0.1	0.63±0.06
KA		0.82±0.11	0.82±0.17	0.82±0.09
C		1.75±0.42	1.12±0.59	1.53±0.51
K		5.87±0.42	4.55±0.41	3.42±0.3
E		0.9±0.07	0.69±0.07	0.5±0.05
AR		0.51±0.01	0.55±0.01	0.58±0.01
I _{x1} (mm ⁴)		881.4±301.64	1324±661.73	1437.65±711.03
I _{y1} (mm ⁴)		0.1±0.02	0.29±0.14	0.65±0.37
I _{xy1} (mm ⁴)		0	0	0
I _{D1} (mm ⁴)		881.5±301.66	1324.3±661.85	1438.3±711.37
I _{x2} (mm ⁴)		881.4±301.64	1324±661.73	1437.65±711.03
I _{y2} (mm ⁴)		0.1±0.02	0.29±0.14	0.65±0.37
I _{xy2} (mm ⁴)		28.43±7.85	58.49±27.89	91.11±47.27
I _{D2} (mm ⁴)		3526±1206.65	5297.18±2647.4	5753.2±2845.48
I _{AA2} (mm ⁴)		0.21±0.05	0.58±0.28	1.29±0.75

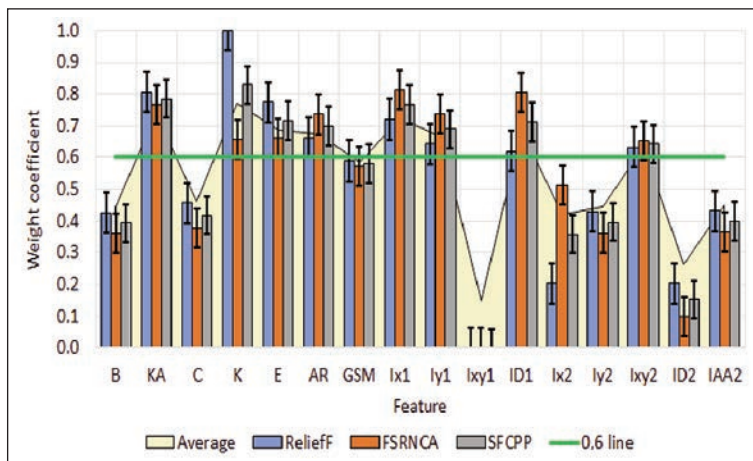


Fig. 5. Results of selection of informative features

be seen that the most informative are the geometric features describing the shape of the drape. Then, there are those obtained from the inertial moments of textile fabrics.

After the selection, the number of traits is reduced by half. The following generalized vector of nine traits (FV) was obtained:

$$FV = [KA \ K \ E \ AR \ GSM \ I_{x1} \ I_{y1} \ I_{D1} \ I_{xy2}] \quad (18)$$

The data from the feature vector is reduced to two principal components and two latent variables. They describe the variance in the experimental data as over 95%.

Regression prediction models for the draping coefficient (DC) by principal components and latent variables have been developed.

The principal component model $DC = f(PC_1, PC_2)$ has a coefficient of determination $R^2 = 0.71$. According to Fisher's criterion $F(3, 86) = 35.44$, which at these degrees of freedom has a critical value of $F_{cr} = 2.71$. The standard error of the model has a value of $SE = 0.072$. The level of significance is $p < 0.01$.

The model for latent variables $DC = f(LV_1, LV_2)$ has a coefficient of determination $R^2 = 0.74$. According to Fisher's criterion $F(3, 86) = 46.43$, which at these degrees of freedom has a critical value of $F_{cr} = 2.71$. The standard error of the model has a value of $SE = 0.07$. The level of significance is $p < 0.01$.

After excluding the insignificant coefficients from the basic model, regression equations were obtained, describing the relationship between DC , the principal components and the latent variables, to which the feature vector FV was reduced. These models have the form:

$$DC = f(PC_1, PC_2)$$

$$DC = 33.61 + 10.01PC_1 - 9.03PC_1^2 + 8.18PC_2^2 \quad (19)$$

$$DC = f(LV_1, LV_2)$$

$$DC = 33.81 + 30.46LV_1 + 8.79LV_2 - 80.78LV_1^2 \quad (20)$$

In general, the obtained models are presented in figure 6. Independent variables are the first two main components and the first two latent variables. In both cases, the dependent variable is the draping coefficient (DC). In both graphs, it can be seen that the prediction will be with the highest accuracy when the DC values are in the upper levels.

Figure 7 shows the distribution of the residuals of the obtained models. The graphs show that in both models the distribution of residuals is close to normal. This analysis shows that the obtained DC prediction models are adequate and describe the experimental data with sufficient accuracy.

Figure 8 displays the outcomes of visualizing the drape's 3D shape. They are obtained by an image processing algorithm. The deviation from the dimensions of the drape is 3–5 mm. The time for obtaining and processing the data, as well as calculating the

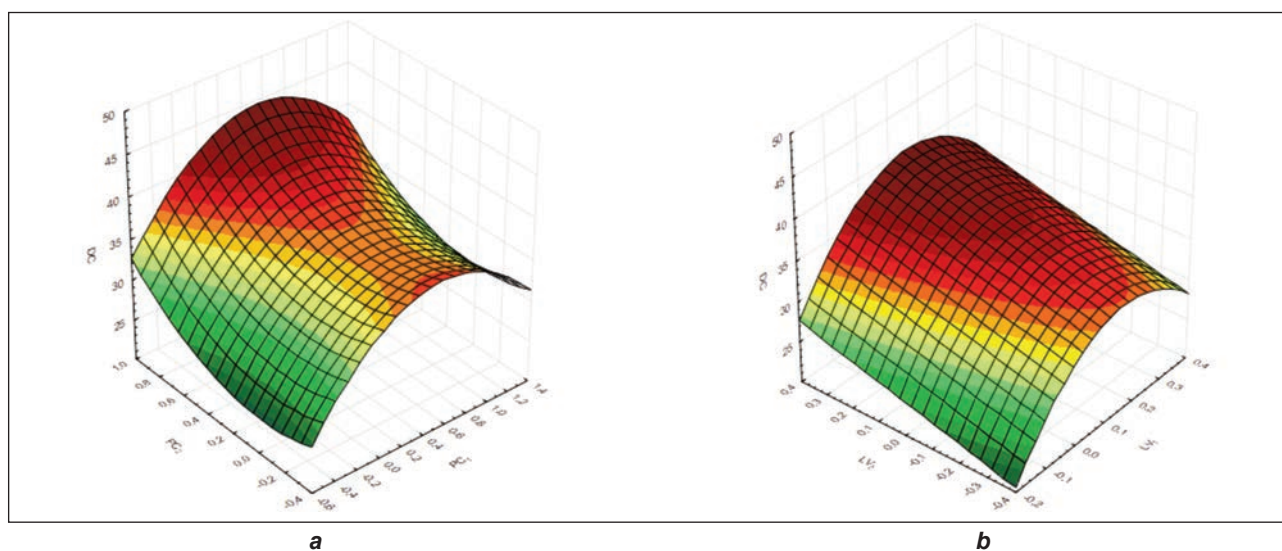


Fig. 6. General view of DC prediction models: a – $DC = f(PC_1, PC_2)$; b – $DC = f(LV_1, LV_2)$

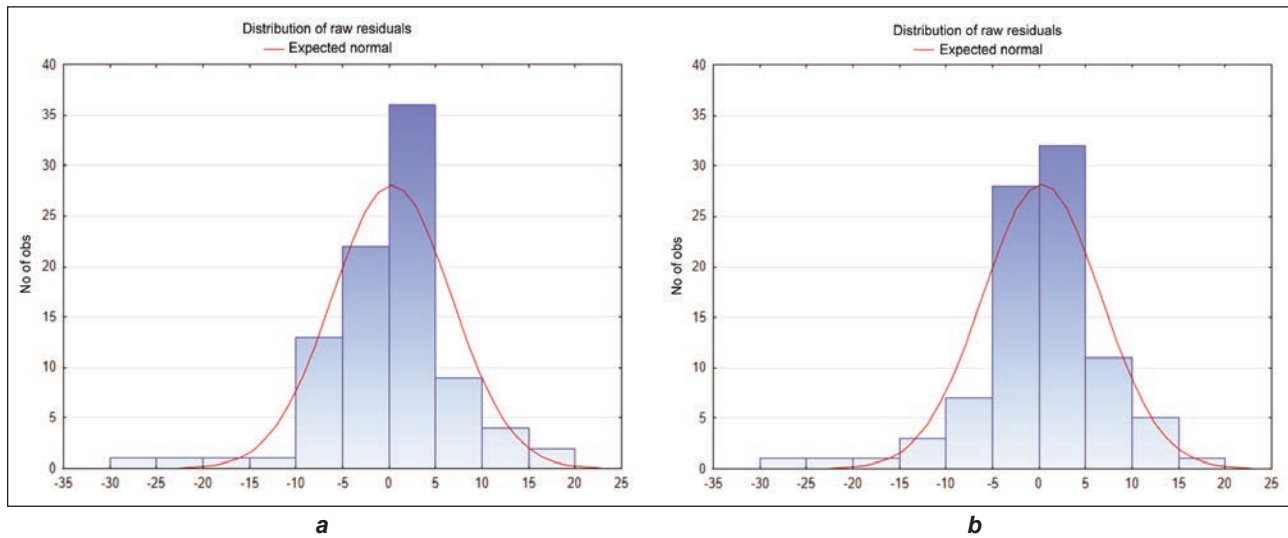


Fig. 7. Distribution of residuals of the obtained models: *a* – $DC=f(PC_1, PC_2)$; *b* – $DC=f(LV_1, LV_2)$

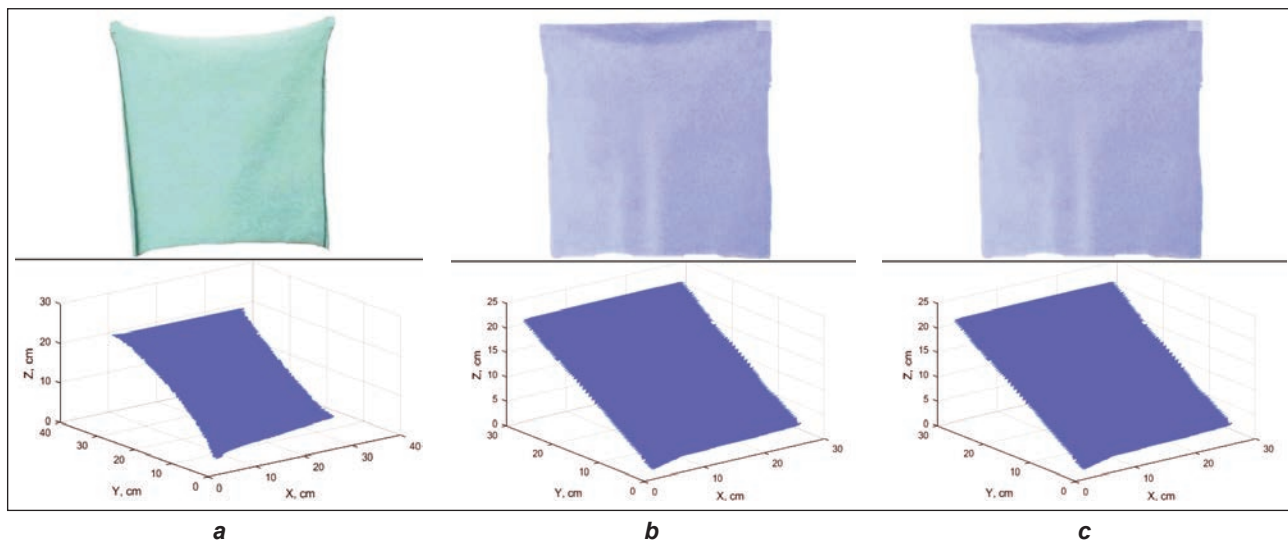


Fig. 8. 3D shapes of drape: *a* – Sample 1; *b* – Sample 2; *c* – Sample 3

parameters for visualization is up to 5 s. When validating the obtained regression models, an accuracy of 68–70% was achieved. This is close to that obtained in their creation.

The results obtained improve those of Bhat et al. [4]. Methods and tools for simulation analysis of rectangular drape are proposed. The proposed procedures do not require complex computational procedures, such as those proposed by Duan et al. [12]. The significant factors that influence the formation of the drape are selected. In addition to the mechanical properties as proposed by Rasheed et al. [13], in the analysis of rectangular drape of fabrics, the present dimensions and coefficients describing the relationship between them are taken into account in the present work.

CONCLUSIONS

An analysis of the characteristics of drape from textiles waste extracted from their colour digital images was made.

Methods and tools for obtaining 3D shapes of hanging drape have been proposed. These approaches have the benefit of not requiring complicated calculation procedures and a long time to measure and obtain a three-dimensional model. It is possible to obtain 3D shapes from 2D images of drape, as the dimensions of the objects in the image are known, as well as the conditions under which they were taken. A predictive model has been created for automated prediction of the drape coefficient of textile fabrics from textiles waste. To create the model, there were used geometric characteristics reduced by principal components and latent variables and features obtained by calculating the moments of inertia of the textile fabric.

The findings in the literature have been improved upon. The developed software tools were used in the study of hanging drape from textile waste. In further research, we can look for other factors that influence

the construction of a 3D contour of drape, on their two-dimensional images. The proposed methods and procedures can be applied in the analysis of drape on video files obtained after exposure to textile fabrics at different airflow rates.

ACKNOWLEDGEMENTS

The research has been funded by the University of Oradea, within the Grants Competition "Scientific Research of Excellence Related to Priority Areas with Capitalization through Technology Transfer: INO – TRANSFER – UO – 2nd Edition", Projects No 232/2022 and 236/2022.

REFERENCES

- [1] Spahiu, T., Shehi, E., Piperi, E., *Personalized avatars for virtual garment design and simulation*, In: UNIVERSI – International Journal of Education, Science, Technology, Innovation, Health and Environment, 2015, 1, 3, 56-63
- [2] Spahiu, T., Fafenrot, S., Grimmelsmann, N., Piperi, E., Shehi, E., Ehrmann, A., *Varying fabric drape by 3D-imprinted patterns for garment design*, In: IOP Conference Series: Materials Science and Engineering, 2017, 254, 172023, 1–6, <https://doi.org/10.1088/1757-899X/254/17/172023>
- [3] Moskvin, A., Wijnhoven, M.A., Moskvina, M., *The equipment of a Germanic warrior from the 2nd–4th century AD: Digital reconstructions as a research tool for the behavior of archaeological costumes*, In: Journal of Cultural Heritage, 2021, 49, 48–58, <https://doi.org/10.1016/j.culher.2021.03.003>
- [4] Bhat, K., Twigg, C., Hodgins, J., Khosla, P., Popović, Z., Seitz, S., *Estimating cloth simulation parameters from video*, In: Proceedings of the 2003 ACM SIGGRAPH/Eurographics symposium on Computer animation (SCA '03), Eurographics Association, Goslar, DEU, 2003, 37–51
- [5] Hunter, L., Fan, J., *Measurement and Prediction of Fabric and Garment Drape*, In: Textile Learner, 2008, 7–25
- [6] Davis, A., Bouman, K., Chen, J., Rubinstein, M., Durand, F., Freeman, W., *Visual vibrometry: Estimating material properties from small motion in the video*, In: Proceedings of IEEE Conference of Computer Vision and Pattern Recognition, 2015, 5335–5343
- [7] Ju, E., Choi, M., *Estimating cloth simulation parameters from a static drape using neural networks*, In: IEEE Access, 2020, 8, 195113–195121
- [8] Bi, W., Jin, P., Nienborg, H., Xiao, B., *Estimating mechanical properties of cloth from videos using dense motion trajectories: Human psychophysics and machine learning*, In: Journal Vision, 2018, 18, 5, 1–20
- [9] Bouman, K., Xiao, B., Battaglia, P., Freeman, W., *Estimating the material properties of fabric from video*, In: Proceedings of IEEE International Conference of Computer Vision, 2013, 1984–1991
- [10] Yang, S., Liang, J., Lin, M., *Learning-based cloth material recovery from video*, In: Proceedings of IEEE International Conference of Computer Vision (ICCV), 2017, 4383–4393
- [11] Maqsood, E., Chen, H-L., Abdulrahman, N., *The impacts of different woven fabrics on three draping techniques*, In: International Design Journal, 2019, 9, 2, 147–155
- [12] Duan, L., Boyd, L., Aragon-Camarasa, G., *Learning physics properties of fabrics and garments with a physics similarity neural network*, In: Pattern Recognition Letters, 2021, arXiv:2112.10727, 1–7
- [13] Rasheed, A., Romero, V., Bertails-Descoubes, F., Wuhrer, S., Franco, J., Lazarus, A., *A visual approach to measure cloth-body and cloth-cloth friction*, In: IEEE Transactions on Pattern Analysis and Machine Intelligence, 2021, 1–13, <https://doi.org/10.1109/TPAMI.2021.3097547>
- [14] Santesteban, I., Thuerey, N., Otaduy, M., Casas, D., *Self-supervised collision handling via generative 3D garment models for virtual try-on*, In: IEEE/CVF Conference on Computer Vision and Pattern Recognition (CVPR), 2021, 11763–11773
- [15] Ilieș, D.C., Lite, M.-C., Indrie, L., Marcu, F., Moș, C., Ropa, M., Sturzu, B., Costea, M., Albu, A.V., Szabo-Alexi, P., Sambou, A., Herman, G.V., Caciora, T., Hodor, N., *Research for the conservation of cultural heritage in the context of the circular economy*, In: Industria Textila, 2021, 72, 1, 50–54, <http://doi.org/10.35530/IT.072.01.1807>, WOS: 000627567800006
- [16] Tripa, S., Indrie, L., *Households textile waste management in the context of a circular economy in Romania*, In: Environmental Engineering and Management Journal, 2021, 20, 1, 81–87, ISSN:1582-9596, eISSN:1843-3707 WOS:000620353800009 IF 0,916
- [17] Albu, A., Caciora, T., Berdenov, Z., Ilies, D.C., Sturzu, B., Sopota, D., Herman, G.V., Ilies, A., Kecse, G., Ghergheles, C.G., *Digitalization of garment in the context of circular economy*, In: Industria Textila, 2021, 72, 1, 102–107, <http://doi.org/10.35530/IT.072.01.1824>
- [18] Tripa, S., Indrie, L., Zlatev, Z., Tripa, F., *Customized clothes – a sustainable solution for textile waste generated by the clothing industry*, In: Industria Textila, 2022, 73, 3, 275–281, <http://doi.org/10.35530/IT.073.03.202112>
- [19] Sanad, R., Cassidy, T., Cheung, T., *Fabric and garment drape measurement – part 1*, In: Journal of Fiber Bioengineering and Informatics, 2012, 5, 4, 341–358
- [20] Spahiu, T., Manavis, A., Kazlacheva, Z., Almeida, H., Kyratsis, P., *Industry 4.0 for fashion products – Case studies using 3D technology*, In: IOP Conference Series: Materials Science and Engineering, 2021, 1031, 1, 012039, 1–9
- [21] Alikhanov, J., Penchev, S., Georgieva, Ts., Moldazhanov, A., Shynybay, Z., Daskalov, P., *An indirect approach for egg weight sorting using image processing*, In: Food Measurement and Characterization, 2017, 12, 1, 87–93

- [22] Mladenov, M., *Complex assessment of the quality of food products through visual images, spectrophotometric and image analysis hyper-spectral characteristics, Monograph*, University publishing Center of Rousse University "A. Kanchev", Rousse, 2015
- [23] Spahiu, T., Zlatev, Z., Ibrahimaj, E., Ilieva, J., Shehi, E., *Drape of Composite Structures Made of Textile and 3D Printed Geometries*, In: *Machines*, 2022, 10, 587, <https://doi.org/10.3390/machines10070587>
- [24] Indrie, L., Affandi, N.D.N., Díaz-García, P., Haji, A., Ilies, D.C., Zlatev, Z., Taghiyari, H.R., Grama, V., Farima, D., *Mechanical and Morphological Properties of Cellulosic Fabrics Treated with Microencapsulated Essential Oils*, In: *Coatings*, 2022, 12, 1958. <https://doi.org/10.3390/coatings12121958>
-

Authors:

LILIANA INDRIE¹, ZLATIN ZLATEV², JULIETA ILIEVA², IOAN PAVEL OANA¹

¹University of Oradea, Faculty of Energy Engineering and Industrial Management, Department of Textiles, Leather and Industrial Management, 1 Universitatii str., Oradea, Romania
e-mail: lindrie@uoradea.ro, oanaioanpavel@yahoo.com

²Trakia University, Faculty of Technics and technologies,
38 Graf Ignatiev str., 8602, Yambol, Bulgaria

Corresponding author:

ZLATIN ZLATEV
e-mail: zlatin.zlatev@trakia-uni.bg

Smart fabric inspection using *Mimosa pudica* plant

DOI: 10.35530/IT.074.02.1719

M. FATHU NISHA
L. MALLIGA
S. MANTHANDI PERIANNASAMY

J. JOHN BENNET
S. AMALORPAVA MARY RAJEE

ABSTRACT – REZUMAT

Smart fabric inspection using *Mimosa pudica* plant

Fabric quality governing and defect detection are playing a crucial role in the textile industry with the development of high customer demand in the fashion market. This work presents fabric defect detection using the sensitive plant segmentation algorithm (SPSA) which, is developed with the sensitive behaviour of the plant biologically named "*Mimosa pudica*". This method consists of two stages. The first stage enhances the contrast of the defective fabric image and the second stage segments the fabric defects with aid of SPSA. The proposed work SPSA is developed for defective pixels identification in both uniform and non-uniform patterns of fabrics. In this work, SPSA has been done by checking with devised condition, correlation and error probability. Every pixel will be checked with the developed algorithm, to get marked either defective or non-defective pixels. The proposed SPSA has been tested on the different types of fabric defect databases and shows a prodigious performance over existing methods like the Differential evolution based optimal Gabor filter model (DEOGF), Gabor filter bank (GFB), Adaptive sparse representation-based detection model (ASR) and Fourier and wavelet shrinkage (FWR).

Keywords: correlation, error probability, sensitive plant, segmentation, uniform pattern

Inspecția inteligentă a materialelor textile folosind planta *Mimosa pudica*

Controlul calității materialelor textile și detectarea defectelor joacă un rol crucial în industria textilă, odată cu dezvoltarea cerințelor ridicate ale clienților pe piața modei. Această lucrare prezintă detectarea defectelor materialului textil folosind algoritmul de segmentare a plantelor sensibile (SPSA), care este dezvoltat pe baza comportamentului sensibil al plantei denumită biologic „*Mimosa pudica*”. Această metodă constă din două etape. Prima etapă îmbunătățește contrastul imaginii materialului textil defect, iar a doua etapă segmentează defectele materialului textil cu ajutorul SPSA. Lucrarea propusă este dezvoltată pentru identificarea pixelilor defecți în modele uniforme și neuniforme ale materialelor textile. În această lucrare, SPSA a fost realizat prin verificarea față de condiția concepută, corelația și probabilitatea de eroare. Fiecare pixel va fi verificat cu algoritmul dezvoltat, pentru a fi marcat fie pixel defect, fie fără defect. SPSA propusă a fost testat pe diferite tipuri de baze de date cu defecte de materiale textile și arată o performanță ridicată față de metodele existente, cum ar fi modelul de filtru optim Gabor bazat pe evoluție diferențială (DEOGF), bancul de filtre Gabor (GFB), modelul de detectare adaptativ bazat pe reprezentare rară (ASR) și contracția Fourier și cea de tip wavelet (FWR).

Cuvinte-cheie: corelație, probabilitate de eroare, plantă sensibilă, segmentare, model uniform

INTRODUCTION

Defect detection is greatly significant for textile quality control. Conventionally, defects are detected by human eyes. The effectiveness of this labour-intensive process is low and the missed rate is high because of eye tiredness. Hence, an automatic examination scheme is compulsory for textile industries [1–9].

Due to the weaving course of cloth products, cloth images naturally encompass periodic texture patterns. The look of fabric defects, though, causes local deformation of the normal texture pattern, which indicates that a class of defects locally produces a dissimilar set of textures [10, 11]. Many diverse weaving patterns are there in creating diverse fabric patterns and finding differences between them is not easy [12, 13].

PROPOSED METHOD

This work proposes a defect detection model which is developed based on the sensitive behaviour of a sensitive plant biologically named *Mimosa pudica*. First, all images are pre-processed through Adaptive Intensity Transformation to enhance image contrast. The second step involves the segmentation process developed with the base of the sensitiveness behaviour of *Mimosa pudica* to segment the various pattern of fabrics. The conditions have been resulting in different patterns of fabric to easily section and segregate the defects with a superior degree of precision and accuracy. On the whole, the proposed process consists of two processes namely, pre-processing and segmentation with a sensitive plant algorithm. Contrast enhancement progresses the perceptibility of objects in the scene by enhancing the clarity difference between the objects and their backgrounds. In this work, a fresh contrast enhancement

approach based on dominant brightness level analysis and adaptive intensity transformation of images has been chosen.

Segmentation using sensitive plant algorithm

The segmentation process has been developed based on the sensitive behaviour of the *Mimosa pudica* plant. The sensitive plant is also known as a humble plant which is the pea family of Fabaceae which is sensitive to touch and other external simulations so instantly closing its leaves and drooping. This plant gives unusually quick responses to the simulation (touch) by sudden water release from leaflets due to the specialized cells. Then the plant comes back to normal after several minutes. It droops in the sense to defend itself against the herbivores. The leaves of the plant also droop in response to darkness and reopen with the daylight known as nyctastic movement shown in figure 1.

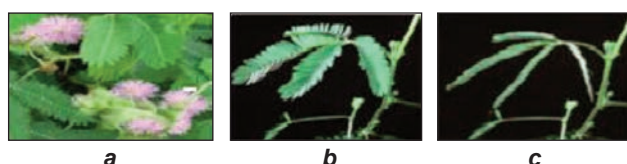


Fig. 1. Images of: a – *Mimosa pudica* plant; b – leaves of the plant in normal environmental conditions; c – leaves drooped in response to the external stimuli

As a result, the leaves of the sensitive plant droop when affected by external stimuli to protect themselves from predators and it does not droop and act normally with normal environmental conditions. With this sensitivity behaviour, the conditions have been derived for various patterns of the fabric to extract the defective pixels. The missing yarn, stain marks, holes and knotted yarns are said to be defects in the fabric textures. Three different patterns of fabrics plain, twill and satin are checked with the conditions derived for each to find the defective pixels.

Uniform pattern – plain texture pattern

The segmentation process to detect the defective pixel in a plain fabric pattern is done by checking the conditions relative to the sensitiveness of the *Mimosa pudica* plant. The image chosen for the detection will have $M \times N$ pixels. Let us take the random pixel $p(x,y)$ which is chosen for checking as the *Mimosa pudica* plant and its intensity the corresponding pixel is denoted as $I\{p(x,y)\}$.

The chosen pixel has to satisfy the two conditions derived to detect the defects in the plain pattern. The first condition checks the pixels at the top, down, right and left of the selected pixel shown in figures 2 and 3. The first condition is the following:

$$I(P_{x,y}) \neq \{I(P_{x+1,y}), (P_{x,y+1}), (P_{x-1,y}), (P_{x+1,y})\} \quad (1)$$

and the second condition checked with the diagonal pixels around the selected pixel.

$$I(P_{x,y}) \neq \{I(P_{x+1,y+1}), (P_{x-1,y+1}), (P_{x-1,y-1}), (P_{x+1,y+1})\} \quad (2)$$

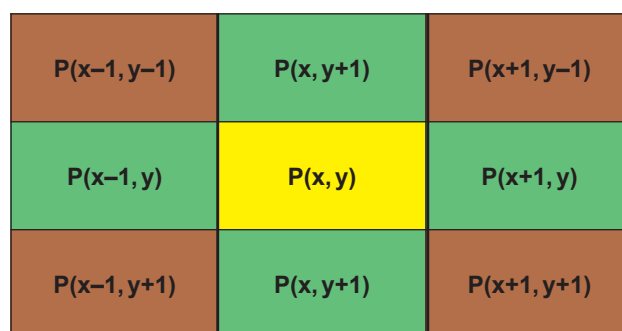


Fig. 2. Green pixels – four neighbourhood pixels of the pixel $p(x,y)$ and brown pixels – diagonal neighbour pixel of the pixel $p(x,y)$

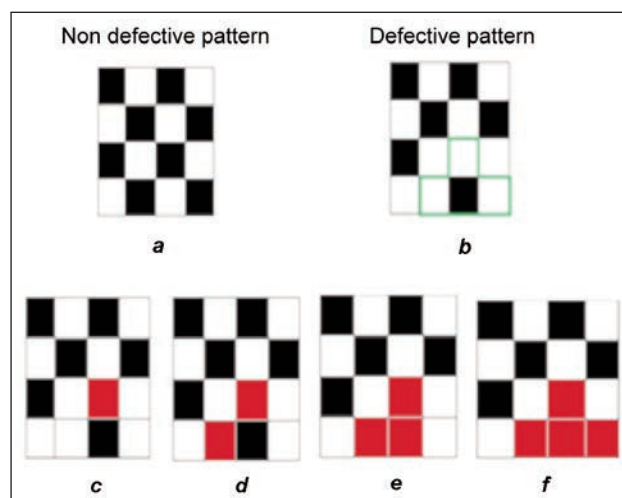


Fig. 3. Step-by-step process of defective pixels identification in a plain pattern

The chosen random pixel (plant) is said to be non-defective, if it satisfies both above conditions. If not, the pixel will be marked (plant droops in response to the stimuli) as the defective one. In this manner, all the pixels in the image will be checked one by one to mark the whole area of the defect. The condition devised will be checked for every pixel starting from the pixel $P_{1,1}$ in the 1st row 1st column. In the above-given pattern while checking the pixel $P_{2,2}$ at the 2nd row 2nd column, it could violate the second condition even though it is not the defective one.

$$\rho(P_{x,y}) = \frac{1}{8} (\text{no of 4 neighbourhood pixel violating condition} + \text{no of diagonal pixel violating condition}) \quad (3)$$

In that case, Error probability checking will be done.

$$\text{Probability} = \rho(P_{x,y}, P_{x+a,y+b}) \quad (4)$$

With the calculated value of probabilities, the pixel with a higher probability will be chosen as a defective one and will be marked for defect identification. By checking condition and error probability, the pixel will either be marked as defective or leave ideal as non-defective.

Twill texture pattern

The twill pattern of the fabric is among the most widely used weaves within textile production shown in

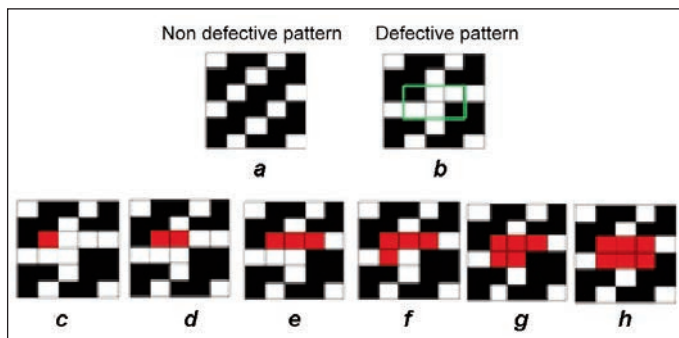


Fig. 4. Step-by-step process of defective pixels identification in a twill pattern

figure 4. It can be easily identified by its pattern of diagonal lines. we check the selected pixel with only its 4 neighbourhood pixels but not with diagonal pixels.

The first condition comprises checking conditions for 8 neighbourhood pixels:

$$\begin{aligned}
 I(P_{x,y}) &= \{I(P_{x+1,y}), I(P_{x,y+1})\} \text{ AND} \\
 I(P_{x,y}) &\neq \{I(P_{x-1,y}), I(P_{x,y-1})\} \\
 \{I(P_{x,y}) = I(P_{x-1,y+1}), I(P_{x+1,y-1}), I(P_{x-1,y-1})\} \text{ AND} \\
 I(P_{x,y}) &\neq I(P_{x+1,y+1}) \quad (5)
 \end{aligned}$$

The second condition is the following:

$$\begin{aligned}
 I(P_{x,y}) &\neq \{I(P_{x+1,y}), I(P_{x,y+1})\} \text{ AND} \\
 I(P_{x,y}) &= \{I(P_{x-1,y}), I(P_{x,y-1})\} \\
 \{I(P_{x,y}) = I(P_{x-1,y+1}), I(P_{x+1,y-1}), I(P_{x-1,y-1})\} \text{ AND} \\
 I(P_{x,y}) &\neq I(P_{x+1,y+1}) \quad (6)
 \end{aligned}$$

The third condition is the following:

$$\begin{aligned}
 I(P_{x,y}) &\neq \{I(P_{x+1,y}), I(P_{x,y+1}), I(P_{x-1,y}), I(P_{x,y-1})\} \\
 \{I(P_{x,y}) = I(P_{x-1,y+1}), I(P_{x+1,y-1})\} \text{ AND} \\
 I(P_{x,y}) &\neq \{I(P_{x-1,y-1}), I(P_{x+1,y+1})\} \quad (7)
 \end{aligned}$$

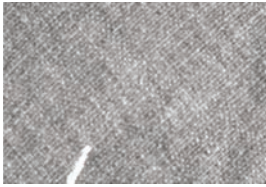
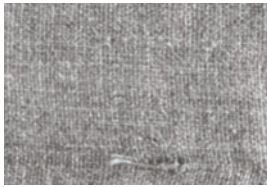
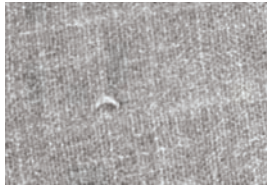
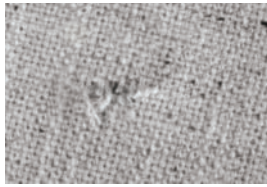

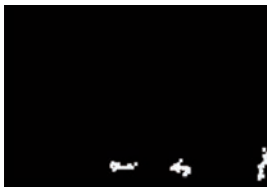

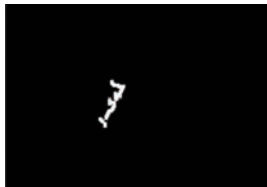
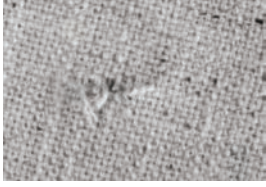
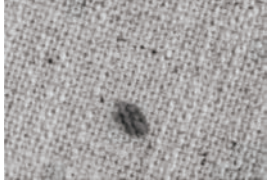
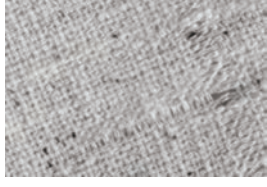
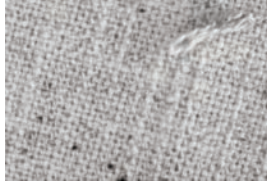




The selected pixel is checked with three conditions developed.

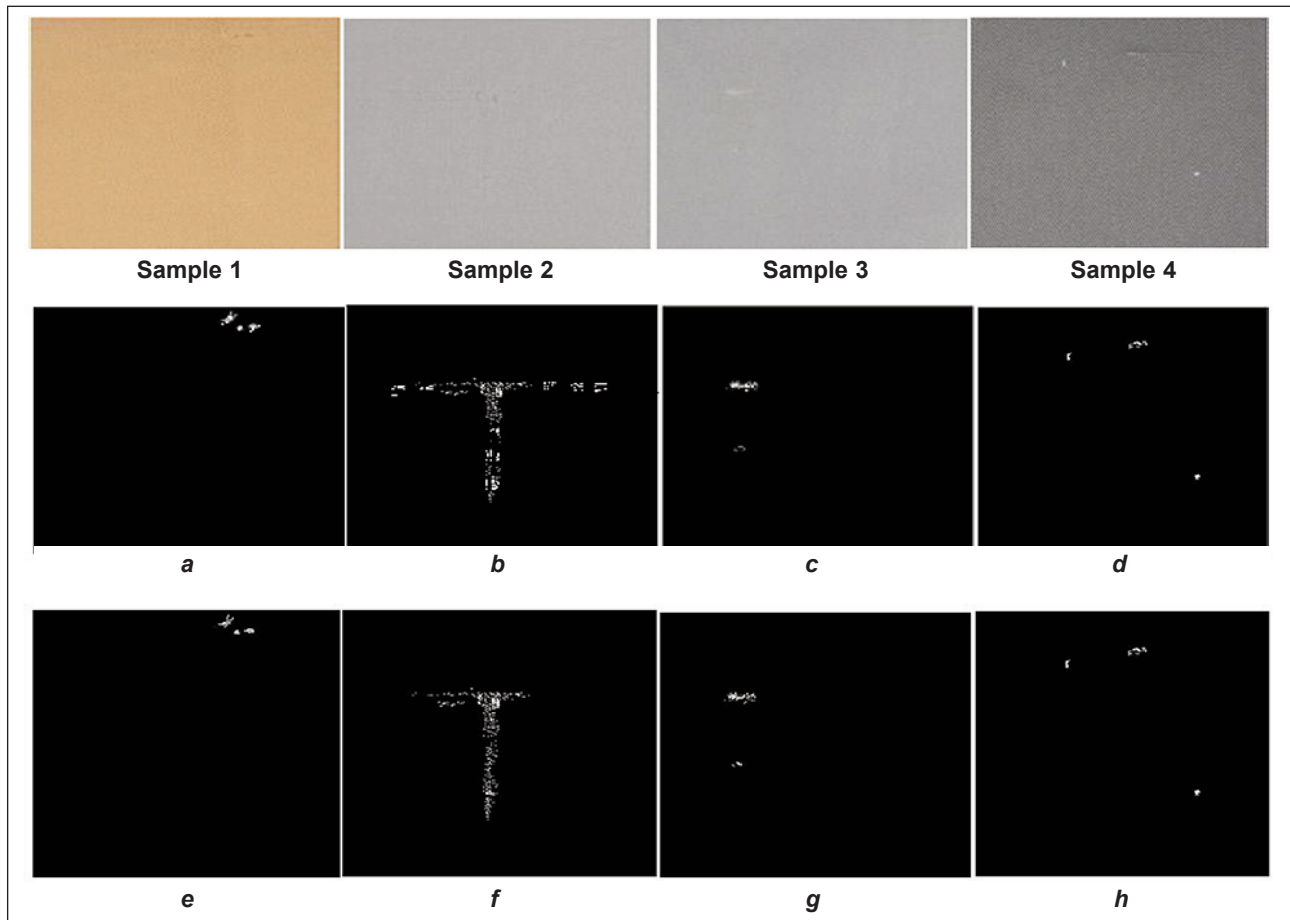
RESULTS AND DISCUSSION

This section consists of a performance evaluation of the proposed fabric defect detection with the two databases. The first database is the TILDA database, which is the outcome of the workshop on texture analysis of Deutsche Forschungsgemeinschaft Germany. The second database comprises both defective and defective free samples acquired from an apparel factory in Mainland China and scanned from the fabric defect handbook (table 1, figure 5).

Table 1

SEGMENTED RESULTS OF THE TILDA DATABASE				
Type/Defects	Holes	Stain	Missing yarn	Spot
I				
II				

Type/Defects	Holes	Stain	Missing Yarn	Spot
III				
				
IV				
				



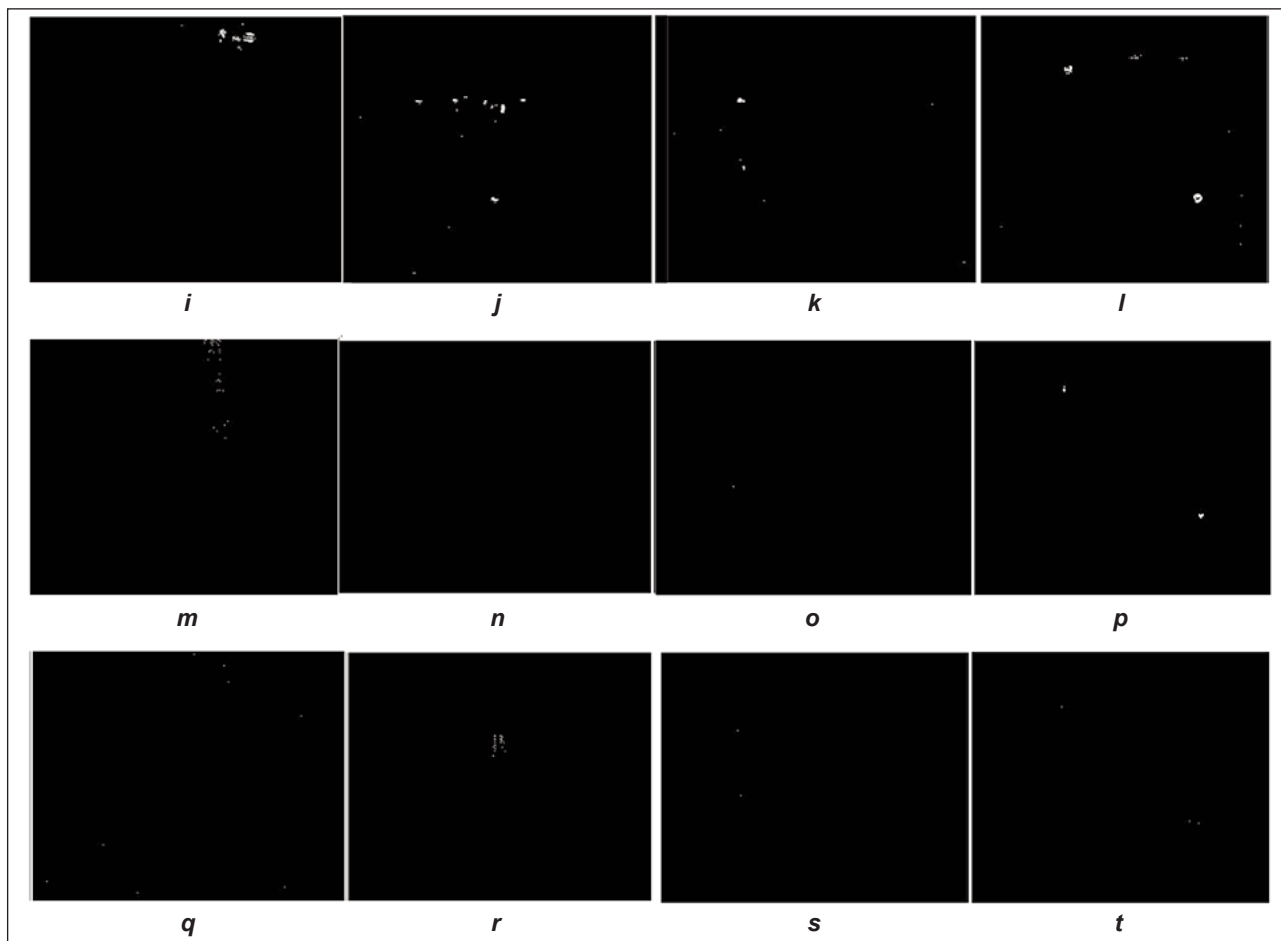


Fig. 5. Detection results of twill fabric compared with existing methods sample image: *a-d* – proposed method; *e-h* – NSR; *i-l* – DEOGF; *m-p* – GBF; *q-t* – ASR

Performance metric

Further, the proposed model is compared with traditional methods to show its efficiency. Compared with

the five defect detection models, its performance depends on the metrics Precision, Sensitivity, specificity and accuracy (table 2, figure 6).

Table 2

PERFORMANCE COMPARISON TABLE OF PROPOSED AND CONVENTIONAL WORK						
Metrics	Proposed method	NSR	DEOGF	GFB	ASR	FWS
Precision	93.6	92.5	94.7	79.3	93.3	82.7
Sensitivity	97.2	96.1	88.2	81.2	82.3	88.2
specificity	92.2	92.2	95.1	95.1	94.1	79.1
Accuracy	95.8	94.1	91.7	91.7	88.2	83.5

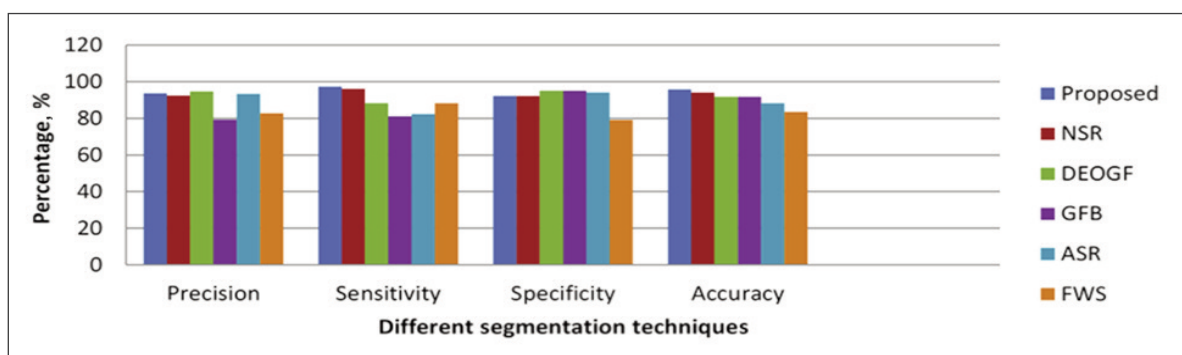


Fig. 6. Performance comparison of different segmentation techniques

CONCLUSION

This work presented a fabric defect detection algorithm developed based on the sensitive behaviour of the sensitive plant algorithm. Detection has been done in two processes: (i) contrast enhancement and (ii) segmentation. The algorithm has developed in a sense to detect defects in both plain and twill texture patterns. The sample images with various types of

defects have been used for defect detection and those results are all compared with past developed research. The result complied that the proposed work can detect the most type of defects even if it is tiny and with uneven illumination. It also achieved a high percentage of precision, sensitivity and accuracy of 96% over the other work with a higher detection rate of true positive pixels and lower false alarm pixels.

REFERENCES

- [1] Li, Y., Zhao, W., Pan, J., *Deformable patterned fabric defect detection with fisher criterion-based deep learning*, In: IEEE Transactions on Automation Science and Engineering, 2017, 14, 2, 1256–1264
- [2] Yang, X., Pang, G., Yung, N., *Robust fabric defect detection and classification using multiple adaptive wavelets*, In: IEEE Proceedings-Vision, Image and Signal Processing, 2005, 152, 6, 715–723
- [3] Mitu, S., Ghalayini, M., Matenciuc, C.C., Porav, M., Manole, M., *Relationship between the mass of a jacket-including clothing structure and body energetic consumptions*, In: Industria Textila, 2010, 61, 1, 17–22
- [4] Hanbay, K., Talu, M.F., Özgüven, Ö.F., *Fabric defect detection systems and methods – A systematic literature review*, 2016, 127, 24, 11960–11973
- [5] Yapi, D., Allili, M.S., Baaziz, N., *Automatic fabric defect detection using learning-based local textural distributions in the contourlet domain*, In: IEEE Transactions on Automation Science and Engineering, 2018, 15, 3, 1014–1026
- [6] Kumar, A., *Computer-vision-based fabric defect detection: A survey*, In: IEEE Transactions on Industrial Electronics, 2008, 55, 1, 348–363
- [7] Celik, H.I., Topalbekroglu, M., Dulger, L.C., *Real time denim fabric inspection using image analysis*, In: Fibers and Textiles in Eastern Europe, 2015, 85–90
- [8] Graniteville, S.C., *Manual of Standard Fabric Defects in the Textile Industry*, Graniteville Company, 1975
- [9] Zhang, K., Yan, Y., Li, P., Jing, J., Liu, X., Wang, Z., *Fabric Defect Detection Using Saliency Metric for Color Dissimilarity and Positional Aggregation*, In: IEEE Access, 2018, 6, 49170–49181
- [10] Tong, L., Wong, W.K., Kwong, C.K., *Fabric defect detection for apparel industry: a nonlocal sparse representation approach*, In: IEEE Access, 2017, 5, 5947–5964
- [11] Nicula, G., Belu, N., Necula, E., *Researches on accomplishing filtering textile materials destined for preventing air and water pollution*, In: Industria Textila, 2008, 59, 3, 113–117
- [12] D.F. Germany, *Tilda textile texture-database*, 1996, Available at: <http://lmb.informatik.uni-freiburg.de/resources/datasets/tilda.en.html>. Version 1.0. [Accessed on March 2019]
- [13] Fathu Nisha, M., Vasuki, P., Mohamed Mansoor Roomi, S., *Survey on Various Defect Detection and Classification Methods in Fabric Images*, In: Journal of Environmental Nano Technology (JENT), 2017, 6, 2, 20–29
- [14] Fathu Nisha, M., Vasuki, P., Mohamed Mansoor Roomi, S., *Effective Contrast Enhancement of Fabric Images Using Adaptive Intensity Transformation*, SSRN Publications, 2019
- [15] Fathu Nisha, M., Vasuki, P., Mohamed Mansoor Roomi, S., *Fabric Defect Detection Using the Sensitive Plant Segmentation Algorithm*, In: Fibres & Textiles in Eastern Europe 2020, 28, 3, 141, 84–88, <https://doi.org/10.5604/01.3001.0013.9025>
- [16] Subtirica, A.-I., Banciu, C.A., Chivu, A.A.-M., Dinca, L.-C., *Nanofibres made from biocompatible and biodegradable polymers, with potential application as medical textiles*, In: Industria Textila, 2018, 69, 1, 55–58, <http://doi.org/10.35530/IT.069.01.1502>
- [17] Girneata, A., Popescu, D.I., Giurgiu, A., Cuc, S., Dobrin, O.C., Voicu, L., Popa, I., *Performance management practices in Romanian textile and clothing companies*, In: Industria Textila, 2015, 66, 2, 108–114
- [18] Gazi, H., Üstütağ, T.S., *Elastic hybrid yarns for denim fabrics*, In: Industria Textila, 2015, 66, 5, 306–312
- [19] Watanabe, T., Ito, S., Yokoi, K., *Co-occurrence histograms of oriented gradients for pedestrian detection*, 3rd IEEE Pacific-Rim Symp. Image Video Technol., 2009, 37–47
- [20] Fathu Nisha, M., Vasuki, P., Mohamed Mansoor Roomi, S., *Various Defect Detection Approaches in Fabric Images-Review*, In: International Journal of Scientific Research in Science and Technology, 2017, 3, 5, 95–100
- [21] Fathu Nisha, M., Vasuki, P., Mohamed Mansoor Roomi, S., *Fabric Defect Detection Using Sparse Representation Algorithm*, In: Journal of Engineering, 2018, 1–7

Authors:

M. FATHU NISHA¹, L. MALLIGA², S. MANTHANDI PERIANNASAMY², J. JOHN BENNET²,
AMALORPAVA MARY RAJEE²

¹Sethu Institute of Technology, Pulloor, 6261116, Virudhunagar District, India

²Mallareddy Engineering College for Women, Secundrabad, 500100, India

Corresponding author:

DR. M. FATHU NISHA, ASSOCIATE PROFESSOR
e-mail: nishahameed2016@gmail.com

Investigation of radiation shielding, antibacterial and some properties of nanosilver applied and coated woven fabrics

DOI: 10.35530/IT.074.02.202216

FEYZA AKARSLAN KODALOĞLU

NACIYE SÜNDÜZ OĞUZ

ABSTRACT – REZUMAT

Investigation of radiation shielding, antibacterial and some properties of nanosilver applied and coated woven fabrics

Antibacterial textiles are widely used in terms of providing hygiene and comfort by protecting human health. Due to its importance in the health sector and increasing customer demands, the trend towards these textiles is increasing day by day. In this study, the antibacterial properties of cotton and cotton/polyester woven fabrics which had applied impregnation and coating processes were examined and compared. For this purpose, nano silver-containing chemicals were applied to the fabrics by impregnation method to give antibacterial properties. After this, the fabrics were coated with tungsten and barium sulphate which have different properties, and coating fabric with antibacterial and radiation shielding properties is obtained. To examine some properties of these antibacterial fabrics, tensile strength, washing fastness, friction fastness tests and SEM analysis were applied to the fabrics. The coating and impregnated fabrics were compared with the fabrics that had been coated only.

Keywords: antibacterial property, nano silver, coating, radiation shielding, woven fabric

Investigarea proprietăților de protecție împotriva radiațiilor, antibacteriene și altor proprietăți ale țesăturilor impregnate și peliculizate cu nanoargint

Textilele antibacteriene sunt utilizate pe scară largă pentru asigurarea igienei și confortului prin protejarea sănătății umane. Datorită importanței lor în sectorul sănătății și a cerințelor în continuă creștere ale clienților, tendința către utilizarea acestor materiale textile crește pe zi ce trece. În acest studiu, au fost analizate și comparate proprietățile antibacteriene ale țesăturilor din bumbac și bumbac/poliester pentru care a fost aplicat un proces de impregnare și peliculizate. În acest scop, substanțe chimice care conțin nanoargint au fost aplicate pe țesături prin metoda de impregnare, pentru a conferi proprietăți antibacteriene. După aceasta, țesăturile au fost peliculizate cu tungsten și sulfat de bariu care au proprietăți diferite și se obțin astfel, țesături peliculizate cu proprietăți antibacteriene și cu rezistență împotriva radiațiilor. Pentru a analiza alte proprietăți ale acestor țesături antibacteriene, au fost realizate teste de rezistență la tracțiune, rezistență la spălare, de rezistență la frecare și analiza SEM. Pelicula și țesăturile impregnate au fost comparate cu țesăturile care au fost doar peliculizate.

Cuvinte-cheie: proprietate antibacteriană, nanoargint, peliculizare, protecție împotriva radiațiilor, țesătură

INTRODUCTION

Antibacterial products are used to eliminate or minimize the effect of microorganisms that harm the textile product and the user [1]. Antibacterial textiles are used as medical garments, surgical applications, sportswear, socks, military uniforms, underwear, tents, curtains, bath covers, outdoor garments, filter making, the construction of various technical fibres, the automotive industry, food industry in many areas [2]. In antibacterial finishing processes, the methods of extraction, impregnation, vacuum application, maximum liquor application, transfer, spraying, foam application and coating are used. Impregnation, coating and spraying methods are the most commonly used methods [3]. Alcohols, metals, phenols and derivatives, halogens, oxidation agents, biquanidines, isothiazolones, ammonium compounds, zeolites, chitin and chitosan are the most important antibacterial agents [4].

To improve the functionality and performance characteristics of woven, knitted and non-woven fabrics, one or two surfaces are applied chemical substances to obtain coating fabric [5, 6]. Properties that are not present on the textile surface are imparted to the textile surface by the coating process [6]. In recent years, with the increasing trend towards technical textiles, the trend towards coating fabrics has also increased [7].

In this study, nano-silver, which is one of the most important antibacterial materials in giving antibacterial properties, had been applied to woven fabrics by impregnation method which is one of the most widely used methods and then was coated with tungsten and barium sulfate, blade coating. Thus, it was aimed to give antibacterial and radiation shielding properties to woven fabrics that had been impregnated and coated. In addition, coated fabrics which weren't applied nanosilver and coated fabrics which were applied nanosilver were compared with each other.

MATERIALS AND METHODS

Material

Cotton fabrics; easily absorbs fluids such as blood and urine from the body due to their liquid-absorbing properties. It has the property of taking liquid and passing gas and water vapour. It has a heat-resistant, insulating, non-allergic soft tissue and is frequently preferred in daily life. Cotton/polyester fabrics are widely used in daily use due to their high strength, and advantages in ironing and are frequently preferred in surgical garments [8, 9]. Because of these properties of cotton and cotton/polyester, cotton (97% cotton, 3% elastane) and cotton/polyester (59% cotton, 39% polyester, 2% elastane) woven fabrics were used in this study. The properties of these fabrics are shown in table 1.

Table 1

FEATURES OF COTTON FABRIC				
Cotton fabric	Density (wire/cm)	Yarn number (Ne)	Fiber type	Weight (g/m ²)
Weft	55	20	Cotton/Lycra	247
Warp 1	33	12	Cotton	
Warp 2	33	12		
FEATURES OF COTTON/POLYESTER FABRIC				
Weft 1	34	28	PES/Lycra	236
Weft 2	34	18		
Warp	60	20	Cotton	

In this study, a 20–25 nm size nanosilver which was provided by NANOKAR® Nano Technological Materials was used to give antibacterial properties to woven fabrics. Nanosilver particles pass through the cell membrane of bacteria and microbes, disrupt DNA and prevent the reproduction of bacteria and microbes [10]. Silver is effective against more than 650 microorganisms that cause diseases [11]. Silver, bacteria and germs with resistance to the product provide a deodorizing property, as well as the use of a certain amount of silver does not harm the human body [12]. It is used in socks, underwear, sheets, armchair upholstery, the military and the medical field in the textile field [13]. Although metal ions such as copper, zinc, gold and titanium have antimicrobial effects, silver shows the best antimicrobial properties. At present, silver-containing products are used in the treatment of burns, wounds, and bacterial infections. In addition, silver-containing wound dressings are used for antibiotic-resistant bacteria [14].

In this study, *Staphylococcus aureus* (ATCC 6538), a common bacterium in hospitals that is the cause of many infections and *Escherichia coli* (ATCC 35218) in the hands and toes, soles, scalp, armpits, palms and stools in contact with textile surfaces were used to test antibacterial properties of the fabrics [15, 16].

It was aimed to compare the effect of nanosilver applied to woven fabrics by impregnation method on the antibacterial properties of the fabrics by coating them with barium sulfate and tungsten having two different properties. In addition, in future studies, it is thought that functional textile products can be obtained by using the properties of barium sulfate and tungsten. Tubicoat CRO was used as a coating chemical and was provided by CHT Kimya A.Ş. The barium sulphate was provided by Emir Kimya and the tungsten was provided by Baymet Foreign Trade Limited Company. Barium sulfate is a cheap mineral, it has a resistant structure. It is used in sports equipment, coating of carpets and similar products, the pharmaceutical sector due to its toxin cleansing properties, the paint sector due to its whitening and thinning properties, drilling works, nuclear power plants, hospitals, X-ray works, in many processes such as paper production [17, 18]. Tungsten is a metal that has more hardness than many sheets of steel, can be easily processed, has good abrasion resistance and thermal conductivity, has a high melting and boiling point, and is resistant to acids and alkalis for a long time. It is used in the arms and defence industry, space technology, ships, airplanes, automotive, bulb wires, X-ray devices, anti-radiation screens, television tubes, and jewellery as an alternative to platinum and gold [19].

Methods

In this study, after the nanosilver impregnation method was applied to cotton and cotton/polyester woven fabrics, the fabrics were coated with tungsten and barium sulfate. The fabrics which were applied impregnation and coating process and the fabrics that applied only the coating process were tested for antibacterial properties with AATCC 100 method.

1% nano silver and pure water were applied to cotton and cotton/polyester fabrics at Ataç brand FY 350 fulars under two bar atmospheric pressure [20, 21]. The impregnated fabrics were dried at 80°C for 15 minutes and fixed for 3 minutes at 100°C in Mathis fixing machine.

The homogeneous mixture was obtained by using 60% Tubicoat CRO as the coating chemical and 40% barium sulphate and tungsten were coated with the help of a stripper on the fabrics which were applied nanosilver. In figure 1, barium sulfate (a) and tungsten (b) coated fabrics are shown. After coating, the barium sulfate-coated fabric was dried for 15 minutes at 80°C, the tungsten-coated fabric was dried for 10 minutes at 80°C and the fixation process was carried out for 3 minutes at 100°C.

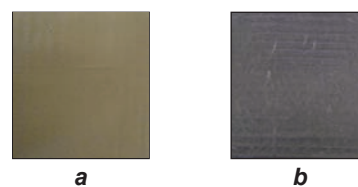


Fig. 1. Fabrics coated with:
a – barium sulfate; b – tungsten

AATCC 100 antibacterial test method was used to quantitatively investigate the antibacterial properties of woven fabrics that were impregnated and coated. To determine the effect of impregnation and coating methods applied to woven fabrics on the tensile strength of fabrics, the tensile strength test of Llyod brand LR5K model strength tester according to TS EN ISO 13934-1 standard, SEM analysis on Quanta FEG 250 SEM device to determine the change in fabric structure, to determine the effect of washing process on fabrics, washing fastness test in ISO 105-C06 standard and to determine the effect of friction on fabrics, friction fastness test according to TS EN ISO 105-X12 standard was applied.

In this study, the neutron absorption properties of coated woven fabric samples were experimentally measured. Neutron measurement was made by a removable He-3 proportional detector. The fabrics used in the study and the applications made are shown in table 2.

Table 2

Fabrics	Application
1	Untreated Cotton
2	Cotton-Nano Silver
3	Cotton-Barium Sulfate
4	Cotton-Nano Silver-Barium Sulfate
5	Cotton-Tungsten
6	Cotton-Nano Silver-Tungsten
7	Untreated Cotton/Polyester
8	Cotton/Polyester -Nano Silver
9	Cotton/Polyester-Barium Sulfate
10	Cotton/Polyester-Nano Silver-Barium Sulfate
11	Cotton/Polyester-Tungsten
12	Cotton/Polyester-Nano Silver-Tungsten

FINDINGS

Antibacterial test

According to AATCC 100 antibacterial test method cotton and cotton/polyester woven fabrics' antibacterial activity, values are given in table 3 against *S.aureus* and antibacterial activity values are given in table 4 against *E.coli*.

In AATCC 100 Antibacterial test method, (-) values indicate a decrease in the number of bacteria, and (-) 100 indicates that all bacteria are dead.

When the antibacterial properties of the samples against *S.aureus* bacteria were examined, it was seen that all bacteria killed in cotton and cotton/polyester samples coated with barium sulphate and nanosilver and other coating samples had antibacterial properties. The antibacterial properties of barium sulfate-coated samples were found to be slightly better than tungsten-coated samples.

When the antibacterial properties of the samples against *E.coli* bacteria were examined, it was determined that all bacteria were killed in the nanosilver-coated samples. Bacterial growth was observed on

Table 3

ANTIBACTERIAL ACTIVITY OF SAMPLES AGAINST <i>S.aureus</i>	
Fabrics	Bacteria reduction (%)
1	-56.08
2	-100
3	-99.96
4	-100
5	-99.43
6	-99.35
9	-99.78
10	-100
11	-99.46
12	-99.57

Table 4

ANTIBACTERIAL ACTIVITY OF SAMPLES AGAINST <i>E.coli</i>	
Fabrics	Bacteria reduction (%)
1	7.22
2	-99.98
3	118.18
4	-100
5	130.30
6	-99.58
9	143.64
10	-100
11	180
12	-99.70

cotton and cotton/polyester fabrics coated with tungsten and barium sulfate.

Tungsten-coated nano silver applied samples were found to have antibacterial properties. Antibacterial properties of barium sulfate-coated samples were detected to be slightly better than tungsten-coated samples.

Tensile strength

Tensile strength and elongation at break values of the samples are given in table 5.

When table 5 is examined, it has been determined that barium sulfate-coated fabrics have better breaking strength values than tungsten-coated fabrics, cotton fabrics coated with barium sulphate have lower breaking elongation values than tungsten-coated fabrics, and in other samples barium sulfate-coated fabrics have higher breaking elongation than tungsten-coated fabrics.

Washing fastness

The washing fastness values of the samples are given in table 6.

When table 6 is examined, it has been determined that coating and impregnation processes do not have

Table 5

TENSILE STRENGTH AND ELONGATION VALUES OF SAMPLES				
Fabrics	Tensile strength (N)		Elongation at break (%)	
	Warp	Weft	Warp	Weft
1	1077	285	29	75
2	1078	337	28	77
3	1246	315	30	84
4	1200	317	27	82
5	1225	56	35	94
6	1104	57	20	77
9	1936	705	31	84
10	1603	409	27	92
11	1200	150	22	30
12	961	209	20	39

Table 6

WASHING FASTNESS VALUES OF SAMPLES						
Fabrics	Fading					
	Acetate	Cotton	Polyamide	Polyester	Acrylic	Wool
3	5	5	5	5	5	5
4	5	5	5	5	5	5
5	5	5	5	5	5	5
6	5	5	5	5	5	5
9	5	5	5	5	5	5
10	5	5	5	5	5	5
11	5	5	5	5	5	5
12	5	5	5	5	5	5

a negative effect on the fastness of washing of fabrics.

Friction fastness

Friction fastness values of the samples are given in table 7.

Table 7

FRICTION FASTNESS VALUES OF SAMPLES		
Fabrics	Friction fastness	
	Dry	Wet
3	5	4-5
4	5	5
5	5	5
6	5	4-5
9	5	4-5
10	5	5
11	5	4
12	5	4-5

When table 7 is examined, it has seen that coating and impregnation processes have no negative effect on the friction fastness of the fabrics. The dry friction

fastness values of the samples are 5 and the wet friction fastnesses are 4, 4-5, 5.

SEM Analysis

Samples were magnified in the range of 500–10.000 and the most suitable samples were selected. SEM analysis images of the samples were indicated in figures 2 and 3.

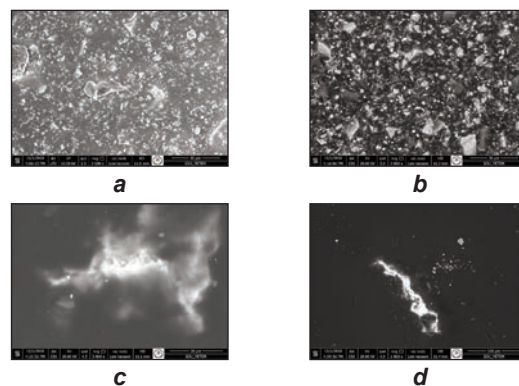


Fig. 2. Cotton fabrics coated with: a – barium sulfate; b – barium sulfate-nano silver; c – tungsten; d – tungsten-nano silver

As shown in figure 2, barium sulphate applied cotton fabric (figure 2, a) and barium sulfate-nano silver applied cotton fabric (figure 2, b) 3000 times, tungsten applied cotton fabric (figure 2, c) 5000 times, tungsten-nano silver applied cotton fabric (figure 2, d) 1000 SEM image was taken enlarged.

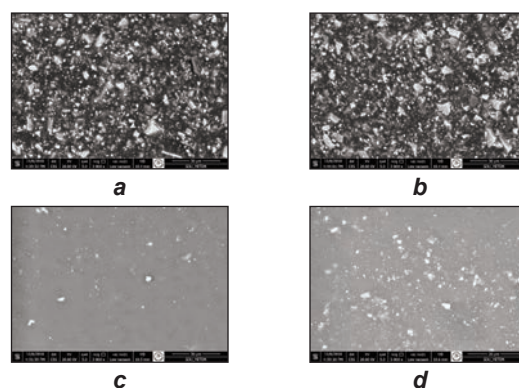


Fig. 3. Cotton/polyester fabrics coated with: a – barium sulfate; b – barium sulfate-nano silver; c – tungsten; d – tungsten-nano silver

As shown in figure 3, barium sulphate applied cotton/polyester fabric (figure 3, a) and barium sulfate-nano silver applied cotton/polyester fabric (figure 3, b) and tungsten applied cotton/polyester fabrics (figure 3, c) 3000 times, tungsten-nano silver applied cotton/polyester fabric (figure 3, d) 5000 SEM image was taken enlarged.

When figures 2 and 3 were examined, the surface distribution of barium sulfate and tungsten was observed to be different. It was seen that barium sulfate covered the whole surface in cotton and cotton/polyester fabrics and tungsten covered a narrower

area in coated fabrics. The distribution of tungsten on the surface of cotton/polyester fabric was found to be higher than cotton fabric. Because the application rate of nanosilver to the fabric was 1%, it wasn't clearly seen on the fabric surfaces.

Radiation shielding

The neutron measurement of the device is provided by the Helium-3 proportional detector. Measurements were made with a neutron detector at 2.3 MeV neutron energy emitted from a ^{252}Cf neutron source. By using the dose values obtained as a result of the measurements, the linear absorption coefficient of a sample of x thickness was calculated with the following formula [22].

$$N(x) = N_0 e^{-\mu x} \quad (1)$$

Here, μ is the linear absorption coefficient, x – the thickness of the sample, $N(x)$ – the dose measured when there is a sample of x thickness between the detector and the source, and N_0 – the dose value measured when there is no sample between the detector and the source. The neutron absorption coefficients of the fabrics were measured. The results obtained are given in figure 4.

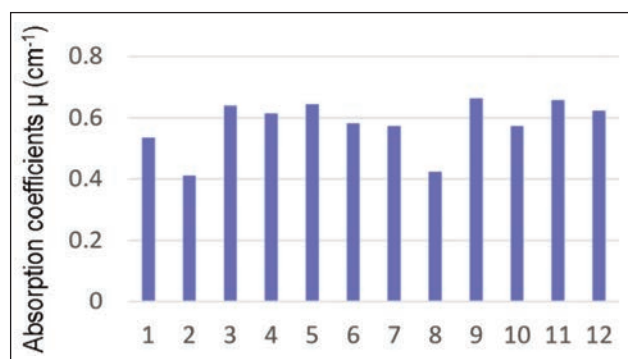


Fig. 4. Neutron absorption coefficients of fabrics

When the neutron absorption coefficient values of the treated fabrics given in figure 4 are examined, the values vary between 0.6616 and 0.4114. The highest value belongs to the barite-coated cotton/polyester fabric, while the lowest value belongs to the Nanosilver-applied cotton/polyester fabric. Tungsten and barite coating increased the neutron absorption coefficient values. Neutron absorption coefficient values of tungsten-applied fabrics are higher than barite-applied fabrics. It has been observed that nano silver application reduces the neutron absorption coefficient values of the fabrics. Neutron absorption coefficient values of cotton/polyester fabric are generally higher than cotton fabric.

CONCLUSION

When the results of antibacterial properties of gram-positive and gram-negative bacteria according to the AATCC 100 antibacterial test method after applying

to the woven fabrics by nano silver impregnation method coated with tungsten and barium sulfate and woven fabrics only coated with tungsten and barium sulfate were examined, all coating woven fabrics with nano silver have antibacterial properties. While antibacterial properties were observed against *S. aureus* bacteria in nano silver not applied coated fabrics, antibacterial properties were not observed in nano silver not applied coated fabrics using *E. coli* bacteria. When the non-nano silver coated coating fabrics were considered, *E. coli* bacteria are more resistant than *S. aureus* bacteria was observed. When the antibacterial properties of barium sulfate and tungsten-coated fabrics were compared, it was seen that barium sulfate-coated fabrics had slightly more antibacterial properties than tungsten-coated fabrics. In this study, gamma ray shielding properties of coated woven fabrics were investigated. The advantage to being provided to the fabric in this study is to obtain an antibacterial fabric that can absorb neutron rays. The neutron absorption properties of coated woven fabric samples were experimentally measured. The neutron measurement of the device is provided by the Helium-3 proportional detector. Measurements were made with a neutron detector at 2.3 MeV neutron energy emitted from a ^{252}Cf neutron source. Barium sulfate-coated cotton/polyester fabric has the highest neutron absorption coefficient, while nano silver applied cotton/polyester fabric has the lowest neutron absorption coefficient. Tungsten and barite coating have affected the neutron absorption coefficient values in the direction of increase. Neutron absorption coefficient values of tungsten-coated fabrics are higher than barium sulfate-coated fabrics. Nanosilver application negatively affected the neutron absorption coefficient values of the fabrics. When the tensile strength of the samples is examined, it is observed that barium sulfate-coated fabrics are more durable than tungsten-coated fabrics. It was determined that barium sulfate used fabrics for nanosilver-applied antibacterial fabrics would be more suitable in terms of durability. When washing fastness and friction fastness tests were examined, it was seen that there was no negative situation in the washing and friction fastness of the fabrics with the coating process and these fabrics were resistant to washing and friction. When SEM images of the samples were examined, it was observed that barium sulfate spread is more than tungsten on the sample. In terms of antibacterial properties of nanosilver applied to the fabric were not very clear on the surface. In addition to these properties of cotton and cotton/polyester fabrics with good washing, friction fastness and antibacterial properties; functional textile products with different properties can be produced by making use of the properties of tungsten and barium sulfate.

REFERENCES

- [1] Müsiad Teknik Tekstiller, *Teknik Tekstiller: Genel ve Güncel Bilgiler*. Müsiad Araştırma Raporları: 58 İstanbul: Mavi Ofset Basım Yayın Tic. San. Ltd. Şti, 2009
- [2] Ünal, H., *Tek Kullanımlık Hidrofil ve Antibakteriyel Polipropilen Nonwoven Çarşaf Eldesi*, Yüksek Lisans Tezi, İstanbul Teknik Üniversitesi, Fen Bilimleri Enstitüsü, Tekstil Mühendisliği Anabilim Dalı, 123 s, İstanbul, 2009
- [3] Seventekin, N., Öktem, T., Tekeoğlu, S., *Tekstilde Antimikrobiyel Madde Kullanımı*, In: Tekstil ve Konfeksiyon, 2001, 4, 217–224
- [4] Devrent, N., Yılmaz, N.D., *Tekstil Endüstrisinde Kullanılan Antimikrobiyal Lifler*, In: Nonwoven Technical Textiles Technology Dergisi, 2004, 4, 48–55
- [5] Fung, W., *Coated and Laminated Textiles*, The Textile Institute, Woodhead Publishing Limited, England, 2002
- [6] Öner, E., *Tekstilde Kaplama, Tekstil Terbiye Teknolojisi Ders Notları*, Marmara Üniversitesi, Teknik Eğitim Fakültesi, İstanbul, 2006
- [7] İTKİB, *Türkiye’de ve Dünya’da Teknik Tekstiller Üzerine Genel ve Güncel Bilgiler*, AR&GE ve Mevzuat Şubesi, İstanbul, 2008
- [8] Pamuk, O., Öndoğan, Z., *Cerrahi Personelin Ameliyat Önlükleri ile İlgili Görüşlerinin Belirlenmesi Üzerine Bir Araştırma*, In: Tekstil ve Konfeksiyon, 2008, 142–148.
- [9] Yükseloğlu, S.M., Canoğlu, S., *Sağlık ve Hijyen Alanında Kullanılan Nonwoven Kumaşlar*, In: Kimya Teknolojileri, 2003, 29, 64–71
- [10] Aydın, C., İnanç, E., *Nano Teknoloji ve Nano Gümüş*, Selçuk Üniversitesi, Yüksek Lisans Semineri, Konya, 2012
- [11] Süpüren, G., Çay, A., Kanat, E., Tarakçioğlu, I., *Antimikrobiyal Lifler*, In: Tekstil ve Konfeksiyon, 2006, 80–89
- [12] Altuner, E.E., *Nano Kremelerin Üretimi*, Selçuk Üniversitesi, Fen Bilimleri Enstitüsü, Kimya Ana Bilim Dalı, Yüksek Lisans Tezi, 65 s, Konya, 2013
- [13] Babaarslan, O., Erbil, Y., *Fonksiyonel Tekstil Ürünleri Geliştirmek Üzere Ştapel Gümüş Takviyeli Karışım İpliklerinin Tasarım Ve Üretimi*, ÜİB Tekstil ve Konfeksiyon Sektöründe Ar-Ge Proje Pazarı, Bursa, 2010, 125–126
- [14] Rai, M., Yadav, A., Gade, A., *Silver Nanoparticles as a New Generation of Antimicrobials*, In: Biotechnology Advances, 2009, 27, 76–83
- [15] Hacıbektasoğlu, A., Eyigün, C.P., ve Özsoy, M.F., *Gıda Elleyicilerinde Burun ve Boğaz Portörlüğü*, In: Mikrobiyoloji Bülteni, 1993, 27, 62–70
- [16] Orhan, M., *Pamuk, Poliamid ve Poliester Esaslı Tekstil Materyallerinde Antimikrobiyal Bitim Uygulamaları Üzerine Bir Araştırma*, Uludağ Üniversitesi, Fen Bilimleri Enstitüsü, Tekstil Mühendisliği Anabilim Dalı, Doktora Tezi, 175 s, Bursa, 2007
- [17] Eskier, U., *Barit: Mineral Ailesinden Çok Amaçlı Taş*, 2017, Available at: <https://www.makaleler.com/barit-tasi-ozellikleri-ve-kullanim-alanlari> [Accessed on August 1st, 2018]
- [18] Molla, T., *Radyasyon Zirhlanmasında Kullanılacak Baritli Kumaş Üretimi Ve Özellikleri*, Süleyman Demirel Üniversitesi, Yapı Eğitimi Anabilim Dalı, Yüksek Lisans Tezi, 61 s, Isparta, 2011
- [19] Eskier, U., *Tungsten (Volfram) Nedir? (Özellikleri, Kullanımı)*, 2017, Available at: <https://www.makaleler.com/tungsten-volfram-nedir-ozellikleri-kullanimi> [Accessed on August 1st, 2018]
- [20] Bilget, Ö., *Nano Boyutta Gümüş/Çinko Katkılı Pigment Baskı Uygulanmış Kumaşların Antibakteriyel Özelliklerinin Araştırılması*, Erciyes Üniversitesi, Fen Bilimleri Enstitüsü, Tekstil Mühendisliği Anabilim Dalı, Yüksek Lisans Tezi, 97 s., Kayseri, 2013
- [21] El-Rafie, M.H., Mohamed, A.A., Shaheen, T.I., Hebeish, A., *Antimicrobial Effect of Silver Nanoparticles Produced by Fungal Process on Cotton Fabrics, Carbohydrate Polymers*, 2010, 80, 779–782
- [22] Albarhoum, M., Soufan, A.H., Mustafa, H., *Experimental determination of the shielding characteristics of the dwelling houses’ building materials against neutrons in the Central Region of Syria*, In: Annals of Nuclear Energy, 2012, 47, 134–139

Authors:

FEYZA AKARSLAN KODALOĞLU¹, NACİYE SÜNDÜZ OĞUZ²

¹Süleyman Demirel University, Department of Textile Engineering, 32260, Isparta, Turkey

²Kastamonu University, Araç Rafet Vergili Voc. School, Dept. of Textile, Clothing, Shoes and Leather, 37800, Kastamonu, Turkey
e-mail: noguz@kastamonu.edu.tr

Corresponding author:

FEYZA AKARSLAN KODALOĞLU
e-mail: feyzaakarslan@sdu.edu.tr

Evaluation of the mechanical properties of chopped carbon fibre reinforced polypropylene, polyethylene, polyamide 6, and polyamide 12 composites

DOI: 10.35530/IT.074.02.202214

ARI ALI
BAYRAM ALI

KARAHAN MEHMET
KARAGÖZ SEÇGİN

ABSTRACT – REZUMAT

Evaluation of the mechanical properties of chopped carbon fibre reinforced polypropylene, polyethylene, polyamide 6, and polyamide 12 composites

In this study, a comparative assessment of the mechanical properties of chopped carbon fibre (CF) reinforced polypropylene (PP), polyethylene (PE), polyamide 6 (PA6), and polyamide 12 (PA12) composites was performed. A variation in the composites was obtained by changing the fibre volume fraction of the composite elements under the same manufacturing method and conditions. After blending reinforcement and matrix materials using the extrusion method, the composite materials were manufactured in the shape of plates with thermoforming. The composites' tensile and 3-point bending tests were carried out, and the surface morphology of the fractured surfaces was examined by Scanning Electron Microscope (SEM). As the fibre content in all matrices increased, the efficiency of the fibre in the composites decreased. Finally, ANOVA analysis and mathematical model development by the least square optimization method were performed to analyse and fit experimental data. As a result of the ANOVA analysis, it was seen that the matrix type was more effective on the composite than the fibre type. The error of the modelling performed is less than 20% for the tensile and three-point bending tests.

Keywords: polymer-matrix composites, carbon fibre, mechanical properties, ANOVA analysis, experimental data

Evaluarea proprietăților mecanice ale compozitelor din polipropilenă, polietilenă, poliamidă 6 și poliamidă 12 armate cu fibre de carbon tăiate

În acest studiu, a fost efectuată o evaluare comparativă a proprietăților mecanice ale compozitelor din polipropilenă (PP), polietilenă (PE), poliamidă 6 (PA6) și poliamidă 12 (PA12) armate cu fibre de carbon (CF). S-au obținut diferite materiale compozite prin modificarea fracției de volum de fibre, utilizând însă aceeași metodă și aceleași condiții de fabricație. După amestecarea materialelor de armare și matrice prin metoda extrudării, materialele compozite au fost fabricate sub formă de plăci cu termoformare. Au fost efectuate testele de tracțiune și îndoire în trei puncte ale compozitelor, iar morfologia suprafețelor fracturate a fost analizată cu microscopul electronic cu scanare (SEM). Pe măsură ce conținutul de fibre din toate matricele a crescut, eficiența fibrei din compozite a scăzut. În cele din urmă, analiza ANOVA și dezvoltarea modelului matematic prin metoda de optimizare a celor mai mici pătrate au fost efectuate pentru a analiza datele experimentale. Ca rezultat al analizei ANOVA, s-a observat că tipul de matrice a fost mai eficient pe compozit decât tipul de fibră. Eroarea modelării efectuate este mai mică de 20% pentru încercările de tracțiune și îndoire în trei puncte.

Cuvinte-cheie: compozite polimer-matrice, fibră de carbon, proprietăți mecanice, analiză ANOVA, date experimentale

INTRODUCTION

Polymer matrix composites are increasingly used in the plastics industry due to their high strength and low density [1]. Especially, chopped fibre-reinforced thermoplastic composites have become very appealing because of their ease of production, economy, and better mechanical properties and are widely used in many fields such as aircraft, aerospace, defence, and automotive industries [2]. In general, higher fibre volume fractions in composites are required to achieve a high-performance composite, and increasing the fibre volume fraction substantially increases the strength properties. Thus, the impact of fibre content on the mechanical properties of composites is significant [3]. Similarly, the mechanical properties of composites such as strength, modulus,

and toughness usually up with increasing chopped fibre length; so, the mechanical properties of the composites are identified by the fibre volume fraction, as well as the size of the chopped fibre [4]. The properties of CF-reinforced polymers do not depend solely on the properties of the matrix and fibre; It also depends on the carbon fibre content, distribution, and fibre/matrix adhesion [1]. In the literature, it is reported that the mechanical performance of the composite increases with low and medium fibre content. However, high fibre content (more than 30 vol.%) indicates that the homogeneous distribution is impaired and weak fibre-matrix adhesion occurs. In this case, it is extremely important to achieve good fibre distribution to improve composite performance [5]. Moreover, the chemical structures of the fibre and

the matrix determine the degree of interfacial adhesion. In this context, the fibre surface needs to be modified by chemical or plasma treatment [6]. Extrusion and injection moulding are the common methods to prepare CF reinforced polymer composites [7]. However, a significant amount of fibre breakage occurs during production, caused by the fibre-polymer, fibre-to-fibre, and fibre-processing equipment surface wall interactions. Fibre breakage resulting from these interactions causes a reduction in fibre length, which results in reduced fibre efficiency [8]. Therefore, the effects of fibre length and volume ratio, key factors that determine the final mechanical properties of composites, on CF reinforced polymer composites' mechanical properties are considered a combined impact [9]. Moreover, the mechanical behaviour of the fibre-reinforced composites mainly depends on the fibre's strength, chemical stability, matrix strength, and the interfacial bond between the fibre and the matrix to ensure stress transfer [10].

Relating CF reinforced polymer composites; there are various studies published in the literature [11, 12]. Zhou et al. investigated fibre breakage and dispersion for CF reinforced PA6/clay nanocomposites and drew attention to the effects of processing conditions on fibre breakage and dispersion [12]. Karsli and Aytacı prepared the chopped CF reinforced PA6 composites by injection method and investigated the effect of mixing ratios and fibre lengths on the mechanical properties of the composite [13]. Chen and Qiang produced PP and polyamide composites reinforced with CF by injection moulding. The study concluded that as the CF content of the composite increased, the tensile and impact strength increased [14]. Tiesong Lin et al. (2008) investigated the effects of 2 mm, 7 mm, and 12 mm CF reinforced geopolymer matrix composites on the mechanical properties and fracture behaviour. It was observed that the bending strength reached the highest value at 7 mm fibre length [15]. Based on the studies available in the literature, injection moulding is reported to be faster, easier to manufacture, and highly efficient [16, 17]. Sivas et al. produced fibre reinforced thermoplastic composite by injection and extrusion production method. Composites produced by extrusion showed a 17% superior performance [18].

In addition to experimental research, there are studies in the literature that expand experimental research by including correlation through numerical modelling. These models were used to predict the mechanical properties of fibre-reinforced composites, such as tensile strength, elastic modulus, and Poisson's ratio [19]. Cox published his work using the shear lag model for the interfacial strength between fibre and matrix [20]. Halpin and Kardos proposed a model to evaluate the properties of composites in terms of matrix and fibre properties. This model is based on the Halpin-Tsai equations, which are empirical type equations and are very often used to predict the tensile properties of composites [21]. Liang proposed a model to correlate the tensile strength of short fibre reinforced polymer composites. The model

formulation was based on the force balance between matrix, fibre and composite [22].

The main objective of this work is to perform a comparative study for assessing the mechanical properties of chopped CF reinforced PP, PE, PA6, and PA12 composites. To do that, the focus is to gain a deep understanding of the tensile and 3-point bending properties of the CF-PP, CF-PE and CF-PA6, and CF-PA12 composites couples. In this context, 12 different composite materials were manufactured by adding 10 vol.%, 20 vol.%, and 30 vol.% chopped CF reinforcement materials to each PP, PE, PA6, and PA12 matrix elements under the same manufacturing method and conditions. To provide detailed and collective information to the literature, the rest of the paper is structured as follows: the material selection and production method explain why CF is chosen for this study. Next, the experimental design and ANOVA Analysis structure are introduced. Subsequently, in the results and discussion section, the comparative assessment of the mechanical properties of the fibre-polymer couples is performed by results tables, plots, SEM images, and ANOVA analysis. Finally, a least-square optimization study is carried out to obtain mathematical expression by fitting experimental data.

EXPERIMENTAL DETAILS

Materials and methods

For the experimental design, based on the literature survey, CF was preferred because of having a higher surface energy of 42.1 mJm^{-2} [23] compared to the other alternatives such as glass fibre (surface energy is 32.5 mJm^{-2}) [24] and aramid fibre (surface energy is 34.9 mJm^{-2}) [25]. In general, the main factors for good interfacial adhesion can be defined as the wettability between fibre-matrix and chemical bonding and mechanical interlocking on rough fibre surfaces [26]. Good wetting between the fibre and the matrix is required to achieve good interfacial adhesion and comprehensive and suitable interfacial contact. Wettability mainly depends on the surface energy of the two materials. The high surface energy of the fibre contributes to good adhesion and ensures good fibre-matrix interface compatibility [27, 28].

As a result, the high surface energy of the fibre has a positive effect on the performance of the composite. Since CF has the highest surface energy among the aforementioned fibres, its performance is expected to be higher than other fibres. On the other hand, the surface energy of the matrix should be low.

Molecules in a liquid with low surface energy are not strongly attracted to each other; instead, they tend to spread and adhere to the surface, so a liquid with high free energy will not bond to the fibre surface [29, 30].

In experimental studies, a 6 mm length of chopped fibre was used in the composites. Fibre volume fractions were determined as 10 vol.%, 20 vol.%, and 30 vol.%, and PP, PE, PA6, and PA12 were used as matrix materials. Mechanical properties of matrix and fibre materials were taken from catalogue values.

Preparation of test samples and all related tests were carried out in Bursa Technology Coordination and R&D Centre (Bursa, Turkey). A twin-screw extruder (Polmak Plastik 22 mm Lab type research extruder) was used to produce composites. The temperature values for the five zones in the extruder were determined using the literature and the product catalogue of the materials (195°C – 215°C – 225°C – 225°C – 240°C for PP, 170°C – 195°C – 220°C – 220°C – 230°C for PE, 240°C – 240°C – 250°C – 260°C – 285°C for PA6, 190°C – 200°C – 210°C – 220°C – 230°C for PA12) [31–34]. After the composites were obtained, they were granulated with a cutter.

500 mm × 500 mm composite plates were obtained by the granular press moulding method. Moulding consists of 3 stages, and all samples taken were kept in the first stage for 120 seconds, in the second stage for 180 seconds, and for 60 seconds in the third stage. The test samples were prepared by cutting the relevant moulds in standard sizes on the CNC machine.

Experimental design and ANOVA analysis

The experimental factors and levels shown in table 1 were selected. Sing these factors and levels; the experimental design was performed as illustrated in table 2 used to observe, achieve and interpret the impacts on the response variable by making the desired changes on the input variables [35].

EXPERIMENT FACTORS AND LEVELS				
Factors	1. Level	2. Level	3. Level	4. Level
A – Matrix Type	PP	PE	PA6	PA12
B – Fibre volume fraction %	0*	10	20	30

Note: *0 represents the no fibre condition or matrix itself.

The analysis of variance shows to what extent the examined factors affect the output value chosen to measure quality and what kind of various levels cause. On top of that, the statistical reliability of the achieved results is also tested. For this purpose, firstly, the SS_T value (sum of total squares), which shows the total variability of the signal/noise (S/N) ratio, is calculated according to equation 1 [36].

$$SS_T = \sum_{i=1}^n (\eta_i - \eta_m)^2 \quad (1)$$

$$SS_j = \sum_{i=1}^n [n_{ji} \times (\eta_{ji} - \eta_m)^2] \quad j = A \text{ or } B \quad (2)$$

$$F = \frac{SS_T/k - 1}{SS_E/N - k} \quad (3)$$

In equation 1, η_i is the signal-to-noise ratio calculated over the measured value, η_m – is the average of the signal-to-noise ratios calculated over the measured value, and n – the total number of experiments [36, 37]. The SS_T value is the sum of the squares of the two factors of SS_A (sum of squares of factor A) and SS_B (sum of squares of factor B), and the SS_E value is the sum of the squares of the margin of error. The sum of the squares of each factor was calculated separately by using equation 2.

In equation 2, k_j represents the number of levels of the A or B factor, n_{ji} – the number of experiments at the i level of the A or B factor, η_{ji} – the S/N ratio of the A or B factor at the i level, and η_m – the average S/N ratio [36,37]. For the next step, the F-Test is performed by calculating equation 3 to present how much each experimental factor affects the test results. For the next step, the F-Test is performed by calculating equation 3 to present how much each experimental factor affects the test results.

In equation 3, $k-1$ is the degree of freedom for the numerator by subtracting one from the number of groups, $N-k$ is the degree of freedom for the denominator, which is determined by subtracting the number of groups from the number of observations in all groups [38].

RESULTS AND DISCUSSION

Tensile properties and fractography

Tensile tests were carried out with Besmak-BMT 100E brand Universal Tensile Tester (100 kN). Tensile test samples were prepared according to TS EN ISO 527-2 type 2 standards. The tensile speed was set as 2 mm/min, and the pre-stress value was set as 10N. The measuring length was 50 mm for the video extensometer was. The tests were performed at 21°C. Fractured surface images of 30 vol.% fibre reinforced samples were examined with Hitachi TM3000 brand SEM at Bursa Technology Coordination and R&D Center (Bursa, Turkey).

It was observed that the tensile strength of all composite materials increased as the proportion of reinforcement material went up; so, the highest tensile strength values were achieved at the ratio of 30 vol.% reinforcement material. In terms of fibre efficiency factor, when the matrix materials are compared, 10 vol.% reinforcement PA12 shows the best performance, while the worst is seen in 30 vol.% reinforcement PE.

EXPERIMENTAL DESIGN																
Experiment no.	1	2	3	4	5	6	7	8	9	10	11	12	13	14	15	16
A – Matrix type	1	2	3	4	1	1	1	2	2	2	3	3	3	4	4	4
B – Fibre volume fraction	1	1	1	1	2	3	4	2	3	4	2	3	4	2	3	4

S.Y. Fu and B. Lauke investigated fibre efficiency in chopped glass fibre and chopped CF reinforced PP composites. The tensile test of the composite materials with 8%, 16%, and 25% reinforcement materials was carried out. They concluded that the fibre efficiency in the glass and CF-reinforced composite decreased as the fibre volume fraction increased [8]. Choudhari and Kakhandki, on the other hand, investigated the mechanical properties of the chopped CF reinforced PA66 composite. It was observed that the tensile stress values decreased as the fibre volume fraction (10%, 20%, and 30% reinforcement materials used) increased on the matrix material. The SEM images of the 30% reinforced composite were examined, and it was observed that the fibres were not covered with the polymeric matrix, and most of the fibres were pulled out [39]. Karsli and Aytac, on the other hand, investigated the mechanical properties of CF-reinforced PA6 composite material. It was determined that the amount of deformation in the matrix increased with the increase in the number of fibre rods in the matrix material, thus causing the fibres to pull out more easily [13]. Y. Zhang et al. interpreted the decrease in tensile strength and bending of the fibres as the fibre volume fraction increased as the fibre not being able to form a good interface with the matrix due to its smooth surface, thus causing the fibres to be stripped from the matrix [40]. The efficiency of fibres on matrix materials can be calculated using the Kelly–Tyson model [8, 31].

$$\sigma_c = \lambda_f \sigma_f V_f + \sigma_m (1 - V_f) \quad (4)$$

In equation 4, σ_c (composite), σ_f (fibre), and σ_m (matrix) are the tensile strengths. V_f is the fibre volume ratio of the composite and λ_f – the fibre efficiency factor. When the tensile test results were inspected, it was clear that the mechanical properties of the matrix materials were greatly improved with the addition of fibres (figure 1). Nonetheless, fibre efficiency factors (figure 2) decreased with increasing fibre volume fractions [41]. SY Fu et al. explain this decrease in fibre efficiency: Average fibre length decreases as fibre volume ratios increase. This indicates that a higher fibre content causes significant damage to fibre length. The increased damage in fibre to length at higher fibre volume ratios is primarily attributed to the higher fibre-fibre interaction. It is also noted that the average length of CF is less than the average length of glass and aramid fibre. This is because carbon fibres are more fragile. Therefore, it is explained as being more easily broken during processing [8]. As the fibre volume fraction increased, the deformation ratio increased between the matrix and the fibre, and the weakening of the interface adhesion gave

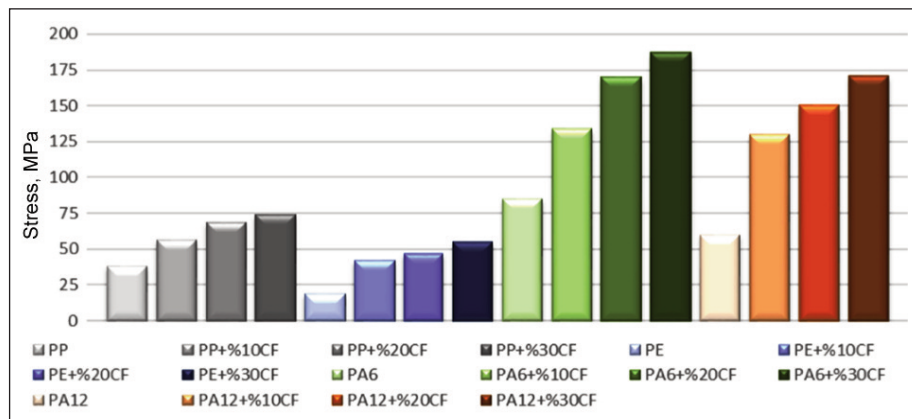


Fig. 1. Tensile test results of composites

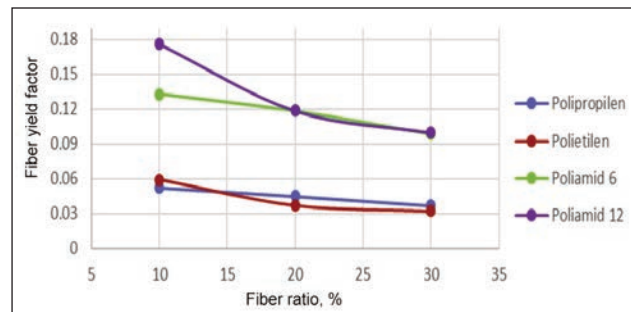


Fig. 2. CF efficiency factor in composites

this result [25, 42]. In addition, another reason for the low fibre efficiency can be explained as follows; when figure 3 is examined, it is seen that the CF is not homogeneously dispersed in the matrixes. Wang et al. (2008) examined the effect of fibre dispersion on the mechanical properties of CFRC samples. They concluded that the inhomogeneity of the fibre dispersion negatively affects the strength of the composite [43]. Therefore, in our study, it can be supposed that while the fibre volume fraction increases in CF reinforced matrixes, one reason for the decrease in fibre efficiency is the deterioration of homogeneous distribution as this fibre percentage increases. Among the 30% CF reinforced composites, the lowest fibre efficiency was observed with those made with PE and PP. The main reason is that PE and PP have lower tensile strength than other matrices. Therefore, it is necessary to evaluate each fibre-matrix efficiency in itself. Normally, CF increases the tensile strength of PE by about 3 times. When the 30% fibre-reinforced composites were examined, the CF efficiency decreased as the fibre volume fraction increased in the four matrices. However, when we look at the highest-fibre efficiency, it is seen that the composite made with 10% CF added PA12. This means that as the CF ratio increases, the amount of deformation in the matrix increases, and the fibres do not provide the desired level of adhesion to the matrix. But CF showed the highest effect in PE. The 30% CF reinforcement increased the tensile strength of PE by 3 times, increasing it from 19 MPa to 56 MPa.

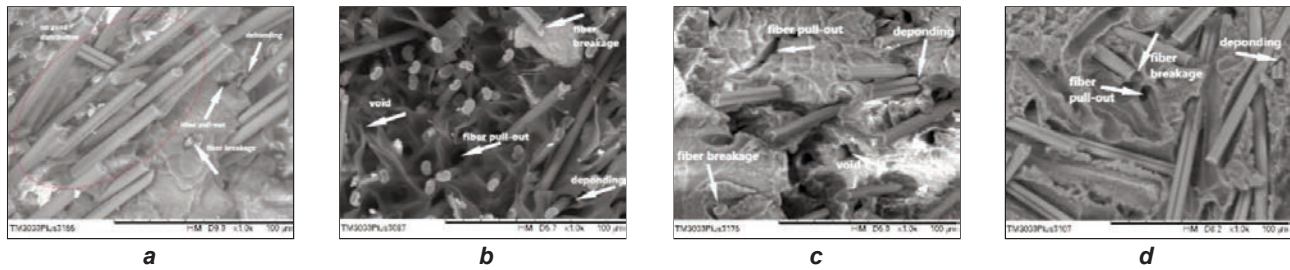


Fig. 3. SEM images of 30% CF reinforced composites: a – PP; b – PE; c – PA6; d – PA12 matrix

However, it only increased the tensile strength of PA6 by 2 times. It was observed that all samples had brittle fractures. This shows that damage occurred with fibre breakage.

SEM images of 30% fibre-reinforced composites can be seen in figure 3, a–d. It is seen that the damage mechanism in composite materials occurs in three stages. In the first stage, micro cracks

were formed in the matrix material. Then, the separation between the fibre and the matrix, and finally, the split at the interface and the breakage of the fibres caused damage. The physical adhesion between fibres and polymer matrices and the formation of voids at the interface between these two materials is controlled mainly by the wetting properties of the fibres [44]. Good wettability means that the reinforcing material that covers the rough surface of the matrix will flow over and take in all the air. Pull-out appears in the composites if good wetting does not occur between the matrix and the fibre [42]. When figure 3, a–d is inspected, it is observed that pull-out occurs in the fibres, and it is not covered with the polymeric matrix. This means poor interface adhesion between the fibre and the matrix [31]. Dark circles around the fibres show local deformation in the matrix around the fibres.

Additionally, these dark circles at the interface show the fibres have been unbonded with the matrix. The dark circle is because of the local deformation of the matrix around the fibre once the fibres separate from the matrix [25]. Some of the fibres were pulled from the matrix during deformation. It can be seen in figure 3, that the CF is not homogeneously dispersed in the PP matrix. When the fracture surfaces of 30% CF-reinforced composites in figure 3 were examined, it was seen that bending and crossing occurred in the fibres with the increase in fibre content, and the surface of the fibres was clean and smooth [40].

Three-point bending properties

The bending tests were carried out on a SHIMADZU brand three-point bending tester. According to TS EN ISO 178-3 three-point bending standards, the test

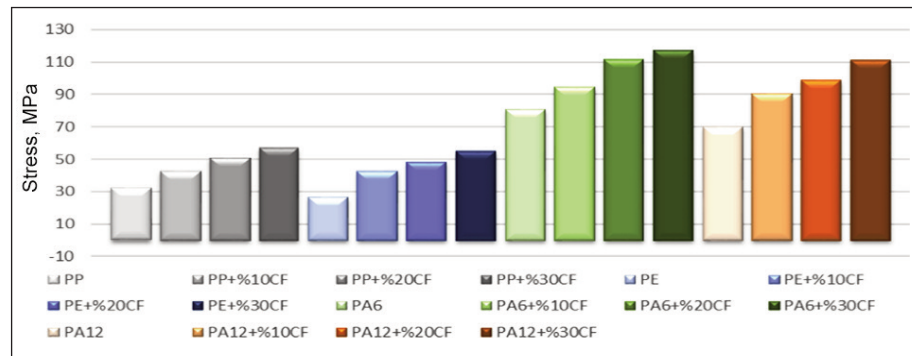


Fig. 4. Three-point bending test results of the composites

samples were ready. The test conditions are set as the distance between the supports is 64 mm, the test speed is 2 mm/min, and the ambient temperature is 21°C. The 3-point bending test results are shown in figure 4. The results indicate that a higher bending strength ensures that the samples have better-bending strength. Moreover, it was observed that the bending stress of the composites increased, and the flexibility decreased as the fibre volume fractions increased. However, mechanical properties such as fibre-matrix interface adhesion levels and random dispersion of fibres were also adversely affected [39, 45]. In addition, molecules in a liquid with low surface energy are not strongly attracted to each other; instead, they tend to spread and adhere to the surface, so a liquid with high free energy will not bond to the fibre surface. To form a better bond, the matrix surface energy must be low [29]. Since the surface energy of the PE matrix is lower than other matrices, composites with the PE matrix performed better than the others [30]. The summary of the test results: (1) It was observed that the highest enhancement for each composite was obtained for 30% CF reinforcement cases, (2) 30% CF reinforcement increased the flexural strength of PP approximately 1.7 times by enhancing it from 32 MPa to 55.3 MPa, (3) 30% CF reinforcement increased the flexural strength of PE 2 times by enhancing it from 27 MPa to 55.1 MPa, (4) 30% CF reinforcement increased the flexural strength of PA6 1.4 times by enhancing it from 81 MPa to 117 MPa and (5) 30% CF reinforcement the flexural strength of PA12 1.6 times by enhancing it from 70 MPa to 110 MPa.

Analysis of experimental results

Signal value (S) stands for the actual value presented by the system and intended to be measured. The noise factor (N) represents the share of undesired factors in the measured value. In this method, the goal is to achieve higher S/N values, and the following equation 5 is used for the S/N ratio calculations [36, 38]. The S/N ratios of the test results are shown in table 3.

$$S/N = -10 \log_{10} \left[\frac{1}{n} \sum_{i=1}^n \frac{1}{y_i^2} \right] \quad (5)$$

where y is the measurement value, and n – the number of experiments.

In the next section, the impact of each factor at each level is investigated. For this aim, the average of the S/N ratios (table 3) is calculated for each factor level. When the S/N rates of the tensile and 3-point bending tests are analysed (figure 5), it can be observed that the mechanical properties increase significantly under the presence of fibre. The reason for this is that as the fibre percentage increase, the deformation energy of the composite rises, and the bond becomes stronger between the matrix and the fibre. In addition, molecules in a liquid with low surface energy are not strongly attracted to each other; instead, they tend to spread and adhere to the surface, so a liquid with high free energy will not bond to the fibre surface. To form a good bond, the matrix surface energy must be low [29]. Since the surface energy of the PE matrix is lower than other matrices, composites with the PE matrix performed better than the others [30]. On the other hand, it is observed that the effect in percentage decreases as the fibre percentage increases. As seen in figure 5, the matrix type significantly affected the mechanical properties of the composites. The highest effect was observed with composites made with PA6. This is because PA6

has the best mechanical properties among other matrices.

To explain to what length each experimental factor impacts the experiment results, the ANOVA analysis was performed for each factor. The calculated F values ensure the targeted 95% confidence level. The analysis details are shown in table 4. It can be observed from table 4 that matrix kind has the dominant impact on the mechanical properties. The second significant factor is fibre content s . However, it is seen that the impact on the matrix material increases as the fibre additive rate rises. It can be concluded that even though fibre addition has an enormous impact on the mechanical properties, of the composites, the mechanical properties of the composites have more sensitivity regarding the matrix type.

Mathematical modelling and data analysis by regression

This section has developed mathematical models to measure the relationship between input and output parameters. The model constants are obtained by the nonlinear multivariable optimization method. In the model, the fibre volume fraction (W) and the type of polymer matrix (P) are defined as the independent variable to result in dependent variables ($y(W,P)$ = the mechanical properties of the composites). The general representation of the proposed model equation is shown as follows:

Nonlinear equation (NLE):

$$y(W,P) = a_0 \times W^{a_1} \times P^{a_2} \quad (6)$$

where y is the model predicted outcomes and are the model coefficients (determined by the data fitting process) [46]. The above model constants are found by performing regression analysis shown in table 5 for mechanical properties of tensile, three-point, and bending respectively. In the modelling study, W and P are considered 4 levels. For W , the levels are

Table 3

S/N RATIOS OF EXPERIMENTAL RESULTS																
Experiment no.	1	2	3	4	5	6	7	8	9	10	11	12	13	14	15	16
Tensile (MPa)	38	19	85	60	56.8	69.2	74.2	42.6	47.3	55.2	133.7	169.9	186.9	129.7	150.0	170.7
S/N	31.6	25.6	38.6	35.6	35.0	36.8	37.4	32.6	33.5	34.9	42.5	44.6	45.4	42.2	43.5	44.6
Three-Point Bend	32	27	81	70	42.9	51.2	57.4	42.9	48.2	55.0	95.0	111.1	117.0	90.7	99.1	111
S/N	30.1	28.6	38.1	36.9	32.6	34.2	35.1	32.6	33.6	34.8	39.5	40.9	41.3	39.1	39.9	40.9

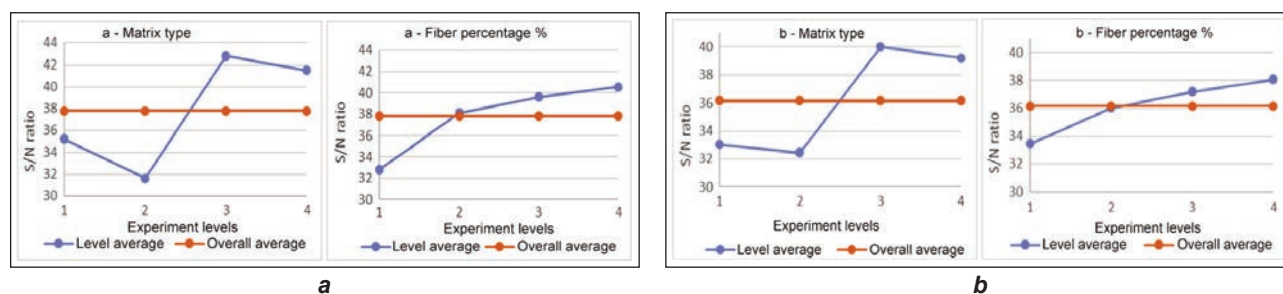


Fig. 5. Graphical representation of: a – S/N ratios for tensile strength; b – Three-point bending

Table 4

ANOVA TABLE FOR TENSILE TEST									
S/N ratio: 37.78	Average S/N Values								
	Degrees of Freedom	Level 1	Level 2	Level 3	Level 4	Sum of Squares	Variance	F	Contribution (%)
A- Matrix Type	3	35.22	31.63	42.79	41.5	333.27	111.09	137.8	69.58
B- Fibre volume fraction %	3	32.83	38.11	39.61	40.58	143.26	47.75	59.25	29.91
Error	8					6.45	0.81		0.5
Total	14					482.98	159.65		

ANOVA TABLE FOR 3-POINT BEND TEST									
S/N ratio: 36,18	Average S/N Values								
	Degrees of Freedom	Level 1	Level 2	Level 3	Level 4	Sum of Squares	Variance	F	Contribution (%)
A- Matrix Type	3	33.03	32.44	40.00	39.22	190.88	63.63	155.93	79.45
B- Fibre volume fraction %	3	33.45	36.01	37.18	38.07	48.15	16.05	39.33	20.04
Error	8					3.26	0.41		0.51
Total	14					242.29	80.08		

Table 5

MATHEMATICAL MODELS FOR PREDICTING THE MECHANICAL PROPERTIES OF COMPOSITES			
Model conditions			
Property	W	P	Model Equation
Tensile	1=0, 2=0.1, 3=0.2, 4=0.3	1=PE, 2=PP, 3=PA12, 4=PA6	$y(W, P) = 22.25175 \cdot W^{0.5764774} \cdot P^{1.014976}$
Three Point Bending	1=0, 2=0.1, 3=0.2, 4=0.3	1=PE, 2=PP, 3=PA12, 4=PA6	$y(W, P) = 27.59192 \cdot W^{0.3237031} \cdot P^{0.7525528}$

described as 1=0, 2=0.1, 3=0.2 and 4=0.3. On the other hand, the various type of matrixes used in this study is assigned to different levels to obtain more accurate model equations for the mechanical properties of the composites (table 5).

The comparative assessments' results between the experimental values and the model-predicted values are performed. The evaluation is carried out for tensile and three-point bending by taking into account the error between the experimental values, and the model-predicted values [38]. The obtained errors indicate that 75% are less than 20% of the tensile and three-point bending error. These results imply that the model (even though having a highly nonlinear nature) predictions against experimental values are very close and at acceptable levels [19].

CONCLUSIONS

In this study, a comparative assessment of the mechanical properties of chopped CF reinforced PP, PE, PA6, and PA12 composites was performed. It is concluded that the presence of reinforcement material, the type of matrix, the degree of adhesion between the matrix and the interface, matrix/fibre volume fraction, distribution, and orientation in the matrix are effective parameters in the mechanical behaviour of the composites.

The tests' results indicate that the mechanical properties increase significantly under the presence of fibre. On the other hand, it is observed that the effect in percentage decreases as the fibre percentage increases. Among the matrices of PE, PP, PA6, and PA12, CF-reinforced composites made with PA6 show the highest-fibre efficiency, but the PE matrix shows the highest performance improvement than the others because having the lowest matrix surface energy, which enables to form good form with the fibre. From the results of S/N ratios and ANOVA analysis, it can be seen that the percentage of the impact of matrix and fibre volume fraction on the mechanical properties of composite materials is various. It is observed that the matrix kind has the dominant impact on the mechanical properties.

Finally, nonlinear mathematical models to correlate the experimental values are developed. Based on the results, it is inferred that the predictions from the proposed models are found to be in good agreement with experimental data. Thus, it can be concluded that the proposed models are robust enough to correlate the experimental response of the polymer composites.

REFERENCES

- [1] Li, J., Cai, C.L., *The carbon fibre surface treatment and addition of PA6 on tensile properties of ABS composites*, In: Current Applied Physics, 2011, 11, 50–54
- [2] Botelho, E.C., Figiel, Rezende, M.C., Lauke B., *Mechanical behavior of carbon fibre reinforced polyamide composites*, In: Composites Science and Technology, 2003, 63, 1843–1855
- [3] Fu, S.Y., Lauke, B., *Fracture resistance of unfilled and calcite-particle-filled ABS composites reinforced by short glass fibres (SGF) under impact load*, In: Composites Part A: Applied Science and Manufacturing, 1998, 29, 631–641
- [4] Tjong, S.C., Xu, S.A., Mai, Y.W., *Impact fracture toughness of short glass fibre-reinforced polyamide 6,6 hybrid composites containing elastomer particles using essential work of fracture concept*, In: Materials Science and Engineering A, 2003, 347, 338–345
- [5] Capela, C., Oliveira, S.E., Pestana, J., Ferreira, J.A.M., *Effect of fibre length on the mechanical properties of high dosage carbon reinforced*, In: Procedia Structural Integrity, 2017, 5, 539–546
- [6] Zhao, S., Cheng, L., Guo, Y., Zheng, Y., Li B., *PA6 and Kevlar fibre reinforced isotactic polypropylene: Structure, mechanical properties and crystallization and melting behavior*, In: Materials and Design, 2012, 35, 749–753
- [7] Fu, S.Y., Lauke, B., Mäder, E., Hu, X., Yue C.Y., *Fracture resistance of short-glass-fibre-reinforced and short-carbon-fibre-reinforced polypropylene under Charpy impact load and its dependence on processing*, In: Journal of Materials Processing Technology, 1999, 89–90, 501–507
- [8] Fu, S.Y., Lauke, B., Mäder, E., Yue, C.Y., Hu, X., *Tensile properties of short-glass-fibre- and short-carbon-fibre-reinforced polypropylene composites*, In: Composites Part A: Applied Science and Manufacturing, 2000, 31, 1117–1125
- [9] Fu, S.Y., Mai, Y.W., Ching, E.C.Y., Li, R.K.Y., *Correction of the measurement of fibre length of short fibre reinforced thermoplastics*, In: Composites Part A: Applied Science and Manufacturing, 2002, 33, 1549–1555
- [10] Awan, G.H., Ali, L., Ghauri, M., Ramzan, E., Ehsan, E., *Effect of Various Forms of Glass Fibre Reinforcements on Tensile Properties of Polyester Matrix Composite*, In: Journal of Faculty of Engineering & Technology, 2009
- [11] Akindoyo, J.O., et al., *Simultaneous impact modified and chain extended glass fibre reinforced poly(lactic acid) composites: Mechanical, thermal, crystallization, and dynamic mechanical performance*, In: Journal of Applied Polymer Science, 2021 138, 1–14
- [12] Zhou, H., et al., *Fibre breakage and dispersion in carbon-fibre-reinforced nylon 6/clay nanocomposites*, In: Journal of Applied Polymer Science, 2007, 106, 1751–1756
- [13] Karsli, N.G., Aytac, A., *Tensile and thermomechanical properties of short carbon fibre reinforced polyamide 6 composites*, In: Composites Part B: Engineering, 2013, 51, 270–275
- [14] Chen, X., et al., *Research on mechanical properties of carbon fibre /polyamide reinforced PP composites*, In: AIP Conference Proceedings, 2017, 1890, 1–5
- [15] Lin, T., Jia, D., He, P., Wang, M., Liang, D., *Effects of fibre length on mechanical properties and fracture behavior of short carbon fibre reinforced geopolymer matrix composites*, In: Materials Science and Engineering A, 2008, 497, 181–185
- [16] Hassan, A., Hornsby, P.R., Folkes, M.J., *Structure-property relationship of injection-molded carbon fibre-reinforced polyamide 6,6 composites: The effect of compounding routes*, In: Polymer Testing, 2003, 22, 185–189
- [17] Kim, Y.S., Kim, J.K., Jeon, E.S., *Effect of the compounding conditions of polyamide 6, carbon fibre, and Al₂O₃ on the mechanical and thermal properties of the composite polymer*, In: Materials, 2019, 12, 1–14
- [18] Siva R., Sundar Reddy Nemali S., Kishore Kunchapu S., Gokul K., Arun Kumar T., *Comparison of Mechanical Properties and Water Absorption Test on Injection Molding and Extrusion – Injection Molding Thermoplastic Hemp Fibre Composite*, In: Materials Today: Proceedings, 2021, 47, 4382–4386
- [19] Junaedi, H., Baig, M., Dawood, A., Albahkali, E., Almajid, A., *Modeling analysis of the tensile strength of polypropylene base Short Carbon Fibre reinforced composites*, In: Journal of Materials Research and Technology, 2021, 11, 1611–1621
- [20] Cox H.L., *The elasticity and strength of paper and other fibrous materials*, In: British Journal of Applied Physics, 1952 3, 72
- [21] Afddl J.C.H., Kardos J.L., *The Halpin-Tsai equations*, In: A review. Polymer Engineering and Science, 1976, 16, 344–352
- [22] Liang J.Z., *Predictions of tensile strength of short inorganic fibre reinforced polymer composites*, In: Polymer Testing, 2011, 30, 749–752
- [23] SIGRAFIL Short Carbon Fibres | SGL Carbon, Available at: <https://www.sglcarbon.com/en/markets-solutions/material/sigrafil-short-carbon-fibres/> [Accessed on February 2022]
- [24] Park, J.M., et al., *Interfacial and hydrophobic evaluation of glass fibre/CNT-epoxy nanocomposites using electro-micromechanical technique and wettability test*, In: Composites Part A: Applied Science and Manufacturing, 2009, 40, 1722–1731
- [25] Hao, W., Yao, X., Ke, Y., Ma, Y., Li, F., *Experimental characterization of contact angle and surface energy on aramid fibres*, In: Journal of Adhesion Science and Technology, 2013, 27, 1012–1022
- [26] Wang, Y., Hansen, C.J., Wu, C.C., Robinette, E.J., Peterson, A.M., *Effect of surface wettability on the interfacial adhesion of a thermosetting elastomer on glass*, In: RSC Advances 2021, 11, 31142–31151

- [27] Tran, L.Q.N., Fuentes, C.A., Vuure, A.W. Van., Verpoest, I., Leuven, K.U., *Investigating the interfacial compatibility and adhesion of coir fibre composites, materials engineering*, In: 18th International Conference on Composite Materials Investigating, 1–5
- [28] Kim, J.-K., Mai, Y.W., *Engineered interfaces in fibre reinforced composites*, 1998, 401
- [29] Lu, C., et al., *Wettability and Interfacial Properties of Carbon Fibre and Poly(ether ether ketone) Fibre Hybrid Composite*, In: ACS Applied Materials and Interfaces, 2019, 11, 31520–31531
- [30] Fenouillot, F., Cassagnau, P., Majesté, J.C., *Uneven distribution of nanoparticles in immiscible fluids: Morphology development in polymer blends*, In: Polymer, 2009, 50, 1333–1350
- [31] Delli, E., Giliopoulos, D., Bikiaris, D.N., Chrissafis, K., *Fibre length and loading impact on the properties of glass fibre reinforced polypropylene random composites*, In: Composite Structures, 2021, 263
- [32] Crabtree, S.L., Spalding, M.A., Pavlicek, C.L., *Single-screw extruder zone temperature selection for optimized performance*, In: Technical Papers, Regional Technical Conference – Society of Plastics Engineers, 2008, 3, 1406–1411
- [33] da Costa, H.M., Ramos, V.D., de Oliveira, M.G., *Degradation of polypropylene (PP) during multiple extrusions: Thermal analysis, mechanical properties and analysis of variance*, In: Polymer Testing, 2007, 26, 676–684
- [34] Ghislandi, M., Luis, L.A.S., Schulte, K., Barros-Timmons, A., *Effect of filler functionalization on thermo-mechanical properties of polyamide-12/carbon nanofibres composites: A study of filler-matrix molecular interactions*, In: Journal of Materials Science, 2013, 48, 8427–8437
- [35] Savaşkan, M., Taptık, Y., Ürgen, M., *Performance optimization of drill bits using design of experiments*, In: Itüdergisi/D 2004, 117–128
- [36] Özçelik, B., Özbay, B., *Determination of effect on the mechanical properties of polypropylene product of molding materials using taguchi method*, In: Sigma 29, 2011, 289–300
- [37] Fu, T., Haworth, B., Mascia, L., *Analysis of process parameters related to the single-screw extrusion of recycled polypropylene blends by using design of experiments*, In: Journal of Plastic Film and Sheeting, 2017, 33, 168–190
- [38] Ravi Kumar, N., Srikant, P., Ranga Rao, C.H., Meera Saheb, K., *Statistical analysis of mechanical properties of vakka fibre reinforced polypropylene composites using Taguchi method*, In: Materials Today: Proceedings, 2017, 4, 3361–3370
- [39] Choudhari, D.S., Kakhandki, V.J., *Comprehensive study and analysis of mechanical properties of chopped carbon fibre reinforced nylon 66 composite materials*, In: Materials Today: Proceedings, 2020, 44, 4596–4601
- [40] Zhang, Y., Zhang, Y., Liu, Y., Wang, X., Yang, B., *A novel surface modification of carbon fibre for high-performance thermoplastic polyurethane composites*, In: Applied Surface Science, 2016, 382, 144–154
- [41] Karahan, M., Karahan, N., *Influence of weaving structure and hybridization on the tensile properties of woven carbon-epoxy composites*, In: Journal of Reinforced Plastics and Composites, 2014, 33, 212–222
- [42] Wang, J., et al., *Wettability of carbon fibres at micro- and mesoscales*, In: Carbon, 2017, 120, 438–446
- [43] Wang, C., et al., *Effect of carbon fibre dispersion on the mechanical properties of carbon fibre-reinforced cement-based composites*, In: Materials Science and Engineering A, 2008, 487, 52–57
- [44] Huang, B.Z., Zhao, L.J., *Bridging and toughening of short fibres in SMC and parametric optimum*, In: Composites Part B: Engineering, 2012, 43, 3146–3152
- [45] Karahan, M., Gul, H., Karahan, N., Ivens, J., *Static behavior of three-dimensional Integrated core sandwich composites subjected to three-point bending*, In: Journal of Reinforced Plastics and Composites, 2013, 32, 664–678
- [46] Manikandan, A., Rajkumar, R., *Evaluation of mechanical properties of synthetic fibre reinforced polymer composites by mixture design analysis*, In: Polymers and Polymer Composites, 2016, 24, 455–462

Authors:

ARI ALI¹, BAYRAM ALI², KARAHAN MEHMET³, KARAGÖZ SEÇGİN⁴

¹OSTİM Technical University, Vocational School of Higher Education, Department of Weapon Industry Technician, 06374, Ankara, Turkey

²Bursa Uludag University, Department of Mechanical Engineering, 16059, Bursa, Turkey

³Bursa Uludag University, Vocational School of Higher Education, Department of Textile, 16059, Bursa, Turkey

⁴Qatar University, Department of Chemical Engineering, 2713, Doha, Qatar

Corresponding author:

ARI ALI
e-mail: ali.ari@ostimteknik.edu.tr

An investigation on non-flammability properties of polypropylene knitted fabrics

DOI: 10.35530/IT.074.02.202178

ÖZKAN HACIOĞULLARI SELCEN

BABAARSLAN OSMAN

ABSTRACT – REZUMAT

An investigation on non-flammability properties of polypropylene knitted fabrics

The research performed in recent years regarding synthetic filament yarns is improving the structures and properties of such yarns, and diversifying their usage areas. Most of the current studies being carried out in this field are in the form of bringing functionality to filament yarns. And one of these functional properties is the production of flame-retardant yarns from different types of polymers. In this study, polypropylene (PP) raw material was mixed with organophosphate based flame retardancy additive at rates in between 1% and 8% in the feed hopper of a laboratory-type melt spinning machine during PP filament yarn production and then knitted fabric structures were obtained from these yarns. Then the flame retardancy properties of these PP knitted fabrics were tried to be determined by vertical flammability tests and Limit Oxygen Index (LOI) tests. Test results indicated that after flame time and char length values had significantly decreased and values of LOI had increased in knitted fabrics by the increase in additive rate. In conclusion, it was observed that the increase in the rate of flame retardancy additive had significantly improved the non-flammability properties of the PP samples.

Key-words: flame retardancy (FR), knitted fabric, mechanical properties, polypropylene filament yarn, vertical flammability and Limited Oxygen Index (LOI)

O investigație asupra proprietăților de neinflamabilitate ale tricotelor din polipropilenă

Cercetările efectuate în ultimii ani cu privire la firele filamentare sintetice îmbunătățesc structurile și proprietățile unor astfel de fire și le diversifică domeniile de utilizare. Cele mai multe dintre studiile actuale care se desfășoară în acest domeniu sunt sub forma aducerii în stadiul de funcționalitate a firelor filamentare. Și una dintre aceste proprietăți funcționale se referă la producerea de fire ignifuge din diferite tipuri de polimeri. În acest studiu, materia primă din polipropilenă (PP) a fost amestecată cu aditiv ignifug pe bază de organofosforați în proporții cuprinse între 1% și 8% în buncărul de alimentare al unei mașini de filat din topitură de laborator, în timpul producției de fire filamentare PP și apoi au fost obținute structuri tricotate din aceste fire. Apoi, proprietățile de ignifugare ale acestor tricoteuri PP au fost testate, prin teste de inflamabilitate verticală și teste cu Indice Limită de Oxigen (LOI). Rezultatele testelor au indicat că, după timpul de ardere și lungimea rezidului de carbon, valorile de ardere au scăzut semnificativ, iar valorile LOI au crescut în tricoteuri prin creșterea proporției aditivilor. În concluzie, s-a observat că creșterea proporției aditivului de ignifugare a îmbunătățit semnificativ proprietățile de neinflamabilitate ale probelor PP.

Cuvinte-cheie: ignifugare (FR), tricot, proprietăți mecanice, fire filamentare de polipropilenă, inflamabilitate verticală și Indice Limită de Oxigen (LOI)

INTRODUCTION

Polypropylene (PP) based fibres are raw materials that are frequently preferred and used in the textile industry due to their outstanding properties such as low density, easy processability, a sufficient level of tenacity, high chemical resistance and low cost even if they vary. PP fibres, due to their above-listed advantageous properties, are mainly being used in the fields of carpet, upholstery, clothing, technical textile applications etc. In addition to these properties of fibres and of products being obtained from these fibres, bringing in additional properties to these products depending on their place and purpose of use is one of the accentuated issues. For instance, textile products must possess flame retardancy properties, especially in respect of safety. Thus, various studies are being performed in recent years to improve the

flame retardancy property of PP fibres in addition to their already available properties. Bringing in flame retardancy property to textile products consisting of PP fibres is generally ensured by the addition of an additive having flame retardancy (FR) properties. Moreover, despite having various additives used for this purpose (phosphorus, boron, intumescent, SiO₂ etc.), the action mechanisms and effectiveness degrees of these additives differ from each other. Today, there are many scientific studies regarding the examination of the action mechanisms and synergistic actions of flame retardancy additives and the production of new types of additives [1–3]. When the results of these studies were reviewed, it was being observed that the flame retardancy property of PP could be improved by substances and that this property was generally being increased to the required

level. Also, it was seen that the textile materials gain a good level of flame retardancy property by the phosphorus-based flame retardancy additives which were based on in this study [1, 4–6]. Examining the permeability properties (air permeability, water vapour permeability, etc.) of knitted fabrics and determining the effects of these properties on their flammability are also important research topics [7–9]. This subject has been evaluated as another study. This study aims to investigate the non-flammability properties of PP knitted fabrics in detail. Hence, the large control group (1–8% FR added PP knitted structure) has been used. As a result, the effect of organophosphonate based FR additive on the flammability properties of PP knitted fabrics has been determined. In this study, the production of PP filament yarn by the addition of FR substance at rates of 1%, 2%, 3%, 4%, 5%, 6%, 7% and 8% was performed, and the structures and properties of these yarns were examined. The yarns produced afterwards were converted to the knitted fabric surface, and the effect of additive on flame retardancy properties was tried to be determined through vertical flammability and LOI tests. During production, all other production parameters were kept fixed, and only the rate of additive was determined as a variable factor. The originality of this study can be defined as a detailed examination of the burning properties of PP knitted fabrics which have been obtained by the addition of FR additive at a wide range changing from 1% to 8%.

MATERIAL AND METHODS

Polypropylene polymer chips (Sabic PP 518P) and particles of additive providing flame retardancy properties were used as raw materials in this study. Sabic PP 518P, an isotactic PP (IPP) chips with a melt flow index of 24 g/10 min. and 905 kg/m³ density was used as a polymer substance. The properties of these PP chips are given in table 1.

Also, an organophosphonate based FR additive (CESA-Flam CFR1) was used in this study and spin-finish oil (Polymast-MKL) was used as an auxiliary chemical during the production of yarns to prevent

Table 1

PROPERTIES OF PP CHIPS USED IN THIS STUDY		
Properties	Value	Standards
Resin properties		
Melt flow rate (MFI) (230°C&2.16 kg load density)	24 g/10 min. 905 kg/m ³	ASTM D 1238 ASTM D 792
Mechanical properties		
Tensile strength at yield	32 MPa	ASTM D 638
Tensile elongation at yield	12%	ASTM D 638
Flexural modulus (1% secant)	1550 MPa	ASTM D 790A
Notched izod impact strength at 23°C	30 J/m	ASTM D 256
Rockwell hardness, R-Scale	100	ASTM D 785
Thermal properties		
Vicat softening point	152°C	ASTM D 1525B
Heat deflection temperature at 455 KPa	118°C	ASTM D 648

fibre-metal and fibre-fibre frictions after the spinneret and to prevent adhesion of filaments to each other. Yarns have been produced according to the melt spinning principle by using a laboratory-type filament yarn machine (figure 1). The PP polymer chips and FR additives were fed into the hopper consisting of a single-screw extrusion system. The heating along the screw was adjusted to obtain a temperature gradient from 220°C to 245°C and a volumetric pump regulated the injection of molten polymer towards the dies at a flow rate of 350 cm³ per minute. Then, the filaments were air-cooled and a spin finish was applied on the filaments before their passage in the drawing godets. Then filaments were drawn using heated godets before being wound. The speeds of the two godets serve to adjust the drawing ratio: the first godet speed was set at 400 rpm, whereas the second one was set at 800 rpm, giving a drawing ratio of 2. Finally, the filament yarns were wound on a cheese

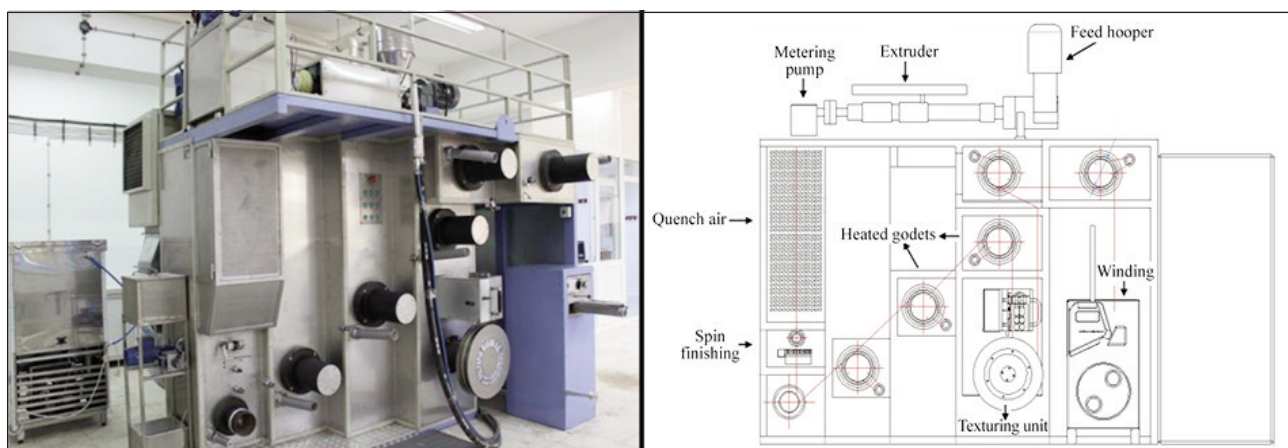


Fig. 1. Laboratory-type melt spinning machine used for yarn production [10]

PRODUCTION PARAMETERS OF PP FILAMENT YARNS			
Extruder parameters		Drawing unit parameters	
Zone-1 temperature	220°C	Godet-1 speed	390 rev/min.
Zone-2 temperature	240°C	Godet-2 speed	400 rev/min.
Zone-3 temperature	245°C	Godet-3 speed	800 rev/min.
Zone-4 temperature	245°C	Godet-4 speed	680 rev/min.
Extruder speed	143 rev/min.	Godet-5 speed	680 rev/min.
Extruder pressure	6.6 bar	Speed of textured drum	400 rev/min.
Pump speed	70 rev/min.	Winding speed	2050 m/min.

package. In addition, during the production process, all other parameters except for the factors whose effects were aimed to be investigated (ratio of additive material) were kept constant. Production parameters of PP filament yarns are given in table 2.

STRUCTURE AND PROPERTIES OF PP FILAMENT YARNS

PP polymer chips and FR additive were mixed at determined rates (99/1%, 98/2%, 97/3%, 96/4%, 95/5%, 94/6%, 93/7% and 92/8%) and fed to the system during production. First of all, 100% PP reference yarns have been produced and then, FR added PP filament yarns were produced. Also, these yarns have round cross-sectional shape and structure and the fineness of produced yarns were determined as "144f918denier" (figure 2).

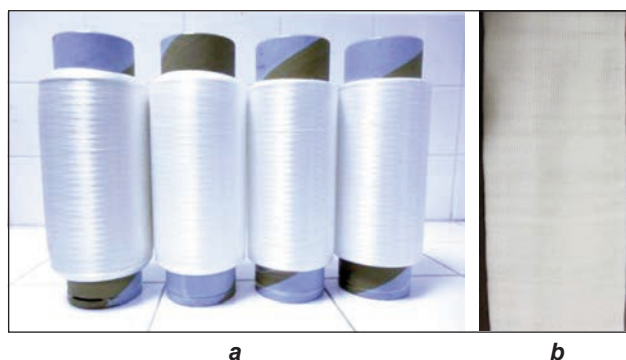


Fig. 2. Produced materials in the scope of this study: *a* – PP filament yarns; *b* – structure of supreme knitted fabric [11]

To determine the structure and properties of the yarns, tenacity-breaking elongation, unevenness and intermingled tests were applied to the yarns. Filament yarn samples were conditioned for 24 hours at $20^{\circ}\text{C}\pm 2$ temperature and $65\pm 2\%$ relative humidity, which are the standard atmospheric conditions before the tests. Tenacity-Elongation tests were carried out with a Uster Tensorapid-3 test device according to BS EN ISO 2062, 1995 test standard and unevenness tests were carried out with a Uster Unevenness Measurement device according to DIN 53817-1 test standard ("Using BS EN ISO 2062", 1995; "Using DIN 53817-1", 1983) [12, 13]. Also, the

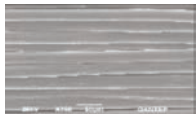
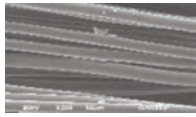
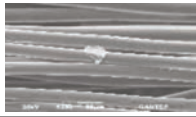
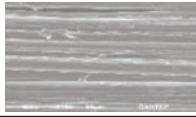
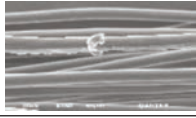
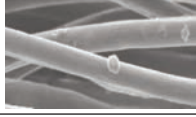
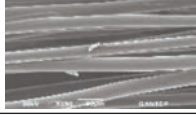
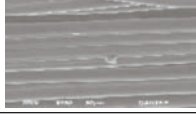
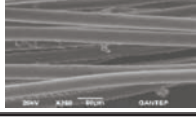
intermingling test was realized with the Rothschild Entanglement Tester R-2070 test device according to the "Internal Method". Additionally, the surface morphology of filament yarns was investigated with the help of a Scanning Electron Microscope-SEM (Jeol JSM-6390 LV) at a voltage of 20 kV. SEM images of PP filament yarns and test results are given in table 3.

As will be seen in table 3, while additive-free PP filament yarns have a smooth structure, granules caused by additives which had not been completely integrated into the structure are being observed on the surfaces of filament yarns produced by FR additive. Moreover, it was determined that the tenacity-breaking elongation and unevenness values of PP filament yarns do not change in a specific direction depending on the rate of additive in the structure. Intermingling numbers of filament yarns per meter were determined as 9–12 units [11].

KNITTED FABRIC PRODUCTION FROM PP FILAMENT YARNS AND FLAME RETARDANCY TEST

PP filament yarns were converted to a knitted fabric structure (Supreme) to perform the flame retardancy tests. The knitting operation was performed at Lonati Goal-6715 brand knitting with a cylinder diameter of $3\frac{1}{2}$ inches and by automatic yarn tension settings. As the result of the knitting operation performed by 54 needles and a machine speed of 160 rpm, yarns with supreme knitting structure were obtained. Supreme (Single jersey) is one of the basic knitted structures. Single jersey fabric is produced with the RL knitting technique. RL plain knitted fabrics have plain (R) loops on one side and only reverse (L) loops on the other. Supreme knitted fabrics are widely used in home textiles. As it is known, the flame retardancy property is desired from home textile products for safety. Therefore, a single jersey knitted structure was preferred in this study. The GSM of supreme knitted samples which are used in this study is 352 g/m^2 . Also, the thickness of these knitted fabrics is 0.4 mm.

300×76 mm samples were prepared from the fabrics for vertical flammability test according to ASTM D 6413 testing standard and the relevant test was

SEM (LONGITUDINAL) OBSERVATIONS AND MECHANICAL PROPERTIES OF PP FILAMENTS [11]						
Sample	SEM Pictures	Tenacity (cN/tex)	Breaking elongation (%)	Uster (U%)	CVm (%)	Intermingling (number of nips per meter)
PP filament yarn		22.8	28.4	6.94	7.49	10.1
1% FR		23.6	28.4	5.29	6.63	10.2
2% FR		23.0	27.4	5.45	6.88	11.0
3% FR		22.5	26.7	5.60	6.95	8.9
4% FR		22.7	27.3	5.98	7.53	10.1
5% FR		22.8	26.2	5.95	7.41	9.7
6% FR		23.4	26.6	5.37	6.64	10.0
7% FR		23.7	28.7	5.97	7.50	12.0
8% FR		22.5	26.7	6.17	7.63	9.2

applied to Atlas Brand Fire Science Product-AGC Automatic Gas Control device ("Using ASTM D 6413", 2011) [14]. By the beginning of the test, the ignition source at the central lower point of knitted fabrics was lit up, and the fabrics were exposed to flame with a length of 19 mm for 12 seconds. In this test, the ignition source dies following a period of 12 seconds and the period of continuation of the burning of the fabric is measured by a chronometer ("Using ASTM D 6413", 2011) [14]. Limit Oxygen Index (LOI) test was applied to knitted fabric samples as well. These samples were prepared with a dimension of 140×52 mm as per ASTM-D 2863 testing standard by using a Dynisco brand device ("Using ASTM D 2863-10", 2009) [15]. For both tests, the samples were exposed to the same process 15 times, and the averages of the results were taken. Before tests, the knitted fabric samples were conditioned for 24 hours at 20°C±2 temperature and 65±2% relative humidity which are

the standard atmospheric conditions. After testing, the effect of the rate of FR additive on the PP knitted fabrics was statistically analysed by using the "One-Way Variance Analysis (ANOVA)" method. The statistical study was realized at $\alpha=0,05$ reliability level.

RESULTS AND DISCUSSION

Vertical flammability test-char length

Vertical flammability test is being used under controlled laboratory conditions to measure the reaction of textile materials against heat and flame ("Using ASTM D 6413", 2011) [14]. This test is being applied in order to determine whether the fabric continues to burn or not after cutting the source of flame applied to the sample fabric. During the test, as the sample is directly exposed to flame from its central lower point, significant results are obtained by the end of the test in respect of determining the flame retardancy property of the samples. By this test, many burning

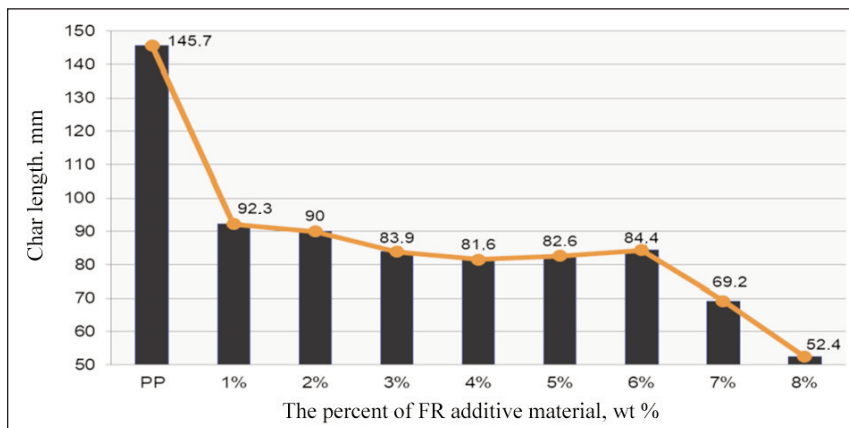


Fig. 3. Effect of flame-retardant additives on char length of PP knitted fabrics (Significant: 0.000)

properties of the fabrics such as “afterflame”, “afterglow”, “aftertime”, dripping behaviour and burning behaviour are determined. This test in the subject is generally used to determine the flame retardancy property of textile materials such as apparel fabrics, upholstery, curtains etc.

During the study, the char length and after-flame time of the fabrics were determined by the vertical flammability test being applied to PP knitted fabrics. The change of char length values of PP knitted fabrics according to different rates of FR additive are presented in figure 3.

Descriptive statistical data table of the char length of FR added filament yarns is given in table 4.

ANOVA table of char length of FR added filament yarns is given in table 5.

From figure 3, it is seen that the increase in the amount of FR additive significantly decreases the vertical char length of the samples. From the graph (figure 3), it is seen that the PP knitted fabric which doesn't include FR additive has a char length of 145.7 mm and that the PP knitted fabric with additive has a char length much lower than this value. Especially, the 52.4 mm char length of the PP knitted fabric with 8% FR additive is remarkable.

This result indicates that 8% significantly improves the flame retardancy property of knitted fabrics. And another remarkable result is the similarity among the char lengths of knitted fabrics including an additive in between 3–6%; not a significant decrease tendency but similarities were observed among these results. The change in the additive rate of 3–6% had not improved the FR property of fabrics. Consequently, this condition can be defined by similar flame retardancy properties of test samples including FR at rates of 3%, 4%, 5% and 6%. By the addition of additive at a rate of 7%, it was observed that the flame retardancy property of the fabrics significantly improves. Moreover, according to the

Table 4

DESCRIPTIVES								
Sample	N	Mean	Std. Deviation	Std. Error	95% Confidence interval for mean		Minimum	Maximum
					Lower bound	Upper bound		
100% PP	9	145.667	37.1113	12.3704	117.140	174.193	90.0	200.0
1% FR	9	92.333	11.5217	3.8406	83.477	101.190	79.0	118.0
2% FR	9	90.000	13.8203	4.6068	79.377	100.623	60.0	101.0
3% FR	9	83.889	8.1001	2.7000	77.663	90.115	73.0	100.0
4% FR	9	81.556	17.0449	5.6816	68.454	94.657	59.0	111.0
5% FR	9	82.556	14.9592	4.9864	71.057	94.054	60.0	105.0
6% FR	9	84.444	7.6012	2.5337	78.602	90.287	71.0	95.0
7% FR	9	69.222	19.7976	6.5992	54.004	84.440	30.0	89.0
8% FR	9	52.444	11.8544	3.9515	43.332	61.557	35.0	71.0
Total	81	86.901	29.2539	3.2504	80.433	93.370	30.0	200.0

Note: Char length (mm).

Table 5

ANOVA					
Description	Sum of squares	df	Mean square	F	Sig.
Between groups	45493.877	8	5686.735	17.826	0.000
Within groups	22969.333	72	319.019		
Total	68463.210	80			

Note: Char length (mm).

results of statistical analysis, as the significance value of test results of the char lengths of knitted fabrics was found to be 0.000 at $\alpha=0,05$ reliability level, the effect of the amount of additive on the char lengths of knitted fabric samples was also statistically significant.

Vertical flammability test-after-flame time

Another data obtained as the result of the vertical flammability test applied on PP knitted fabric samples is the time in which the fabrics continue to burn following the duration of exposure to flame. Figure 4 indicates the effect of change in FR additive rate on after-flame time values of PP knitted fabrics.

Descriptive statistical data table of after flame time of FR added filament yarns is given in table 6. ANOVA table of after flame time of FR added filament yarns is given in table 7.

From figure 4, it is seen that against the increase in the amount of FR additive, after-flame time following 12 seconds of exposure to the ignition source significantly decreases. It was determined that the additive-free PP knitted fabric samples burn for about 46 seconds

following 12 seconds of exposure to flame and that the fabrics produced by adding additive have much lower after-flame times than this value. The change in the direction of the increase-decrease of the after-flame time of knitted fabrics including FR additive in between 5% and 8% can be assessed as a remarkable result. This condition can be interpreted as reaching a specific flame retardancy level of knitted fabrics including 5% additive and as observing similar burning behaviours in samples even by the addition of a higher rate of additive in the yarn. Moreover, as the significance value of test results of the after-flame time values of PP knitted fabrics was found to

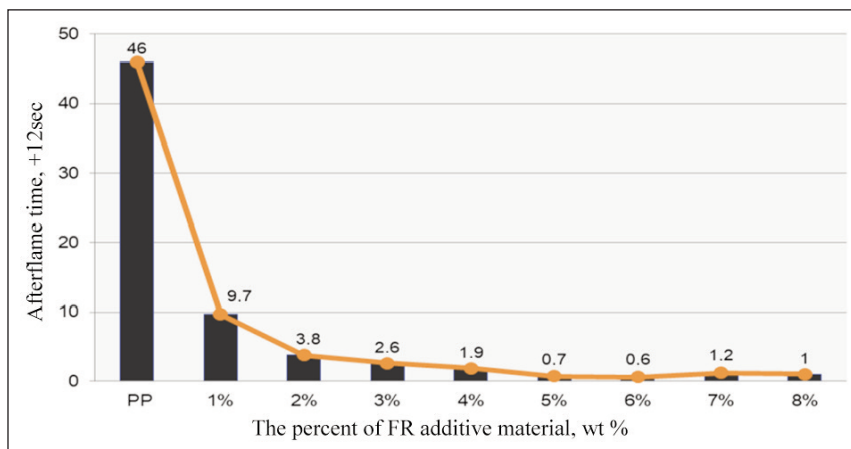


Fig. 4. Effect of flame-retardant additives on after-flame time of PP knitted fabric (Significant: 0.000)

Table 6

DESCRIPTIVES								
Sample	N	Mean	Std. Deviation	Std. Error	95% Confidence interval for mean		Minimum	Maximum
					Lower bound	Upper bound		
100% PP	9	46.067	20.6870	6.8957	30.165	61.968	27.9	91.5
1% FR	9	9.689	5.3471	1.7824	5.579	13.799	4.5	19.6
2% FR	9	3.822	2.7730	0.9243	1.691	5.954	0.0	8.0
3% FR	9	2.633	1.6793	0.5598	1.343	3.924	0.0	4.9
4% FR	9	1.911	1.0764	0.3588	1.084	2.738	0.6	3.7
5% FR	9	0.656	0.5341	0.1780	0.245	1.066	0.0	1.3
6% FR	9	0.578	0.9667	0.3222	-0.165	1.321	0.0	2.9
7% FR	9	1.167	0.9975	0.3325	0.400	1.933	0.0	2.6
8% FR	9	1.044	0.6598	0.2199	0.537	1.552	0.0	2.1
Total	81	7.507	15.5730	1.7303	4.064	10.951	0.0	91.5

Note: Afterflame time (+12 sec).

Table 7

ANOVA					
Description	Sum of squares	df	Mean square	F	Sig.
Between groups	15634.562	8	1954.320	37.355	0.000
Within groups	3766.893	72	52.318		
Total	19401.456	80			

Note: Afterflame time (+12 sec).

be 0.000 at $\alpha=0.05$ reliability level, the effect of the amount of additive on the after-flame times of knitted fabric samples was also found to be statistically significant. Another result of the vertical flammability test is relevant to afterglow behaviours of knitted fabrics; along with the vertical flammability test applied on PP knitted fabrics with and without additive, afterglow had not been observed on any of the fabrics. And a significant dripping behaviour was also not observed on the samples during the tests, and dripping was observed only on additive-free PP and on a few knitted fabric test samples with 1% and 2% additive.

Limit Oxygen Index (LOI)

LOI test was also applied on knitted fabric samples produced from PP filament yarns to support the results of the vertical flammability test. By this test method, the reactions of materials against heat and flame under controlled conditions are measured and defined ("Using ASTM D 2863-10", 2009) [15]. By the end of the test, the minimum oxygen amount required to be available in the environment for the continuation of burning is being determined. The LOI test method provides a good measurement regarding the flammability properties of polymeric materials, and it can determine the flame retardancy characteristics of the materials. In these respects, this test was deemed to be significant and was used in this study. Figure 5 indicates the change in LOI values of fabrics as per the flame retardancy additive rate.

As the oxygen amount in the air is about 21%, any material with an LOI value lower than that value can easily burn in the current air condition. On the contrary, the materials with an LOI value over 21% slow down or stop burning when the ignition source is removed. Figure 5 shows that the LOI value of additive-free PP was calculated as 19% and LOI values of samples in which FR additive was added had significantly increased as per that reference value. It is known that the LOI value for PP polymeric materials is about 17–18%, and the LOI value of the PP sample fabric structure used in the study was higher. It can be interpreted as it had arisen from the condition that the linear density (918 denier) of continuous fila-

ment yarn was high [11]. It was also observed that the LOI values of PP knitted fabrics significantly increased by the addition of FR additive at a rate of 1%. According to the literature, it was determined that the samples including FR substances at rates of 1%, 2%, 3%, 4%, 5% and 6% are in the "Slowly Flammable" products category due to their LOI values of 25, 26, 27 and 28 respectively and that the samples including additive at a rate of 7% and 8% are in the "Flame Retardancy-Self-Extinguishing Material" class due to LOI value of 30 [16, 17]. When studies are included in the literature relevant to improving the flame retardancy properties of textile products, it is observed that the LOI test determining the resistance of materials against burning had been used in many scientific studies. In these studies, the LOI test had generally been used to support the other flame retardancy tests [2, 11, 18].

CONCLUSION

Polypropylene fibre is significantly being used in the textile industry and especially in the field of technical textiles. However, it is a significant disadvantage that polypropylene fibre has lower resistance to flame. Thus, many research and application studies are being performed today to bring flame retardancy properties to PP textile products. In this study, knitted fabric samples were produced by additive-free and FR added PP filament yarns, and then Vertical Flammability and LOI tests were applied to these samples to examine their flame retardancy properties. When the test results were examined, it was observed that the increase in the additive rate of the samples significantly decreases both the after-flame times and char lengths of PP knitted fabrics. The average char length value of additive-free PP knitted fabrics was determined as 145.7 mm, and this value decreased to 52.4 mm with the increase in the additive rate. Again, the average after-flame time value for additive-free PP knitted fabrics was calculated as 46 seconds, and this value gradually decreased with the increase in additive rate, and it had decreased below 1 second by the addition of 5% additive.

Moreover, the results of the LOI test supported the vertical non-flammability test results. While the LOI value of additive-free PP knitted fabric was found as 19%, it was observed that this value significantly increases with the increase in the additive amount. LOI values of the samples with 7% and 8% FR were found as "30". The obtained result indicated that these samples have "Self-Extinguishing" properties. Consequently, this study showed us that the flame retardancy properties of knitted fabrics produced from PP filament yarns

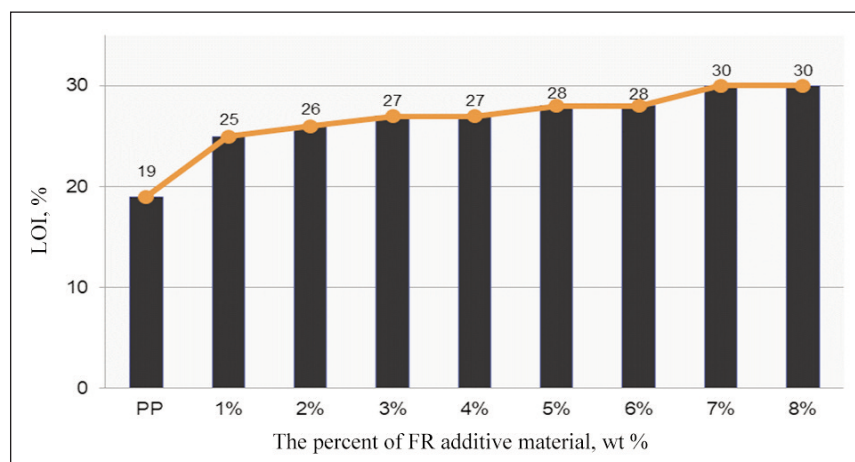


Fig. 5. Effect of flame-retardant additives on LOI value of PP knitted fabrics

can be improved significantly by the organophosphate-based additive.

Investigation of the lifetime and performance of the functional properties (such as non-flammability) of fabrics is an important issue. Investigation of the flammability performance of fabrics after washing and abrasion was determined as the next study. In addition, the effect of permeability properties of knitted fabrics on non-flammability is another important research topic. Also, another future work is currently

being prepared and the subject of this study is examining the burning behaviour of these fabrics. Images of samples before and after the vertical flame test will be given in this future work.

ACKNOWLEDGEMENTS

This work was financially supported by the "Turkey Ministry of Science, Industry and Technology" within the research program called SAN-TEZ, Project Number: 00428.STZ.2009-2.

REFERENCES

- [1] Zhang, S., Horrocks, A.R., *Review of flame retardant polypropylene fibres*, In: Progress in Polymer Science, 2003, 28, 11, 1517–1538, <https://doi.org/10.1016/j.progpolymsci.2003.09.001>
- [2] Li, Q., Jiang, P., Su, Z., Wei, P., Wang, G., Tang, X., *Synergistic effect of phosphorus, nitrogen, and silicon on flame-retardant properties and char yield in polypropylene*, In: Journal of Applied Polymer Science, 2005, 96, 3, 854–860, <https://doi.org/10.1002/app.21522>
- [3] Fontaine, G., Bourbigot, S., Duquesne, S., *Neutralized flame retardant phosphorus agent: facile synthesis, reaction to fire in PP and synergy with zinc borate*, In: Polymer Degradation and Stability, 2008, 93, 68–76, <https://doi.org/10.1016/j.polymdegradstab.2007.10.019>
- [4] Song, L., Hu, Y., Lin, Z., Xuan, S., Wang, S., Chen, Z., Fan, W., *Preparation and properties of halogen-free flame-retarded polyamide 6/organoclay nanocomposite*, In: Polymer Degradation and Stability, 2004, 86, 535–540, <https://doi.org/10.1016/j.polymdegradstab.2004.06.007>
- [5] Wang, L., Kang, H., Wang, S., *Solubilities, thermostabilities and flame retardance behaviour of phosphorus-containing flame retardants and copolymers*, In: Fluid Phase Equilibria, 2007, 258, 2, 99–107, <https://doi.org/10.1016/j.fluid.2007.04.031>
- [6] Xiao, J., Hu, Y., Yang, L., Cai, Y., Song, L., Chen, Z., Fan, W., *Fire retardant synergism between melamine and triphenyl phosphate in poly(butylene terephthalate)*, In: Polymer Degradation and Stability, 2006, 91, 9, 2093–2100, <https://doi.org/10.1016/j.polymdegradstab.2006.01.018>
- [7] Mikučionienė, D., Milašiūtė, L., Baltušnikaitė, J., Milašius, R., *Influence of plain knits structure on flammability and air permeability*, In: Fibres & Textiles in Eastern Europe, 2012, 20, 5, 94, 66–69
- [8] Özcan, G., Dayıoğlu, H., Candan, C., *Effect of Gray Fabric Properties on Flame Resistance of Knitted Fabric*, In: Textile Research Journal, 2003, 73, 10, 883–891, <https://doi.org/10.1177/004051750307301006>
- [9] Bivainytė A., Mikučionienė D., *Investigation on the air and water vapour permeability of double-layered weft knitted fabrics*, In: Fibres & Textiles in Eastern Europe, 2011, 19, 3, 86, 69–73, <https://doi.org/10.5755/j01.ms.18.3.2438>
- [10] Hacıoğulları, S.O., Babaarslan, O., *Structural analysis and mechanical properties of polypropylene filament yarns containing flame retardant additive*, In: 15th Romanian Textiles and Leather Conference-CORTEP-2014, 2014, Poiana Braşov, Romania, 25–30
- [11] Hacıoğulları, S.O., *Design and manufacture of laboratory type filament yarn machine and development of original product*, Doctoral dissertation, Çukurova University, Adana, Turkey, 2014, Available at: <http://libra.cu.edu.tr/libra.aspx?IS=DETAY&KN=9994> [Accessed on March 2021]
- [12] BS EN ISO 2062. *Textile-yarns from packages: Determination of single-end breaking force and elongation at break*, 1995
- [13] DIN 53817-1. *Textile-testing of textiles: Determination of unevenness of slivers and yarns; general basis*, 1983
- [14] ASTM D 6413. *Standard test method for flame resistance of textiles (Vertical test)*, 2011
- [15] ASTM D 2863–10. *Standard test method for measuring the minimum oxygen concentration to support candle-like combustion of plastics (Oxygen index)*, 2009
- [16] Fenimore, C.P., *Candle-type test for flammability of polymers*, In: Flame Retardant Polymeric Materials, 1975, 1, 371–397, https://doi.org/10.1007/978-1-4684-2148-4_9
- [17] Horrocks, A.R., Tunc, M., Price, D., *The burning behavior of textiles and its assessment by oxygen index methods*, In: Textile Progress, Harrison, PW: Manchester, 1989, 18, 1, 1–205, <https://doi.org/10.1080/00405168908689004>
- [18] Almeras X., Le Bras M., Hornsby P., Bourbigot S., Marosi Gy., Keszei S., Poutch F., *Effect of fillers on the fire retardancy of intumescent polypropylene compounds*, In: Polymer Degradation and Stability, 2003, 82, 325–331, [https://doi.org/10.1016/S0141-3910\(03\)00187-3](https://doi.org/10.1016/S0141-3910(03)00187-3)

Authors:

ÖZKAN HACIOĞULLARI SELCEN, BABAARSLAN OSMAN

Çukurova University, Textile Engineering Department, Balcalı Campus, 01330, Adana, Turkey
e-mail: teksob@cu.edu.tr

Corresponding author:

ÖZKAN HACIOĞULLARI SELCEN
e-mail: selcenozkan@gmail.com

Effect of trade barriers on export performance during COVID-19 pandemic: a comparative study among South Asian textile industries

DOI: 10.35530/IT.074.02.2021110

SADIA AZIZ
MUHAMMAD ABDULLAH KHAN NIAZI
USMAN GHANI

SAMRA KIRAN
MISBAH NOOR

ABSTRACT – REZUMAT

Effect of trade barriers on export performance during COVID-19 pandemic: a comparative study among South Asian textile industries

The study focused on determining essential government policies and trade barriers affecting the textile industry's export performance during the COVID-19 pandemic. This study has analysed the effect of government export policies on the export performance of the textile industry. This study has also compared factors among three South Asian textile industries, including Pakistan, India, and Bangladesh. The study identified nine essential government export policies and trade barriers based on Industrial Organization View (I/O View). A panel regression model was used to analyse the significance of each government policy and trade barrier affecting textile export performance. Results of the study showed that currency exchange rates, the cost to export, time to export, political stability of the country, quality of infrastructure in the country, freedom from corruption, business cost of terrorism and economic stability in the country have a significant effect on export performance of the industry. In contrast, taxes on doing business have an insignificant effect on export performance. The Seemingly Unrelated Estimation (SUEST) test compared the differences in export performance of Pakistani, Indian and Bangladeshi textile industries due to government policies. The results showed that a higher level of time to export, cost to export and business cost of terrorism lead to the low export performance of the textile industry. At the same time, a higher level of currency exchange rates, political stability of the country, quality of infrastructure, freedom from corruption and economic stability in-country lead to the high export performance of the textile industry. Further, taxes on doing business have an insignificant effect on export performance.

This study is among the few contributing to the textile industry during the COVID-19 pandemic. Due to uncertain circumstances, it becomes hard for the government to identify important factors which could help textile exporters to survive and grow during the COVID-19 pandemic. The study has identified important government policies and trade barriers affecting textile exports based on strong theoretical support and has also compared and elaborated on the importance of each factor across three South Asian countries. This study will help policymakers reconsider export-related factors to enhance their textile exports and revive their economy after the COVID-19 pandemic.

Keywords: COVID-19 pandemic, export performance, textile industry, industrial organization view

Influența barierelor comerciale asupra performanței exporturilor în timpul pandemiei de COVID-19: un studiu comparativ între industriile textile din Asia de Sud

Studiul s-a concentrat pe determinarea politicilor guvernamentale esențiale și a barierelor comerciale care afectează performanța exporturilor industriei textile în timpul pandemiei de COVID-19. Acest studiu a analizat influența politicilor guvernamentale de export asupra performanței la export a industriei textile. Acest studiu a comparat, de asemenea, factori din trei industrii textile din Asia de Sud, respectiv Pakistan, India și Bangladesh. Studiul a identificat nouă politici guvernamentale de export esențiale și bariere comerciale bazate pe vizualizarea organizației industriale (Vizualizarea I/O). A fost utilizat un model de regresie de tip panel pentru a analiza semnificația fiecărei politici guvernamentale și barierele comerciale care afectează performanța exporturilor de produse textile. Rezultatele studiului au arătat că ratele de schimb valutar, costul de export, timpul de export, stabilitatea politică a țării, calitatea infrastructurii din țară, libertatea din corupție, costul de afaceri al terorismului și stabilitatea economică în țară au un efect semnificativ asupra performanței la export a industriei. În schimb, taxele pentru desfășurarea afacerilor au un efect nesemnificativ asupra performanței la export. Testul de Estimare aparent fără legătură (SUEST) a comparat diferențele de performanță la export ale industriilor textile din Pakistan, India și Bangladesh datorate politicilor guvernamentale. Rezultatele au arătat că un nivel mai ridicat de timp pentru export, costul de export și costul pentru desfășurarea afacerilor terorismului duc la performanța scăzută la export a industriei textile. În același timp, un nivel mai ridicat al cursurilor de schimb valutar, stabilitatea politică a țării, calitatea infrastructurii, libertatea din corupție și stabilitatea economică în țară duc la performanțe ridicate la export ale industriei textile. Mai mult, taxele pentru desfășurarea afacerilor au un efect nesemnificativ asupra performanței la export.

Acest studiu este printre puținele care abordează industria textilă în timpul pandemiei de COVID-19. Din cauza circumstanțelor incerte, va fi greu pentru guvern să identifice factori importanți care ar putea ajuta exportatorii de textile să supraviețuiască și să se dezvolte în timpul pandemiei de COVID-19. Studiul a identificat politici guvernamentale importante și bariere comerciale care afectează exporturile de textile pe baza unui sprijin teoretic solid și a comparat și a elaborat, de asemenea, importanța fiecărui factor în trei țări din Asia de Sud. Acest studiu va ajuta factorii de decizie să-și reconsidere factorii legați de export pentru a-și spori exporturile de textile și pentru a-și relansa economia după pandemia de COVID-19.

Cuvinte-cheie: pandemie de COVID-19, performanță la export, industria textilă, vizualizarea organizației industriale

INTRODUCTION

The COVID-19 pandemic has hit the economies of countries all over the world. Overall, industries and businesses worldwide have been suffering during the COVID-19 pandemic. The textile industry is the most affected industry, along with tourism and hoteling, due to the forced change in the consumption behaviour of consumers during the COVID-19 lockdown. Currently, selling and buying habits have changed. At the organisational level, the governments have also reacted and changed their trade policies in reaction to the international scenario [1]. The global sales of textile and fashion brands decreased by 11% in 2020–2021 compared to 2019. It is further expected that the industry will experience a decline of up to 30% in the coming six months. The export volume for almost every country is noticeably decreased during the COVID-19 pandemic, as shown in figure 1. Even China and the European

Union, the leading textile and clothing exporters, have faced an export decline of 6.6% and 8.2%, respectively, from 2020 to 2021. Customers' purchase behaviour has also changed; they focus more on primary clothing products than fashion brands. In addition, the Work From Home (WFH) culture has changed the clothing preferences of consumers [2]. South Asian countries, including India and Pakistan, significantly contribute to world export, as shown in figure 2. The share of India is 4.2%, and Pakistan contributes 2% in overall world textile exports. Still, while many countries are well-positioned in the raw materials or the production stage of the textile and apparel Global Value Chain (VGC), they are only playing a limited role in the absence of retail (comprised of marketing, branding and sales). Thus, they have the potential waiting to be unlocked to reap more benefits from the global markets [3]. Many countries are well-positioned in the raw materials or the production stage of the textile and apparel

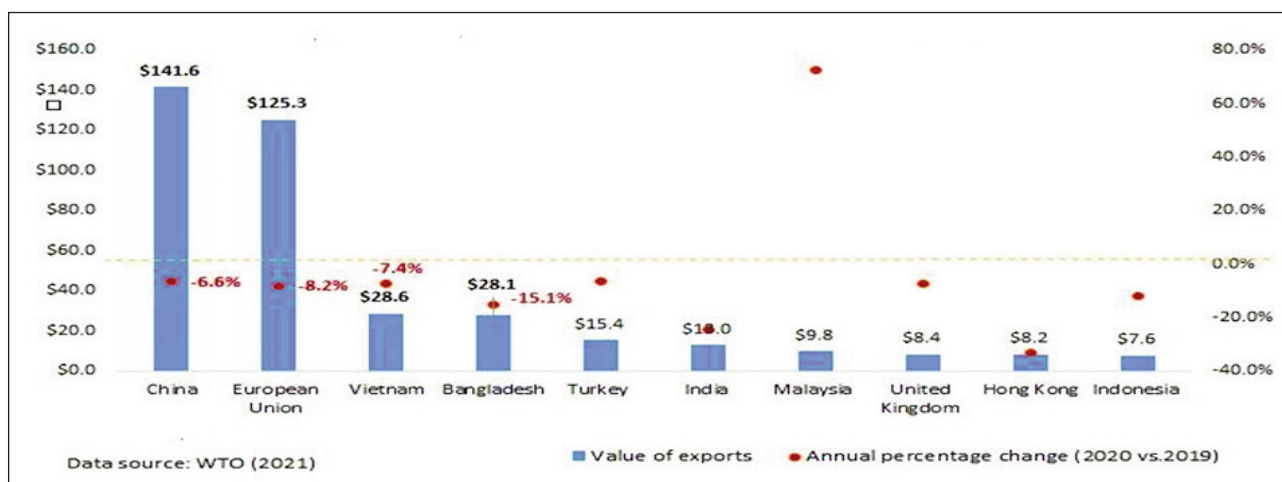


Fig. 1. Percentage change in exports during 2020–2021 [1]

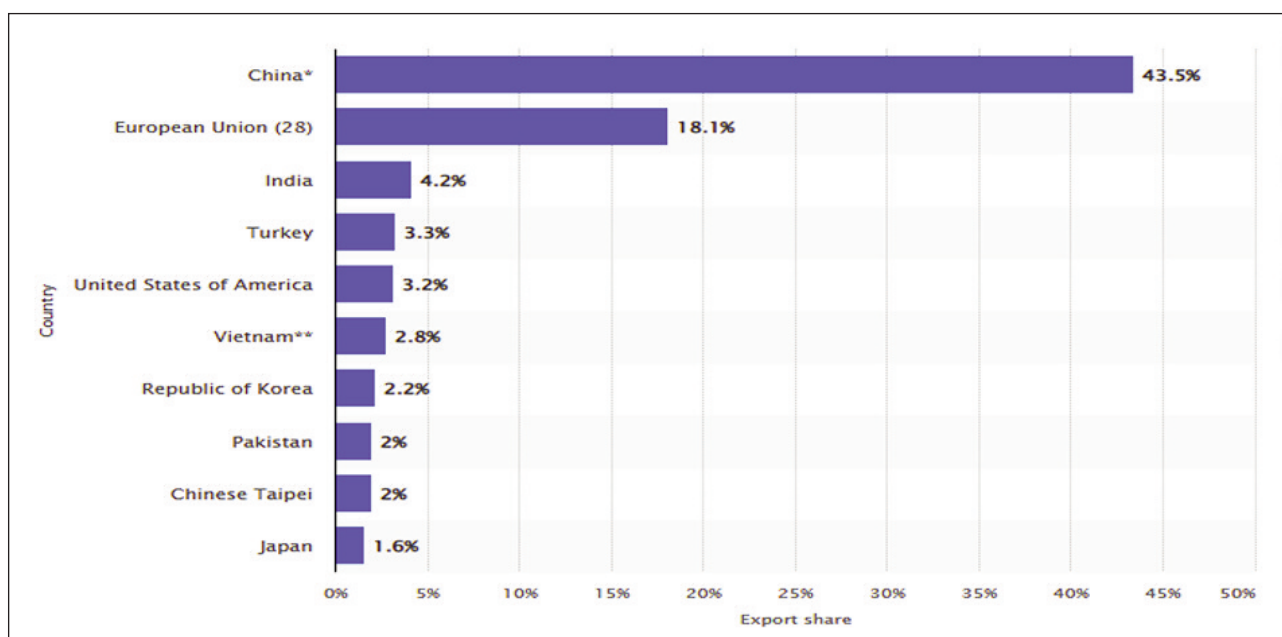


Fig. 2. Share in world exports of the leading clothing exporters in 2020, by country

Global Value Chain (GVC); they are only playing a limited role in the absence of retail (comprised of marketing, branding and sales). Thus, they have the potential waiting to be unlocked to reap more benefits from the global markets [3].

Now, governments are trying to influence industry-related factors to ease the pressure on the export industry. Textile export-dependent countries like Pakistan, China, India, and Bangladesh are developing more export-friendly policies in the region. Different government policies and trade barriers, including the cost of doing business, tax on exports, time to export, and other factors, have been changed. Countries are trying to develop export-friendly policies in reaction to the international business scenario as exports assist in the economic development and growth of a country. Countries interact and make relationships through international trade to achieve their economic goals [4]. Exports help improve foreign exchange reserves and increase economic growth and expansion opportunities. Exports enhance the level of competition, enhance technology acceptance and enhance the knowledge and skills of the workforce in a country [5].

Exports-led growth of East Asian countries and India and China's recent high export achievements have brought export promotion to the forefront in the development policy agendas of most developing countries [6]. The behaviour of the Asian textile industry is uncertain because of differences in economic levels, trade policies and political uncertainty. Initially, cheap labour and low cost of production were supposed to be the critical determinants of export performance. Asian countries such as Bangladesh, China and Thailand have achieved the lowest production cost and earned high positions as international textile exporters [7].

It has become hard for exporting firms to work in the international market because of high international trade barriers during the COVID-19 pandemic. Now exporting firms from developing countries are asking for export subsidies. In this downturn of economies, it is hard for developing countries to offer subsidies. The only solution is to make export-friendly policies and reduce trade barriers for textile exporters. The current study identifies essential government policies and trade barriers affecting export performance. The study focused on determining important textile-related government policies and trade barriers contributing to the industry's export performance during the COVID-19 pandemic. The study has identified nine government policies and trade barriers based on Industrial Organization View (I/O View).

LITERATURE REVIEW

Coronavirus SARS-CoV-2 (severe acute respiratory syndrome coronavirus 2, COVID-19) has drastic impacts on the economy and global health. According to WHO, over 274M cases were confirmed across the globe, and 5.35M deaths were reported cumulatively on 29th December 2021. The pandemic of

COVID-19 has shown a severe impact concerning transmissibility and mortality compared to previous viruses such as influenza in countries worldwide. COVID-19 impacted international trade significantly and in various ways. In exporting countries, the COVID-19 damage manifested as a reduction in the production scale and the export supply. Exports are expected to drop, particularly in manufacturing industries and specifically in countries where remote work/operation is less feasible. The COVID-19 damage in an importing country is mainly due to the decrease in aggregate demand. Reduced people's earnings and limited visits to retail outlets led to low demand [8].

At the beginning of the first wave, it was not known how to "behave" during the COVID-19 pandemic. Many countries forced people to stay at home, and all operational activities were suspended [9]. COVID-19 has increased trade costs among countries. For instance, high infection and death cases reduced the workforce, including port workers and truck drivers in the transport and shipping sectors. Lockdown policies and port restrictions reduce air flights and marine transportation between countries [10]. According to Lau et al. [11], container transportation through ships decreased by 29% compared to 2019 in the first week of April 2020. These issues in the transportation industry have decreased export performance.

Theoretical framework and hypotheses

The I/O view explains the critical determinants of export performance across industries. It focuses on the characteristics of industry (external factors of the firm) such as tariffs, political stability, technological change, export promotion program, barriers to market entry and infrastructure of the country [9]. According to the Industrial Organization View, government policies and trade barriers substantially influence export performance [12]. Mason has proposed a strong relationship between the industry's structure and firm performance.

The Industrial Organization View has four underlying assumptions. First, top management must have a high commitment to developing and implementing export strategies. Second, firms competing within an industry must have common relevant resources and should develop similar strategies with the help of those resources. Third, the resources and capabilities of firms must be highly mobile across firms. Fourth, government policies and trade barriers create pressure and constraints, which lead to high export performance strategies [13].

Researchers have also paid good attention to government policies and trade barriers affecting the industry's export performance [14]. LiPuma and Park found that trade barriers, including tax and corruption in a country, harmed export performance [15]. Government policies and trade barriers, including the cost of doing business, availability of electricity, road facilities and economic situation in a country, are considered significant determinants of industry export performance [16]. Researchers have considered the

Industrial Organization View a reliable predictor of high export performance [17]. Athukorala found exporting firms cannot survive in the international market without having a complete analysis of the industry [18]. This study has given great importance to government policies and trade barriers and considers the following determinants of export performance derived from the Industrial Organization View.

Currency exchange rates

The currency exchange rate is a significant determinant of export performance and predicts the industry's export performance. The currency exchange rate is essential in enhancing the industry's export performance [19]. Limao and Venables found that depreciation in currency results in low prices of products in the international market and high export performance of the industry [20]. Depreciation of currency offers high profits to exporters and vice versa [21]. The COVID-19 pandemic has also affected the currency market [22]. The dollar gained strength at the beginning of the pandemic, and the currency of developing countries depreciated over time. Though international trade declined during the pandemic due to the depreciation in currency against the dollar, many developing countries got benefited from exports [23]. Therefore, based on the previous literature, the following hypotheses are proposed:

H1 (a): Depreciation of currency in a country positively affects the industry's export performance.

H1 (b): High depreciation of the currency in a country will lead to the high export performance of the industry

Cost to export

Hummels and Klenow [24] estimated the cost to export for developing countries, and their findings revealed that developing countries have a 55% higher cost to export than developed countries. These findings show that the high cost to export slows down a country's export growth. Yasar [25] pointed out some reasons for the high cost to export, including poor infrastructure, poor law and order situations and energy crises in the country. Cost to export remained a significant trade barrier to the high export performance of industry [26]. During the COVID-19 pandemic, countries failed to provide sufficient infrastructural facilities to exporters, which resulted in low export performance [27]. Moreover, the lack of international transportation services, including air cargo and ship cargo services, cost almost three times during the COVID-19 pandemic, which increased the cost of exports significantly [28]. Therefore, based on the previous literature, the following hypotheses are proposed:

H2 (a): Cost to export in a country has a negative effect on the industry's export performance.

H2 (c): High cost to export in the country will lead to the low export performance of the industry.

Time to export

Researchers have suggested time to export as a significant determinant of industry export performance [29]. Differences exist in the time required to perform export activities across countries. For China, Indonesia and Australia, the average time to export a 20-foot container from the production unit to the port, including all formalities, is 18 days. For Bangladesh and Sri Lanka, the average time to export is 32 days [30]. Time delay due to the unavailability of international transportation services during COVID-19 has created problems for exporters [31]. According to Hummels [32], the time to export has increased by almost 30% because of the unavailability of transportation services and trade restrictions during COVID-19 spreads. Therefore, based on the previous literature, the following hypotheses are proposed:

H3 (a): Time to export in a country has a negative effect on the export performance of the industry.

H3 (b): The requirement for more time to export in a country will lead to the low export performance of the industry.

Political stability in the country

According to Kessides [33], political instability is when the government is forced to go or is taken over following a coup, and the machinery of governance is confronted by groups working from outside the normal process of the political system. Political stability plays a vital role in the international trade of a country. The country's political conditions mainly depend on high-quality control by the government [34]. Political consistency in a country portrays an excellent image to the rest of the world, and political instability adversely affects exports [35]. Almost all countries have redefined their international trade policies during the COVID-19 pandemic [36]. Travelling restrictions, quarantine policies, and trade policies have influenced exports negatively [37]. Therefore, based on the previous literature, the following hypotheses are proposed:

H4 (a): Political stability in a country positively affects industry export performance.

H4 (b): High political stability in a country will lead to high export performance of the industry.

Quality of infrastructure in the country

Valbona et al. [38] argued that a potent infrastructure in a country reduces export costs and improves international trade. Export growth depends on tariff liberalisation and the quality of infrastructure and related services [39].

Arize et al. [40] have pointed out the reasons for the low export performance of the industry. According to them, poor transportation facilities and interrupted supply of electricity and gas to the industry are the main reasons for low export performance. Poor infrastructure in a country makes it difficult for firms to compete in the international market, as they cannot

ensure low-cost and timely delivery [41]. Ocampo and Guerra [42] suggest that most firms do not even think to participate in international trade because of poor infrastructure. Countries can improve their export performance by improving electricity supply, telephonic services and road facilities [43]. Due to economic crises during the COVID-19 pandemic, most developing countries are trying to improve their country's health infrastructure. As a result, trade infrastructure has been ignored [44]. Therefore, based on the previous literature, the following hypotheses are proposed:

H5 (a): The quality of infrastructure in a country positively affects industry export performance.

H5 (b): High quality of infrastructure in a country will lead to the high export performance of the industry.

Freedom from corruption

According to Marks et al. [45], corruption exists in a country whenever an official has discretion in granting the distribution of a "good" or avoidance of a "bad" in the public sector. Warr [46] has argued that corruption in both tangible (such as ineffective government administration) and intangible (such as the loss of trust in the economy) forms negatively affect the industry's export performance. According to the Corruption Perceptions Index 2021(CPI) report, the corruption level in developing countries has increased during the COVID-19 pandemic. Due to instability in the government export policies during COVID-19, it has been reported that in some developed countries, government officials are asking for bribes to facilitate the export process [47]. Therefore, we propose the following hypotheses:

H6 (a): Freedom from corruption positively affects the industry's export performance.

H6 (b): High level of freedom from corruption will lead to the high export performance of the industry.

The business cost of terrorism

According to Hamzah [48], terrorism is a planned political or non-politically influenced aggression against non-militants. The COVID-19 pandemic has created health-threat in the security workforce, and security workers are hesitant to contact other persons personally. Due to a less secure workforce and the risk of COVID-19 transfer, security workers are not as effective as in the pre-COVID-19 situation. Therefore there is more threat of terrorism, which could affect exports negatively [36]. Ackerman and Peterson [49] described terrorism as an activity of violence against people or government to achieve social, political or ideological objectives. Terrorism incidents affect the export performance of countries in the long run. In developing countries, the adverse effects of terrorism activities are seen immediately after the incident [50]. According to Valbona [51], an uncertain security situation negatively affects importers' purchasing behaviour. Therefore, based

on the previous literature, the following hypothesis is proposed:

H7 (a): The business cost of terrorism in the country has a negative effect on the export performance of the industry.

H7 (b): High business cost of terrorism in a country will lead to low export performance of the industry.

Economic stability of the country

Espinosa-Méndez and Arias [52] have suggested that economic instability has a negative effect on the export performance of countries in both the short run and the long run. Arize et al. [53] investigated the effect of financial instability across developed and developing countries, including Chile, Colombia, Denmark, Japan, Kenya, Malaysia and Uruguay. Their findings indicate that financial instability negatively affects the export performance of developing countries [41]. Another group of studies on developing countries showed the negative effect of economic instability on countries' export performance. After examining economic instability in 21 African countries, Ocampo and Guerra [52] concluded that unstable economic indicators affect export performance negatively. COVID-19 has hit the economies of many developed and developing countries [54]. Padhan and Prabheesh [55] have categorised the economic effect of COVID-19 into two categories, decreased supply due to a reduction in the business working hours and decline in aggregate demand due to unemployment because of lockdowns which ultimately affects export negatively. Liu et al. [56] claimed that COVID-19 has affected the economy by reducing employment and increasing international transaction costs, and demand reduction. So, we propose the following hypotheses:

H8 (a): Economic stability in a country positively affects industry export performance.

H8 (b): High economic stability in a country will lead to high export performance of the industry.

Taxes on doing business

Researchers have studied the effect of taxation on export performance [44]. Marks et al. [45] studied the direct effect of taxation on export performance. Their results showed that tax on doing business significantly affects countries' export performance. Warr [46] examined the effect of tax on doing business and found that tax had a negative effect on countries' export performance. Zulkarnaen et al. [57] conducted a similar study and calculated economic gains and losses due to taxes on businesses. His results showed that export drops in periods of high taxation. Countries have changed their tax policies during COVID-19 because of limited trade activities. Many countries offered tax relaxation for the business community to survive during a pandemic [58]. For exporters, subsidies were offered, and many countries reduced monetary trade barriers to encourage international trade [58]. Therefore, based on the previous literature, the following hypothesis is proposed:

- H9 (a): Taxes on doing business in the country have a negative effect on the export performance of the industry.
- H9 (b): High taxes on doing business in a country will lead to low export performance of the industry.

RESEARCH METHODOLOGY AND METHODS

The research employed a quantitative method to test hypotheses empirically. Country-level secondary data for three countries' government policies and trade barriers have been used. Monthly base data from November 2020 to November 2021 has been considered to explain government policies and trade barriers regarding exports. Data for currency exchange rates, cost to export, time to export, political stability of the country, quality of infrastructure, freedom from corruption, business cost of terrorism and economic stability of country and Taxes on doing business is purchased from the Global Competitiveness Index, 2021.

To test the model, Panel Regression Models were used for panel data. Panel Regression models included Pooled OLS Model, Random Effect Model and Fixed Effect Model. Panel diagnostic tests, including the Chow test, Breusch-Pagan test and Hausman Specification Test, were used to choose the appropriate model. The white test was used to examine the problem of heteroscedasticity in the data. The Variance Inflation Factor test (VIF) was used to examine the multicollinearity problem of the data.

The difference in export performance of Pakistani, Indian and Bangladeshi textile industries was compared due to differences in government policies and trade barriers. Differences in the effect of government policies and trade barriers on export performance were compared with the Seemingly Unrelated Estimation (SUEST) test in Stata software.

RESULTS AND ANALYSIS

Analysis of government policies and trade barriers affecting the export performance of the industry

The Panel Regression model examined the significance of nine government policy-related factors of export performance.

Panel diagnostic tests

The study used Panel Regression models for the panel data. Diagnostic tests such as the Chow test, Breusch-Pagan test and Hausman specification test were used to find the appropriate Panel Regression model. Panel diagnostics tests are explained below.

Chow test

To select the most suitable model between a pooled regression and a fixed-effect model, the Chow test was used. If P's value is greater than 0.05, then the pooled Ordinary least squares are considered the appropriate model. The minimum P-value required for the model is given below. The results from table 1

show that the P-value (0.173073) is greater than 0.05; hence we conclude that the pooled Ordinary least squares model is better than the fixed effect model.

Table 1

SUMMARY OF THE PANEL DIAGNOSTIC TESTS			
Tests	Null hypothesis (H0)	P-Value	Recommended model
Chow test	Pooled Ordinary least squares model is better than Fix Effect Model	0.17308	Pooled OLS model
Breusch-Pagan test	Pooled Ordinary least squares model is better than Random Effect Model	0.34692	Pooled OLS model

Breusch-Pagan test

Breusch-Pagan test was used to decide the best model between Pooled OLS model and the random effect model. The results from table 1 show that the P-value (0.346917) is greater than 0.05; hence pooled OLS is better than the random-effects model. Thus, based on the Chow and Breusch-Pagan test, we concluded that the pooled OLS model is better than the random effect and fixed-effect models.

Assumptions for the Panel Regression model

Assumptions for the Panel Regression model (heteroscedasticity and multicollinearity) were satisfied through the following tests.

Test for heteroscedasticity

A heteroscedasticity problem occurs when variance is not constant for all observations. The basic assumption of ordinary least square is constant variables, i.e. the variables must be homoscedastic. To check this assumption, the White test was used. The P-value of the White test must be greater than 0.05.

Table 2

WHITE'S TEST OF HETEROSCEDASTICITY	
Chi ²	P-Value
20.549695	0.302737

The variance in the data is constant. As shown in table 2, P-value is greater than 0.05. So, there is no problem of heteroscedasticity in the data.

Test for multicollinearity

To check the multicollinearity among the independent variables in the data, the Variance Inflation Factor (VIF) was used.

Table 3

VIF FOR GOVERNMENT POLICIES AND TRADE BARRIERS AFFECTING EXPORT PERFORMANCE OF INDUSTRY	
Government Policies and Barriers	VIF
Currency exchange rates	2.086
Cost to export	1.539
Time to export	2.137
Political stability in the country	1.829
Quality of infrastructure in the country	1.058
Freedom from corruption	2.294
Business cost of terrorism	1.666
Economic stability in the country	2.753
Tax on doing business	2.971

Results of VIF in table 3 indicate that all the variance inflation factor test values are below 10. So, there is no problem with multicollinearity in the model.

Hypotheses testing

The pooled regression model was used to examine the significant effect of government policies and trade barriers on the industry's export performance.

Analysis of Pooled Regression Model

Table 4 reports the results of the pooled regression. The R-square value of 38.96% reflects that a reasonable proportion of variance in export performance is explained by currency exchange rates, the cost to export, time to export, political stability of the country, quality of infrastructure, freedom from corruption, business cost of terrorism and economic stability of the country. In table 4, F-value and its underlying P-value show the overall fitness of the model. Since the P-value is less than 0.05 (0.000), it indicates a good model fit.

Hypotheses results

Results in table 4 show that Currency exchange rates (H1a), Political stability of the country (H4a), Quality of infrastructure in the country (H5a), Freedom from

corruption (H6a) and Economic stability in the country (H8a) have a significant positive effect on export performance. While the cost to export (H2a), time to export (H3a), and business cost of terrorism (H7a) has a significant negative effect on export performance. Tax on doing business (H9a) has an insignificant effect on export performance. Therefore except for Taxes on doing business, all hypotheses are accepted.

Comparative analysis of government policies and trade barriers and export performance

Results in table 5 show that the mean coefficient value of the currency is more depreciated for Pakistan and has a high positive effect on the export performance of the Pakistani textile industry compared to the Bangladeshi and Indian textile industries. So, we accept H1 (b).

Results in table 5 show that the mean coefficient value of cost to exports is high for Bangladesh and also has a high negative affects on the Bangladeshi textile industry's export performance compared to the Pakistan and Indian textile industry. Therefore, we accept H2 (b).

Results in table 5 show that the mean coefficient value of time to exports is high for Bangladesh and has a higher negative effect on the Bangladeshi textile industry's export performance than the Pakistan and Indian textile industry. Therefore, we accept H3 (b).

Results in table 5 show that the mean coefficient value of political stability is high for Indian and has a higher positive effect on the export performance of the Indian textile industry as compared to Bangladesh and Pakistan. Therefore, we accept H4 (b).

Results in table 5 show that the mean coefficient value of the quality of infrastructure is higher for India and has a higher positive effect on the export performance of the Indian textile industry. Hence, we accept H5 (b).

Results in table 5 show that the mean coefficient value of freedom from corruption is higher for India

Table 4

POOLED OLS MODEL GOVERNMENT POLICIES AND TRADE BARRIERS AFFECTING EXPORT PERFORMANCE OF INDUSTRY							
Firm's external factors	Coefficient	Std. Error	t-ratio	p-value	R-square	F	P-value
Constant	23.5926	0.330416	71.402	0.0000	0.389	29.3	0.000
Currency exchange rates	0.0104114	0.0014836	7.0174	0.0000			
Cost to export	-0.0004054	0.0001551	-2.614	0.0165			
Time to export	-0.0305705	0.0035951	-8.503	0.0000			
Political stability of the country	0.609771	0.0437238	13.946	0.0000			
Quality of infrastructure in the country	0.248317	0.0467149	5.3156	0.0000			
Freedom from corruption	0.0057723	0.0020482	2.8183	0.0106			
Business cost of terrorism	-0.0498401	0.0222966	-2.235	0.0369			
Economic stability in the country	0.0098918	0.0046291	2.1368	0.0451			
Taxes on doing business	-0.0003122	0.0009051	-0.345	0.7337			

COMPARATIVE ANALYSIS OF GOVERNMENT POLICIES AND TRADE BARRIERS							
External factor	Countries	Coefficients	T	Sig.	SUEST Test for comparison of coefficients		
					Differences In coefficients	Chi ²	SIG.
Currency exchange rates	Bangladesh	0.0551384	5.49	0.00	Bangladesh: India	1.21	0.230
	India	0.0155939	3.41	0.00	Pakistan: Bangladesh	15.80	0.00
	Pakistan	0.1077742	6.53	0.00	India: Pakistan	14.41	0.00
Cost to export	Bangladesh	-0.0953443	-9.22	0.00	Bangladesh: India	5.89	0.00
	India	-0.0546394	-8.05	0.00	Pakistan: Bangladesh	9.22	0.00
	Pakistan	-0.0113381	-7.05	0.00	India: Pakistan	5.52	0.00
Time to export	Bangladesh	-0.119794	-9.97	0.00	Bangladesh: India	7.18	0.00
	India	-0.0523489	-8.56	0.00	Pakistan: Bangladesh	11.52	0.00
	Pakistan	-0.0310657	-3.37	0.00	India: Pakistan	0.16	0.875
Political stability in the country	Bangladesh	0.1627201	5.29	0.00	Bangladesh: India	9.15	0.00
	India	2.49915	4.19	0.00	Pakistan: Bangladesh	0.323	0.747
	Pakistan	0.1247469	6.19	0.00	India: Pakistan	10.21	0.00
Quality of infrastructure in the country	Bangladesh	0.2079503	3.84	0.00	Bangladesh: India	8.28	0.00
	India	0.9007808	5.45	0.00	Pakistan: Bangladesh	7.71	0.00
	Pakistan	0.7744854	7.089	0.00	India: Pakistan	8.09	0.19
Freedom from corruption	Bangladesh	0.0175171	6.28	0.00	Bangladesh: India	12.65	0.00
	India	0.0681908	5.99	0.00	Pakistan: Bangladesh	1.56	0.123
	Pakistan	0.0087161	9.08	0.00	India: Pakistan	14.25	0.00
Business cost of terrorism	Bangladesh	-0.7655221	10.36	0.00	Bangladesh: India	1.55	0.68
	India	-0.5133019	12.55	0.00	Pakistan: Bangladesh	6.22	0.01
	Pakistan	-1.18344	8.05	0.00	India: Pakistan	9.21	0.00
Economic stability in the country	Bangladesh	0.0150767	9.22	0.00	Bangladesh: India	11.28	0.00
	India	0.1353135	6.35	0.00	Pakistan: Bangladesh	9.56	0.00
	Pakistan	0.0053135	8.19	0.00	India: Pakistan	14.95	0.00
Tax on doing business	Bangladesh	-0.0025588	-3.25	0.00	Bangladesh: India	6.24	0.00
	India	-0.0545854	-4.02	0.00	Pakistan: Bangladesh	0.492	0.624
	Pakistan	-0.002554	-0.58	0.72	India: Pakistan	7.05	0.00

and has a higher positive effect on the Indian textile industry's export performance compared to the Bangladeshi and Pakistani textile industries. Therefore, we accept H6 (b).

Results in table 5 show that the mean coefficient value of the business cost of terrorism is worst for Pakistan and has a more negative effect on textile exports than the Bangladeshi and Indian textile exports. So, we accept H7 (b).

Results in table 5 show that the mean coefficient value of economic stability is higher for Indians and has a higher positive effect on the export performance of the Indian textile industry compared to the Pakistan textile industry. So, we accept H8 (b).

Results in table 5 show the insignificant effect of taxes on doing business on the export performance of the Pakistani textile industry. So, based on insignificant results, we reject H9 (b).

CONCLUSION

This study is among the few contributing to the textile industry during the COVID-19 pandemic. Due to

uncertain circumstances, it becomes hard for the government to identify essential factors which could help textile exporters to survive and grow during the COVID-19 pandemic. The study has identified important government policies and trade barriers affecting textile exports based on strong theoretical support and has also compared and elaborated on the importance of each factor across three South Asian countries. This study will help policymakers reconsider export-related factors to enhance their textile exports and revive their economy during the COVID-19 pandemic.

The study focused on determining essential government policies and trade barriers affecting the textile industry's export performance during the COVID-19 pandemic. To achieve the objective, a study has identified nine textile export-related factors based on Industrial Organization View. The significance of each textile export performance factor was seen using the panel regression model. Results of the study showed that currency exchange rates, the cost to export, time to export, political stability of the country, quality of

infrastructure in the country, freedom from corruption, business cost of terrorism and economic stability in the country have a significant effect on export performance of the industry. In contrast, taxes on doing business have an insignificant effect on export performance. Supporting the study's findings, Collins and Gagnon [59] has discussed that the currency of developing countries has depreciated during the COVID-19 pandemic and resulted in high export returns. They also pointed out that the cost of imports increases with currency depreciation, and import-dependent industries may get affected negatively. Moreover, the findings of Barbero et al. [60] align with the current study results, as during the COVID-19 pandemic, countries have imposed trade restrictions that have increased the cost and time of exports and are negatively affecting exports. Supporting the findings of the study, Verschuur [61] indicated the negative effect of government policies on the export performance of the industry; moreover, they argued that the government had ignored infrastructure during the COVID-19 pandemic and the lack of political stability in the country has also increased worries for the exporters.

To identify the difference in export performance of Pakistani, Indian and Bangladeshi textile industries due to differences in the level of government policies and trade barriers, the Seemingly Unrelated Estimation test was used to compare the difference in export performance due to government policies and trade barriers of Pakistani, Indian and Bangladeshi textile industry. The results showed that a higher level of time to export, cost to export and business cost of terrorism lead to low export performance. At the same time, a higher level of currency exchange rates, political stability of the country, quality of infrastructure, freedom from corruption and economic stability in-country lead to high export performance. Further, taxes on doing business have an insignificant effect on export performance.

Bas et al. [62] have compared the cross-country data, and their results are aligned with the current study. According to their results, low trade restrictions and friendly export policies can enhance the country's export performance. Delays in the export process and healthcare measures for the employee during the COVID-19 pandemic have increased the cost of export. Countries that are imposing strict lockdowns, working from home, and forcing industries to purchase health care equipment resulted in high costs of production.

For policymakers, this study has identified important factors to work on to increase the export performance of the textile industry. Policymakers should decrease the export barriers by decreasing taxes, improving infrastructure, minimising time to export and improving law and order in the country. The depreciated currency could also be beneficial to enhancing the textile industry's export performance. Finally, corruption is the most critical barrier to export performance. Corruption increases the cost of doing business and morally demotivates firms to export. All sort of corruption is harmful to export performance.

Research has also significant managerial implications for exporting firms as efficient exporting strategies at the firm level are required to manage exports during COVID-19 successfully. Managers of the textile exporting firm should continuously review the national and international trade policies during the COVID-19 pandemic, as the current pandemic has created political and economic instability in the countries. So, exporting firms should monitor local and foreign countries' dynamic international trade policies. Due to transportation and carriage problems during COVID-19, exporting firms should efficiently manage production time to avoid delays in delivering products. Exporting firms should also determine their production cost by anticipating exchange rates and the cost of doing business before quoting rates. Work from home and lockdown have negatively affected the production process of exporting firms. Exporting firms should follow all standard operating procedures (SOPs) for COVID-19 in the workplace to protect their employees from infection so that they can work in a safe environment.

Though research has presented a comprehensive model to explore the effect of export barriers across South Asian countries, still some areas are required to be addressed in future studies. First of all, some firm-level capabilities can be included to compare internal and external factors contributing to export performance during COVID-19. Secondly, as the current study has only considered developing countries, future studies are required to empirically test and compare the presented model in developed and developing countries. Finally, the current study has only considered the data for the period of the COVID-19 pandemic; further study can also pre COVID-19 data to make a more depth comparison of factors affecting export performance.

REFERENCES

- [1] TO, *The COVID-19 pandemic and trade-related developments in Idcs*, 2021, Available at: https://www.wto.org/english/tratop_e/COVID19_e/Idcs_report_e.pdf [Accessed on December 5, 2021]
- [2] ITC, *Impact of COVID19 on the global market and local industry of textile & clothing*, 2020, Available at: https://www.intracen.org/uploadedFiles/intracenorg/Content/Redesign/Projects/GTEX/ImpactofCOVIDonTCindustry_Egypt_eng.pdf [Accessed on December 5, 2021]

- [3] Reliefweb, *How the textile industry can help countries recover from COVID-19*, 2020, Available at: <https://reliefweb.int/report/world/how-textile-industry-can-help-countries-recover-COVID-19> [Accessed on December 15, 2021]
- [4] Chaney, T., *Distorted gravity: the intensive and extensive margins of international trade*, In: American Economic Review, 2008, 98, 4, 1707–1721
- [5] Tiia, Vi., Oliver, L., Maria, J., Segovia, V., *Interconnecting exporter types with export growth and decline patterns: Evidence from matched mature Estonian and Spanish firms*, In: Review of International Business and Strategy, 2018, 28, 1, 61–76
- [6] Musleh, Ghani, E., Mahmood, T., *Determinants of Export Performance of Pakistan: Evidence From The Firm-Level Data*, In: The Pakistan Development Review, 2009, 48, 3, 227–240
- [7] Kumar, P., *Characteristics of Domestic Service Sector and Financial Enterprises of India in the Context of Export Performance*, In: Journal of International Economics, 2016, 7, 2, 13–22
- [8] Kumar, R., *Processed Food Industry in India: An Analysis of Export Competitiveness*, In: Clear International Journal of Research in Commerce & Management, 2017, 8, 2, 37–39
- [9] Hoskisson, R., Hitt, M., Wan, W., Yiu, D., *Theory and research in strategic management: Swings of a pendulum*, In: Journal of Management, 1999, 23, 3, 417–456
- [10] Bowman, E.H., Helfat, C.E., *Does corporate strategy matter?*, In: Strategic Management Journal, 2001, 22, 1, 1–23
- [11] Lau, C.K., To, K.M., Zhang, Z., Chen, J., *Determinants of competitiveness: Observations in China's textile and apparel industries*, In: China and World Economy, 2009, 17, 2, 45–64
- [12] Abraham, V., Sasikumar, S.K., *Labor cost and export behavior of firms in Indian textile and clothing industry*, In: Economics, Management, and Financial Markets, 2011, 6, 1, 258–282
- [13] Sultana, S., Alam, M.A., Saha, A.K., Ashek, U.M., Sarker, M.A.T., *Likely impacts of quota policy on RMG export from Bangladesh: Prediction and the reality*, In: International Journal of Business and Management, 2011, 6, 11, 275–284
- [14] Bilquees, F., Mukhtar, T., Malik, S.J., *Exchange rate volatility and export growth: Evidence from selected South Asian Countries*, In: Zagreb International Review of Economics and Business, 2010, 13, 2, 27–37
- [15] LiPuma, J.A., Park, S., *Venture capitalists' risk mitigation of portfolio company internationalization*, In: Entrepreneurship Theory and Practice, 2014, 38, 5, 1183–1205
- [16] Scherer, F.M., Ross, D., *Industrial Market Structure and Economic Performance*, Boston, MA: Houghton Mifflin, 1990
- [17] Palazzo, G., Rapetti, M., *Real exchange rate and export performance in Argentina, 2002–2008*, In: Journal of Post Keynesian Economics, 2017, 40, 1, 75–94
- [18] Athukorala, P., Jayasuriya, S., Oczkowski, E., *Multinational firms and export performance in developing countries: Some analytical issues and new empirical evidence*, In: Journal of Development Economics, 1995, 46, 1, 109–122
- [19] Nicholas, R.G., Jonathan, D.R., Edward, D.W., Andrew, T.W., *Forecasting foreign currency exchange rates for department of defense budgeting*, In: Journal of Public Procurement, 2017, 17, 3, 315–336
- [20] Limao, N., Venables, A.J., *Infrastructure, Geographical Disadvantage, Transport Costs, and Trade*, In: World Bank Economic Reviews, 2001, 15, 3, 451–479
- [21] Rudaheranwa, N., *Trade Policy and Transport Costs in Uganda*, 2006
- [22] Xinming, H., Zhibin, Lin., Yingqi, W., *International market selection and export performance: a transaction cost analysis*, In: European Journal of Marketing, 2016, 50, 5, 916–941
- [23] Djankov, S., Freund, C., Pham, C.S., *Trading on time*, In: The Review of Economics and Statistics, 2010, 92, 1, 166–173
- [24] Hummels, D., Klenow, P.J., *The variety and quality of a nation's exports*, In: American Economic Review, 2005, 95, 704–723
- [25] Yasar, M., Rejesus, M., Chen, Y., Chakravorty, U., *Political influence of firms in the tradables and non-tradables sectors: A cross-country analysis*, In: Economics and Politics, 2011, 23, 3, 297–312
- [26] Mamunur, R., Xuan, H.L., Shao, J.W., *Political stability and FDI in the most competitive Asia Pacific countries*, In: Journal of Financial Economic Policy, 2017, 9, 2, 140–155
- [27] Chor, F.T., Abosedra, S., *The impacts of tourism, energy consumption and political instability on economic growth in the MENA countries*, In: Energy Policy, 2014, 68, 458–464
- [28] Limao, N., Venables, A.J., *Infrastructure, Geographical Disadvantage, Transport Costs, and Trade*, In: World Bank Economic Reviews, 2001, 15, 3, 451–479
- [29] De Soto, H., *The Mystery of Capital: Why Capitalism Triumphs in the West and Fails Everywhere Else*, New York, NY: Basic Books, 2003
- [30] Nordas, H., Pinali, K.E., Grosso, M.G., *Logistics and Time as a Trade Barrier*, In: OECD Trade Policy Working, 2006, Papers no. 35
- [31] Zhiyang, W., Sizhong, Sun., *Transportation infrastructure and rural development in China*, In: China Agricultural Economic Review, 2016, 8, 3, 516–525
- [32] Hummels, D., *Time as a Trade Barrier*, GTAP Working Papers 1152, Center for Global Trade Analysis, Department of Agricultural Economics, Purdue University, 2001
- [33] Kessides, I.N., *Infrastructure privatization and regulation: Promise and perils*, In: The World Bank Research Observer, 2005, 20, 1, 81
- [34] Rose Ackerman, S., *Corruption and Government Causes, Consequences, and Reform*, Cambridge: Cambridge University Press, 1999
- [35] Ades, A., Tella, R., *Rents, competition, and corruption*, In: American Economic Review, 1999, 89, 4, 982–993
- [36] Whitaker, B., *The definition of terrorism*, 2001, Available at: www.guardian.co.uk [Accessed on June 2016]
- [37] Gearson, J., *The nature of modern terrorism*, In: The Political Quarterly, 2002, 73, 4, 7–24

- [38] Valbona, Z., Michael, R., Gary, K., *Terrorism, competitiveness, and international marketing: an empirical investigation*, In: International Journal of Emerging Markets, 2018, 13, 2, 310–329
- [39] Kant, I., *Fundamental Principles of the Metaphysics of Morals*, 2008
- [40] Arize, A.C., Osang, T., Slottje, D.J., *Exchange-rate Volatility in Latin America and Its Impact on Foreign Trade*, In: International Review of Economics & Finance, 2008, 17, 1, 33–44
- [41] Rousseau, P.L., Wachtel, P., *What is Happening to the Impact of Financial Deepening on Economic Growth?*, Working Papers 0915, Department of Economics, Vanderbilt University, 2009
- [42] Ocampo, J.A., Guerra, S.C., *Exports and Economic Development in Colombia: A Regional Perspective*, In: The First Export Era Revisited: Reassessing its Contribution to Latin American Economies, 2018, 23, 191–201
- [43] Martins, P., Yang, Y., *The impact of exporting on firm productivity: A metaanalysis of the learning-by-exporting hypothesis*, In: Review of World Economics, 2009, 145, 3, 431–445
- [44] Bruce, L., Perez-Garcia, J.M., *The Economic Impact of a Log Export Tax: Who Gains and Who Losses*, Center for International Trade in Forest Products, Special Paper Series SP-02, University of Washington, Seattle, WA, 1992
- [45] Marks, S.V., Larson, D.F., Pomeroy, J., *Economic Effects of Taxes on Exports of Palm Oil Products*, In: Bulletin of Indonesia Economic Studies, 1998, 34, 3, 37–58
- [46] Warr, P.G., *General Equilibrium Welfare and Distributional Effects of Thailand's Rice Export Tax*, Canberra: Research School of Pacific and Asian Studies, Department of Economics, Australian National University, 1997
- [47] Ades, A., Tella, R., *Rents, competition, and corruption*, In: American Economic Review, 1999, 89, 4, 982–993
- [48] Hamzah, H., *Civil law agreement and its implication on regulation for prevention of corruption within Covid-19 Pandemic*, In: Journal of Social Studies Education Research, 2020, 11, 3, 156–176
- [49] Ackerman, G., Peterson, H., *Terrorism and COVID-19*, In: Perspectives on Terrorism, 2020, 14, 3, 59–73
- [50] Gearson, J., *The nature of modern terrorism*, In: The Political Quarterly, 2002, 73, 4, 7–24
- [51] Valbona, Z., Michael, R., Gary, K., *Terrorism, competitiveness, and international marketing: an empirical investigation*, In: International Journal of Emerging Markets, 2018, 13, 2, 310–329
- [52] Espinosa-Méndez, C., Arias, J., *Herding behaviour in Australian stock market: Evidence on COVID-19 effect*, In: Appl. Econ. Lett., 2020, 1–4, <http://dx.doi.org/10.1080/13504851.2020.1854659>
- [53] Arize, A.C., Osang, T., Slottje, D.J., *Exchange-rate Volatility in Latin America and Its Impact on Foreign Trade*, In: International Review of Economics & Finance, 2008, 17, 1, 33–44
- [54] Chakraborty, L., Thomas, E., *COVID-19 and Macroeconomic Uncertainty: Fiscal and Monetary Policy Response*, 2020, 20/302, Available at: https://www.nipfp.org.in/media/medialibrary/2020/04/WP_302_2020.pdf [Accessed on December 5, 2021]
- [55] Padhan, R., Prabheesh, K.P., *The economics of COVID-19 pandemic: A survey*, In: Economic Analysis and policy, 2021, 70, 220–237
- [56] Liu, D., Sun, W., Zhang, X., *Is the Chinese economy well positioned to fight the COVID-19 pandemic? The financial cycle perspective*, In: Emerg. Mark. Finance Trade, 2020, 56, 10, 2259–2276
- [57] Zulkarnaen, W., Erfiansyah, E., Syahril, N.N.A., Leonandri, D.G., *Comparative Study of Tax Policy Related to COVID-19 in ASEAN Countries*, In: International Journal of TEST Engineering & Management, 2020, 83, 2, 6519–6528
- [58] Clemens, J., Veuger, S., *Implications of the COVID-19 pandemic for state government tax revenues*, In: National Tax Journal, 2020, 73, 3, 619–644
- [59] Collins, C.G., Gagnon, J.E., *Exchange rate policy in the COVID-19 pandemic*, Peterson Institute for International Economics, 2021
- [60] Barbero, J., de Lucio, J.J., Rodríguez-Crespo, E., *Effects of COVID-19 on trade flows: Measuring their impact through government policy responses*, In: PLoS ONE, 2021, 16, 10, e0258356, <https://doi.org/10.1371/journal.pone.0258356>
- [61] Verschuur, J., Koks, E.E., Hall, J.W., *Observed impacts of the COVID-19 pandemic on global trade*, In: Nature Human Behaviour, 2021, 5, 305–307
- [62] Bas, M., *A Fernandes and C Paunov*, The Resilience of Trade to COVID-19, 2021

Authors:

SADIA AZIZ¹, MUHAMMAD ABDULLAH KHAN NIAZI², USMAN GHANI³, SAMRA KIRAN¹, MISBAH NOOR¹

¹Management Sciences, Shaheed Benazir Bhutto Women University, Peshawar, Pakistan
e-mail: sadia_aziz11@yahoo.com, samra.kiran@sbbwu.edu.pk, misbahnoor86@yahoo.com

²IBMS, University of Agriculture Peshawar, Pakistan

³Institute of management sciences, 1-A, Sector E-5, Phase VII, Hayatabad, Peshawar, Pakistan
e-mail: usman.ghani@imsciences.edu.pk

Corresponding author:

DR. MUHAMMAD ABDULLAH KHAN NIAZI
e-mail: makniazikhani@yahoo.com

Gamma-rays shielding and antibacterial properties of coated fabrics

DOI: 10.35530/IT.074.02.202218

NACIYE SÜNDÜZ OĞUZ

FEYZA AKARSLAN KODALOĞLU

ABSTRACT – REZUMAT

Gamma-rays shielding and antibacterial properties of coated fabrics

Today, with the development of technology, radiation exposure is more common. Therefore, alternative methods have been developed because shielding, which is used as the most effective method for radiation protection, has risks in terms of health. With the awareness of consumers, the use of antibacterial textile products has increased in terms of hygiene and comfort. In this study, for this purpose nano-silver which has antibacterial properties was applied to woven fabrics with the impregnation method and the fabrics were coated with tungsten and barium sulfate, which have radiation shielding properties. The radiation shielding properties of fabrics against ^{137}Cs source emitting γ radiation were investigated. In this study, woven fabrics with radiation protection and antibacterial properties, which are very important for the health sector, were obtained and compared with each other.

Keywords: radiation shielding, antibacterial property, woven fabric

Proprietățile de ecranarea împotriva radiațiilor gamma și cele antibacteriene ale țesăturilor peliculizate

În prezent, odată cu dezvoltarea tehnologiei, expunerea la radiații este mai frecventă. Prin urmare, s-au dezvoltat metode alternative de ecranare, care sunt folosite ca cele mai eficiente metode pentru protecția împotriva radiațiilor, ce prezintă riscuri în ceea ce privește sănătatea. Odată cu conștientizarea consumatorilor, utilizarea produselor textile antibacteriene a crescut în ceea ce privește igiena și confortul. În acest studiu, în acest scop a fost aplicat nano-argint care are proprietăți antibacteriene pe țesături prin metoda de impregnare, iar țesăturile au fost peliculizate cu tungsten și sulfat de bariu, care au proprietăți de protecție împotriva radiațiilor. Au fost investigate proprietățile de protecție împotriva radiațiilor ale țesăturilor împotriva sursei de ^{137}Cs care emite radiații γ . În acest studiu, au fost obținute și comparate țesături cu proprietăți antibacteriene și de protecție împotriva radiațiilor, care sunt foarte importante pentru sectorul sănătății.

Cuvinte-cheie: ecranare împotriva radiațiilor, proprietăți antibacteriene, țesătură

INTRODUCTION

The energy emitted or transmitted in wave or particle form, in matter or space is called radiation [1]. There are natural and artificial radiation sources such as cosmic rays, radioactive elements in the human body, radon gas, gamma rays, radioactive materials taken from food, medical applications, nuclear power plants, and consumer products [2, 3]. Base stations, mobile phones, and Internet networks can affect the quality of life of all living things [4]. Radiation has serious biological effects such as radiation burns and diseases, hereditary disorders, shortening of human life, cancer and sudden death [5]. Radiation is used in the diagnosis and treatment of diseases, energy production, industrial products, agriculture, nuclear weapons, consumer products and forensic medicine [6]. Radiation, which is used in many areas today, besides making human life easier, it is necessary to be protected from radiation due to the risks it poses in terms of health.

Humans are in contact with a wide variety of microorganisms in daily life, and these microorganisms can reproduce very quickly with the effect of appropriate humidity, temperature and food. With the effect of

microorganisms on textile surfaces, conditions such as stains, bad odour and loss of strength can be encountered [7]. With antibacterial textile products, it is desired to reduce and eliminate the negative situations caused by microorganisms on the textile surface and the damage that they cause to the user. Antibacterial textile products are especially preferred in environments such as hospitals and nurseries where microorganisms multiply rapidly [8]. Apart from killing microorganisms, the antibacterial substances used should not harm the user, the environment and the textile product [9].

Antibacterial textile surfaces are obtained by adding antibacterial substances to the fibre polymer structure and finishing processes [8]. Alcohols, metals, ammonium compounds, phenol and its derivatives, halogens, zeolites, oxidizing agents, biquanidins, isothiazolones, chitin and chitosan are the most important antibacterial agents [9]. Extraction, impregnation, spraying, foam application, vacuum application, maximum liquor application, transfer and coating methods are used in antibacterial finishing processes [10]. With antibacterial finishing processes, it is desired to prevent negative changes in fabric

performance, limit bacterial re-growth, to prevent odour formation and the spread of pathogens [11]. In the field of radiation shielding, work is underway to develop materials that are lightweight, economical, non-toxic and have high shielding properties. Researchers have focused on many types of materials, from traditional materials to natural minerals, and composite materials to various building materials, such as the absorption of various types of radiation. In some studies in the literature of Harish et al., different proportions of lead monoxide (PbO) and isophthalate-based unsaturated polyester resin composites were prepared and gamma ray absorption tests were performed from ^{137}Cs source. According to the test results, it was stated composites filled with PbO of more than 30% showed higher performance for gamma rays with an energy of 0.662 MeV than armour materials such as silver, copper and concrete [12]. In 2015, Badawy and Latif investigated the performance of composites containing polyvinyl alcohol (PVA) and magnetite (Fe_2O_3) nanoparticles in ^{60}Co , ^{137}Cs , and ^{22}Na gamma sources. As a result of the experiments, they stated that this composite film can be an alternative to lead due to its lightness and flexibility advantage [13]. Gülbicim examined the radiation permeability of samples created with vermiculite and different proportions of Borax mineral (25–50%) in his study. Using ^{60}Co (Cobalt), ^{152}Eu (Europium) and ^{226}Ra (Radium) radiation sources, it was noted that the boron-doped vermiculite sample at energy values in the range of 0.186–1.728 MeV showed higher performance than lead at energy values of 1–3 MeV [14]. As a filler Carbon Black (CB) and lead tungstate (PbWO_4) dust used in the study of EPDM (Ethylene-Propylene-Diene Monomer) matrix composites produced by three different gamma source (^{155}Eu , ^{137}Cs and ^{60}Co radiation attenuation performance have been investigated and the absorption of gamma rays increasing in the percentage of rubber to increase the performance of the PWO is stated [15]. The head of laminated composites containing Basalt Fiber Reinforced with epoxy resin produced by Kev in energy between 31 and 80 has protective qualities against the values of X and gamma rays indicated that [16]. The work of an Unsaturated Polyester Resin matrix in different proportions in lead monoxide (PbO) and 5 WT.-%nanoclay composite samples produced by participating in ^{192}Ir , ^{137}Cs , and ^{60}Co gamma sources in the measurements with the increase of PBO content, the shielding performance increase, however, it has been stated that composites can be used as an armour material at low energies [17]. Gamma-rays reduce to 8 different polymers (polyamide (PA-6), polyacrylonitrile (PAN) polivinilidendeklorur (PVDC), polyaniline (PANI), poliileneterftalat (PET), polifenile sulfide (PPS), poliprol (PP) and polyethylene (PPR)) for high-resolution HPGe detector with the help of the 81 keV – 1333 keV in the energy range examined using different radioactive sources. They observed that the linear reduction coefficients of all polymers decrease rapidly

at low energies [18]. Kacal et al. have studied the gamma-ray reduction properties of Zn-reinforced polymer composites. Using the HPGe detector, they measured the mass reduction coefficients of composites in the energy December of 59.5 keV – 1408.0 keV. As the addition of Zn increases, they have observed that the property of armouring increases [19]. The gamma-ray shielding properties of polymer composites doped in CdTe at different rates (5%, 10%, 15% and 20%) using an HPGe detector have been investigated theoretically and experimentally. As the contribution increases, it has been determined that there is an increase in protection efficiency [20]. In this study, both medical and protective technical textiles, which are very important for the health sector in terms of the functional properties of technical textiles, have been studied both radiation-protective and antibacterial properties have been given to woven fabrics.

MATERIALS AND METHODS

Material

In this study, cotton woven fabric (97% cotton, 3% elastane) with a weight of 247 g/m², weft density of 55 wire/cm, a warp density of 33 wire/cm; cotton/polyester woven fabric (59% cotton, 39% polyester, 2% elastane) with a weight of 236 g/m², weft density 34 wire/cm, warp density 60 wire/cm were used.

Antibacterial properties of the fabrics were investigated by applying nanosilver in 20–25 nm size. In recent years, antibacterial textile products with silver applied have been used intensively. The most important reasons for this are that bacteria are prevented from multiplying by passing through the cell membrane, it is an odour remover, the use of a certain amount does not harm the human body, and it is effective on more than 650 microorganisms that cause disease [21]. It is used in many areas such as socks, underwear, sheets, sofa upholstery, antibacterial food packages, wounds and burns [2, 22, 23].

Staphylococcus aureus (ATCC 6538), which is frequently encountered in hospitals and causes infection, and *Escherichia coli* (ATCC 35218) which is in intense contact with textile surfaces, were used for antibacterial tests [24, 25].

Tubicoat CRO was used as a coating chemical with tungsten and barium sulfate, which have radiation shielding properties, to give the fabrics radiation shielding properties [26, 27].

Method

The impregnation method, which is an application process in a short time and a short liquor ratio, was used in the treatment bath for cotton and cotton/polyester fabrics. With this method, the solution obtained by mixing 1% nano silver with distilled water on cotton and cotton/polyester fabrics in Ataç brand FY 350 model foulard was poured between two bar pressure cylinders and impregnated [28]. The

fabrics were dried at 80°C for 15 minutes and fixed at 100°C for 3 minutes.

A homogeneous coating material was obtained by mixing Tubicoat CRO, which is a coating chemical, with barium sulfate and tungsten separately. 60% tubicoat, 40% barium sulfate and 40% tungsten were used in the study. The coating material was applied to the fabrics using a squeegee. After the coating process, the drying and fixation processes of the fabrics were carried out in the fixing machine. The barium sulfate-coated fabric was dried at 80°C for 15 minutes, the tungsten-coated fabric was dried at 80°C for 10 minutes, and both fabrics were fixed at 100°C for 3 minutes.

To examine the radiation shielding properties of fabrics, ¹³⁷Cs source, which is widely used in medical applications, has been used. By using the gamma spectrometer measurement system ORTEC brand, GEM50P4-83 model high purity coaxial Ge detector, 600 seconds of radiation shielding was applied to the fabrics. The ¹³⁷Cs source has an energy of 661.6 keV and an abundance of 85% with a half-life of 11022 days. The gamma spectrometer system consists of a detector, a preamplifier, a spectroscopy amplifier, an ADC system that converts analogue counts into electronic signals, and a multi-channel analyzer (MCA) [29].

AATCC 147 antibacterial test method, which is an easy and fast method, was applied to examine the antibacterial properties of woven fabrics qualitatively. In this method, bacteria were vaccinated and the fabrics were placed in petri dishes by making contact with the fabric, and the antibacterial properties of the samples, which were kept in an oven at 37°C for 24 hours, were determined according to the formation of the inhibition area [30].

RESEARCH FINDINGS

The fabrics were classified as no treatment applied, only nanosilver applied, only tungsten and barium sulfate applied, and nanosilver and tungsten and barium sulfate applied fabrics.

Radiation shielding

In table 1, the number of particles per second and radiation shielding rates (%) of the fabrics against the ¹³⁷Cs source with 662 keV energy are given.

$$\text{Radiation Shielding (\%)} = [(I_0 - I) / I_0] \cdot 100 \quad (1)$$

where I_0 is the intensity of the incident photons on the fabric before they are absorbed and I – intensity of photons absorbed through the fabric.

The radiation shielding percentage of the fabrics was found using the formula given in equation 1.

When the radiation shielding values were examined, it was seen that tungsten and barium sulfate gave the fabrics radiation shielding properties, while nano silver reduced the radiation shielding properties of the fabrics. It has been observed that tungsten-treated cotton fabric has better radiation shielding properties than barium sulphate-treated cotton fabric and barium

Table 1

ENERGY AND RADIATION SHIELDING VALUES OF FABRICS AGAINST ¹³⁷ CS SOURCE		
Samples	Number of incoming particles per second	Radiation shielding (%)
The Source Itself	168510±413	
Cotton	156194±397	7.3
Cotton-Nano silver	165191±408	1.9
Cotton-Barium Sulphate	151571±391	10
Cotton-Nano silver-Barium Sulphate	153143±393	9.1
Cotton-Tungsten	149812±389	11
Cotton-Nano silver-Tungsten	155194±396	7.9
Cotton/Polyester	155290±396	7.8
Cotton/Polyester-Nano silver	165324±408	1.8
Cotton/Polyester-Barium Sulphate	142279±379	15
Cotton/Polyester-Nano silver-Barium Sulphate	156186±397	7.3
Cotton/Polyester-Tungsten	146518±384	13
Cotton/Polyester-Nano silver-Tungsten	152216±392	9.6

sulfate-treated cotton polyester fabric has better radiation shielding properties than tungsten-treated cotton polyester fabric.

Antibacterial test

The antibacterial activities of cotton and cotton/polyester woven fabrics, with the sample removed, against *S. aureus* and *E. coli* bacteria according to the AATCC 147 Antibacterial test method results are shown in figures 1–4.

It was observed that an inhibition area was formed in all fabrics on which nanosilver was applied, and these fabrics gained antibacterial properties against *E. coli* and *S. aureus* bacteria. Bacterial growth was observed on the surface of some of the coated fabrics. The fabrics were classified among themselves and compared with each other and radiation-shielding fabrics with antibacterial properties were obtained.

CONCLUSION

In this study, nano silver with antibacterial properties was applied to cotton and cotton/polyester woven fabrics by impregnation method. Tungsten and barium sulfate, which have radiation protection properties, are coated on fabrics using a squeegee. It has been observed that cotton/polyester fabrics generally have better radiation shielding properties than cotton fabrics against ¹³⁷Cs source emitting γ radiation. When the radiation shielding values were examined, it was seen that tungsten and barium sulfate gave the fabrics radiation shielding properties, while nano silver reduced the radiation shielding properties of the

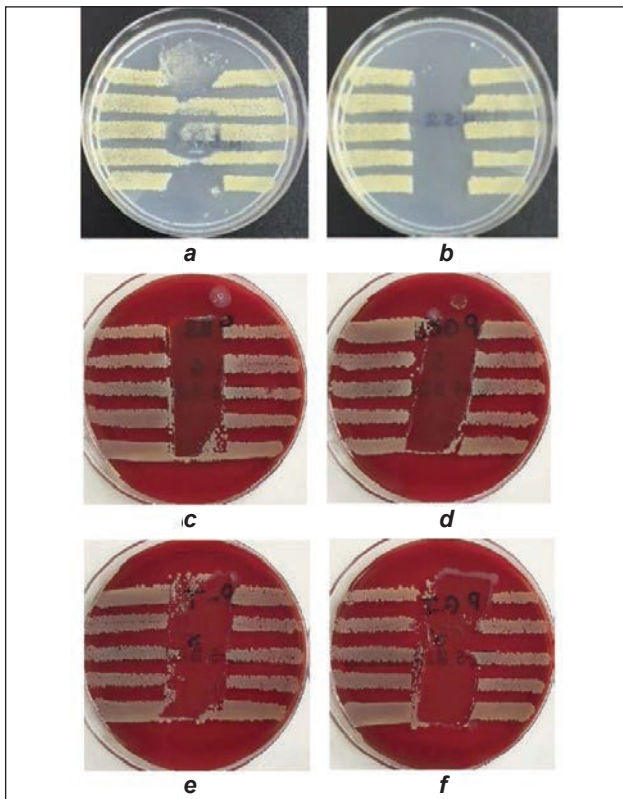


Fig. 1. Antibacterial activities against *S. aureus* bacteria of: *a* – untreated; *b* – nanosilver treated; *c* – barium sulfate treated; *d* – barium sulfate-nano silver treated; *e* – tungsten treated; *f* – tungsten-nano silver treated cotton fabric

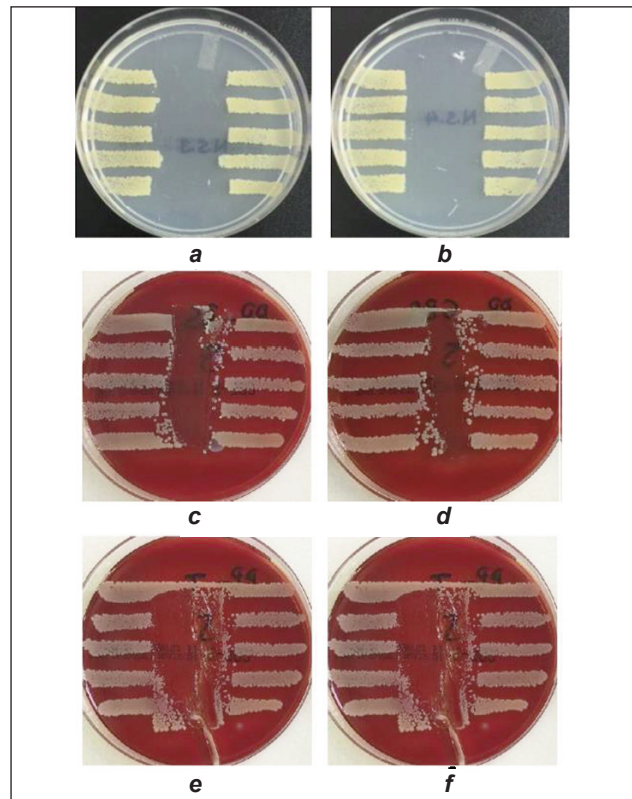


Fig. 2. Antibacterial activities against *E. coli* bacteria of: *a* – untreated; *b* – nanosilver treated; *c* – barium sulfate treated; *d* – barium sulfate-nano silver treated; *e* – tungsten treated; *f* – tungsten-nano silver treated cotton fabric

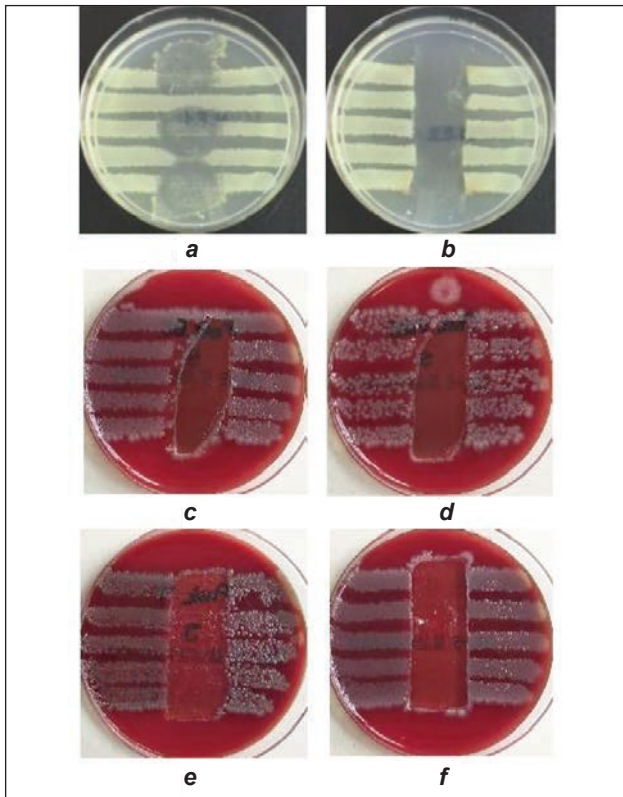


Fig. 3. Antibacterial activities against *S. aureus* bacteria of: *a* – untreated; *b* – nanosilver treated; *c* – barium sulfate treated; *d* – barium sulfate-nano silver treated; *e* – tungsten treated; *f* – tungsten-nano silver treated cotton/polyester fabric

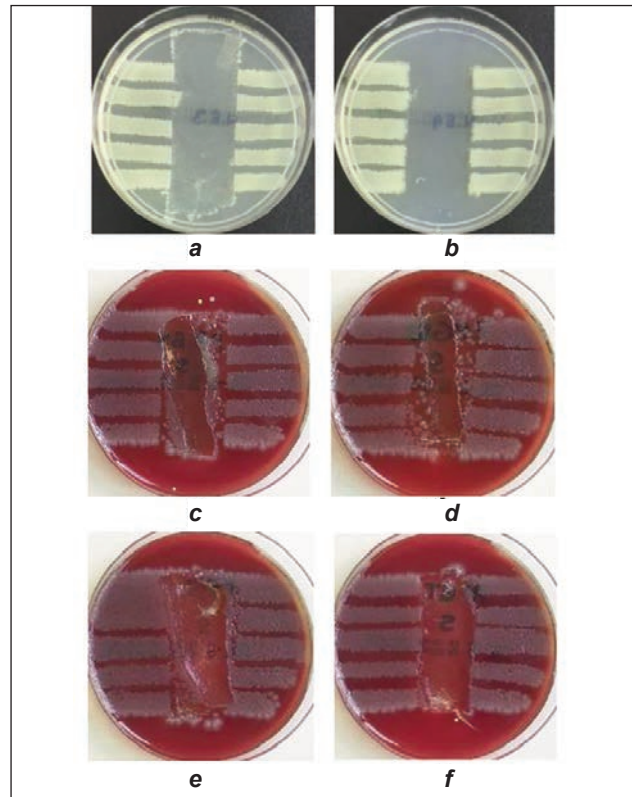


Fig. 4. Antibacterial activities against *E. coli* bacteria of: *a* – untreated; *b* – nanosilver treated; *c* – barium sulfate treated; *d* – barium sulfate-nano silver treated; *e* – tungsten treated; *f* – tungsten-nano silver treated cotton/polyester fabric

fabrics. Bacterial growth was observed on the surface of some of the coated fabrics that were not coated with nanosilver. It would be more appropriate to

prefer fabrics with tungsten and barium sulfate applied as nano silver coating material to obtain a radiation-protective and antibacterial fabric.

REFERENCES

- [1] Bushberg, J.T., Seibert J.A., Leidholdt, E.M., Boone, J. M., *The essential physics of medical imaging*, Lippincott Williams & Wilkins, 2011
- [2] Bozbıyık, A., Özdemir, Ç., Hancı, H., *Radyasyon yaralanmaları ve korunma yöntemleri*, In: Sürekli Tıp Eğitimi Dergisi, 2002, 11, 7, 272–274
- [3] Gökharman, F.D., Aydın, S., Koşar, P.N., *Radyasyon güvenliğinde mesleki olarak bilmemiz gerekenler*, In: SDÜ Sağlık Bilimleri Dergisi, 2016, 7, 2, 35
- [4] Günaydın, G.K., Aydın, Ö., *Elektromanyetik Kalkanlama Amaçlı Koruyucu Tekstiller*, In: Akdeniz Sanat, 2011, 4, 7
- [5] Türkiye Atom Enerjisi Kurumu, *Radyasyon, İnsan ve Çevre: İyonlaştırıcı Radyasyon, Etkileri ve Kullanım Alanları, Güvenli Kullanımı İçin Uygulamada Olan Tedbirler*, Ankara, 2009
- [6] Kaçar, A., *Yapılarda Radyasyon Kalkanı Olarak Kullanılan Barit Agregalı Ağır Beton Elemanların Zırh Kalınlık Hesaplarının Belirlenmesi*, Süleyman Demirel Üniversitesi, Fen Bilimleri Enstitüsü, Yüksek Lisans Tezi, 60s, Isparta, 2006
- [7] Sarı, Ç., *Antibakteriyel Ajan İçeren B-Siklodekstrin Kompleksinin Ve Türevinin Pamuklu Kumaşlara Uygulanması ve Karakterize Edilmesi*, Fen Bilimleri Enstitüsü, Tekstil Mühendisliği Ana Bilim Dalı, Yüksek Lisans Tezi, 156 s, Denizli, 2020
- [8] Akpınar, E.S., *Antibakteriyel Bitim İşleminin Pamuklu Çarşafılık Kumaşların Bazı Mekanik Özellikleri Üzerindeki Etkilerinin İncelenmesi*, Fen Bilimleri Enstitüsü, Tekstil Mühendisliği Ana Bilim Dalı, Yüksek Lisans Tezi, 89 s, Denizli, 2019
- [9] Devrent, N., Yılmaz, N.,D., *Tekstil Endüstrisinde Kullanılan Antimikrobiyal Lifler*, In: Nonwoven Technical Textiles Technology Dergisi, 2004, 4, 48–55
- [10] Seventekin, N., Öktem, T., Tekeoğlu, S., *Tekstilde Antimikrobiyel Madde Kullanımı*, In: Tekstil ve Konfeksiyon, 2001, 4, 217–224
- [11] Mucha, H., Hofer, D., Abfalğ, S., Swerev, M., *Antimicrobial Finishes and Modifications*, In: Melliand International, 2002, 8, 148–151
- [12] Harish, V., Nagaiah, N., Prabhu, T.N., Varughese, K.T., *Thermo-mechanical analysis of lead monoxide filled unsaturated polyester based polymer composite radiation shields*, In: Journal of Applied Polymer Science, 2010, 117, 6, 3623–3629
- [13] Badawy, S.M., Abd El-Latif, A.A., *Synthesis and Characterizations of Magnetite Nanocomposite Films for Radiation Shielding*, In: Polymers and Polymer Composites, 2015, 38, 5, 974–980
- [14] Gülbiçim, H., *Saf ve bor katkılı vermikülit'in gama radyasyon geçirgenliğinin belirlenmesi*, Ondokuz Mayıs Üniversitesi, Fen Bilimleri Enstitüsü, Fizik Anabilim Dalı, Yüksek lisans tezi, 73 s, Samsun, 2015
- [15] Huang, W., Yang, W., Ma, Q., Wu, J., Fan, J., Zhang, K., *Preparation and characterization of γ -ray radiation shielding PbWO₄/EPDM composite*, In: Journal of Radioanalytical and Nuclear Chemistry, 2016, 309, 3, 1097–1103
- [16] Li, R., Gu, Y., Zhang, G., Yang, Z., Li, M., Zhang, Z., *Radiation shielding property of structural polymer composite: Continuous basalt fiber reinforced epoxy matrix composite containing erbium oxide*, In: Composites Science and Technology, 2017, 143, 67–74
- [17] Bagheri, K., Razavi, S.M., Ahmadi, S.J., Kosari, M., Abolghasemi, H., *Thermal resistance, tensile properties, and gamma radiation shielding performance of unsaturated polyester/nanoclay/PbO composites*, In: Radiation Physics and Chemistry, 2018, 146, 2017, 5–10
- [18] Kaçal, M.R., Akman, F., Sayyed, M.I., Akman, F., *Evaluation of gamma-ray and neutron attenuation properties of some polymers*, In: Nuclear Engineering and Technology, 2019, 51, 818–824
- [19] Kaçal, M.R., Polat, H., Oltulu, M., Akman, F., Agar, O., Tekin, H.O., *Gamma shielding and compressive strength analyses of polyester composites reinforced with zinc: an experiment, theoretical, and simulation based study*. Applied Physics A 126:205, 2020.
- [20] Akman, F., Ogul, H., Kaçal, M.R., Polat, H., Dilsiz, K., Agar, O., *Gamma attenuation characteristics of CdTe-Doped polyester composites*, In: Progress in Nuclear Energy, 2021, 131, 103608
- [21] Süpüren, G., Çay, A., Kanat, E., Tarakçioğlu, I., *Antimikrobiyal Lifler*, In: Tekstil ve Konfeksiyon, 2006,16, 2, 80–89
- [22] Babaarslan, O., Erbil, Y., *Fonksiyonel Tekstil Ürünleri Geliştirmek Üzere Ştapel Gümüş Takviyeli Karışım İpliklerinin Tasarım ve Üretimi*, ÜB Tekstil ve Konfeksiyon Sektöründe Ar-Ge Proje Pazarı, Bursa, 2010, 125–126
- [23] Rai, M., Yadav, A., Gade, A., *Silver Nanoparticles as a New Generation of Antimicrobials*, In: Biotechnology Advances, 2009, 27, 1, 76–83
- [24] Hacıbektazoğlu, A., Eyigün, C.P., ve Özsoy, M.F., *Gıda Elleyicilerinde Burun ve Boğaz Portörlüğü*, In: Mikrobiyoloji Bülteni, 1993, 27, 62–70
- [25] Orhan, M., *Pamuk, Poliamid ve Poliester Esaslı Tekstil Materyallerinde Antimikrobiyal Bitim Uygulamaları Üzerine Bir Araştırma*. Uludağ Üniversitesi, Fen Bilimleri Enstitüsü, Tekstil Mühendisliği Anabilim Dalı, Doktora Tezi, 175 s, Bursa, 2007

- [26] Eskier, U., *Barit: Mineral Ailesinden Çok Amaçlı Taş*, 2017, Available at: <https://www.makaleler.com/barit-tasi-ozellikleri-ve-kullanim-alanlari> [Accessed on August 1, 2020]
- [27] Eskier, U., *Tungsten (Volfram) Nedir? (Özellikleri, Kullanımı)*, 2017, Available at: <https://www.makaleler.com/tungsten-volfram-nedir-ozellikleri-kullanimi> [Accessed on August 1, 2020]
- [28] El-Rafie, M.H., Mohamed, A.A., Shaheen, T.I., Hebeish, A., *Antimicrobial Effect of Silver Nanoparticles Produced by Fungal Process on Cotton Fabrics*, In: Carbohydrate Polymers, 2010, 80, 3, 779–782
- [29] Kurnaz, A., *Trabzon İlinin ve Şebinkarahisar İlçesinin Doğal Radyoaktivite Düzeylerinin Belirlenmesi ve Yıllık Etkin Doz Eşdeğerleri*, Karadeniz Teknik Üniversitesi, Fen Bilimleri Enstitüsü, Doktora Tezi, 279s, Trabzon, 2009
- [30] Altınok, U.B., *Tekstil Yüzeylerinin Antibakteriyel Özelliklerinin Araştırılması*, Süleyman Demirel Üniversitesi, Fen Bilimleri Enstitüsü, Tekstil Mühendisliği Ana Bilim Dalı, Yüksek Lisans Tezi, 97 s, Isparta, 2008

Authors:

NACIYE SÜNDÜZ OĞUZ¹, FEYZA AKARSLAN KODALOĞLU²

¹Kastamonu University, Araç Rafet Vergili Vocational School, Department of Textile, Clothing, Shoes and Leather, 37800, Kastamonu, Turkey
email: noguz@kastamonu.edu.tr

²Süleyman Demirel University, Engineering Faculty, Department of Textile Engineering, 32260, Isparta, Turkey

Corresponding author:

FEYZA AKARSLAN KODALOĞLU
email: feyzaakarслан@sdu.edu.tr

The optimal factoring type with partial credit guarantee in the textile industry: disclosed or undisclosed

DOI: 10.35530/IT.074.02.202222

ZHAO SHENGYING
ZHONG MINGJUN

LU XIANGYUAN

ABSTRACT – REZUMAT

The optimal factoring type with partial credit guarantee in the textile industry: disclosed or undisclosed

Small and medium-sized textile enterprises generally experience financial difficulties, with a high default risk because of the textile industry's characteristics of low concentration, long industrial chains, and large seasonal fluctuations. Using a two-echelon supply chain model of the textile industry comprising a core retailer and capital-constrained supplier, this study investigates disclosed and undisclosed factoring while considering the default risk of both the supplier and retailer under two guarantee mechanisms: no guarantee and a third-party partial credit guarantee. Utilizing a Stackelberg game model, this study finds that both the default risk and financial institutions' loan-to-value ratio for accounts receivable significantly affect optimal financing decisions and financing efficiency. First, excessively pursuing higher loan-to-value ratios lowers financing efficiency. In addition, a partial credit guarantee from a third party can effectively reduce the financing interest rate but cannot improve financing efficiency if the supplier assumes the guarantee fee. Thus, while introducing a guarantee mechanism to control financing risk, financial institutions should consider supply chain participants, rather than the supplier, to assume the guarantee fees. Furthermore, both the supplier and retailer should finance through disclosed factoring regardless of a guarantee. Our findings offer textile industry-specific financing insights regarding the options of guarantee and factoring financing type based on the accounts receivable.

Keywords: factoring, guarantee, game model, default risk, efficiency

Tipul optim de factoring cu garanție parțială a creditului în industria textilă: divulgat sau nedivulgat

Întreprinderile textile mici și mijlocii se confruntă în general cu dificultăți financiare, cu un risc mare de nerambursare din cauza caracteristicilor industriei textile de concentrare scăzută, lanțuri industriale lungi și fluctuații sezoniere mari. Folosind un model de lanț de aprovizionare cu două eșaloane al industriei textile, care cuprinde un comerciant cu amănuntul de bază și un furnizor cu capital limitat, acest studiu investighează factoringul divulgat și nedivulgat, luând în considerare riscul de neplată atât al furnizorului, cât și al comerciantului cu amănuntul în cadrul a două mecanisme de garanție: fără garanție și garanția parțială a creditului pentru terța parte. Folosind un model de joc Stackelberg, acest studiu constată că atât riscul de nerambursare, cât și raportul împrumut-valoare al instituției financiare pentru conturile de încasat afectează în mod semnificativ deciziile optime de finanțare și eficiența finanțării. În primul rând, urmărirea excesivă a unor rapoarte credit/valoare mai ridicate scade eficiența finanțării. În plus, o garanție parțială a creditului de la o terță parte poate reduce efectiv rata dobânzii de finanțare, dar nu poate îmbunătăți eficiența finanțării dacă furnizorul își asumă comisionul de garanție. Astfel, în timp ce se introduce un mecanism de garantare pentru controlul riscului de finanțare, instituțiile financiare ar trebui să ia în considerare participanții lanțului de aprovizionare, mai degrabă decât furnizorul, să își asume taxele de garanție. În plus, atât furnizorul, cât și comerciantul cu amănuntul ar trebui să finanțeze prin factoring divulgat, indiferent de garanție. Constatările noastre oferă perspective de finanțare specifice industriei textile cu privire la opțiunile de finanțare cu garanție și factoring pe baza conturilor de încasat.

Cuvinte-cheie: factoring, model de joc, risc implicit, eficiență

INTRODUCTION

The textile industry is an important pillar of people's livelihood and employment generation. However, because the textile industry has a long industrial chain and many subdivisions, approximately 80% of textile enterprises are small- and medium-sized enterprises (SMEs). These SMEs generally experience financing difficulties and a high default risk because of problems such as information asymmetry and the textile industry's characteristics of low concentration, long industrial chains, and large seasonal fluctuations. The capital constraint is a key factor that commonly affects firms' operations, especially those of SMEs. In

particular, the COVID-19 outbreak has severely affected manufacturing industries such as textiles; for example, many enterprises – even large or core ones – have suffered from raw material and capital shortages. SMEs face a more severe situation because of the shortage of cash flows, especially those with accounts receivable as their main business in supply chain operations, with longer account periods and greater financing difficulties.

A potential method to free up cash flows is factoring in financing. Factoring is a type of short-term supplier financing in which suppliers sell their accounts receivable receipts at a discount (loan-to-value ratio)

and receive immediate cash from factors such as banks or other financial institutions [1]. Factoring can be disclosed or undisclosed based on whether the core enterprise is notified. Disclosed factoring (DF) seems to be the main form of factoring. However, with higher pressures on capital flow and supplier selection, an increasing number of capital-constrained enterprises, especially suppliers, have begun utilizing undisclosed factoring (UF). For example, as the largest brokerage company specializing in insurance and financing of receivables and a partner of the A.U. Group, ARFIN secures business transactions worth more than EUR 200 billion and has over 15 years of experience in the field of factoring, including recourse factoring, reverse factoring, and UF. However, UF is subject to two risks, as the core enterprise (the debtor) is not notified about the transfer of accounts receivable by the capital-constrained supplier (the creditor): i) The core enterprise may default, and ii) the capital-constrained supplier may cheat on loans through forged receipts. This reveals that the factoring company must conduct strict reviews before granting credit to the capital-constrained suppliers to mitigate and prevent financing risks from UF.

In this financing environment, financial institutions, such as banks, usually require a guarantee mechanism in the process of factoring to reduce financing risks. Many studies have examined the guarantee issues in financing from various perspectives, such as third-party [2–4], insurance [5], and core enterprise [6]. However, to the best of our knowledge, few have considered the guarantee issue under UF. Furthermore, no study has performed a comparative analysis of the optimal decisions and financing efficiency between DF and UF under guarantee to provide insights into the optimal factoring type in the context of the textile industry.

Here, we aim to answer the following research questions:

- How does a guarantee affect the financing decisions under both DF and UF?
- In the textile industry, what is the optimal factoring type between DF and UF under both guarantee and no guarantee scenarios?

Using a two-echelon supply chain comprising a core retailer and capital-constrained supplier, this study analyses the impact of guarantee on the optimal factoring decisions and types while considering the default risks of the retailer and supplier utilizing a Stackelberg game model. We show that the bank's loan-to-value ratio for accounts receivable and default risk significantly affect financing decisions and profits. First, the profits of both the supplier and retailer decrease with the loan-to-value ratio and default risk. Thus, the capital-constrained supplier cannot always benefit from a higher loan-to-value ratio because of higher financing costs. In addition, a partial credit guarantee (PCG) from a third party can effectively reduce the financing interest rate but cannot improve the financing efficiency if the supplier assumes the guarantee fee. Furthermore, the optimal

profits of both the supplier and retailer under DF are always higher than those under UF regardless of a guarantee.

This study makes several contributions. First, from a theoretical perspective, our study is the first to analyse the optimal factoring type between DF and UF in the textile industry while considering guarantee. Studies on factoring mainly focus on DF [1,7] and reverse factoring [1,8]. Meanwhile, studies in the field of guarantee mainly focus on scenarios such as PCG [9,10], buy-back [3,11], and core enterprise guarantee [6,12]; rarely do they comprehensively consider the guarantee under both DF and UF, especially the optimal factoring type between the two. Finally, studies on the textile industry primarily focus on material reserves [13,14], inventory management [15], and supply chain management [16,17]. Our study fills the research gap on factoring and guarantee under UF in the textile industry.

Second, by using the Stackelberg game model, our study provides some guidelines for supply chain participants and financial institutions on the factoring business in the textile industry, especially under UF. We show that a capital-constrained supplier may not find it profitable to pursue a higher loan-to-value ratio for accounts receivable. In addition, while introducing a guarantee mechanism to control financing risk, banks should consider supply chain participants, rather than the supplier, to assume the guarantee fees. Finally, both the supplier and retailer should finance through DF regardless of a guarantee.

The remainder of this paper is organized as follows. Section 2 discusses DF and UF models under different guarantee scenarios. Section 3 explores the impact of guarantee and factoring types on financing efficiency. Finally, Section 4 presents the conclusions of this study.

DISCLOSED AND UNDISCLOSED FACTORING MODELS

Model setup

We consider a two-echelon supply chain comprising a capital-constrained supplier and a core retailer. After the supplier offers the product to the retailer, its capital is not enough to support its operations, and it needs financing from banks and other financial institutions for accounts receivable. The supplier can choose between two types of factoring: DF and UF. Under DF, the supplier enters into a factoring agreement with the bank and assigns the benefit of the debts created by the sales transaction to them. The retailer is then notified and sends payment to the bank. The DF arrangement is usually on a non-recourse basis. Meanwhile, UF, which is usually undertaken on a recourse basis, does not involve the retailer. The agreement is made between the bank and supplier, and the retailer must pay as per the sales contract. While receiving payments, the supplier holds the funds in a separate bank account as a trustee for the bank. Finally, we also consider two scenarios: no guarantee and PCG.

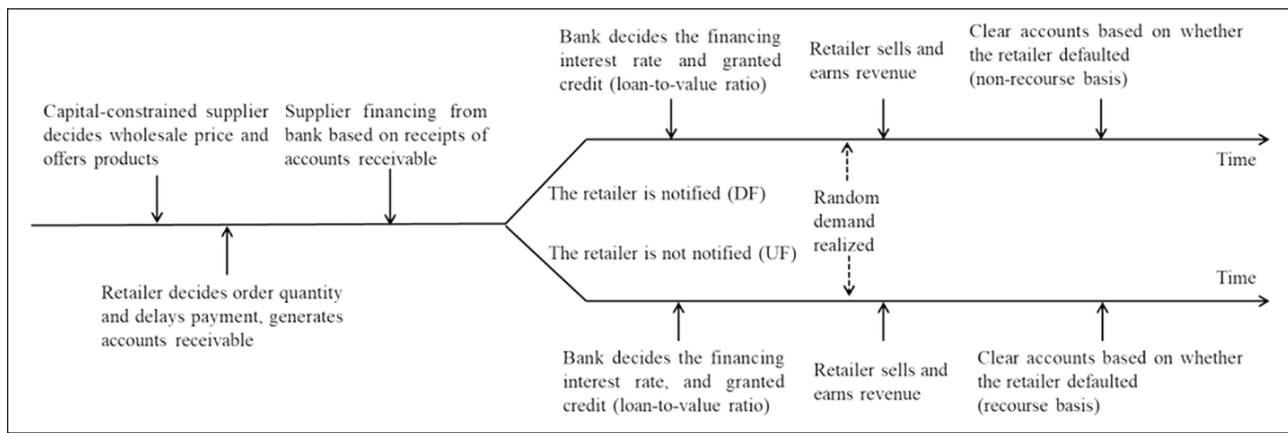


Fig. 1. The sequence of events in DF and UF when no guarantee

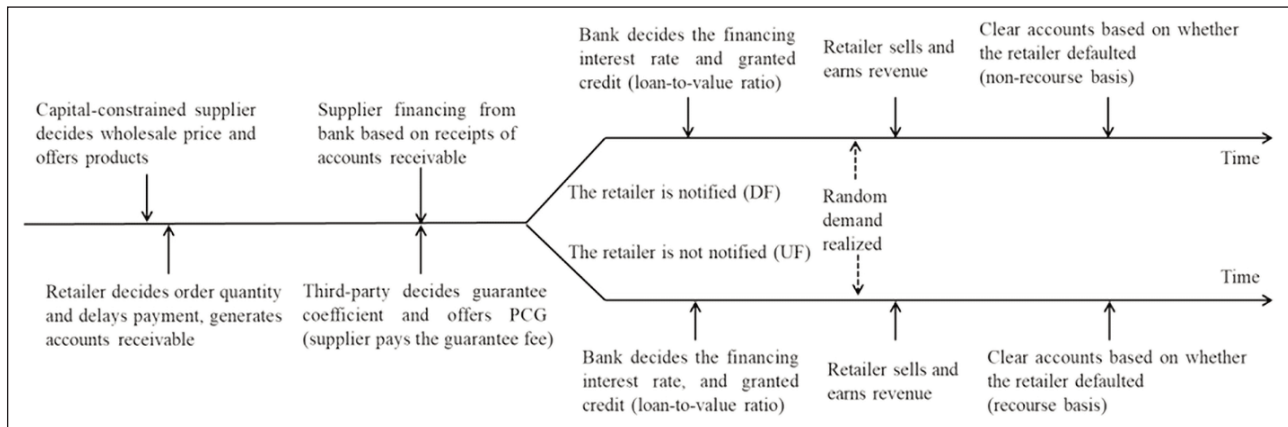


Fig. 2. The sequence of events in DF and UF with PCG from the third-party

Scenario 1: No guarantee. The sequence of events in this scenario is shown in figure 1.

As shown in figure 1, at the end of the sales period, the sequence of clearing accounts under DF is as follows: The bank pays the remaining credit to the supplier if the retailer pays the bank (and does not default), and the supplier pays the financing interest to the bank simultaneously. Otherwise, if the retailer defaults at the end of the sales period, the bank claims financing interest from the supplier and does not pay the remaining credit.

Meanwhile, the sequence of clearing accounts at the end of the sales period under UF is as follows: If the retailer does not default, it pays the supplier first. The supplier then pays the financing amount and interest to the bank, which then pays the remaining credit to the supplier. If the retailer defaults at the end of the sales period, the bank seeks direct recourse with the supplier and does not pay the remaining credit.

Scenario 2: PCG from the third party. The sequence of events is shown in figure 2.

Table 1

NOTATIONS	
Parameters	Decision variables
p : Retailer's unit retail price in the market	w_{ij} : Wholesale price
c : Supplier's unit production cost	q_{ij} : Order quantity
α : The probability of retailer default	r_{ij} : Bank's financing interest under
β : The probability of supplier default	Functions:
λ : The PCG coefficient	Π_{ij}^t : The expected profit
δ : The unit guarantee fee for the third-party PCG	$q(p,\varepsilon)$: Demand curve
r_f : The risk-free interest rate	Abbreviations
ε : Random variable with mean 0, variance σ^2	R: Retailer; S: Supplier; SC: Supply Chain
θ_{ij} : Bank's loan-to-value ratio to the supplier under scenario I and factoring type j	D&U: Disclosed & Undisclosed factoring
A: Supplier's asset (asset can be recourse)	$i = 1,2$: no guarantee, third-party offers PCG
	$j = D,U; t = R,S,SC$

As shown in figure 2, the sequence of events under both DF and UF is similar to figure 1. The only difference in the PCG scenario is that the bank can claim a share (guarantee coefficient) of the loan loss from the third party when the retailer defaults.

Notations in this paper are summarized in table 1.

Our assumptions are as follows:

1. The bank, retailer, supplier, and the third party are all risk neutral. The bank's market is competitive.
2. The default risk of both the retailer and supplier is exogenous, which may be driven by the exogenous credit shock associated with the credit rating or moral hazard [1, 18].
3. Similar to the demand curve used in [19] and [20], we assume that $q(p, \varepsilon) = a - bp + \varepsilon$, where ε has mean 0 and variance σ^2 .
4. The salvage value of unsold products at the end of the sales period is zero. Furthermore, we assume that $\lambda < \theta_{ij} < 1$; that is, the PCG coefficient does not exceed the bank's loan-to-value ratio for the accounts receivable.

DF model under no guarantee

The sequence of events is shown in figure 1. First, the supplier decides w_{1D} based on equation 1.

$$\begin{aligned} \Pi_{1D}^S(w_{1D}) = & \max_{w_{1D}} \theta_{1D} w_{1D} q_{1D} + \\ & + (1-\alpha)(1-\theta_{1D})w_{1D}q_{1D} - w_{1D}q_{1D}r_{1D} - cq_{1D} \quad (1) \end{aligned}$$

The first term on the right side of equation 1 is the bank's financing amount for accounts receivable; the second is the remaining financing amount that the bank should pay if the retailer does not default; and the third and fourth terms are the supplier's financing interest and production, respectively.

The retailer's decision on its order quantity, q_{1D} , can then be formulated as equation 2.

$$\Pi_{1D}^R(q_{1D}) = \max_{q_{1D}} E_{\varepsilon}[pq(p, \varepsilon)] - w_{1D}q_{1D}(1-\alpha) \quad (2)$$

The first term on the right side of equation 2 is the retailer's sales revenue. The second term is the payment to the bank if the retailer does not default.

Finally, the bank decides the financing rate, r_{1D} , which can be formulated as equation 3.

$$\begin{aligned} \theta_{1D} w_{1D} q_{1D} (1+r_f) = & (1-\alpha)\theta_{1D} w_{1D} q_{1D} + \\ & + w_{1D} q_{1D} r_{1D} \quad (3) \end{aligned}$$

The left side of equation 3 is the bank's risk-free income. The first term on the right side is the payment received by the bank if the retailer does not default and the second is the financing interest.

Equations 1–3 represent a Stackelberg game. We proceed backwards and derive Lemma 1.

Lemma 1: When no PCG in DF, $w_{1D}^* = \frac{a\rho_2 + bc\rho_1}{2b\rho_1\rho_2}$, $q_{1D}^* = \frac{a\rho_2 - bc\rho_1}{4\rho_2}$, $r_{1D}^* = \theta_{1D}(\alpha + r_f)$, where $\rho_1 = 1 - \alpha$, $\rho_2 = \rho_1 - \theta_{1D}r_f$.

Proposition 1: In the DF model when no PCG,

(1) $w_{1D}^* \propto \alpha$, $q_{1D}^* \propto \frac{1}{\alpha}$, $r_{1D}^* \propto \alpha$, and

$$\Pi_{1D}^S = \frac{(a\rho_2 - bc\rho_1)^2}{8b\rho_1\rho_2} \propto \frac{1}{\alpha}, \quad \Pi_{1D}^R = \frac{(a\rho_2 - bc\rho_1)^2}{16b(\rho_2)^2} \propto \frac{1}{\alpha}$$

where “ \propto ” means a positive effect. For example, $w_{1D}^* \propto \alpha$ means increases with α ;

(2) $w_{1D}^* \propto \theta_{1D}$, $q_{1D}^* \propto \frac{1}{\theta_{1D}}$, $r_{1D}^* \propto \theta_{1D}$, and

$$\Pi_{1D}^S \propto \frac{1}{\theta_{1D}}, \quad \Pi_{1D}^R \propto \frac{1}{\theta_{1D}}.$$

In factoring practice, the supplier usually expects the bank to provide a larger payment (loan-to-value ratio) for the accounts receivable, thereby reducing their own risk when a retailer defaults. However, Proposition 1 shows that a higher loan-to-value ratio will lead to lower financing efficiency. This is because the bank will set a higher financing interest rate to avoid financing risks while providing a larger loan-to-value ratio because of the retailer's default risk. Consequently, the supplier experiences higher financing costs. This increases the wholesale price and lowers the order quantity, consequently lowering the supply chain's financing efficiency.

UF model under no guarantee

The sequence of events is shown in figure 1. Similarly, the supplier decides w_{1U} based on equation 4.

$$\begin{aligned} \Pi_{1U}^S(w_{1U}) = & \max_{w_{1U}} \theta_{1U} w_{1U} q_{1U} + \\ & + (1-\alpha)(1-\theta_{1U})w_{1U}q_{1U} - w_{1U}q_{1U}r_{1U} - cq_{1U} - \alpha A \quad (4) \end{aligned}$$

The fifth term is the amount of the bank's recourse to the supplier if the retailer defaults.

Then the retailer decides on the orders based on equation 5.

$$\Pi_{1U}^R(q_{1U}) = \max_{q_{1U}} E_{\varepsilon}[pq(p, \varepsilon)] - w_{1U}q_{1U}(1-\alpha) \quad (5)$$

Finally, the bank decides the financing rate r_{1U} , which can be formulated as equation 6.

$$\begin{aligned} \theta_{1U} w_{1U} q_{1U} (1+r_f) = & (1-\alpha)[(1-\beta)\theta_{1U} w_{1U} q_{1U} + \beta A] + \\ & + \alpha A + w_{1U} q_{1U} r_{1U} \quad (6) \end{aligned}$$

The first term on the right side of equation (6) is the bank's expected revenue received from the supplier if the retailer does not default; the second is the payment received by the bank from the supplier if the retailer defaults; and the third term is the financing interest.

Similarly, we proceed backwards and derive Lemma 2 based on equations 4 to 6.

Lemma 2: When no PCG in UF, and without loss of generality, we assume that the supplier's asset can be recourse is zero ($A=0$), then $w_{1U}^* = \frac{a\rho_3 + bc\rho_1}{2b\rho_1\rho_3}$, $q_{1U}^* = \frac{a\rho_3 - bc\rho_1}{4\rho_3}$, $r_{1U}^* = \theta_{1U}[(1-\alpha)\beta + \alpha + r_f]$, where

$$\rho_3 = (1-\alpha)(1-\beta\theta_{1U}) - \theta_{1U}r_f.$$

Lemma 2 indicates that both the retailer's default and supplier's default have a large impact on the financing decisions and financing efficiency under UF, which is shown in Proposition 2 below.

Proposition 2: In the UF model when no PCG,

$$(1) w_{1U}^* \propto \alpha, q_{1U}^* \propto \frac{1}{\alpha}, r_{1U}^* \propto \alpha, \text{ and}$$

$$\Pi_{1U}^S = \frac{(a\rho_3 - bc\rho_1)^2}{8b\rho_1\rho_3} \propto \frac{1}{\alpha}, \Pi_{1U}^R = \frac{(a\rho_3 - bc\rho_1)^2}{16b(\rho_3)^2} \propto \frac{1}{\alpha}$$

$$(2) w_{1U}^* \propto \beta, q_{1U}^* \propto \frac{1}{\beta}, r_{1U}^* \propto \beta, \text{ and}$$

$$\Pi_{1U}^S \propto \frac{1}{\beta}, \Pi_{1U}^R \propto \frac{1}{\beta};$$

$$(3) w_{1U}^* \propto \theta_{1U}, q_{1U}^* \propto \frac{1}{\theta_{1U}}, r_{1U}^* \propto \theta_{1U}, \text{ and}$$

$$\Pi_{1U}^S \propto \frac{1}{\theta_{1U}}, \Pi_{1U}^R \propto \frac{1}{\theta_{1U}}.$$

Similar to Proposition 1, under UF, both the supplier's wholesale price and the bank's financing interest rate increase with the retailer's default risk and the bank's loan-to-value ratio; meanwhile, the retailer's orders and the profits of both the supplier and retailer decrease. Therefore, under UF, excessively pursuing higher loan-to-value ratios for the accounts receivable increases (decreases) financing costs (financing efficiency). In addition, as the supplier's default risk increases under UF, the bank sets a higher interest rate, which increases financing costs for the capital-constrained supplier, consequently lowering the supply chain's financing efficiency.

DF model with a third-party PCG

The sequence of events is shown in figure 2. Similarly, the supplier decides w_{2D} based on equation 7.

$$\begin{aligned} \Pi_{2D}^S(w_{2D}) = & \max_{w_{2D}} \theta_{2D}w_{2D}q_{2D} + \\ & + (1-\alpha)(1-\theta_{2D})w_{2D}q_{2D} - w_{2D}q_{2D}r_{2D} - \\ & - cq_{2D} - \delta w_{2D}q_{2D} \end{aligned} \quad (7)$$

The fifth term of equation 7 represents the guarantee fees that the supplier pays to the third party.

The retailer's decision on its order quantity q_{2D} can be formulated as equation 8.

$$\Pi_{2D}^R(q_{2D}) = \max_{q_{2D}} E_\varepsilon [pq(\rho, \varepsilon)] - w_{2D}q_{2D}(1-\alpha) \quad (8)$$

The third party decides the guarantee coefficient λ_{2D} , which can be formulated as equation 9.

$$\lambda_{2D}w_{2D}q_{2D}\alpha = \delta w_{2D}q_{2D} \quad (9)$$

The term on the left side of equation 9 represents the guarantee costs of the third party if the retailer defaults, and the term on the right side is the third party's income by offering a PCG.

Finally, the bank decides the financing rate r_{2D} based on equation 10.

$$\begin{aligned} \theta_{2D}w_{2D}q_{2D}(1+r_f) = & (1-\alpha)\theta_{2D}w_{2D}q_{2D} + \\ & + w_{2D}q_{2D}r_{2D} + \lambda_{2D}w_{2D}q_{2D}\alpha \end{aligned} \quad (10)$$

Similarly, we proceed backwards and derive Lemma 3 below.

Lemma 3: When no PCG in DF, $w_{2D}^* = \frac{a\rho_2 + bc\rho_1}{2b\rho_1\rho_2}$, $q_{2D}^* = \frac{a\rho_2 - bc\rho_1}{4\rho_2}$, $r_{2D}^* = \theta_{2D}(\alpha + r_f) - \alpha\lambda_{2D}$.

Proposition 3: In DF model when third-party offers PCG,

$$(1) w_{2D}^* \propto \alpha, q_{2D}^* \propto \frac{1}{\alpha}, r_{2D}^* \propto \alpha, \text{ and}$$

$$\Pi_{2D}^S = \frac{(a\rho_2 - bc\rho_1)^2}{8b\rho_1\rho_2} \propto \frac{1}{\alpha}, \Pi_{2D}^R = \frac{(a\rho_2 - bc\rho_1)^2}{16b(\rho_2)^2} \propto \frac{1}{\alpha};$$

$$(2) w_{2D}^* \propto \theta_{2D}, q_{2D}^* \propto \frac{1}{\theta_{2D}}, r_{2D}^* \propto \theta_{2D}, \text{ and}$$

$$\Pi_{2D}^S \propto \frac{1}{\theta_{2D}}, \Pi_{2D}^R \propto \frac{1}{\theta_{2D}}.$$

(3) For a given α and θ_{2D} , then $w_{2D}^* \perp \lambda_{2D}$, $q_{2D}^* \perp \lambda_{2D}$, $r_{2D}^* \propto \frac{1}{\lambda_{2D}}$, $\Pi_{2D}^S \perp \lambda_{2D}$, $\Pi_{2D}^R \perp \lambda_{2D}$, where " \perp " means no relationship. For a given and interest rate r_{2D}^* , then $\theta_{2D} \propto \lambda_{2D}$, $w_{2D}^* \propto \lambda_{2D}$, $q_{2D}^* \propto \frac{1}{\lambda_{2D}}$.

Proposition 3 notes that the PCG coefficient significantly affects decisions and profits. First, if the bank's loan-to-value ratio remains unchanged, a third-party PCG can reduce the financing rate. Interestingly, a PCG does not affect the optimal decisions of the supplier and retailer even when the supplier assumes the guarantee fees. This is because the decline in the financing interest rate reduces the supplier's financing cost; this enables the supplier (retailer) to maintain the optimal wholesale price (optimal order quantity). In addition, if the bank sets a fixed interest rate, a third-party PCG can increase the bank's loan-to-value ratio for the accounts receivable. However, the supplier will charge a higher wholesale price when a third party offers a PCG and the wholesale price increases with the PCG coefficient. This is because a higher PCG coefficient can reduce the bank's financing interest rate or improve its loan-to-value ratio, which in turn offsets the guarantee costs borne by the supplier.

UF model with a third-party PCG

The sequence of events is shown in figure 2. Similarly, the supplier decides w_{2U} based on equation 11.

$$\begin{aligned} \Pi_{2U}^S(w_{2U}) = & \max_{w_{2U}} \theta_{2U}w_{2U}q_{2U} + \\ & + (1-\alpha)(1-\theta_{2U})w_{2U}q_{2U} - \alpha A - w_{2U}q_{2U}r_{2U} - \\ & - cq_{2U} - \delta w_{2U}q_{2U} \end{aligned} \quad (11)$$

Then the retailer decides on the orders q_{2U} based on equation 12.

$$\Pi_{2U}^R(q_{2U}) = \max_{q_{2U}} E_\varepsilon [pq(\rho, \varepsilon)] - w_{2U}q_{2U}(1-\alpha) \quad (12)$$

The third party decides the guarantee coefficient λ_{2U} based on equation 13.

$$\lambda_{2U}w_{2U}q_{2U}[\alpha + (1-\alpha)\beta] = \delta w_{2U}q_{2U} \quad (13)$$

Finally, the bank decides the financing interest rate r_{2U} based on equation 14.

$$\theta_{2U}w_{2U}q_{2U}(1+r_f) = (1-\alpha)[(1-\beta)\theta_{2U}w_{2U}q_{2U} + \beta A] + \alpha A + w_{2U}q_{2U}r_{2U} + \lambda_{2U}w_{2U}q_{2U}[\alpha + (1-\alpha)\beta] \quad (14)$$

Similarly, we proceed backwards and derive Lemma 4 below.

Lemma 4: When the third-party offers PCG in UF,

$$w_{2U}^* = \frac{a\rho_3 + bc\rho_1}{2b\rho_1\rho_3}, q_{2U}^* = \frac{a\rho_3 - bc\rho_1}{4\rho_3},$$

$$r_{2U}^* = (\theta_{2U} - \lambda_{2U})[(1-\alpha)\beta + \alpha] + \theta_{2U}r_f.$$

Proposition 4: In UF model when third-party offers PCG,

$$(1) w_{2U}^* \propto \alpha, q_{2U}^* \propto \frac{1}{\alpha}, r_{2U}^* \propto \alpha, \text{ and}$$

$$\Pi_{2U}^S = \frac{(a\rho_3 - bc\rho_1)^2}{8b\rho_1\rho_3} \propto \frac{1}{\alpha}, \Pi_{2U}^R = \frac{(a\rho_3 - bc\rho_1)^2}{16b(\rho_3)^2} \propto \frac{1}{\alpha}$$

$$(2) w_{2U}^* \propto \beta, q_{2U}^* \propto \frac{1}{\beta}, r_{2U}^* \propto \beta, \text{ and}$$

$$\Pi_{2U}^S \propto \frac{1}{\beta}, \Pi_{2U}^R \propto \frac{1}{\beta};$$

$$(3) w_{2U}^* \propto \theta_{2U}, q_{2U}^* \propto \frac{1}{\theta_{2U}}, r_{2U}^* \propto \theta_{2U}, \text{ and}$$

$$\Pi_{2U}^S \propto \frac{1}{\theta_{2U}}, \Pi_{2U}^R \propto \frac{1}{\theta_{2U}}.$$

$$(4) \text{ For a given } \alpha, \beta \text{ and } \theta_{2U}, \text{ then } w_{2U}^* \perp \lambda_{2U}, w_{2U}^* \perp \lambda_{2U}$$

$$r_{2U}^* \propto \frac{1}{\lambda_{2U}}, \Pi_{2U}^S \perp \lambda_{2U}, \Pi_{2U}^R \perp \lambda_{2U}. \text{ For a given } \alpha, \beta$$

and interest rate r_{2U}^* , then $\theta_{2U} \propto \lambda_{2U}, w_{2U}^* \propto \lambda_{2U},$

$$q_{2U}^* \propto \frac{1}{\lambda_{2U}}.$$

Proposition 4 states that the impact of the default risks of both the retailer and supplier and the bank's loan-to-value ratio on the optimal decisions and profits are consistent with Proposition 2 in Section 2.3. Furthermore, the PCG coefficient significantly affects decisions and profits. First, if the bank's loan-to-value ratio remains unchanged, a third-party PCG can reduce the negative effect of default risk on the bank. The supplier's financing cost is thus lower, enabling the supplier and retailer to maintain the optimal wholesale price and order quantity. Furthermore, this PCG can increase the bank's loan-to-value ratio if the bank sets a fixed financing interest rate. However, the supplier's wholesale price increases with the PCG coefficient. This is because the decrease in the financing interest rate or increase in the loan-to-value ratio can offset the guarantee costs borne by the supplier.

IMPACT OF GUARANTEE AND FACTORING TYPE

The impact of PCG under DF and UF

For the impact of guarantee under DF, we deduce Proposition 5 based on Lemmas 1 and 3.

Proposition 5: Under DF, if $\theta_{1D} = \theta_{2D} = \theta$, then $w_{1D}^* = w_{2D}^*, q_{1D}^* = q_{2D}^*, r_{1D}^* > r_{2D}^*, \Pi_{1D}^S = \Pi_{2D}^S,$ and $\Pi_{1D}^R = \Pi_{2D}^R.$

For the impact of guarantee under UF, we deduce Proposition 6 based on Lemmas 2 and 4.

Proposition 6: Under UF, if $\theta_{1U} = \theta_{2U} = \theta$, then $w_{1U}^* = w_{2U}^*, q_{1U}^* = q_{2U}^*, r_{1U}^* > r_{2U}^*, \Pi_{1U}^S = \Pi_{2U}^S,$ and $\Pi_{1U}^R = \Pi_{2U}^R.$

Propositions 5 and 6 states that whether under DF or UF, a third-party PCG can effectively reduce the bank's interest rate; however, the wholesale price, order quantity, and financing efficiency remain the same as that under no guarantee. This is because the positive impact of the decrease in the interest rate or increase in the loan-to-value ratio under PCG is offset by the guarantee costs borne by the supplier. Consequently, the supplier maintains the wholesale price rather than reducing it. Therefore, the optimal profit of each participant remains unchanged. Propositions 5 and 6 show that when the supplier assumes the guarantee fee, a third-party PCG can reduce the bank's financing risk and interest rate; however, it cannot improve the supply chain's financing efficiency.

The optimal factoring type between DF and UF

For the optimal factoring type under no guarantee and a third-party PCG, we deduce Proposition 7 based on Lemmas 1 and 2 and Proposition 8 based on Lemmas 3 and 4.

Proposition 7: Under factoring with no guarantee, if $\theta_{1D} = \theta_{1U} = \theta$, then $w_{1D}^* \leq w_{1U}^*, q_{1D}^* \geq q_{1U}^*,$ $r_{1D}^* \leq r_{1U}^*, \Pi_{1D}^S \geq \Pi_{1U}^S, \Pi_{1D}^R \geq \Pi_{1U}^R,$ and $\Pi_{1D}^{SC} \geq \Pi_{1U}^{SC};$ the equality holds if and only if $\beta = 0.$

Proposition 8: Under factoring with a third-party PCG, if $\theta_{2D} = \theta_{2U} = \theta$, then $w_{2D}^* \leq w_{2U}^*, q_{2D}^* \geq q_{2U}^*,$ $r_{2D}^* \leq r_{2U}^*, \Pi_{2D}^S \geq \Pi_{2U}^S, \Pi_{2D}^R \geq \Pi_{2U}^R,$ and $\Pi_{2D}^{SC} \geq \Pi_{2U}^{SC};$ the equality holds if and only if $\beta = 0.$

Propositions 7 and 8 show that the financing efficiency under UF is always lower than that under DF with or without PCG. The reasons are as follows. First, the bank's financing interest rate under UF is higher than that under DF because the supplier's factoring financing does not inform the retailer (core enterprise as the debtor). Simultaneously, there is an information asymmetry between the bank and the supplier on whether the supplier will default. The bank thus assumes the double default risk from both the retailer and supplier and chooses a higher financing interest rate under UF. Therefore, the financing cost of the capital-constrained supplier increases, leading to a

higher wholesale price and lower order quantity, consequently lowering the supply chain's financing efficiency.

CONCLUSIONS

As an important pillar of people's livelihood, SMEs generally experience financing difficulties because of the textile industry's characteristics of low concentration, long industrial chains, and large seasonal fluctuations. To solve financing difficulties, this study investigates the optimal factoring type between DF and UF and the impact of guarantee on factoring. We find that an excessive pursuit of a loan-to-value ratio for the accounts receivable leads to lower financing efficiency. Furthermore, a third-party PCG can effectively

reduce the financing interest rate but cannot improve the financing efficiency if the supplier assumes the guarantee fee. Finally, the profits of both the supplier and retailer are higher under DF than under UF. Our analysis provides guidelines for supply chain and financial institutions regarding the factoring business in the textile industry. First, a capital-constrained supplier may not find it profitable to pursue a higher loan-to-value ratio for accounts receivable. Moreover, while introducing a guarantee mechanism to control financing risk, financial institutions should consider supply chain participants, rather than the supplier, to assume the guarantee fees. Furthermore, both the supplier and retailer should choose financing under DF regardless of a guarantee.

REFERENCES

- [1] Kouvelis, P., Xu, F.S., *A supply chain theory of factoring and reverse factoring*, In: Management Science, 2021, 67, 10, 6071–6088
- [2] Yan, N.N., Sun, B.W., Zhang, H., et al., *A partial credit guarantee contract in a capital-constrained supply chain: Financing equilibrium and coordinating strategy*, In: International Journal of Production Economics, 2016, 173, 122–133
- [3] Huang, B., Wu, A., Chiang, D., *Supporting small suppliers through buyer-backed purchase order financing*, In: International Journal of Production Research, 2018, 56, 18, 6066–6089
- [4] Lu, Q.H., Gu, J., Huang, J.Z., *Supply chain finance with partial credit guarantee provided by a third-party or a supplier*, In: Computers & Industrial Engineering, 2019, 135, 440–455
- [5] Yu, X., Chen, H.Z., Xiang, K.Z., et al., *Supply chain financing mechanism with guarantee insurance*, In: Managerial and Decision Economics, 2021, 42, 2, 308–318
- [6] Zhou, W.H., Lin, T.T., Cai, G.S., *Guarantor financing in a four-party supply chain game with leadership influence*, In: Production and Operations Management, 2020, 29, 9, 2035–2056
- [7] Klapper, L., *The role of factoring for financing small and medium enterprises*, In: Journal of Bank & Finance, 2006, 30, 11, 3111–3130
- [8] Kasper, V., Reindorp, M.J., Fransoo, J.C., *The price of reverse factoring: Financing rates vs. payment delays*, In: European Journal of Operational Research, 2015, 242, 3, 842–853
- [9] Luo, P.F., Wang, H.M., Yang, Z.J., *Investment and financing for SMEs with a partial guarantee and jump risk*, In: European Journal of Operational Research, 2016, 249, 3, 1161–1168
- [10] Xu, S., Fang, L., *Partial credit guarantee and trade credit in an emission-dependent supply chain with capital constrain*, In: Transportation Research Part E: Logistics and Transportation Review, 2020, 135, 101859
- [11] Shi, J.Z., Du, Q., Li, F., et al., *Coordinating the supply chain finance system with buyback contract: A capital-constrained newsvendor problem*, In: Computers & Industrial Engineering 2020, 146, 106587
- [12] Tunca, T.I., Zhu, W.M., *Buyer intermediation in supplier finance*, In: Management Science, 2018, 64, 12, 5631–5650
- [13] Koyuncu, I., Kural, E., Topacik, D., *Pilot scale nanofiltration membrane separation for waste management in textile industry*, In: Water & Science Technology, 2001, 42, 10, 233–240
- [14] Chen, L., Yan, X., Yu, H., *Developing a modular apparel safety architecture for supply chain management: the apparel recycle perspective*, In: Industria Textila, 2018, 69, 1, 24–30, <http://doi.org/10.35530/IT.069.01.1380>
- [15] Milojevic, I., Krstić, S., Ćurčić, M., *Optimisation of accounting model of inventory management in the textile industry*, In: Industria Textila, 2021, 72, 2, 198–202, <http://doi.org/10.35530/IT.072.02.1769>
- [16] Bruce, M., Daly, L., Towers, N., *Lean or agile: A solution for supply chain management in the textiles and clothing industry*, In: International Journal of Operations & Production Management, 2004, 24, 2, 151–170
- [17] Hilletofth, P., Hilmola, O.-P., *Supply chain management in fashion and textile industry*, In: International Journal of Services Sciences, 2008, 1, 2, 127–147
- [18] Devalkar, S.K., Krishnan, H., *The impact of working capital financing costs on the efficiency of trade credit*, In: Production and Operations Management, 2019, 28, 4, 878–889
- [19] Cachon, G.P., Lariviere, M.A., *Supply chain coordination with revenue-sharing contracts: Strengths and limitations*, In: Management Science, 2005, 51, 1, 30–44
- [20] Shunko, M., Do, H.T., Tsay, A.A., *Supply chain strategies and international tax arbitrage*, In: Production and Operations Management, 2017, 26, 2, 231–251

Authors:

ZHAO SHENGYING¹, ZHONG MINGJUN², LU XIANGYUAN¹

¹Dongbei University of Finance and Economics, School of Management Science and Engineering,
217 Jianshan Street, 116025, Dalian, China
e-mail: 995841965@qq.com

²University of Aberdeen, Department of Computing Science,
Aberdeen AB24 3FX, 999020, Scotland, UK
e-mail: mingjun.zhong@abdn.ac.uk

Corresponding author:

LU XIANGYUAN
e-mail: xiangyuan_lu@hotmail.com

The design of experiments in the field of technical textiles as an educational module

DOI: 10.35530/IT.074.02.202266

MARIAN CATALIN GROSU
ION RAZVAN RADULESCU

EMILIA VISILEANU
RAZVAN SCARLAT

ABSTRACT – REZUMAT

The design of experiments in the field of technical textiles as an educational module

Mastering software knowledge for the design of textile fabrics is especially important for students of higher education and offers substantial competitive advantages within the world of work. The Erasmus+ project OptimTex has prepared up-to-date educational materials as a response to the digitization requirements of Industry 4.0 in the textile field. This paper presents the content of an e-learning module conceived by the coordinator of the Erasmus+ OptimTex project. The module addresses the design of experiments in the field of technical textiles for electromagnetic shielding, with the following technical aspects: two input parameters, the weft fabric density (number of yarns per 10 cm) and the thickness of the plasma-coated metallic (copper) layer on both sides of the fabric (nanometre) and one result variable, the electromagnetic shielding effectiveness of the fabrics (dB) at 100 MHz. A Box-Wilson central composite design was applied to optimize shielding effectiveness related to both input parameters. Software such as Excel, MATLAB and MODDE was applied to compute and cross-check the response surface modelling.

Keywords: technical textiles, e-learning, optimization, EMI shielding, plasma

Modul educațional privind proiectarea experimentală în domeniul textilelor tehnice

Deținerea cunoștințelor pentru proiectarea materialelor textile prin aplicații software este deosebit de importantă pentru studenții din învățământul superior și oferă avantaje substanțiale de competitivitate pe piața forței de muncă. Proiectul Erasmus+ OptimTex a pregătit materiale educaționale adaptate la cerințele de digitalizare ale Industriei 4.0 în domeniul textil. Lucrarea prezintă conținutul unui modul de e-learning realizat de coordonatorul proiectului Erasmus+ OptimTex. Modulul abordează proiectarea experimentală în domeniul textilelor tehnice pentru ecranarea electromagnetică, cu următoarele aspecte tehnice: doi parametri de intrare, desimea în bătătură a țesăturii (numărul de fire/10 cm) și grosimea stratului metalic (cupru) deșus prin acoperire cu plasma, pe ambele părți ale țesăturii (nanometri) și o variabilă de rezultat, atenuarea electromagnetică a ecranelor țesute (dB) la 100 MHz. A fost aplicat un program central compozit Box-Wilson pentru a optimiza atenuarea electromagnetică în raport cu cei doi parametri de intrare. Aplicații software precum Excel, MATLAB și MODDE au fost utilizate pentru a calcula și verifica modelarea suprafeței de răspuns.

Cuvinte cheie: textile tehnice, e-learning, optimizare, ecranare EMI, plasmă

INTRODUCTION

This paper aims to present the content of an e-learning software module for the design of experiments for technical textiles.

The novelty of this contribution related to the state of the art is based on three major pillars: technical/e-textiles, e-learning and design and modelling software.

Progress in e-textiles

As a vanguard domain, “e-textiles” and technical textiles are a fast-growing and advanced interdisciplinary research field with promising applications in green wearable electronics, multifunctional smart clothes for health care and human movement detection and smart interior design [1, 2].

The synergy between flexibility, ultralight weight, comfort, stretchability, foldability, low cost of the essential textiles for everyday life and advanced electronic functions of the specific materials (carbon

nanomaterials, metal oxides, metals, silicones, etc.) generates a wide range of advanced applications to serve and improve lifestyle, including continuous monitoring devices for human physiological signals, piezoresistive sensors, piezoelectrical devices, capacitive sensors, field effect transistors [3] portable displays, advanced sportswear and portable energy collection and storage systems [4]. In recent years, there has been an increase in consumer awareness of technological developments and applications, which has led to investments in portable electronics and smart electronic textile systems, along with associated industries [5].

Today's world is characterized by increasing dynamics and complexity in labour market relations and the increasing complexity of global competition [6]. Since digital and smart transformation has impacted how every industry works, the interest in these new technologies continuously increases among teachers,

students, trainees, etc., for their future careers to stay updated in the face of rapid change [7].

Progress in e-learning

In this regard, e-learning and online education have made great strides in the recent past. It has moved from a knowledge transfer model to a highly intellectual, swift and interactive proposition capable of advanced decision-making abilities [8]. Educational software has the primary purpose of teaching or self-learning. Educational software makes learning more effective and attractive, keeping teachers, students, trainees and pupils updated with software technologies, processes, and practices that are popular in industries [9]. Educational software integrates multimedia content and provides users with a high interactivity level. Online education software supports teachers, allowing them to better connect with students and help them keep students interested in a lesson. It also promotes a productive learning environment [10]. There are many examples of educational software, such as GoReact, Canvas, Kahoot!, Edmodo, Socrative, LanSchool, ClassDojo, Dyknow, Workday Student, Wisenet, Litmos, etc., which enable higher educational institutions to support effective learning outcomes, boost stakeholder engagement, increase productivity, and grow businesses [11].

Various software applications provide learners with a portal for taking computerized quizzes and tests and developing interactive didactic applications (IDAs).

Progress in software for modelling & simulation

Computer-aided manufacturing (CAM) and computer-aided design (CAD) apparel and textile software specifically offer the designer a complete design software solution (tools and techniques) to digitally create textile designs from the initial concept to the final presentation [12]. There are numerous textile software programs available in the market, such as Gerber, Lectra, Optitex, Tukatech, CAD CAM Solutions, Assyst, and Polygon, which can be tailored to meet a company's or client's specific needs within any sector of the textile and apparel business.

The educational module presented in this paper is part of the intellectual output of an Erasmus+ project. The project sets out to improve knowledge and skills in the field of software applications for students of higher education, as well as their employability within textile enterprises, by providing six educational modules for their profession. All educational modules were implemented in e-learning format on Moodle (www.advan2tex.eu/portal/) [13] and on the project's website TAB Instrument (www.optimtex.eu) [14]. The module on the design of experiments was prepared by the INCDTP team, and one of the six examples approached the field of technical textiles for electromagnetic shielding, with the following technical aspects: two input parameters, the weft fabric density (number of yarns per 10 cm) and the thickness of the plasma-coated metallic layer on both sides of the

fabric (nanometre) and one result variable, the electromagnetic shielding effectiveness of the fabrics (dB) at 100 MHz. Such educational examples are meant for higher education students in the technical engineering field and focus on mastering software applications and statistics. This paper also includes aspects of the impact achieved by presenting the module within the first intensive study programs organized virtually and hosted by the Technical University of Iasi.

THE ERASMUS+ OPTIMTEX PROJECT

The Erasmus+ project "Software tools for textile creatives – OptimTex" is a strategic partnership project in the field of higher education. It has a two-year implementation period (Dec. 2020 – Nov. 2022) and a prestigious partnership of research and educational providers in Europe: INCDTP – Bucharest coordinates the partnership formed by TecMinho-University of Minho – Portugal, Ghent University – Belgium, University of Maribor – Slovenia, Technical University of Iasi – Romania and University of West Bohemia – Czech Republic. More details are provided on the project's website www.optimtex.eu. The website also includes educational resources in e-learning format with free access by an e-learning instrument (figure 1).

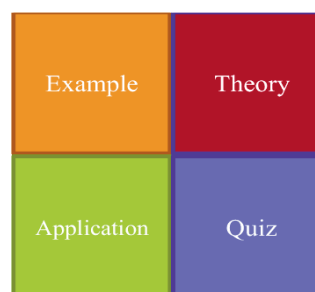


Fig. 1. E-learning instrument in PBL approach

All educational modules were conceived within a problem-based learning approach, starting from examples, the corresponding theory, some of the software applications and quizzes for self-assessment [15].

THE EDUCATIONAL MODULE ON THE DESIGN OF EXPERIMENTS

Software knowledge for design of experiments is useful in the preparation of higher education students. The educational module on the design of experiments addresses four examples with factorial plans and central composite design plans of the practical work within research projects of INCDTP. The second example describes the optimization of a plasma coating for textile fabrics meant for electromagnetic shielding. The rationale of the example is given by the fact that electromagnetic radiation is currently a major problem due to the numerous sources of pollution, mobile phones, Wi-Fi connections, Bluetooth devices, etc. affecting human health [16] and causing

interference with the proper operation of other electronic devices [17].

The presented educational example includes some technical aspects, such as the following:

- A solution to avoid undesired EMI pollution by shielding with flexible textile fabrics [18].
- Electric conductivity represents a main property characterizing electromagnetic interference (EMI) shielding textiles [19].
- Fabrics with enhanced electric conductive properties create eddy currents in reaction to the incident electromagnetic (EM) field, which yields an opposite EM field with a shielding effect [18].
- The effect of shielding can be expressed by measuring the quantity of electromagnetic shielding effectiveness (EMSE), which is defined as:

$$EMSE = 10 \log_{10} \left(\frac{\text{power of incident signal}}{\text{power of transmitted signal}} \right) \text{ [dB]} \quad (1)$$

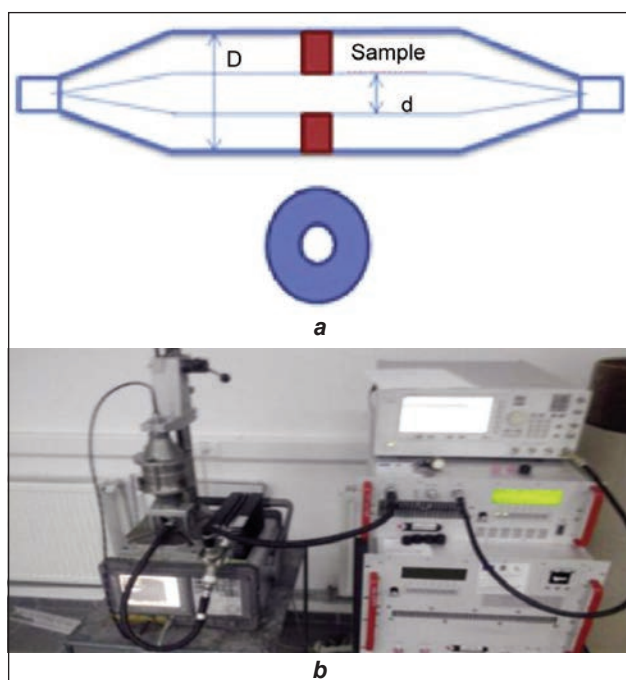


Fig. 2. TEM cell equipment of ICPE-CA: a – operating principle; b – photo of apparatus of the National Institute for R&D in Electrical Engineering – ICPE-CA, Romania

For the measurement of the EMSE, according to the ASTM ES-07 standard, the power of the signal with and without a washer-shaped textile sample within a TEM cell (figure 2) was considered, and the ratio according to equation 1 was computed.

Furthermore, the magnetron plasma deposition of nanometre metallic layers onto the fabric surface was proven to be an advanced technique for enhancing electric conductivity [22] to be used in EMI shielding. Magnetron plasma deposition is a low-pressure plasma technique by which the metallic particles of a target are dislocated by argon ions and driven towards the textile fabric surface. By this technique, using magnetron plasma equipment (figure 3), very thin layers of metallic coating, in the range of 400–6000 nm, can be deposited on the fabric surface.

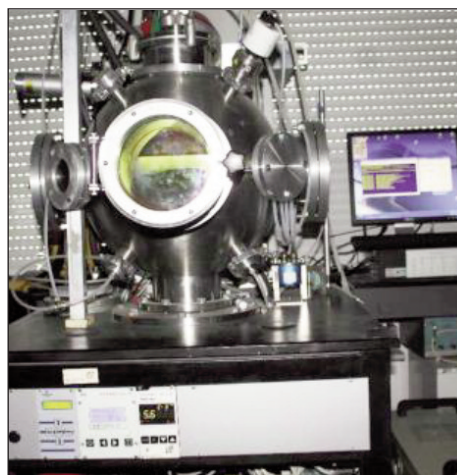


Fig. 3. Magnetron plasma equipment of The National Institute for Laser, Plasma & Radiation Physics – INFLPR, Romania

To optimize the shielding effectiveness of fabric samples, two input parameters were considered: the weft fabric density (number of yarns per 10 cm) and the thickness of the plasma-coated metallic layer on both sides of the fabric. The fabric density was considered a parameter of the fabric structure, while the layer thickness was a parameter of the plasma process. A central composite design (CCD) was applied to optimize the shielding effectiveness related to both input parameters.

CCD is also named the Box-Wilson experimental plan, after the names of the authors. It is one of the most popular experimental plans to optimize a result and determine the response surfaces. There are 3 types of CCD: circumscribed central composite design (CCC), face-centred central composite design (CCF) and inscribed central composite design (CCI). CCD is capable of seizing, in addition to interactions between factors (input parameters), the nonlinear evolution of the response within the experimental domain because it is used for fitting a polynomial equation of second degree or higher. CCD is applied for deep analysis of a phenomenon or in optimization processes. Figure 4 presents the variation levels of the circumscribed central composite design (CCC).

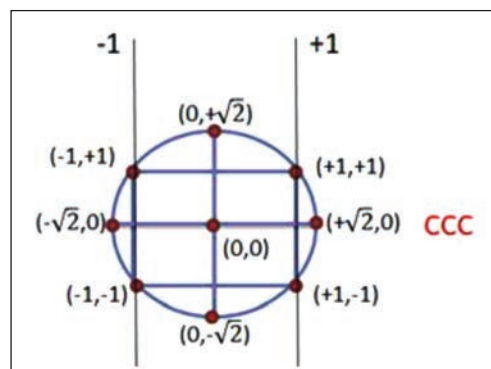


Fig. 4. Variation levels of the circumscribed central composite (CCC) design

Table 1

VARIATION LEVELS OF THE TWO INPUT PARAMETERS		
Level	Fabric density, F_d (No. yarns/10 cm)	Layer thickness, L_t (nm)
upper: $+\sqrt{2}$	404	1975.5
upper: +1	360	1750
medium: 0	260	1200
lower: -1	160	650
lower: $-\sqrt{2}$	116	424.5

The following variation levels were set for fabric density and layer thickness (table 1).

Encoding of the variables fabric density (F_d) and layer thickness (L_t) is used to reach the variation levels ($-\sqrt{2}$, -1, 0, +1, $\sqrt{2}$):

$$x = \frac{F_d - 260}{100} \quad (2)$$

$$y = \frac{L_t - 1200}{550} \quad (3)$$

where F_d is the value of the fabric density and L_t is the value of the layer thickness. The cotton fabrics were designed with different fabric densities in weft according to the experimental matrix (a grid of 4 mm was kept for all fabric samples). The copper plasma coating was subsequently applied to both sides of the fabric with the specified thicknesses in the range of 400–2000 nm according to the experimental matrix. The EMSE was measured for the cotton fabrics with conductive yarns of silver inserted into the warp and weft with a grid of 4 mm and copper plasma coating. The EMSE was measured via TEM cell equipment at 100 MHz as a reference frequency for optimizing the EMSE for these electromagnetic shields. EMSE was expressed in dB (table 2).

Table 2

EXPERIMENTAL MATRIX WITH FABRIC DENSITY AND COATING THICKNESS							
Sample code		Density	Thickness	Parameters			Result
		x	y	xy	x^2	y^2	
P01	1	-1	-1	1	1	1	42
P02	1	1	-1	-1	1	1	35
P03	1	-1	1	-1	1	1	56
P04	1	1	1	1	1	1	55
P05	1	$-\sqrt{2}$	0	0	2	0	52
P06	1	$+\sqrt{2}$	0	0	2	0	48
P07	1	0	$-\sqrt{2}$	0	0	2	40
P08	1	0	$+\sqrt{2}$	0	0	2	62
P09	1	0	0	0	0	0	50
P10	1	0	0	0	0	0	51
P11	1	0	0	0	0	0	53
P12	1	0	0	0	0	0	49
P13	1	0	0	0	0	0	50

The polynomial equation of the second degree for fitting the experimental plans with two input parameters has the following coefficients:

$$f(x,y) = a_0 + a_1x^2 + a_2y^2 + a_3xy + a_4x + a_5y \quad (4)$$

By regression in Excel, we obtain the following coefficients for the polynomial equation (table 3).

Table 3

COEFFICIENTS OF ENCODED POLYNOMIC EQUATION					
a_0	a_1	a_2	a_3	a_4	a_5
50.60	-1.18	-0.67	1.50	-1.71	8.15

By decoding the polynomial equation according to equations 2 and 3, we obtain the following expression of the polynomial model for EMSE:

$$EMSE = 34.61 + 0.012F_d + 0.013L_t + 0.000027F_dL_t - 0.00011F_d^2 - 0.000022L_t^2 \quad (5)$$

The response surface plot of equation 5 may be graphically represented in MATLAB (figure 5).

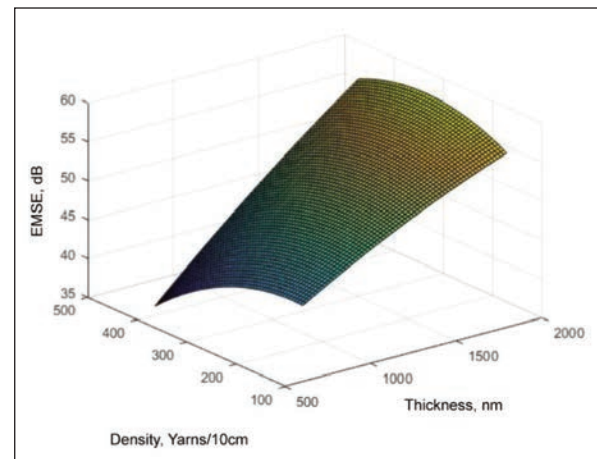


Fig. 5. MATLAB plot of the EMSE response surface

However, there are dedicated software applications for the same procedure. The MODDE software includes a design wizard, which guides the user in the selection of the input parameters, the type of experimental design and the result variables. The first graph generated by the software is the summary of fit, which presents four statistical indicators related to how well the model fits the data (figure 6). High values of the four indicators indicate a good fit of the model to the data.

A second graph shows a 3D response surface plot of the result variable in relation to both input parameters (figure 7). The software computes the values of parameters for optimized EMSE:

$EMSE_{max} = 59.90$ dB for density = -0.021 and thickness = 1.147 .

Considering equations 6 and 7, we can decode the input parameters:

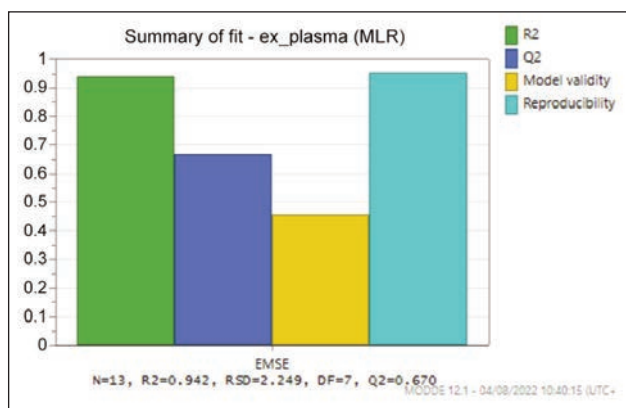


Fig. 6. The four statistic indicators of the summary of fit

$$\frac{F_d - 260}{100} = -0.021 \quad (6)$$

$$\frac{L_t - 1200}{550} = 1.147 \quad (7)$$

By computing the parameters, the maximum obtained value of EMSE = 59.90 dB at 100 MHz, with the following values for the input parameters: fabric density: $F_d = 257.9$ yarns/10 cm and plasma coating thickness: $L_t = 1830.85$ nm.

This experimental plan was conceived only for educational purposes, and both MODDE and MATLAB software offered the same results. The experimental plan was conducted only partially in practice because the nanometre thickness of the copper layer yields similar EMSE results with reduced practical relevance.

There are various methods used to address the design of experiments in the field of technical textiles. The educational module uses the software EXCEL, MATLAB, and MODDE. Different methods yield similar mathematical results. The knowledge of software applications for regression computing and plotting the response surface are useful tools for preparing higher education students.

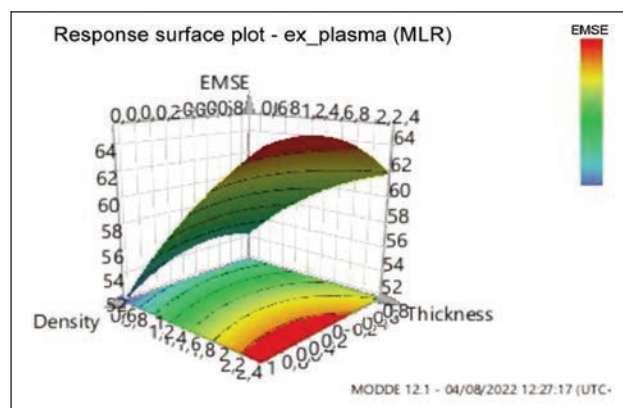


Fig. 7. MODDE plot of the EMSE response surface

CONCLUSIONS

This paper presents an educational module in the field of design experiments for manufacturing technical textiles. The educational module is meant for higher education students and is focused on software for the design of experiments in the context of the digitization trend of Industry 4.0. It is part of the Erasmus+ OptimTex project, having as its main aim to present software for the design and modelling of textiles. Software knowledge offers many competitive advantages for students within the world of work and boosts employability. The initial impact of the prepared educational materials achieved good results within a virtual intensive study program.

ACKNOWLEDGMENTS

This project has been funded with the support of the European Commission, Erasmus+ KA2 project "Software tools for textile creatives – OptimTex", grant agreement number 2020-1-RO01-KA203-079823 and publishing has been funded by the Ministry of Research and Innovation, by Program 1 – Development of the national system for R&D, Subprogram 1.2 – Institutional performance – projects for funding excellence in R&D&I, contract no. 4PFE/30.12.2021.



REFERENCES

- [1] De Medeiros, M.S., Goswami, D., Chanci, D., Moreno, C., Martinez, R.V., *Washable, breathable, and stretchable e-textiles wirelessly powered by omniphobic silk-based coils*, In: *Nano Energy*, 2021, 87, 106155, 1–11, <https://doi.org/10.1016/j.nanoen.2021.106155>
- [2] Maity, S., Singha, K., Pandit, P., *Advanced applications of green materials in wearable e-textiles*, In: S. Ahmed (Ed.), *Applications of Advanced Green Materials*, Woodhead Publishing in Materials, 2021, 239–263, <https://doi.org/10.1016/B978-0-12-820484-9.00010-6>
- [3] Tang, Z., Yao, D., Hu, S., Du, D., Shao, W., Tang, B., Gao, J., *Highly conductive, washable and super-hydrophobic wearable carbon nanotubes e-textile for vacuum pressure sensors*, In: *Sensors and Actuators A: Physical*, 2020, 303, 111710, 1–7, <https://doi.org/10.1016/j.sna.2019.111710>
- [4] Dijie, Y., Tang, Z., Li, Z., Rulong, L., Yuzhou, Z., Hongxin, Z., Jianyong, O., *As-permeable and highly sensitive, washable and wearable strain sensors based on graphene/carbon nanotubes hybrids e-textile*, In: *Composites Part A: Applied Science and Manufacturing*, 2021, 149, 106556, 1–9, <https://doi.org/10.1016/j.compositesa.2021.106556>

- [5] Hardy, D., Wickenden, R., McLaren, A., *Electronic textile reparability*, In: Journal of Cleaner Production, 2020, 276, 142328, 1–10, <https://doi.org/10.1016/j.jclepro.2020.124328>
- [6] Avram, V., Diana, A., *Teachers for the Knowledge Society – Transforming the Knowledge Incorporated in e-Learning Software into an Automatable Explicit Knowledge for the Teacher and the Learner*, In: Procedia Social and Behavioral Sciences, 2011, 11, 180–184, <https://doi.org/10.1016/j.sbspro.2011.01.057>
- [7] Garousi, V., Rainer, A., Lauvås jr, P., Arcuri, A., *Software-testing education: A systematic literature mapping*, In: Journal of Systems and Software, 2020, 165, 110570, 1–34, <https://doi.org/10.1016/j.jss.2020.110570>
- [8] Rani, M., Nayak, R., Vyas, O.P., *An ontology-based adaptive personalized e-learning system, assisted by software agents on cloud storage*, In: Knowledge-Based Systems, 2015, 90, 33–48, <https://doi.org/10.1016/j.knosys.2015.10.002>
- [9] Cico, O., Jaccheri, L., Nguyen-Duc, A., Zhang, H., *Exploring the intersection between software industry and Software Engineering education – A systematic mapping of Software Engineering Trends*, In: Journal of Systems and Software, 2021, 172, 110736, 1–28, <https://doi.org/10.1016/j.jss.2020.110736>
- [10] Nagata, S., *What You Need To Know About Educational Software*, Available at: <https://elearningindustry.com/need-know-educational-software> [Accessed on October 3, 2017]
- [11] *Educational Software Examples*, 2021, Available at: <https://rigorousthemes.com/blog/educational-software-examples/> [Accessed on July 14, 2021]
- [12] Kiron, M.I., *List of CAD/CAM Software Used in Textile and Apparel Industry*, Available at: <https://textilelearner.net/list-of-cad-cam-software/> [Accessed on October 9, 2021]
- [13] Radulescu, I.R., Dinis, A., Malengier, B., Cupar, A., Blaga, M., Polansky, R., *E-learning course of software for textile design*, In: Mobile Learning 2022 Conference Proceedings, 2022, 258–262
- [14] Radulescu, I.R., Grosu, C., Scarlat, R., Dias, A., Malengier, B., Stjepanovic, Z., Blaga, M., Polansky, R., *E-learning instrument and glossary of terms for design and modelling of textiles*, ELSE 2022 Conference Proceedings, 2022, <https://doi.org/10.12753/2066-026X-22-000>
- [15] Radulescu, I.R., Ghituleasa, C., Visileanu, E., Almeida, L., Malengier, B., Stjepanovic, Z., Blaga, M., Dufkova, P., *E-learning instruments for design based learning in textiles*, ELSE 2021 Conference Proceedings, 2021, <https://doi.org/10.12753/2066-026X-21-000>
- [16] Apollonio, F., Liberti, M., et al., *Integrated models for the analysis of biological effects of EM fields used for mobile communications*, In: IEEE Trans. Microwaves Theory, 2000, 48, 2082–2093
- [17] Islam, M.T., Alam, M.S., *Design of high impedance electromagnetic surfaces for mutual coupling reduction in patch antenna array*, In: Materials, 2013, 6, 143–155
- [18] Schwab, A., Kuerner, W., *Electromagnetic compatibility*, AGIR Publishing House, 2013
- [19] Ziaja, J., Jaroszewski, M., *EMI shielding using composite materials with plasma layers*, InTechOpen, 2011
- [20] Standard IEEE 299:2006, *IEEE Standard Method for Measuring the Effectiveness of Electromagnetic Shielding Enclosures*, 2006, Available at: <https://standards.ieee.org/standard/299-2006.html> [Accessed on October 2021]
- [21] Standard ASTM E597:2005, *Test Method for Electromagnetic Shielding Effectiveness of Planar Materials*, Available at: <https://www.astm.org/Standards/E597.htm> [Accessed on October 2021]
- [22] Rădulescu, I.R., Surdu, L., Mitu, B., Morari, C., Costea, M., Golovanov, N., *Conductive textile structures and their contribution to electromagnetic shielding effectiveness*, In: Industria Textila, 2020, 71, 5, 432–437, <http://doi.org/10.35530/IT.071.05.1783>

Authors:

MARIAN CATALIN GROSU, ION RAZVAN RADULESCU, EMILIA VISILEANU, RAZVAN SCARLAT

National Research & Development Institute for Textiles and Leather,
16 Lucretiu Patrascanu, 030508, Bucharest, Romania

Corresponding author:

MARIAN CATALIN GROSU
e-mail: catalin.grosu@incdtp.ro

Tensile and impact properties of chopped carbon fibre reinforced thermoplastics with multiple recycle and regenerate

DOI: 10.35530/IT.074.02.202225

FANGTAO RUAN
QINGYONG YANG
BOBO ZHAO

XINYU XIE
LI YANG
ZHENZHEN XU

ABSTRACT – REZUMAT

Tensile and impact properties of chopped carbon fibre reinforced thermoplastics with multiple recycle and regenerate

The increasing use of high-value carbon fibre in composites is linked with increasing waste generation. A simple and feasible chopped/hot-press method was proposed for multiple recycled carbon fibre-reinforced thermoplastic composites. The effect of regeneration times on the tension and impact properties of carbon fibre-reinforced polypropylene thermoplastic composites was investigated experimentally. The results showed that the r1-CFRTP specimen decreased by 69.34% in tensile strength and 48.66% in tensile modulus compared with v-CFRTP. However, its tensile properties were improved with the increase of regeneration times (before 3 times). The impact strength of r2-CFRTP and r3-CFRTP is 12.65%, 20.85% higher than v-CFRTP, while r1-CFRTP and r4-CFRTP are 8.02% and 7.06% lower than v-CFRTP. When the third regeneration makes relatively excellent mechanical properties for recycled carbon fibre/PP composite, the chopped/hot-press method is a meaningful attempt at recycling and reusing the thermoplastic composites.

Keywords: chopped carbon fibre, multiple recycle, thermoplastic polymer, tensile, impact

Proprietăți de rezistență la tracțiune și la impact ale termoplasticelelor armate cu fibră de carbon tăiată, cu reciclare și regenerare multiplă

Utilizarea tot mai frecventă a fibrei de carbon cu valoare adăugată în compozite este legată de creșterea generării de deșeurii. O metodă simplă și fezabilă de presare la cald/tăiere a fost propusă pentru mai multe compozite termoplastice armate cu fibră de carbon reciclată. Influența timpilor de regenerare asupra proprietăților de rezistență la tracțiune și la impact ale compozitelor termoplastice din polipropilenă armate cu fibre de carbon a fost investigată experimental. Rezultatele au arătat că pentru proba r1-CFRTP, rezistența la tracțiune scade cu 69,34% și modulul de tracțiune cu 48,66%, în comparație cu proba v-CFRTP. Cu toate acestea, odată cu creșterea timpilor de regenerare (până la 3 ori), proprietățile sale de rezistență la tracțiune au fost îmbunătățite. Rezistența la impact a probelor r2-CFRTP și r3-CFRTP este 12,65%, cu 20,85% mai mare decât cea a probei v-CFRTP, în timp ce cea a probelor r1-CFRTP și r4-CFRTP este cu 8,02% și 7,06% mai mică decât cea a probei v-CFRTP. În timp ce cea de-a treia regenerare face ca proprietățile mecanice să fie relativ excelente pentru compozitul din fibră de carbon reciclată/PP, metoda prin presare la cald/tăiere este o încercare semnificativă de reciclare și reutilizare a compozitelor termoplastice.

Cuvinte-cheie: fibră de carbon tăiată, reciclare multiplă, polimer termoplastic, tracțiune, impact

INTRODUCTION

Carbon fibre reinforced polymer composite (CFRP) is used in a wide range of applications in the automotive [1], construction industries [2], and other engineering applications because of its superior specific strength and stiffness and lower density [3–6]. CFRP can be divided by the component matrix polymers as either carbon fibre-reinforced thermosetting composites (CFRP) or thermoplastic composites (CFRTP). CFRTP has been growing at high speed, especially in the civil field, such as sports equipment, and new energy vehicle applications [7]. The main reasons are their better recyclability and ability to be processed more rapidly compared with thermosetting based [1, 4, 8]. Moreover, CFRTP can be applied in construction parts where toughness is more important

than strength and stiffness [9]. CFRP recycling approach can be summarised into three broad methods, mechanical, thermal, and chemical, which use a corresponding source to separate the carbon fibres from the thermoset matrix respectively [10]. Those recovery processes are complex as well as cause carbon fibre damage. A thermoplastic plastic is a kind of linear polymer material, which can realize solid-liquid conversion above the viscous flow temperature and resolidify with the decrease in temperature. Therefore, thermoplastic composites can be recovered using remelting and remodelling. In other words, CFRTP is more recyclable compared with thermosetting-based composites. Since thermoplastic-based composites can be shaped and formed repeatedly by heating and pressing, they can be developed to deal

with the recycling and environmental pressure caused by the waste of thermosetting-based composites.

There are continuous and discontinuous filling forms of carbon fibre in CFRTP, a drawback of continuous CFRTP is the limited formability. Discontinuous fibre shows superiority in complex shape design, which has been widely prepared using compression moulding, injection-moulded, and pultrusion processes, these processes may ensure the fabrication of discontinuous CFRTP with recycled carbon fibres. At present, increased work is conducted on this type of recycling for discontinuous fibre-reinforced thermoplastic composites because the recycled carbon fibres for low-end fields are step-by-step. Carbon fibre sheet moulding composite produced via chopped carbon fibre and thermoplastic plastic hot-press moulding approach presents a balanced solution with excellent mechanical performance and better formability [11]. Yi Wan [11, 12] comprehensively studied the preparation process and influence factors of semi-prepreg carbon fibre chopped tape reinforced thermoplastic composites, a wet type of paper-making method was used for better dispersion. The tape fibre lengths, thickness and moulding pressures have an impact on the mechanical properties. Liu [13] proposed a N-methyl-2-pyrrolidone solution impregnation method to prepare recycled carbon fibre-reinforced Polyetherimide chopped tapes. It is not necessary to dissolve all resin in the fabric thus has improved recovery efficiency.

It is an effective strategy to make full use of resources and save costs by multiple recycling of carbon fibre. Longana [14] adopted resin burning (pyrolysis) as a carbon fibre reclamation process, hot pressure, and vacuum bag moulding as remanufacturing processes and investigated the performance of short carbon fibre reinforced epoxy resin composite after recycling twice. The recovery of carbon fibre was highly oriented by wet suspension and pressure injection. The experimental results show that reduced adhesion between the fibre and matrix caused by residues builds up on the fibre surface during the pyrolysis process. Concerns have been raised regarding the degradation of recycled carbon fibre during the resin removal process. It is evident that the current thermoset material paradigm is not conducive to closed-loop composite recycling [15]. Tapper [15, 16] evaluated a closed-loop recycling methodology for discontinuous carbon fibre-reinforced thermoplastic matrix through a dissolution/precipitation reclamation technique and remanufacturing with the Hi-PerDiF method.

The purpose of this investigation is to determine if thermoplastic composite is multiple recyclables based on the principle of linear polymer melt remodelling. We explored the multiple recovery process of carbon fibre-reinforced polypropylene. The recycle chopped carbon fibre tape is prepared into prepreg by moulding, before that, chopped tapes were vibrated by a modified oscillator to achieve better dispersion and uniformity. The recycled chopped CFRTP

can be used as other discontinuous thermoplastic composites. For instance, application in a cover plate of a vehicle trunk, electrical components, or sports helmet. These new processing steps were introduced to address both the performance and processing issues. The effect of recovery times on fibre morphology, distribution and mechanical properties of each stage was discussed.

EXPERIMENTAL

Materials

Polypropylene was supplied by Shanghai Petrochemical Co., Ltd., China, and its melt index is 26 g/10 min. Carbon fibre plain fabric was supplied by Henan Yongmei Carbon Fibre Co., Ltd., China.

Manufacturing of multiple recoveries CFRTP

1. Firstly, polypropylene pellets were prepared into thin films by hot pressing. Virgin CFRTP for the mechanical characterization and recycling were prepared by compression moulding. 180°C with a pre-pressing step of 20 min at 4 MPa and a pressing step of 6 hours at 2 MPa as the machine cooled naturally.
2. Virgin CFRTP were cut into a specified size (4×4 cm) before the recycling process for simulating the crushing process of waste. The chopped carbon fibre tapes were placed in a special mould to ensure uniformity with a vibrating machine. Prepreg of chopped carbon fibre tapes with 0.5 mm thickness was pressurized at 180°C, 50 s at 4 MPa. Then 4 pieces of prepreg were laminated and hot pressed to prepare the first recycled chopped CFRTP (r1-CFRTP).
3. The process of step 2 was repeated, r1-CFRTP was cut into the chopped carbon fibre tapes and manufactured to r2-CFRTP, four times recovery processes were conducted, v-CFRTP, r1-CFRTP, r2-CFRTP, r3-CFRTP, r4-CFRTP were papered. A schematic diagram of the chopped recycling technique is shown in figure 1.

The weighing method was used to calculate the carbon fibre volume fraction of v-CFRTP specimens, as shown in equation 1:

$$v_f = \frac{w_f / \rho_f}{L \times W \times H} \quad (1)$$

where v_f is the fibre volume fraction; w_f and ρ_f are the weight and density of carbon fibres; L , W and H are the length, width, and thickness of composite specimens. The combustion absorption method was used to calculate the carbon fibre volume fraction of regenerative according to the GB/T31292-2014 method.

Experiments

Tensile test

Tensile testing was carried out on grades using a universal mechanical testing instrument (WDW-20) in a standard laboratory atmosphere. The specimen size is 150 mm × 12.5 mm × 2 mm, and five specimens from each quality were tested, according to the

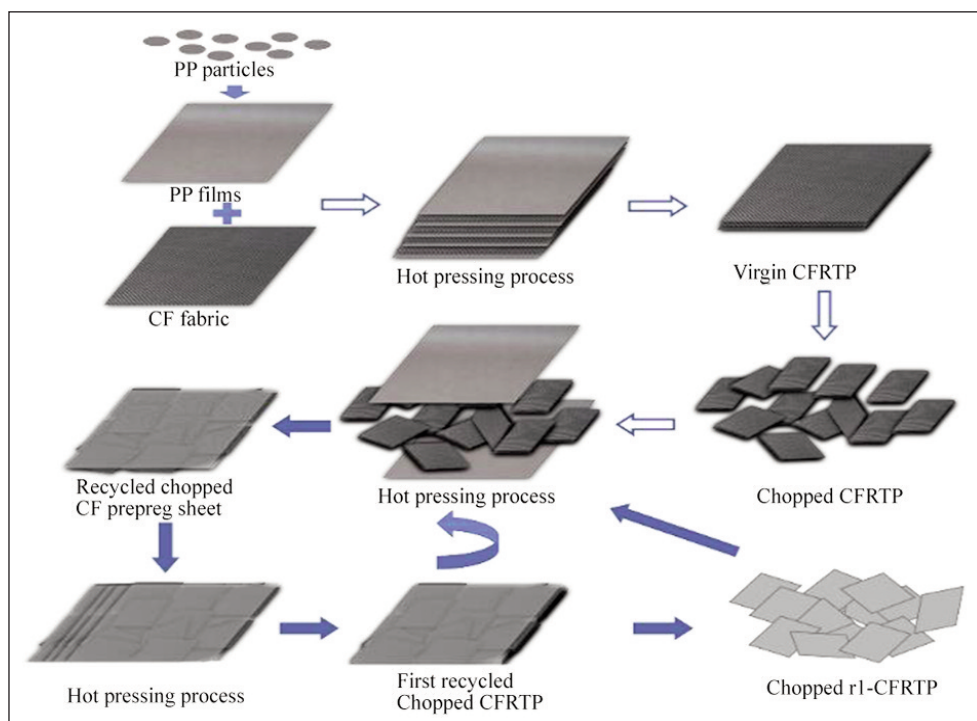


Fig. 1. A schematic diagram of multiple chopped melting recovery process

ASTMD3039 method, at a crosshead speed equal to 2 mm/min.

Notch impact test

The impact tests were carried out using a digital display simple cantilever impact tester (XJJ-50S). The absorbed energy during fracture in an impact test is used as a measure of impact strength. The dimensions of impact test specimens were about 50×10 mm (length and width). A notch was artificially prepared in the middle part of the specimens. Five specimens from each quality were tested.

The impact strengths of the specimen were calculated by the formula which references equation 2:

$$a = \frac{Ak}{W \cdot H} \times 10^3 \quad (2)$$

where a is impact strength, which is available directly from the digital display. W , H , and A are the width of the specimen, the thickness of the specimen, and the absorbed energy of the specimen, respectively.

Morphology observation

The surface and edge of the specimen were performed to observe the microstructure of the specimen after testing using an electronic magnifying camera (Gaoping, GP-300C) aim to understand fibre arrangement and resin impregnation in the composite. The fracture surface of each specimen after the impact test was inspected and analysed using a scanning electron microscope (SEM, Hitachi, S-4800) after the impact test.

RESULTS AND DISCUSSION

Morphology analysis

Representative photographic images are shown in figure 2 for the surface and edge sides of all the tested

specimens, figure 2, shows the vertical and horizontal interleaving structure shape of virgin carbon fibre plain fabric, from the edge side, the fibre waviness and layered structure are obvious due to the lamination process. r1-CFRTTP still shows some characteristics of plain fabrics, that is, the arrangement of fibres is in some order although it has become chopped tapes. With the increase in recycling and regeneration times, the arrangement of fibres in the composite is becoming more and more disordered. Besides, it can be observed from the edge side image that the fusion situation of polypropylene resin in composite was more uniform for regenerated CFRTTP.

Tensile performance

Representative stress-strain curves obtained by the tensile test of CFRTTP for each stage are shown in figure 3. The specimens of virgin CFRTTP showed linear-elastic tensile behaviour and brittle failure. The r-CFRTTP responded linearly under tension initial stage, while they are not brittle like continuous carbon fibre reinforcement. A decrease in stiffness and failure properties can be observed for recycled specimens. The continuous unrecycled carbon fibre reinforcement has the best tensile performance. However, there is no necessarily positive proportional relationship between tensile properties and regeneration times, it is not that the more recycling times, the more tensile performance degradation.

Compared with unrecycled continuous carbon fibre, the tensile strength of the first recycled carbon fibre decreased by 69.34%, as shown in figure 4. It is obvious that continuous fibre becomes discontinuous ones, the tensile strength and modulus will be greatly reduced owing to the change in failure mechanism.

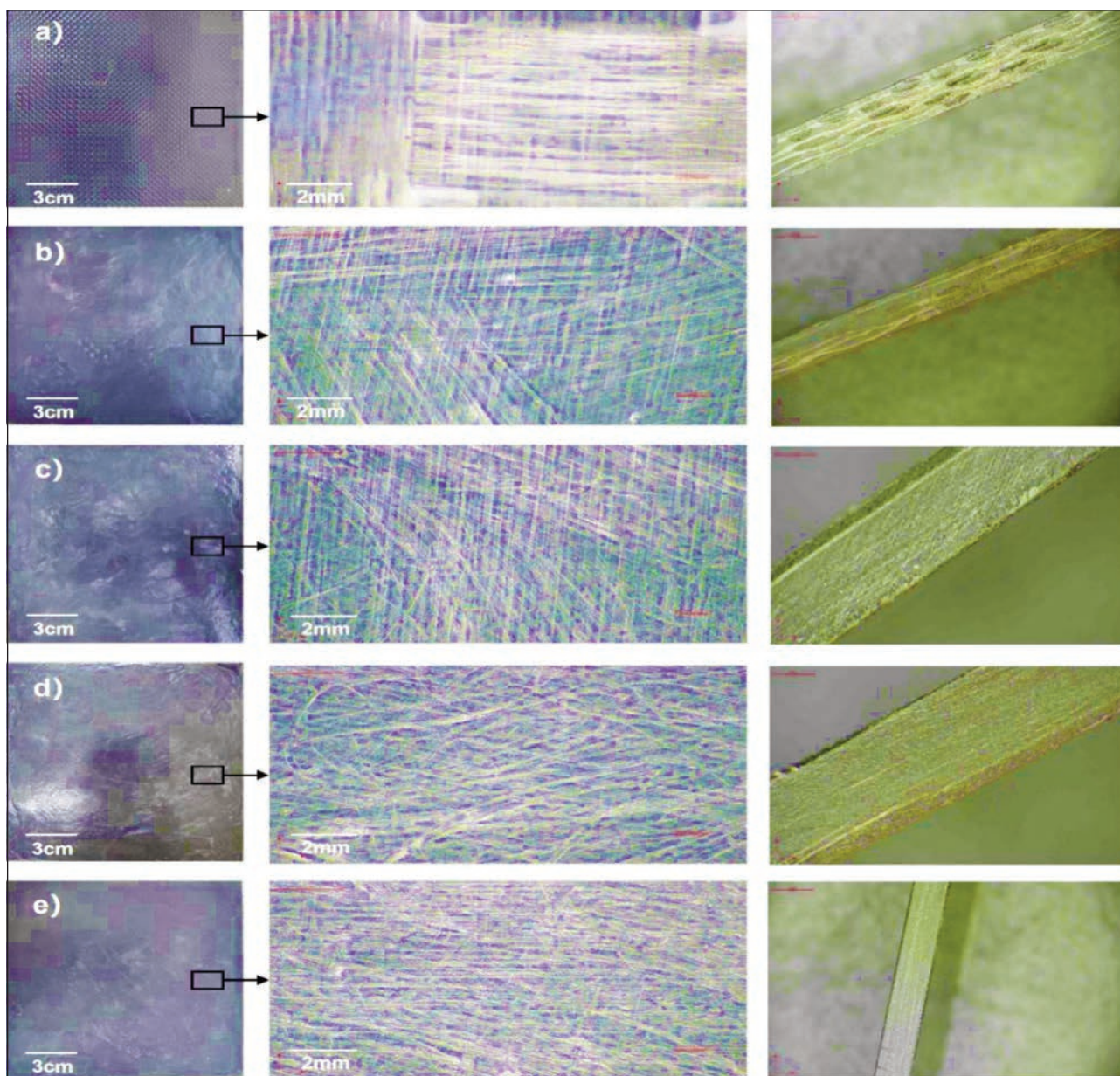


Fig. 2. Electronic photos of surface and edge for: a – CFRTTP; b – r1-CFRTTP; c – r2-CFRTTP; d – r3-CFRTTP; e – r4-CFRTTP

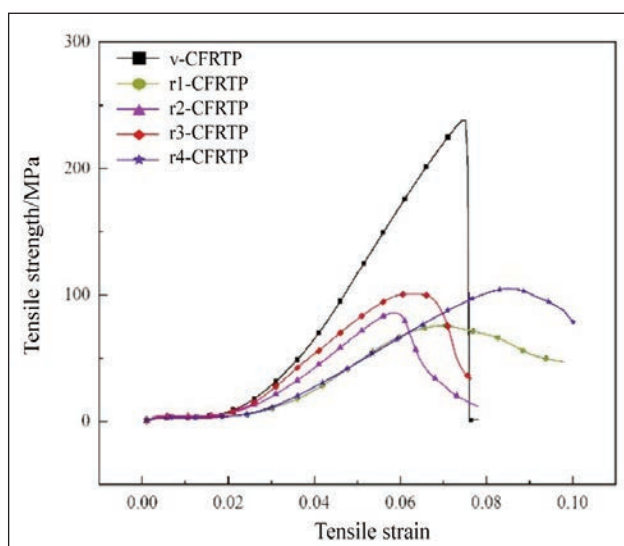


Fig. 3. Stress-strain curves for the tensile specimen

The tensile strength and modulus of second-generation recycled CFRTTP are higher than that of r1-CFRTTP. It may be the fibre waviness in-plane would decrease the strength performance. For sample r1-CFRTTP, the fibre waviness of the fabric is still obvious, which can be observed in figure 2. Young's modulus and tensile strength are degraded seriously with increasing fibre waviness. The fibre waviness gradually decreased after the shearing and chopping process many times. The third-generation recycled CFRTTP further improved. The different fibre length of the composite materials results in different mechanical properties, an equilibrium point was reached at the third recovery. The r3-CFRTTP has the best tensile properties among recycled materials. Tensile failure was strain dominated, which suggests that the fibres failed by pull-out rather than at their cross-section (figure 5).

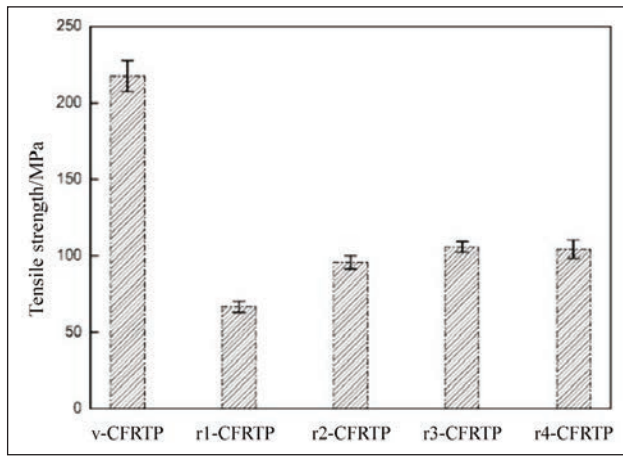


Fig. 4. Tensile strength of five specimens

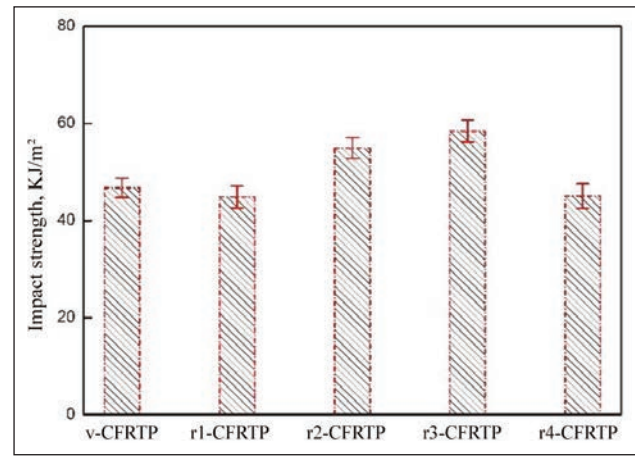


Fig. 6. Impact strength of five specimens

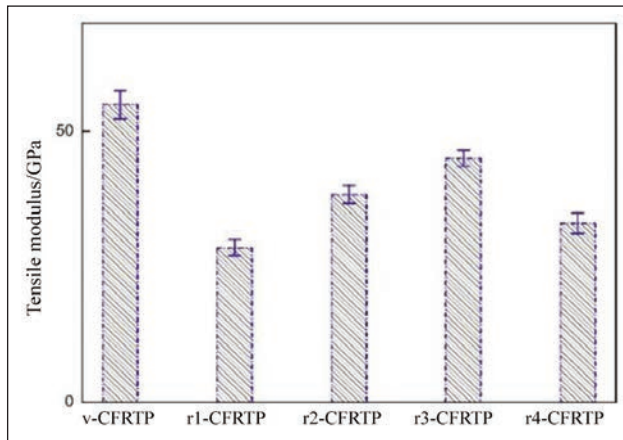


Fig. 5. Tensile modulus of five specimens

Impact performance

In general, impact phenomena are classified as low-velocity impact, high-velocity impact, ballistic impact, and hypervelocity damage impact [17]. In this investigation, the low-velocity impact carried on a cantilever beam tester was used to simulate the damage from dropped tools, bump, or fall during the services

period. From figure 6, the impact strength of regenerated composites is even higher than that of virgin carbon fibre reinforced composite. The impact strength of r2-CFRTP and r3-CFRTP is 12.65%, 20.85% higher than v-CFRTP, while r1-CFRTP and r4-CFRTP are 8.02% and 7.06% lower than v-CFRTP. The results prove that the recovery and regeneration frequency is two or three will help to improve the impact properties of chopped tape CFRTP, which is of great significance for the utilization of waste carbon fibre-reinforced thermoplastic composites.

The duration of contact between the impactor and test sample is very high in the low-velocity impact process, and thus the sample absorbs energy by elastic deformation. In addition to the geometry of carbon fibre, other factors such as resin types and interfacial properties, also affect the impact properties [18]. The prime components of CFRTP are the carbon fibre, the matrix, and a fine interphase region, which determines the bonding strength between fibre and matrix. The properties of these individual components decide how the CFRTP elastic deformation and impact ruptures. Interphase plays a role to transfer stress between resin and reinforcement, whose properties are determined by the surface chemistry

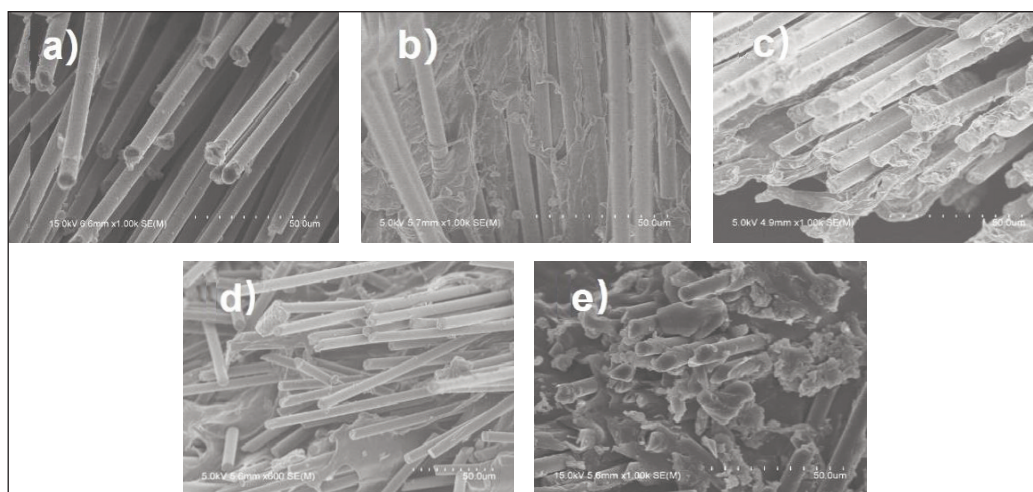


Fig. 7. Fracture surface of each specimen after impact: a – CFRTP; b – r1-CFRTP; c – r2-CFRTP; d – r3-CFRTP; e – r4-CFRTP

of fibres and resins and the composite material preparation process.

To further investigate the impact performance and fracture progress in the specimens, the x SEM picture of the impact section was observed. The obtained morphology results reveal that poor impregnation quality leads to a low impact strength for v-CFRTP. The changes in impregnation quality produce changes in interphase and interface strengths and stress transfer limitations. Besides, from figure 7, *d* and *e*, while at short carbon fibre length or poor impregnation quality, the failure is more likely to occur according to the interphase or interface debonding.

CONCLUSIONS

In this study, the effect of regeneration times on the tension and impact properties of carbon fibric reinforced polypropylene thermoplastic composites was investigated experimentally. From the tensile and notch impact test of the cantilever beam, and micro-graphic inspection, the following conclusions are reached:

- Multiple recycled chopped carbon fibre reinforced thermoplastics is a simple and feasible method for carbon and polymer resin circular and sustainable development.
- The r1-CFRTP specimen showed a total decrease of 69.34% in tensile strength and 48.66 % in tensile modulus compared with v-CFRTP. With the increase of regeneration times (before 3 times), its tensile properties were improved.
- The impact strength of r2-CFRTP and r3-CFRTP are 12.65%, 20.85% higher than v-CFRTP, while r1-CFRTP and r4-CFRTP are 8.02% and 7.06% lower than v-CFRTP. When the third regeneration makes relatively excellent mechanical properties for recycled carbon fibre/PP composite.

ACKNOWLEDGEMENTS

This work was supported by the Natural Science Foundation of China (No. 51903001), Anhui Province University Excellent Talent Cultivation Project (gxgn-fx2021133). Research Program for Students of Anhui Polytechnic University(2022DZ19).

REFERENCES

- [1] Wan, Y., Takahashi, J., *Development of carbon fibre-reinforced thermoplastics for mass-produced automotive applications in Japan*, In: Journal of Composites Science, 2021, 5, 3, 86-86, <https://doi.org/10.3390/jcs5030086>
- [2] Bakis, C.E., Bank, L.C., Brown, V.L., Cosenza, E., Davalos, J.F., Lesko, J.J., Rizkalla, S.H., Triantafillou, T.C., *Fibre-Reinforced Polymer Composites for Construction – State-of-the-Art Review*, In: Perspectives in Civil Engineering: Commemorating the 150th Anniversary of the American Society of Civil Engineers, 2002, 6, 2, 73–87, [https://doi.org/10.1061/\(ASCE\)1090-0268\(2002\)6:2\(73\)](https://doi.org/10.1061/(ASCE)1090-0268(2002)6:2(73))
- [3] Barnett, P.R., Young, S.A., Penumadu, D., *Chopped carbon fibre reinforced thermoplastic composites*, In: 32nd Technical Conference of the American Society for Composites 2017, 2017, 4, <https://doi.org/10.12783/asc2017/15386>
- [4] Pegoretti, A., *Towards sustainable structural composites: A review on the recycling of continuous-fibre-reinforced thermoplastics*, In: Advanced Industrial and Engineering Polymer Research, 2021, 4, <https://doi.org/10.1016/j.aiepr.2021.03.001>
- [5] Alshammari, B.A., Alsuhybani, M.S., Almushaikeh, A.M., Alotaibi, B.M., Alenad, A.M., Alqahtani, N.B., Alharbi, A.G., *Comprehensive review of the properties and modifications of carbon fibre-reinforced thermoplastic composites*, In: Polymers, 2021, 13, 15, <https://doi.org/10.3390/polym13152474>
- [6] Scaffaro, R., Di Bartolo, A., Dintcheva, N.T., *Matrix and filler recycling of carbon and glass fibre reinforced polymer composites: A review*, In: Polymers, 2021, 13, 21, <https://doi.org/10.3390/polym13213817>
- [7] Yao, S.S., Jin, F.L., Rhee, K.Y., Hui, D., Park, S.J., *Recent advances in carbon-fibre-reinforced thermoplastic composites: A review*, In: Composites Part B: Engineering, 2018, 142, 241–250, <https://doi.org/10.1016/j.compositesb.2017.12.007>
- [8] Leblanc, D., Landry, B., Jancik, M., Hubert, P., *Recyclability of randomly-oriented strand thermoplastic composites*, In: ICCM International Conferences on Composite Materials, 2015
- [9] Jogur, G., Nawaz, Khan A., Das, A., Mahajan, P., Alagirusamy, R., *Impact properties of thermoplastic composites*, In: Textile Progress, 2018, 50, 3, 109–183, <https://doi.org/10.1080/00405167.2018.1563369>
- [10] Zhang, J., Chevali, V.S., Wang, H., Wang, C.H., *Current status of carbon fibre and carbon fibre composites recycling*, In: Composites Part B: Engineering, 2020, 193, <https://doi.org/10.1016/j.compositesb.2020.108053>
- [11] Wan, Y., Sukanuma, H., Takahashi, J., *Effects of fabrication processes and tape thickness on tensile properties of chopped carbon fibre tape reinforced thermoplastics*, In: Composites Communications, 2020, 22, <https://doi.org/10.1016/j.coco.2020.100434>
- [12] Wan, Y., Takahashi, J., *Tensile and compressive properties of chopped carbon fibre tapes reinforced thermoplastics with different fibre lengths and molding pressures*, In: Composites Part A: Applied Science and Manufacturing, 2016, 87, 271–281, <https://doi.org/10.1016/j.compositesa.2016.05.005>
- [13] Liu, B., Zhu, P., Xu, AC., Bao, L.M., *Investigation of the recycling of continuous fibre-reinforced thermoplastics*, In: Journal of Thermoplastic Composite Materials, 2019, 32, 3, 342–356, <https://doi.org/10.1177/0892705718759388>

- [14] Longana, M.L., Ong, N., Yu, H.N., Potter, K.D., *Multiple closed loop recycling of carbon fibre composites with the HiPerDiF (High Performance Discontinuous Fibre) method*, In: Composite Structures, 2016, 153, 271–277, <https://doi.org/10.1016/j.compstruct.2016.06.018>
- [15] Tapper, R.J., Longana, M.L., Yu, H.A., Hamerton, I., Potter, K.D., *Development of a closed-loop recycling process for discontinuous carbon fibre polypropylene composites*, In: Composites Part B: Engineering, 2018, 146, 222–231, <https://doi.org/10.1016/j.compositesb.2018.03.048>
- [16] Tapper, R.J., Longana, M.L., Hamerton, I., Potter, K.D., *A closed-loop recycling process for discontinuous carbon fibre polyamide 6 composites*, In: Composites Part B: Engineering, 2019, 179, <https://doi.org/10.1016/j.compositesb.2019.107418>
- [17] Jogur, G., Nawaz, Khan A., Das, A., Mahajan, P., Alagirusamy, R., *Impact properties of thermoplastic composites*, In: Textile Progress, 2018, 50, 3, 109–183, <https://doi.org/10.1080/00405167.2018.1563369>
- [18] McKown, S., *Investigation of strain-rate effects in self-reinforced polypropylene composites*, In: Journal of Composite Materials, 2007; 41, 20, 2257–2470. <https://doi.org/10.1177/0021998307084173>

Authors:

FANGTAO RUAN^{1,2}, QINGYONG YANG¹, BOBO ZHANG¹, XINYU XIE¹, LI YANG^{1,2}, ZHENZHEN XU^{1,2}

¹Anhui Polytechnic University, School of Textile and Garment, 241000, Wuhu, China

²International Cooperation Research Center of Textile Structure Composite Materials, 241000, An Hui Province, China

Corresponding authors:

FANGTAO RUAN

e-mail: ruanfangtao@ahpu.edu.cn

ZHENZHEN XU

e-mail: xuzhenzhen@ahpu.edu.cn

The effect of entrepreneurs' personality on entrepreneurial marketing in textile sector: the mediating role of self-efficacy

DOI: 10.35530/IT.074.02.202179

MUDDASSAR SARFRAZ
MUHAMMAD IBRAHIM ABDULLAH
NAJAF MUMTAZ

SYED IBN-UL-HASSAN
ILKNUR OZTURK

ABSTRACT – REZUMAT

The effect of entrepreneurs' personality on entrepreneurial marketing in textile sector: the mediating role of self-efficacy

The study objective is to analyse the effect of big-five entrepreneurs' personality traits on entrepreneurial marketing while considering the mediating role of self-efficacy. Data were collected through a structured questionnaire; a study of 199 usable questionnaires out of 290 was carried out among young entrepreneurs. Structural equation modelling was used to test the study hypothesis. The results show a significant relationship between personality traits and entrepreneurial marketing. Openness, Extroversion, and Agreeableness personality traits are positively linked with entrepreneurial marketing. The findings also show a positive association between self-efficacy and entrepreneurial marketing. The current study contributes to the literature by analysing an entrepreneur's personality characteristics in entrepreneurial marketing.

Keywords: Big-Five personality traits, entrepreneurial marketing, self-efficacy, non-cognitive skills, entrepreneurship, textile sector

Influența personalității antreprenorilor asupra marketingului antreprenorial în sectorul textil: rolul de mediere al autoeficacității

Obiectivul studiului este de a analiza influența celor cinci mari trăsături de personalitate ale antreprenorilor asupra marketingului antreprenorial, luând în considerare rolul de mediere al autoeficacității. Datele au fost colectate printr-un chestionar structurat; un studiu de 199 de chestionare utilizabile dintr-un total de 290 a fost realizat în rândul tinerilor antreprenori. Modelarea ecuațiilor structurale a fost utilizată pentru a testa ipoteza studiului. Rezultatele arată o relație semnificativă între trăsăturile de personalitate și marketingul antreprenorial. Deschiderea, extroversia și trăsăturile de personalitate sunt pozitiv legate de marketingul antreprenorial. Constatările arată, de asemenea, asocierea pozitivă dintre autoeficacitate și marketingul antreprenorial. Studiul actual contribuie la literatura de specialitate prin analizarea caracteristicilor de personalitate ale unui antreprenor în marketingul antreprenorial.

Cuvinte-cheie: Cele cinci mari trăsături de personalitate (Big-Five), marketing antreprenorial, autoeficacitate, abilități noncognitive, antreprenori, sectorul textil

INTRODUCTION

During the past two decades, entrepreneurial marketing has gained significant attention [1], and it encapsulates the coalition between entrepreneurship and marketing [2, 3]. Marketing and entrepreneurship are separately known significant factors for firm performance [4]. Entrepreneurial marketing is an alternative approach to traditional marketing because it requires innovation in marketing tactics [5]. It is found to offer imperative consequences to the business. In general, the formulation of entrepreneurial marketing proved a crucial indicator of firm performance [6]. Entrepreneurial marketing has a significant relationship to competitive advantage, positively affecting business performance [7, 8].

Past studies have highlighted the need for studies focusing on the antecedents of entrepreneurial marketing [9]. Moreover, Whalen [10] stated that entrepreneurial marketing is at the development

stage and lacks theoretical and empirical support work. Miles [11] mentioned that entrepreneurial marketing requires theoretical and empirical underlying mechanisms. Thus, future research is necessary for the domain of entrepreneurial marketing. The earlier studies have investigated the relationship of personality traits of small and medium enterprises owner with entrepreneurial orientation, intentions, and behaviour; and found a positive nexus among these variables [12, 13].

The entrepreneur's personality shows a decisive role in encouraging entrepreneurial intention [14]. Nga & Shamuganathan [12] explained that personality traits might affect entrepreneurial desirability. Empirical findings show that acting as an entrepreneur and becoming an entrepreneur is a feature of the entrepreneurial learning process. Both are significantly affected by the personality traits of an entrepreneur [15, 16]. While looking at the various personality characteristics, the big five personality

traits have positively influenced entrepreneurial intention [17]. Other personality traits are also found to significantly influence the entrepreneur's innovative and creative actions, other than the big five personality model. Out of such personality traits, self-efficacy is one of the most significant traits [18]. Individuals who have greater self-efficacy can implement a successful strategic plan for their firms [19, 20]. Segal [21] argued that self-efficacy plays a pivotal role in entrepreneurial success.

Urban [22] found that entrepreneurs with high self-efficacy regarding planning and strategies create firm competitiveness than entrepreneurs with less self-efficacy. There is a need to find a statistical relation between Entrepreneurial Self-Efficacy (ESE) and firm performance. The existing literature shows that this relationship should exist; a study of self-efficacy is compelling. Future research should encourage us to explore its relationship with other variables [23]. Prior studies have only shown the positive correlation of self-efficacy with entrepreneurial intention in developed economies [24]; however, there is more need to focus on the outcome of self-efficacy in emerging economies [25].

Moreover, the link between self-efficacy and EM is also unexplored, thus needing future research on it. But it is to assume that self-efficacy can play an essential role in motivating entrepreneurs to adopt creative and innovative marketing methods (i.e., EM). The research aims to investigate the impact of an entrepreneur's characteristics on entrepreneurial marketing. The mediating effect of self-efficacy is rarely studied. There is no such literature to describe the mediating role of self-efficacy in the nexus of personal values and entrepreneurial orientation [17]. The manuscript section 2 presents a literature review, section 3 shows the study methodology, section 4 presents results and section 5 concludes the study.

LITERATURE REVIEW

Personality is the way the individual through which he/she reacts or interacts with others. Early work on personality shows some characteristics of individuals in the form of behaviour, shyness, aggressiveness, laziness, ambition, and loyal. Whenever these traits have analysed at a larger scale, then these are called personality traits of an individual [26]. The social network of individuals leads to more ideas and new venture startups [27]. The social network involves two concepts, i.e., strong and weak tie relationships. Relationship with individuals is called "ties". A strong tie relationship occurs between co-workers, friends, and spouses, while a weak tie relationship occurs between casual acquaintances, and these are unusual interactions. According to the research, an individual with a weak tie relationship generates new ideas for business while a strong tie relationship evolves around the ideas [28].

Openness to experience and entrepreneurial marketing

Schumpeter [29] described that entrepreneurs are creative and innovative people. In past studies, openness was a significant factor in discovering the entrepreneurship and personality relationship [30]. Openness to experience is a pivotal factor for entrepreneurs because it helps to identify entrepreneurial opportunities. Entrepreneurs recognize the opportunities and transform opportunities into business. Alvarez & Barney [31] stated that entrepreneurs are different from non-entrepreneurs because they are more insightful in identifying opportunities, so they are considered greater possible chances to succeed. For new opportunities, a new idea is compulsory [32]. Openness to experience is a personality trait that describes the individual discovery of new ideas, creativity, imagination, and unconventional thoughts. A study conducted by Sahinidis [33] reveals entrepreneurs scoring high in openness to experience exhibit positive entrepreneurial orientation. As a result, the Big Five personality characteristic (i.e., High openness to experience) is positively related to entrepreneurial marketing activities [34]. Openness to experience led entrepreneurs to translate entrepreneurial activities into firms' immediate success. Indeed, this personality attribute forms the core trait, influencing the entrepreneur's strategic choices, and significantly boosting the firm's performance [35]. Hence, the hypothesis prepared based on previous studies concludes

H1: The openness to experience factor will positively relate to Entrepreneurial Marketing.

Conscientiousness and entrepreneurial marketing

Conscientious people are efficient, organized, responsible, dependable, and practical [36]. Entrepreneurs tend to be accountable for decisions; they believe in reliable results than repetitive or routine work. Entrepreneurs gain a high score on the need for achievement, which is observed as a trait of conscientiousness. Conscientiousness shows a leading relationship with entrepreneurship despite other personality factors [37]. As defined earlier, entrepreneurs are organized and systemized, so they go for weak ties and find necessary ventures. This personality attribute explains individual competency and confidence in demonstrating control over the work discipline and social networks. Conscientiousness is a dominant personality trait affecting entrepreneurial activities. It makes entrepreneurs experience successful business ventures [35], thereby taking advantage of strategic business opportunities. Therefore, a recent study marks conscientiousness as a significant dimension of the Big Five personality model, leading to effective business performance.

However, entrepreneurs argue, conscientiousness forms a unique feature for achieving entrepreneurial success [2]. This dominant attribute plays an integral role in fostering entrepreneurial activities by adopting

effective marketing practices [38]. Hence, our findings conclude

H2: The Consciousness factor is positively related to Entrepreneurial Marketing.

Extroversion and entrepreneurial marketing

Extravert inclined to be assertive, active, bold, and energetic. Extraversion shows the best match with a good leader and contributes to achieving an organization's long-term goals [39]. Entrepreneurs can be found high scores on extraversion [40]. Due to extravert, entrepreneurs get more ideas from their surroundings and use them for the business's successful operation. Individuals high on extraversion are socially active, energetic, and confident. However, in line with the mentioned personal traits, entrepreneurs are expected to possess these characteristics for performing efficient marketing practices [41]. Moreover, to embark on a new business venture, extraversion regulates business functions by actively performing entrepreneurial activities [2]. Extraversion has an immediate impact on a firm business performance. Therefore, high social stability encourages entrepreneurs to practice relationship marketing during business ventures [38]. Hence, the finding states

H3: The extraversion factor will be positively related to Entrepreneurial Marketing.

Agreeableness and entrepreneurial marketing

Goldberg [36] described two sides of agreeableness factors; one side is that entrepreneurs act as cooperative, helpful, friendly, and trustful, while on the other hand, they can be cold, disagreeable, harsh, and rude. Kets de Vries [42] described that entrepreneurs are passionate and achievement-oriented, so they found more opportunities for their firms. Most entrepreneurs will make weak ties and relationships and will identify more opportunities. Agreeableness is a dimension that describes individual behaviour towards others. These individuals demonstrate sympathy, trustworthiness, show cooperation, and concern for others. Franco & Prata [41] reveal that the agreeableness personality trait makes entrepreneurs efficiently manage business activities. These traits are widely in need in the entrepreneurial world of environmental vulnerability. Hence, the research shows that this personality trait helps entrepreneurs translate their behaviour into positive actions [43], thus achieving competitive advantage by adopting effective entrepreneurial marketing [44]. Therefore, previous studies conclude the following hypothesis H4: The agreeableness factor will be positively related to Entrepreneurial Marketing

Neuroticism and entrepreneurial marketing

Emotion stability is a pivotal trait for individual achievement [45], and neuroticism is the reverse of emotional stability, which causes a negative association with entrepreneurship. Singh & DeNoble [30] discovered a negative relationship between neuroticism

and entrepreneurship. Goldberg [36] found a negative association between neuroticism and entrepreneurship. Entrepreneurs are the persons who look annoying and uncontrollable due to their provocative ideas and actions. Entrepreneurs who only interact with their friends and co-workers failed to learn stress control skills and possess less self-confidence toward any act. This trait causes barriers for entrepreneurs toward innovation and opportunity recognition. Regardless of the undivided attention, emotional stability is essential for entrepreneurs. Neurotic individuals tend to experience anxiety and stress, potentially lacking the courage for establishing social interactions. According to Franco & Prata [41], neuroticism negatively relates to entrepreneurial business performance. Therefore, the result shows that the insignificant correlation of business practices with neuroticism affects entrepreneurial activities and business performance [46]. However, based on previous findings, the following hypothesis is prepared H5: The neuroticism will be negatively associated with Entrepreneurial Marketing.

Personality traits related to entrepreneurial self-efficacy

Self-efficacy refers to the belief in one's ability to perform some tasks in life [18]. According to Bandura [18], individuals with a high level of self-efficacy tend to perform challenging goals and show positive behaviour toward a problematic situation. In addition, earlier studies showed a positive nexus of self-efficacy with job performance and work satisfaction [47]. Self-efficacy is an individual belief about accomplishing a specific task [48]. Primarily, entrepreneurial self-efficacy produces positive results for entrepreneurial ventures. Consequently, it is essential to understand the outcome of displaying high-level ESE while also recording the adverse effects of low self-efficacy. Entrepreneurship research shows that general self-efficacy positively relates to the intent to start a business [49]. These researches show that self-efficacy can motivate individuals to overcome the difficulties of starting a new venture. Entrepreneurial self-efficacy is specific to self-efficacy in entrepreneurship, which requires innovation. Prior studies showed that personality traits have a positive relationship with self-efficacy. For example, Openness to experience [50], Consciousness [51], Agreeableness [52], Extraversion [53] and emotional stability have a significant association with self-efficacy respectively [51]. Interpersonal relationships are positively associated with self-efficacy in high school students [54]. H6: Personality Traits are positively related to entrepreneurial self-efficacy.

Entrepreneurial self-efficacy and entrepreneurial marketing

Existing literature shows the studies that have been conducted on entrepreneurial motivation, in which self-efficacy plays an explanatory variable. Bandura [18] makes a significant contribution to psychology,

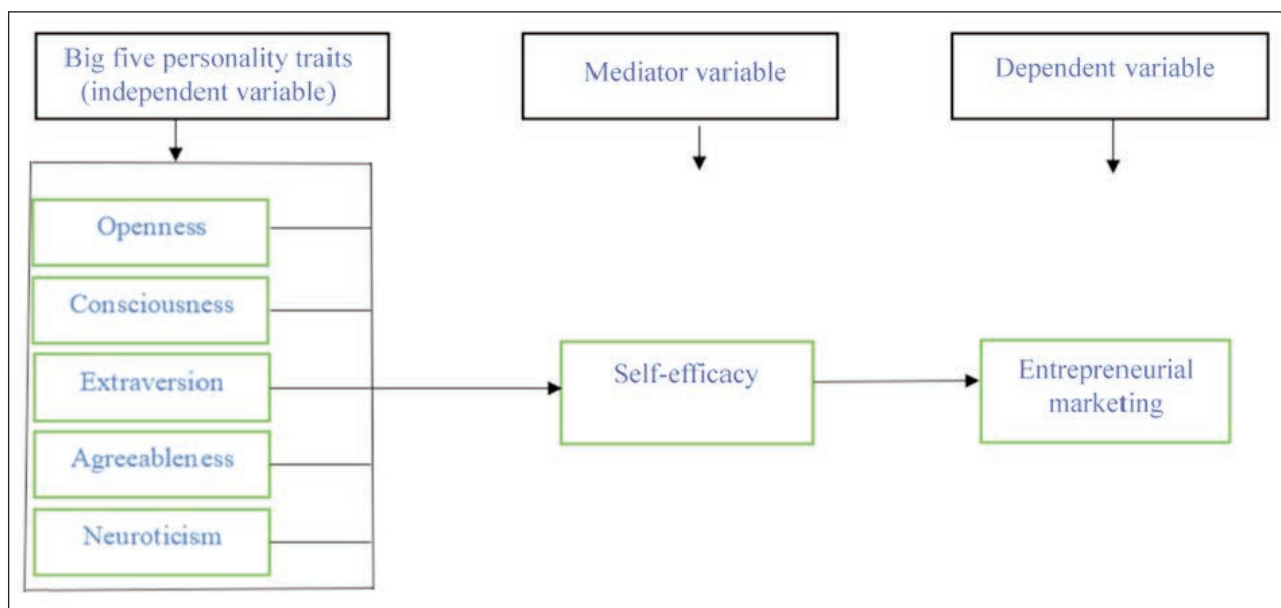


Fig. 1. Theoretical framework

and after that, self-efficacy becomes the major studied topic. Self-efficacy is described as how individuals believe in their capabilities toward motivation and behaviour toward a particular task [18]. In previous study views, self-efficacy has been used as a motivational variable toward entrepreneurs. Bandura & Ramachandran [55] examined people with a high level of self-efficacy to people with a low level of self-efficacy. Individuals with high self-efficacy are more confident in problematic situations, see the situation as challenging tasks, and be committed to achieving it. Early studies show that self-efficacy was significantly associated with the entrepreneurial intention [56]. Some other authors have found a positive relationship between self-efficacy and entrepreneurial intentions [24]. Markman [49] said that the sense of self-efficacy is higher in entrepreneurs despite non-entrepreneurs. Self-efficacy involves greater control to motivate entrepreneurs [57].

H7: Self-efficacy mediates the nexus of the entrepreneur's characteristics and entrepreneurial marketing, where the relationship of each personality dimension is explained/mediated by self-efficacy (H7a-H7e).

H7(a): Self-efficacy mediates between openness to experience and entrepreneurial marketing.

H7(b): Self-efficacy mediates between agreeableness and entrepreneurial marketing

H7(c): Self-efficacy mediates between extroversion and entrepreneurial marketing

H7(d): Self-efficacy mediates between conscientiousness and entrepreneurial marketing

H7(e): Self-efficacy mediates between neuroticism and entrepreneurial marketing

METHODOLOGY

This study has adopted quantitative research methods, and it involves analysing the numerical data and generalising the result. The study's target population

covers young entrepreneurs (who have started a textile business for the first time). There was no source available that may determine the population's size; therefore, the research uses non-probability sampling (as the unknown population frame may hamper the adoption of probability sampling). The research questionnaire was distributed among young entrepreneurs in the city of Lahore and Islamabad (Pakistan). The size sample was comprised, of 199 respondents from different sectors. Data was collected at two different times from the same respondents to avoid biases. Data was collected through a self-administered structured questionnaire.

Study measures

This study uses a questionnaire to gather the data because it is the main source collect the primary data. The questionnaire was based on close-ended questions. These questions were measured on 5-point Likert scales structured from "Strongly Agree" to "Strongly Disagree." The 10-item version measured personality, BFI-10 scale, developed by Rammstedt & John [58] on 5 points Likert scale. Self-efficacy was measured by 4 item scale by Zhao [59] on 3 points Likert scale, which included from no-confidence to complete confidence. A 42-item scale developed by Becherer [7] was used on 5 points Likert scale to measure entrepreneurial marketing.

RESULTS

Table 1 represents the respondents' profile; it covers gender, age, qualification and family business experience. As shown in the table, the study's respondents were both male (159) and female (40), and most of them were below 30 years of age and young entrepreneurs. Entrepreneurs holding a university degree except for 26 respondents. Any family experience did not back the business start-up and background, as 94.4% of the entrepreneurs had no family

Table 1

DEMOGRAPHICS OF RESPONDENTS			
Variable		Frequency	Percentage (%)
Gender	Male	159	84.684
	Female	40	16.317
Age	Less than 30	96	48.241
	31–35	67	33.668
	36–40	36	18.090
Qualification	College diploma	26	13.065
	University degree	173	88.934
Family entrepreneurial venturing	Yes	11	5.527
	No	188	94.472

background or entrepreneurship experience. These results highlight the characteristics of the study sample, which could be believed to be a young group with no entrepreneurial experience in the past. Thus, the business venture would be their first entrepreneurial effort.

Hypotheses testing (Path analysis through SEM)

After establishing the measurement model where CFA and validity assessment was carried out, a structural model was used to test the hypothesized relations. The structural model obtained goodness measures as the fitness indices met the criteria and stood well with fitness requirements. The model fit is regarded well when $DF < 3$, CFI equal or near to 1, $RMSEA < 0.06$ and $SRMR < 0.08$ [60]). Results illustrated a good model fit, with $DF = 2.457$, $CFI = 0.90$, $RMSEA = 0.004$ and $SRMR = 0.004$ (table 2).

Path analysis results are shown in figure 2 and table 3 highlight that all the independent variables had a significant effect on both mediators and dependent variables of the study. For instance, openness to

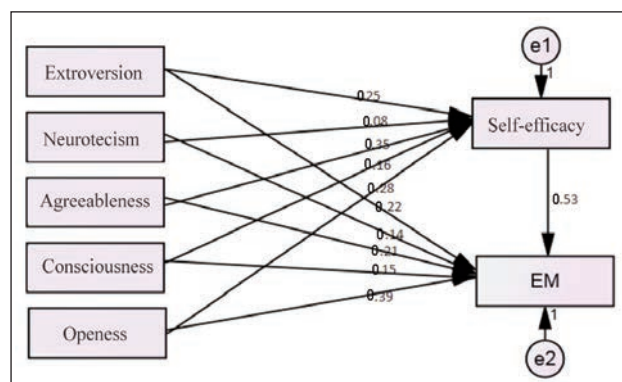


Fig. 2. Path analysis

experiences significantly influenced entrepreneurial marketing ($\beta = 0.39$, $p < 0.001$). Similarly, consciousness predicted entrepreneurial marketing ($\beta = 0.15$, $p < 0.074$), thus showing that the study could not prove the hypothesized relationship between consciousness and entrepreneurial marketing. These results thus supported our hypotheses (H1–H6), except for H2 and H5. Where direct relation was assumed between personality traits, self-efficacy, and entrepreneurial marketing

Mediation analysis

After assessing the direct paths, indirect paths for mediation were also tested using SEM. Each personality type is independently tested as the predictor, both directly and through the mediator's influence. It was hypothesized in H7 (a–e) that personality traits could predict entrepreneurial marketing through self-efficacy. Firstly, openness to experience, extraversion, and agreeableness are found to be partially predicted by self-efficacy. Secondly, consciousness is found to be fully mediated by self-efficacy. In contrast, neuroticism is not related to the criterion variable, and thus could not meet the mediation requirements (table 4).

Table 2

MODEL FIT SUMMARY FOR HYPOTHESIZED STRUCTURAL MODEL								
Model	CMIN/DF	RMR	GFI	AGFI	PGFI	CFI	RMSEA	PCLOSE
Hypothesized	2.457	0.004	0.920	0.899	0.067	0.90	0.004	0.412

Table 3

HYPOTHESIZED RELATIONS				
Hypotheses	Path	Beta	P	Result
H1	Openness – Entrepreneurial Marketing	0.39	0.000	Supported
H2	Consciousness – Entrepreneurial Marketing	0.15	0.074	Not-Supported
H3	Extraversion – Entrepreneurial Marketing	0.22	0.000	Supported
H4	Agreeableness – Entrepreneurial Marketing	0.21	0.05	Supported
H5	Neuroticism – Entrepreneurial Marketing	0.14	0.125	Not-Supported
H6	Self-efficacy – Entrepreneurial Marketing	0.53	0.000	Supported

MEDIATION ANALYSIS					
Hypotheses	Path	B	P	Results	Mediation
Openness to experience – self-efficacy – EM					
H7a	OE-EM	0.39	0.000	Supported	Partial
	OE-SE	0.28	0.05		
	SE-EM	0.53	0.000		
Consciousness – self-efficacy – EM					
H7b	Cons – EM	0.15	0.074	Supported	Full mediation
	Cons – SE	0.16	0.05		
	SE – EM	0.53	0.000		
Extroversion – self-efficacy – EM					
H7c	Extro – EM	0.22	0.000	Supported	Partial
	Extro – SE	0.25	0.000		
	SE – EM	0.53	0.000		
Agreeableness – self-efficacy – EM					
H7d	Agree – EM	0.21	0.000	Supported	Partial
	Agree – SE	0.35	0.000		
	SE – EM	0.53	0.000		
Neuroticism – self-efficacy – EM					
H7e	Neuro – EM	0.14	0.125	Not-supported	No mediation
	Neuro – SE	0.08	0.105		
	SE – EM	0.53	0.000		

CONCLUSION

The study results show entrepreneurial marketing directly and positively influences outcomes related to owner-operated SMEs. Openness, Extroversion, and Agreeableness are positively related to entrepreneurial marketing, while consciousness and neuroticism are not showing a relationship with entrepreneurial marketing. Self-efficacy is also positively mediating between the relationship between personality traits and entrepreneurial marketing. The

use of entrepreneurial marketing in an SME can personally affect goal achievement for an entrepreneur and the company. Entrepreneurial marketing also helps to create a strong company by building a good employee base and culture of innovation that can respond to problems and positively support both customers and employees. While all personality traits do not relate to entrepreneurial marketing, this research shows that alone or in combination, entrepreneurial marketing shows positive outcomes.

REFERENCES

- [1] Kraus, S., Filser, M., Eggers, F., Hills, G.E., Hultman, C.M., *The entrepreneurial marketing domain: A citation and co-citation analysis*, In: Journal of Research in Marketing and Entrepreneurship, 2012
- [2] Sarwoko, E., Nurfarida, I., *Entrepreneurial marketing: between entrepreneurial personality traits and business performance*, In: Entrep. Bus. Econ. Rev., 2021, 9, 2, 105–118
- [3] Morris, M.H., Schindehutte, M., LaForge, R.W., *Entrepreneurial Marketing: A Construct for Integrating Emerging Entrepreneurship and Marketing Perspectives*, In: J. Mark. Theory Pract., 2002
- [4] Krisjanous, J., Carruthers, J., *Walking on the light side: Investigating the world of ghost tour operators and entrepreneurial marketing*, In: Qual. Mark. Res. An Int. J., 2018
- [5] Abdul Rahim, H., Ab. Wahab, K., Saad, A., *The Shift from Traditional Marketing to Entrepreneurial Marketing Practices: A Literature Review*, In: Bus. Manag. Stud., 2015
- [6] Davari, A., Eshghi, N., Akhavan, M., Ghorbani, E., *Investigating the Effect of Entrepreneurial Marketing Dimensions on Innovative Performance in SMEs-Case Study: Guilan Science and Technology Incubator*, In: J. Adm. Manag. Educ. Train., 2016, 12, 3, 567–575
- [7] Becherer, R.C., Helms, M.M., McDonald, J.P., *The effect of entrepreneurial marketing on outcome goals in SMEs*, In: New Engl. J. Entrep., 2012, 15, 1, 3
- [8] Olannye, A.P., Edward, E., *The dimension of entrepreneurial marketing on the performance of fast food restaurants in Asaba, Delta State, Nigeria*, In: J. Emerg. Trends Econ. Manag. Sci., 2016, 7, 3, 137–146
- [9] Yang, M., Gabrielsson, P., *Entrepreneurial marketing of international high-tech business-to-business new ventures: A decision-making process perspective*, In: Ind. Mark. Manag., 2017

- [10] Whalen, P., et al., *Anatomy of competitive advantage: towards a contingency theory of entrepreneurial marketing*, In: J. Strateg. Mark., 2016
- [11] Miles, M., Gilmore, A., Harrigan, P., Lewis, G., Sethna, Z., *Exploring entrepreneurial marketing*, In: J. Strateg. Mark., 2015
- [12] Nga, J.K.H., Shamuganathan, G., *The influence of personality traits and demographic factors on social entrepreneurship start up intentions*, In: J. Bus. Ethics, 2010, 95, 2, 259–282
- [13] Marcati, A., Guido, G., Peluso, A.M., *The role of SME entrepreneurs' innovativeness and personality in the adoption of innovations*, In: Res. Policy, 2008, 37, 9, 1579–1590
- [14] Karabulut, A.T., *Personality traits on entrepreneurial intention*, In: Procedia-Social Behav. Sci., 2016, 229, 12–21
- [15] Littunen, H., *Entrepreneurship and the characteristics of the entrepreneurial personality*, In: Int. J. Entrep. Behav. Res., 2000
- [16] Bachmann, J.-T., Ohlies, I., Flatten, T., *Effects of entrepreneurial marketing on new ventures' exploitative and exploratory innovation: The moderating role of competitive intensity and firm size*, In: Ind. Mark. Manag., 2021, 92, 87–100
- [17] Alam, S.S., Mohd, R., Kamaruddin, B.H., Nor, N.G.M., *Personal values and entrepreneurial orientations in Malay entrepreneurs in Malaysia*, In: Int. J. Commer. Manag., 2015
- [18] Bandura, A., *Self-efficacy: toward a unifying theory of behavioural change*, In: Psychol. Rev., 1977, 84, 2, 191
- [19] Forbes, D.P., *The effects of strategic decision making on entrepreneurial self-efficacy*, In: Entrep. theory Pract., 2005, 29, 5, 599–626
- [20] Prihadini, D., *Role of Entrepreneurial Marketing in increasing product innovation during a pandemic: A Case Study on MSMEs managed by students in Jakarta*, In: Tech. Soc. Sci. J., 2021, 24, 468
- [21] Segal, G., Borgia, D., Schoenfeld, J., *The motivation to become an entrepreneur*, In: Int. J. Entrep. Behav. Res., 2005
- [22] Urban, B., *Tracking the venture creation phases in terms of entrepreneurial self-efficacy: Links to competitiveness of South African ventures*, In: South African J. Econ. Manag. Sci., 2012, 15, 4, 352–366
- [23] McGee, J.E., Peterson, M., *The long-term impact of entrepreneurial self-efficacy and entrepreneurial orientation on venture performance*, In: J. Small Bus. Manag., 2019, 57, 3, 720–737
- [24] Utami, C.W., *Attitude, subjective norm, perceived behaviour, entrepreneurship education and self-efficacy toward entrepreneurial intention university student in Indonesia*, 2017
- [25] Farrukh, M., Khan, A.A., Khan, M.S., Ramzani, S.R., Soladoye, B.S.A., *Entrepreneurial intentions: the role of family factors, personality traits and self-efficacy*, In: World J. Entrep. Manag. Sustain. Dev., 2017
- [26] Buss, A.H., *Personality as traits*, In: Am. Psychol., 1989, 44, 11, 1378
- [27] Audretsch, D.B., Bönnte, W., Keilbach, M., *Entrepreneurship capital and its impact on knowledge diffusion and economic performance*, In: J. Bus. Ventur., 2008, 23, 6, 687–698
- [28] Zhao, H., Seibert, S.E., Lumpkin, G.T., *The relationship of personality to entrepreneurial intentions and performance: A meta-analytic review*, In: J. Manage., 2010, 36, 2, 381–404
- [29] Schumpeter, J., *The theory of economic development. Harvard Economic Studies. Vol. XLVI*, Cambridge, MA: Harvard University Press, 1911
- [30] Singh, G., DeNoble, A., *Views on self-employment and personality: An exploratory study*, In: J. Dev. Entrep., 2003, 8, 3, 265
- [31] Alvarez, S.A., Barney, J.B., *Discovery and creation: Alternative theories of entrepreneurial action*, In: Strateg. Entrep. J., 2007, 1, 1–2, 11–26
- [32] Sarasvathy, S.D., Dew, N., Velamuri, N.R., Venkataraman, S., *Three views of entrepreneurial opportunity*, Handbook of Entrepreneurship Research, Springer, 2003, 141–160
- [33] Sahinidis, A.G., Stavroulakis, D., Kossieri, E., Sdrolas, L., *Using the Theory of Planned Behaviour and the Big Five Personality Trait Model in Predicting Entrepreneurial Intention: A Comparison Study of the Two Models*, Strategic Innovative Marketing and Tourism, Springer, 2019, 245–251
- [34] Fritsch, M., Obschonka, M., Wyrwich, M., Gosling, S.D., Rentfrow, P.J., Potter, J., *Regionale Unterschiede der Verteilung von Personen mit unternehmerischem Persönlichkeitsprofil in Deutschland—ein Überblick*, In: Raumforsch. und Raumordnung| Spat. Res. Plan., 2018, 76, 1, 65–81
- [35] Hachana, R., Berraies, S., Ftiti, Z., *Identifying personality traits associated with entrepreneurial success: does gender matter?*, In: J. Innov. Econ. Manag., 2018, 3, 169–193
- [36] Goldberg, L.R., *An alternative "description of personality": the big-five factor structure.*, In: J. Pers. Soc. Psychol., 1990, 59, 6, 1216
- [37] Zhao, H., Seibert, S.E., *The big five personality dimensions and entrepreneurial status: A meta-analytical review*, In: J. Appl. Psychol., 2006, 91, 2, 259
- [38] Caliskan, A., *Applying the right relationship marketing strategy through big five personality traits*, In: J. Relatsh. Mark., 2019, 18, 3, 196–215
- [39] Zadel, A., *Impact of personality and emotional intelligence on successful training in competences*, In: Manag. Glob. Transitions, 2006, 4, 4, 363–376
- [40] Howard, P.J., Howard, J.M., *The Big Five Quickstart: An Introduction to the Five-Factor Model of Personality for Human Resource Professionals*, 1995

- [41] Franco, M., Prata, M., *Influence of the individual characteristics and personality traits of the founder on the performance of family SMEs*, In: Eur. J. Int. Manag., 2019, 13, 1, 41–68
- [42] Kets de Vries, M.F.R., *The dark side of entrepreneurship*, In: Harv. Bus. Rev., 1985, 63, 6, 160–167
- [43] Fard, M.H., Amiri, N.S., *The effect of entrepreneurial marketing on halal food SMEs performance*, In: J. Islam. Mark., 2018
- [44] Mansion, S.E., Bausch, A., *Intangible assets and SMEs' export behaviour: a meta-analytical perspective*, In: Small Bus. Econ., 2020, 55, 3, 727–760
- [45] Baum, J.R., Frese, M., Baron, R.A., *Born to be an entrepreneur? Revisiting the personality approach to entrepreneurship*, The psychology of entrepreneurship, Psychology Press, 2014, 73–98
- [46] Kraus, S., Berchtold, J., Palmer, C., Filser, M., *Entrepreneurial orientation: the dark triad of executive personality*, In: J. Promot. Manag., 2018, 24, 5, 715–735
- [47] Dormann, C., Fay, D., Zapf, D., Frese, M., *A state-trait analysis of job satisfaction: on the effect of core self-evaluations*, In: Appl. Psychol., 2006, 55, 1, 27–51
- [48] Stroe, S., Parida, V., Wincent, J., *Effectuation or causation: An fsQCA analysis of entrepreneurial passion, risk perception, and self-efficacy*, In: J. Bus. Res., 2018, 89, 265–272
- [49] Markman, G.D., Balkin, D.B., Baron, R.A., *Inventors and new venture formation: The effects of general self-efficacy and regretful thinking*, In: Entrep. Theory Pract., 2002, 27, 2, 149–165
- [50] Wang, J.-H., Chang, C.-C., Yao, S.-N., Liang, C., *The contribution of self-efficacy to the relationship between personality traits and entrepreneurial intention*, In: High. Educ., 2016, 72, 2, 209–224
- [51] Karwowski, M., Lebuda, I., Wisniewska, E., Gralewski, J., *Big five personality traits as the predictors of creative self-efficacy and creative personal identity: Does gender matter?*, In: J. Creat. Behav., 2013, 47, 3, 215–232
- [52] Nauta, M.M., *Self-efficacy as a mediator of the relationships between personality factors and career interests*, In: J. Career Assess., 2004, 12, 4, 381–394
- [53] Tams, S., *Self-directed social learning: the role of individual differences*, In: J. Manag. Dev., 2008
- [54] Wang, D.F., Cui, H., *The Chinese personality traits: interpersonal relationship*, In: Psychol Explor, 2008, 4, 41–45
- [55] Bandura, A., Ramachandran, V.S., *Encyclopedia of human behaviour*, In: New York Acad. Press, 1994, 4, 71–81
- [56] Mei, H., Ma, Z., Jiao, S., Chen, X., Lv, X., Zhan, Z., *The sustainable personality in entrepreneurship: the relationship between big six personality, entrepreneurial self-efficacy, and entrepreneurial intention in the Chinese context*, Sustainability, 2017, 9, 9, 1649
- [57] Markman, G.D., Baron, R.A., Balkin, D.B., *Are perseverance and self-efficacy costless? Assessing entrepreneurs' regretful thinking*, In: J. Organ. Behav. Int. J. Ind. Occup. Organ. Psychol. Behav., 2005, 26, 1, 1–19
- [58] Rammstedt, B., John, O.P., *Measuring personality in one minute or less: A 10-item short version of the Big Five Inventory in English and German*, In: J. Res. Pers., 2007, 41, 1, 203–212
- [59] Zhao, H., Seibert, S.E., Hills, G.E., *The mediating role of self-efficacy in the development of entrepreneurial intentions*, In: J. Appl. Psychol., 2005, 90, 6, 1265
- [60] Nunnally, J., Bernet, J.J., Peter, J.P., *Reliability: A review of psychometric basics and recent marketing practices*, In: J. Mark. Res., 1978, 16, 1, 6–17

Authors:

MUDDASSAR SARFRAZ¹, MUHAMMAD IBRAHIM ABDULLAH², NAJAF MUMTAZ²,
 SYED IBN-UL-HASSAN³, ILKNUR OZTURK⁴

¹School of Management, Zhejiang Shuren University, 310015 Hangzhou, China

²Department of Management Sciences, COMSATS University Islamabad – Lahore Campus, Lahore, Punjab, Pakistan
 e-mail: najafmumtazjanjua@gmail.com

³Department of Commerce & Business, Government College University Faisalabad, Layyah Campus, Pakistan
 e-mail: ibnulhassan_bukhari@yahoo.com

⁴Faculty of Economics, Administrative and Social Sciences, Nisantasi University, Istanbul, Turkey
 e-mail: ilknur.ozturk@nisantasi.edu.tr

Corresponding authors:

MUDDASSAR SARFRAZ
 e-mail: muddassar.sarfraz@gmail.com
 MUHAMMAD IBRAHIM ABDULLAH
 e-mail: miabdullah@cuilahore.edu.pk

ARIMA model to forecast the RSS-1 rubber price in India: A case study for textile industry

DOI: 10.35530/IT.074.02.2022132

KEPULAJE ABHAYA KUMAR
PRAKASH PINTO
CRISTI SPULBAR
RAMONA BIRAU

IQBAL THONSE HAWALDAR
SAMARTHA VISHAL
IULIANA CARMEN BĂRBĂCIORU

ABSTRACT – REZUMAT

ARIMA model to forecast the RSS-1 rubber price in India: A case study for textile industry

Various rubber products are used in the textile industry. Due to increased foreign supply and synthetic rubber production, the price of natural Rubber in India has become more volatile. This paper aims to develop an appropriate model to predict the weekly price using the Box Jenkins methodology. The weekly price for Indian RSS-1 Rubber for the sample period from January 2002 to December 2019 has been collected from the official website of the Indian Rubber Board. ACF and PACF correlograms check the series stationarity and identify the model parameters. A model with the maximum number of significant coefficients, lowest volatility, lowest Akaike's information criterion (AIC), lowest Schwarz criterion and highest Adjusted R-squared is tentatively selected as the appropriate model and for the same model diagnostic check is carried out. An appropriate model to forecast the weekly price for the RSS-1 variety of Rubber is ARIMA (1, 1, 4).

Keywords: volatility, speculative price bubbles, natural rubber price, univariate forecasting model, Box Jenkins methodology, textile industry

Utilizarea modelului ARIMA pentru a preziona evoluția prețului cauciucului natural clasificat în categoria RSS-1 în India: Un studiu de caz pentru industria textilă

În industria textilă sunt utilizate diverse produse din cauciuc. Datorită creșterii ofertei externe și producției de cauciuc sintetic, prețul cauciucului natural din India a devenit mai volatil. Acest studiu de cercetare își propune să dezvolte un model adecvat pentru a preziona prețul săptămânal folosind metodologia Box Jenkins. Bazele de date care includ informațiile privind prețul săptămânal pentru cauciucul natural clasificat în categoria RSS-1 în India, pentru perioada de analiză din ianuarie 2002 până în decembrie 2019 au fost colectate de pe site-ul oficial al Indian Rubber Board. Corelogramele ACF și PACF verifică staționaritatea seriei și identifică parametrii modelului. Un model cu numărul maxim de coeficienți semnificativi, cea mai scăzută volatilitate, cel mai scăzut nivel privind criteriul de informații Akaike sau AIC, cel mai scăzut nivel privind criteriul Schwarz și cel mai ridicat nivel al R-pătrat ajustat se selectează provizoriu ca model adecvat și pentru același model este efectuată o verificare bazată pe diagnosticare. Modelul potrivit pentru a preziona prețul săptămânal pentru varietatea RSS-1 de cauciuc natural din India este modelul ARIMA (1, 1, 4).

Cuvinte-cheie: volatilitate, bule speculative de preț, preț cauciuc natural, model de previziune univariat, metodologia Box Jenkins, industria textilă

INTRODUCTION

A wide range of rubber materials is used in the textile manufacturing process. One of such key consuming areas in the rubber calendaring process in the textile industry is to make various types of fabrics. Rubber rollers, rubber moulded products, rubber coating and rubber suit are some of the other major forms of rubber consumption in the textile industry. India is the second major producer and consumer of natural Rubber globally. China, Thailand, Indonesia and Malaysia are the few other major players in production and consumption. In addition to the above-mentioned, USA and Vietnam are the major consumers and producers respectively in the world. Historically natural rubber industry in India was protected from

strong tariffs and other legal protections. But today, nearly 40% of natural rubber consumption depends on imports from other countries. As India imports 40% of its natural Rubber from other countries and as the role of synthetic Rubber in the country's rubber industry is vital, the price of Natural Rubber in India is more volatile [1]. Volatile rubber prices in India have resulted in the poor lifestyle of many rubber farmers and workers. Farmers were finding it difficult to pay the loan instalments, stoppage of their children's education, entertainment and difficulty for daily livelihood. It is not just farmers and farm workers. On the other hand, corporations taking Rubber as their core raw material will also suffer from the volatile natural rubber price [2]. The government in the central will find it difficult to balance the fair price

demand of farmers and minimum cost supply expectations of the natural Rubber based industries. As the Natural Rubber price is more volatile, developing an appropriate price risk management tool is necessary. Market-based price risk management tools like futures or options will help to hedge the price risk. However, in Indian commodities exchanges, the futures on natural Rubber are not traded regularly. In this situation, the tyre makers, other rubber-dependent industries, traders, and natural rubber growers are exposed to price volatility. Hence, it is necessary to develop an appropriate statistical model to predict the price of natural Rubber [3]. Univariate time series models like AR, MA and ARIMA have become the interest of many researchers today to develop forecast models using time series data. Box Jenkins ARIMA methodology has become very popular today to forecast financial time series because of the simplicity and optimal model-building process [4]. In the univariate forecasting methodology, ARIMA will allow the investigator to model the time series even with multiple external events [5]. Using Box Jenkins methodology, this work aims to develop an appropriate univariate model to predict the price of natural Rubber in India.

Literature review

There are good numbers of literature in which discussions on price volatility in Natural Rubber have appeared. The volatility in the Natural Rubber price is increasing because of the production and supply of synthetic Rubber [6–10]. As the cost of production of synthetic Rubber is directly dependent on the cost of crude and as the cost of crude fluctuates in the market, the price of natural Rubber is also very unstable after the Second World War. Kannan, Lekshmi et al. and Khin et al. have stated that production, consumption, stock, international natural rubber price and import-export are major economic factors contributing to price instability [11–13]. Other authors have stated that Natural Rubber prices are affected by the Asian Crisis [14–16]. Thailand, Indonesia and Malaysia are large producers of natural rubber. The exchange rate between US Dollar and their domestic currencies affected the natural rubber price in these countries. All the above studies have used regression and correlation methods except Khin et al. [13, 14] have used the Vector Error Correction Model to identify the reasons for price volatility in the natural rubber industry.

Zahari et al. [3] and Kumar et al. [17] have used Box Jenkins ARIMA methodology to develop a forecast model to predict the natural rubber price in Malaysia. Sakan [18] used ARIMA, VAR and VECM methods to develop the rubber price forecast model in Malaysia. To develop the forecast model for world Natural Rubber prices, Khin et al. [19] have used ARIMA and MARMA methodology. Many studies have appeared so far on applying ARIMA methodology to develop forecast models for other agricultural commodity prices. For example, Ohyver and Pudjihastuti [20] for medium quality Rice price, Mishra et al. [21] for

Potato price, Shil et al. [22] for Arecanut price, Darekar and Reddy [23] for Cotton price and Sukiyono [24] for Cacao price.

ARIMA methodology has been widely used in other disciplines as well. Some authors have used ARIMA methodology to develop the forecasting model for Gold bullion selling price, GDP, stock price, global solar radiation, private residential price, mineral commodity prices, import-exports values of the country, electricity price, rainfall, oil prices and month temperature respectively [25–38].

DATA AND METHODOLOGY

The weekly data from January 2002 to December 2019 for this study are gathered from the official website of the Indian Rubber Board which is indiannatural.com. There are five varieties of Rubbers trading in the market; RSS-1 is the highest quality among those five varieties. Hence, we consider the price series of RSS-1 in this study.

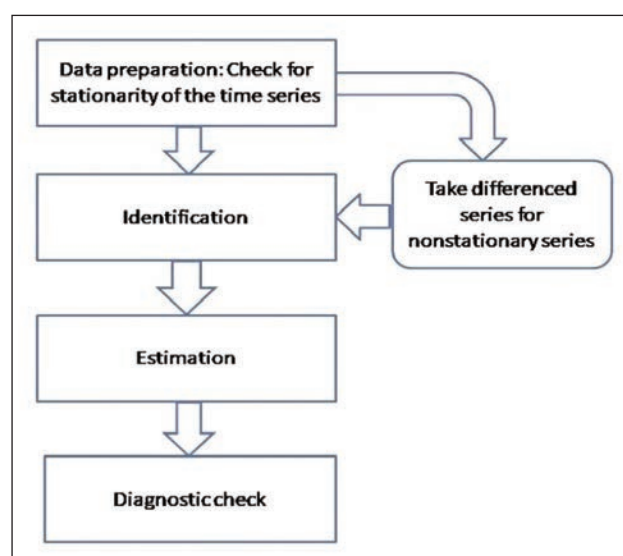


Fig. 1. Flowchart of Box-Jenkins ARIMA methodology

Box Jenkins ARIMA methodology is a systematic process which follows four steps [20–24, 28, 39, 40] have used ACF and PACF correlograms to check the stationarity of time series. We have used time plot correlograms, ACF and PACF correlograms to check the stationarity of the RSS – Rubber price series. The correlograms proved that the series is not stationary and to make the series stationary, we have taken the first-order difference of the raw series. To identify the model parameters (p, d, q) some authors [37, 39, 41] have advised looking at the ACF and PACF correlograms of differenced series; hence we have used the same in this study. For the identified tentative models, we have run the Box Jenkins methodology and the following five statistics are extracted and tabulated from the computer outputs. A model with the maximum number of significant coefficients, lowest volatility, lowest Akaike's information criterion, lowest Schwarz criterion and highest Adjusted R-squared is tentatively selected as the appropriate model and for

the same model diagnostic check is carried out. The same authors [37, 39, 41] have suggested taking residuals of the appropriate model and using the ACF and PACF correlograms of these residuals to decide whether the selected model is statistically appropriate or not.

Linear regression is a common tool used for forecasts. The general term of a bivariate linear regression model is shown in equation 1.

$$y_t = \alpha + \beta(x_t) + \varepsilon_t \quad (1)$$

In this simple form of a linear regression equation, y_t is the dependent variable, x_t – the explanatory or independent variable, α and β are the constants, and ε_t is the error of the model [42]. The same model has been extended for multi-variate predictions; this model could be suitable when the researcher has more than one independent variable for the dependent variable of his interest. The general form of this multivariate regression model is shown in equation 2.

$$y_t = \alpha + \beta_1(x_{1t}) + \beta_2(x_{2t}) + \dots + \beta_n(x_{nt}) + \varepsilon_t \quad (2)$$

In the second equation, we can observe multiple independent variables with names x_1 , x_2 , and x_n and their relationship factors β_1 , β_2 , and β_n with dependent variables y_t . The above two regression equations or methodology can be used only when the determinants of y_t are measurable. In the short run, although explanatory variables are constant, the y_t might vary due to market trends. In such situations, the application of univariate models such as Auto-Regressive (AR), Moving Average (MA), Auto Regressive Moving Average (ARMA), or Auto-Regressive Integrated Moving Average (ARIMA) would be most appropriate [43]. These models' very common pervasive characteristic is that the explanatory variables in all these models are the past values of the dependent series or its error terms [44]. This is evident from the following third, fourth, and fifth equations.

$$y_t = \mu + \beta_1 y_{t-1} + \beta_2 y_{t-2} + \dots + \beta_p y_{t-p} + u_t \quad (3)$$

$$y_t = \mu + u_t + \theta_1 u_{t-1} + \theta_2 u_{t-2} + \dots + \theta_q u_{t-q} \quad (4)$$

$$y_t = \mu + \beta_1 y_{t-1} + \beta_2 y_{t-2} + \dots + \beta_p y_{t-p} + \theta_1 u_{t-1} + \theta_2 u_{t-2} + \dots + \theta_q u_{t-q} + u_t \quad (5)$$

Equations 3–5 are the general form of the AR, MA, and ARMA process, where y_t is the value of the dependent variable. In equations 3–5, u_t denotes the white noise error term, where $p \wedge q$ denotes the optimal number of lags for the AR(p) and MA(q) processes. AR model implies the present value of the dependent variable, y , depending on its past values. MA model implies that the current value of the dependent variable is the function of the present and the past values of a white noise error term [45]. Equation five shows the characteristics of the ARIMA model, where the current value of the dependent variable, y , is the function of its past values plus the blend of the present and past values of a white noise disturbance term [43]. If the raw series is stationary at its base level, then the model applicable would be ARMA(p, q); however, if the series is not stationary, then such series calls for integrated or differenced return series to avoid spurious regression. Such differenced series would be used to identify the AR(p) and MA(q) terms for the ARMA model [46]. Hence, Box and Jenkins ARIMA modelling differs from ARMA, with additional terms 'integrated' and 'I' in the acronym.

DATA PREPARATION

Figures 2 and 3 show the time plot of the RSS-1 rubber price raw series and the return series. The raw series shows trends, specifically upward trends till the end of 2011 and downward trends. Therefore, the raw series of RSS-1 Rubber price is a non-stationary time series; hence we have taken the first order difference return series to make the series stationary. In figure 3, the series does not follow any particular

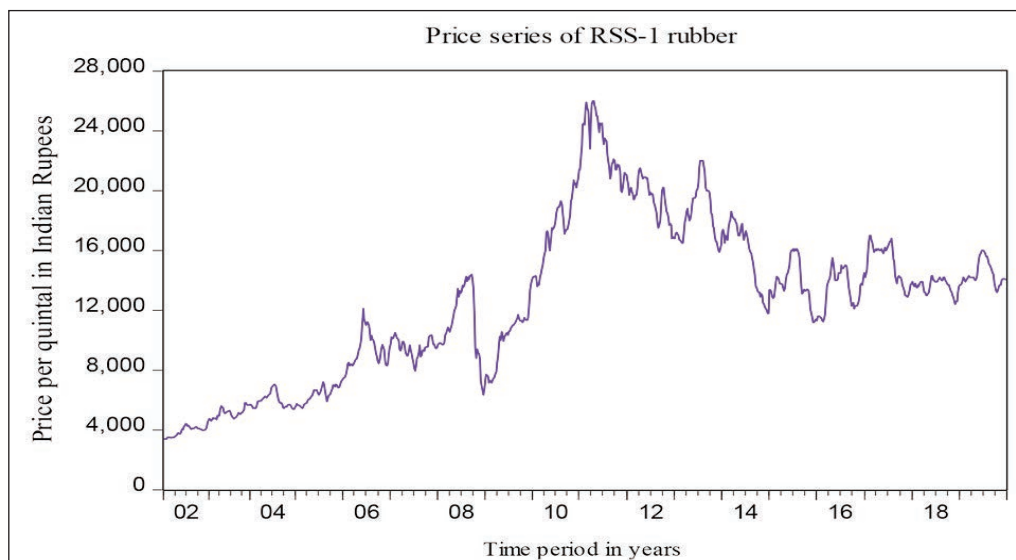


Fig. 2. Price series of RSS-1 Natural Rubber in India (Source: authors processing using EViews package)

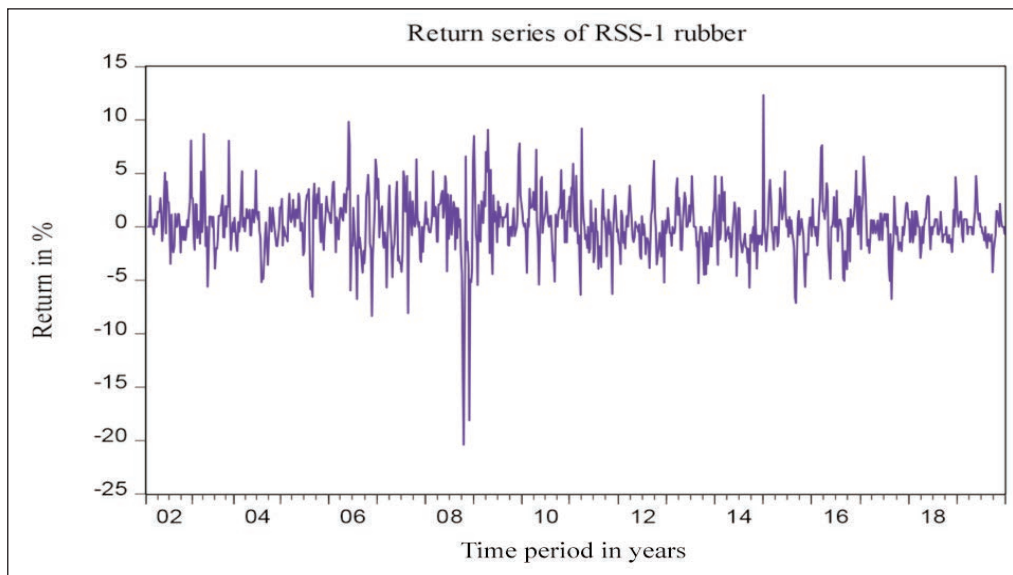


Fig. 3. Return series of RSS-1 Natural Rubber in India
(Source: authors processing using EViews package)

trend, which gives a clue that the mean of the log of RSS-1 rubber return is not changing. This perhaps indicates that the differenced RSS-1 rubber return series is stationary. But this time plot will give just an initial clue to confirm the stationarity of the series, and it is necessary to run ACF and PACF functions on the series to make the decision more precise.

Figure 4 shows the computer output for ACF and PACF with its correlograms for the RSS-1 Rubber price series for the period January 2002 to December 2019. One can observe the autocorrelation and partial Autocorrelation values up to 10 lags of the price series in figure 4. The autocorrelation coefficient at the 1st lag (0.996) is very high, and the coefficients decline slowly until the 10th lag (0.939). The correlograms of ACF for rubber price shown in figure 4 show that up to 10th lags the ACF are individually different from zero and are statistically significant. The partial autocorrelation coefficients in figure 4 show dramatically decline after the first lag, and this indicates that the RSS-1 Rubber price series is non-stationary.

Now the autocorrelation and partial autocorrelation values of the return series in figure 5 gives different interpretation compared to figure 4. The AC coeffi-

cients for the first and second lag (0.417 and 0.141) are very small compared to figure 4 values (0.996 and 0.991). Secondly, the AC coefficients in figure 4 decreased very slowly throughout up to the 10th lag and AC coefficients at each lag are not equal to zero, but in figure 5, AC coefficients decline very sharply and they have got negligible *r* value (less than 0.10) for majority lags. The ACF correlograms for the return series shown in figure 5 that is different from the correlograms of the raw series in figure 4. This confirms that the return series is not serially correlated; hence, the same is a stationary time series. As the first order differenced RSS-1 Rubber price series is a stationary series, we will carry this series for all our computations of Box Jenkins methodology. Further, as the first-order return series is stationary, the ARIMA (*p, d, q*) model identified value for *d* will be 1.

The Augmented Dickey-Fuller (ADF) test is performed to test the unit root in the RSS-1 rubber price series. The results of the ADF test are presented in table 1. The p-values of the ADF test for the price series is 0.27 and the return series is 0.00. This formally confirms that the price series of Rubber is not stationary and the return series is stationary.

Correlogram of RSS-1 rubber price series						
Autocorrelation	Partial Correlation	AC	PAC	Q-Stat	Prob	
█	█	1	0.996	0.996	921.90	0.000
█	█	2	0.991	-0.238	1834.4	0.000
█	█	3	0.984	-0.029	2736.4	0.000
█	█	4	0.978	-0.010	3627.5	0.000
█	█	5	0.972	0.054	4508.4	0.000
█	█	6	0.966	-0.020	5379.2	0.000
█	█	7	0.959	-0.052	6239.4	0.000
█	█	8	0.953	-0.006	7088.6	0.000
█	█	9	0.946	-0.005	7926.9	0.000
█	█	10	0.939	-0.030	8753.8	0.000

Fig. 4. AC and PAC values with correlograms for RSS-1 rubber price series
(Source: authors processing using EViews package)

Correlogram of the return series of RSS-1						
Autocorrelation	Partial Correlation	AC	PAC	Q-Stat	Prob	
█	█	1	0.443	0.443	181.77	0.000
█	█	2	0.158	-0.047	205.00	0.000
█	█	3	0.059	0.008	208.27	0.000
█	█	4	-0.092	-0.144	216.19	0.000
█	█	5	-0.049	0.063	218.39	0.000
█	█	6	0.061	0.094	221.89	0.000
█	█	7	0.063	0.006	225.62	0.000
█	█	8	0.082	0.033	231.99	0.000
█	█	9	0.084	0.025	238.60	0.000
█	█	10	0.025	-0.012	239.17	0.000

Fig. 5. AC and PAC values with correlograms for the return series of RSS-1 Rubber
(Source: authors processing using EViews package)

Table 1

ADF TEST RESULTS				
Level of significance	Price series		Return series	
	t-Statistic	Probability	t-Statistic	Probability
ADF test	-2.04	0.27	-15.1485	0.00
1% level	-3.44		-3.43723	
5% level	-2.86		-2.86447	
10% level	-2.57		-2.56838	

DATA ANALYSIS & INTERPRETATION

Identification

We are using the autocorrelation function (ACF), partial autocorrelation function (PACF) of the return series and their correlograms to identify the (p , and q) values for the model. In figure 5, the PACF cut-off sharply beginning lags (0.417 to -0.0470); it can be called an AR process. Further, the partial autocorrelation coefficient in the first lag and autocorrelation coefficient in the first lag is positive and statistically significant; hence, the RSS-1 rubber return series follows the ARIMA process. The pattern of correlograms of AC and PAC in figure 5 are almost similar; hence this is an indication of the ARIMA model. In other words, the first lag of the ACF coefficient is not negative (0.417); hence it is not an MA process. Therefore adding just the AR term or MA term to the model does not make sense. The AC coefficients are statistically significant at lags 1, 2, 18, 19 and 20; the PAC coefficients are statistically significant at lags 1, 4, 5 and 6. And hence any combination of these terms may give the appropriate model. But according to Box and Jenkins, parsimonious models give a better prediction; hence we are dropping parameters 18, 19, 20, 5 and 6 from our identification process. Gujarati et al. [41] have advised doing experiments with different alternative models to select an appropriate model. Identified alternative models for the estimation process are (1, 1, 1) (1, 1, 2) (4, 1, 1) (1, 1, 4) (4, 1, 2).

Estimation

The rubber return series is used to generate the estimates for above mentioned tentative models. In the ARIMA (p , d , and q) model, the value for parameter d is already defined: the number of differences we take to make the series stationary. In the case of the

RSS-1 rubber price series, the series became stationary with first-order differencing. We have extracted significant coefficients, volatility, adjusted R-squared, Akaike's information criterion and Schwarz criterion and tabulated in table 2 from the estimates of tentative models.

Among four tentative models, models (1, 1, 4) and (4, 1, 2) are the most appropriate models based on significant coefficients. Among these two models, the volatility of model (1, 1, 4) is less compared to model (4, 1, 2). Furthermore, Akaike's information criterion and Schwarz criteria for model (4, 1, 1) are lower than model (4, 1, 2). Hence the appropriate model to forecast RSS-1 Rubber price is ARIMA (1, 1, 4). The model accuracy measured by the Adjusted R-squared of ARIMA (1, 1, 4) is higher than other tentative models.

Diagnostic check

Once the appropriate model is selected and the parameters are estimated, the diagnostic check has to be made using the ACF and PACF correlograms of the residuals. ACF and PACF for model residuals (1, 1, 4) are plotted in figure 6; the correlograms of the residuals are flat in this image. The lags are within the 95% confidence level or the standard error bounce; this indicates that all the information's captured in the model. The selected model (1, 1, 4) is the perfect model because, in figure 5, the residuals are not serially correlated, which is statistically significant. This says that all the information's covered in the model and it is not necessary to look for some other ARIMA model to predict the RSS-1 Rubber price in India.

Correlogram of residuals for ARIMA (1,1,4)						
Autocorrelation	Partial Correlation	AC	PAC	Q-Stat	Prob	
1	0.009	0.009	0.0703			
2	-0.042	-0.042	1.7071			
3	0.055	0.055	4.4835	0.034		
4	-0.004	-0.007	4.4997	0.105		
5	-0.045	-0.041	6.4284	0.093		
6	0.082	0.080	12.708	0.013		
7	0.013	0.008	12.856	0.025		
8	0.034	0.045	13.926	0.030		
9	0.065	0.056	17.832	0.013		
10	0.030	0.030	18.665	0.017		

Fig. 6. Correlograms of the residuals of estimated ARIMA (1, 1, 4) model
(Source: authors processing using EViews package)

Table 2

EXTRACTED PARAMETERS					
Tentative models	(1, 1, 1)	(1, 1, 2)	(4, 1, 1)	(4, 1, 2)	(1, 1, 4)
Significant coefficients	2	2	2	3	3
Volatility	0.000584	0.000583	0.0005870	0.000695	0.000574
Adjusted R-squared	0.191950	0.192380	0.1877050	0.038182	0.205335
Akaike's information criterion	-4.599200	-4.599700	-4.5939000	-4.425101	-4.61583
Schwarz criterion	-4.578300	-4.578800	-4.5730000	-4.404215	-4.59494

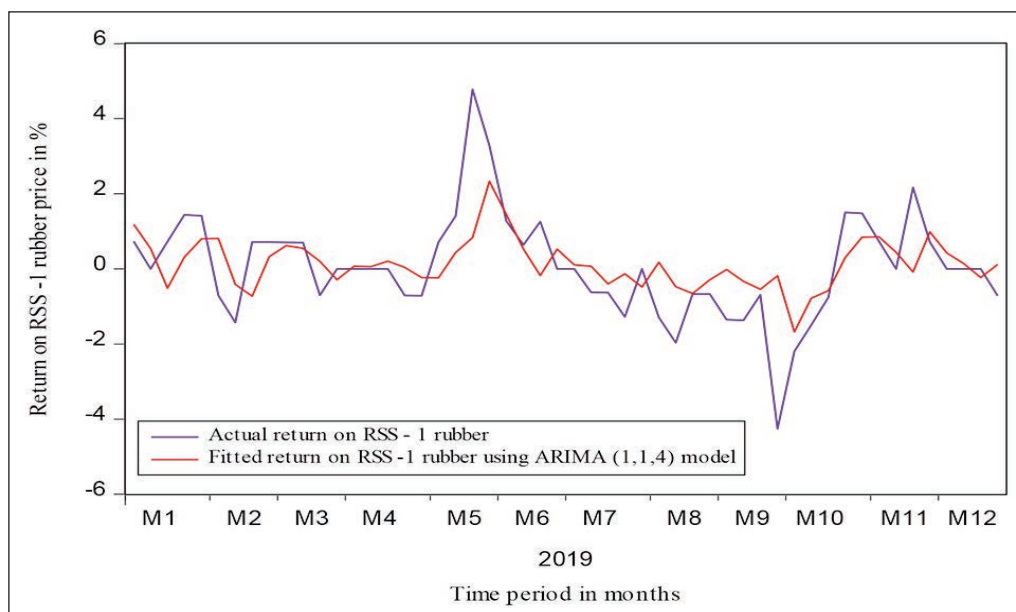


Fig. 7. Actual and fitted weekly returns on RSS-1 Rubber
(Source: authors processing using EViews package)

The estimated coefficients of the appropriate ARIMA (1, 1, 4) model are presented in equation 6. Where is the return of rubber price, 0.0015 is the intercept, 0.50 is the estimated slope for AR term, that is the autoregressive coefficient, and y_{t-1} is the first lag of the rubber return series. -0.14 is the slope for the MA term, that is, the moving average coefficient, and y_{t-4} is the 4th lag of the moving average.

$$y_t = 0.0015 + 0.50y_{t-1} - 0.14y_{t-4} \quad (6)$$

CONCLUSION

A wide range of rubber materials is used in the textile manufacturing process. One of such key consuming areas in the rubber calendaring process in the textile industry is to make various types of fabrics. Rubber rollers, rubber moulded products, rubber coating and rubber suit are some of the other major forms of rubber consumption in the textile industry. The price of natural Rubber in India is unstable, and market-based price risk management tools like futures and

options are not regularly traded for this commodity. Natural rubber growers, traders and industrial buyers suffer from this volatile price. In this situation, looking for good price risk management tools is essential. This study aims to develop a price forecast model to manage the price risk of natural Rubber in India. Using Box Jenkins methodology, we have developed an appropriate model to forecast the price of RSS-1 Rubber in India. The selected best model for prediction is ARIMA (1, 1, 4), that is, AR (1), I (1) and MA (4). The AR (1) term coefficient is 0.50, and MA (4) is -0.14 ; the line plot of the actual and fitted values confirms that the developed model is a good fit. This model will help rubber growers, traders, corporations, and governments make accurate managerial decisions. ARIMA is a univariate time series model; many studies on different price determinants of rubber prices in the world market have identified various price determinants. Hence using multivariate models like VAR and VECM, one can develop a multivariate forecast model to predict the Rubber price in India.

REFERENCES

- [1] Nambiar, R.S., Balasubramanian, P., *A study on the impact of fall in rubber prices concerning farmers in Kottayam district*, In: Int. J. Appl. Bus. Econ. Res., 2016, 14, 14, 10463–10478
- [2] Pareed, A.O., Kumaran, M.P., *Price volatility and its impact on rubber cultivation in India – an analysis of recent trends*, 2018, February
- [3] Zahari, F.Z., et al., *Forecasting natural rubber price in Malaysia Using Arima*, In: J. Phys., 2017, 995, Conference Series, 1–7
- [4] Adhikari, R., Agrawal, R.K., *An Introductory Study on Time Series Modeling and Forecasting*, 2013
- [5] Liu, L., Hudak, G.B., Box, G.E.P., Muller, M.E., Tiao, G.C., *Forecasting and Time Series Analysis Using The SCA Statistical System*, vol. 1. Chicago: Scientific Computing Associates Corp, 1992
- [6] Arunwarakorn, S., Suthiwartnarueput, K., Pornchaiwiseskul, P., *Forecasting equilibrium quantity and price on the world natural rubber market*, In: Kasetsart J. Soc. Sci., 2017, 1–9
- [7] Raju, K.V., *Instability in natural rubber prices in India: An empirical analysis*, In: IOSR J. Econ. Financ., 2016, 7, 3, 24–28

- [8] Chowdappa, P., Cheriyan, H., *Areca nut: Production, Consumption and Marketing*, In: Indian J. Areca nut, Spices Med. Plants, 2017, 18, 4, 6–15
- [9] Basri, M.F., Jaafar, M.N., Muhamat, A.A., *Determinants of the price of natural rubber in Malaysia*, In: Int. J. Bus. Manag., 2018, 6, 12, 50–54
- [10] Chiun Fong, Y., Tunku Abdul Rahman, U., Chee Seong, L., Aye Khin, A., Seong Lim, C., *Determinants of Natural Rubber Price Instability For 4 Major Producing Countries*, 2019
- [11] Kannan, M., *The determinants of production and export of natural rubber in India*, In: J. Econ. Financ., 2013, 1, 5, 41–45
- [12] Lekshmi, S., Moganakumar, S., Tharian, G.K., *The trend and pattern of natural rubber price in India: an exploratory analysis*, In: Indian J. Nat. Rubber Res., 1996, 9, 2, 82–92
- [13] Khin, A.A., Leh Bin, R.L., Keong, O.C., Yie, F.W., Liang, N.J., *Critical Factors of The Natural Rubber Price Instability in The World Market*, In: Humanit. Soc. Sci. Rev., 2019, 7, January, 199–208
- [14] Khin, A.A., et al., *Examining between Exchange Rate Volatility and Natural Rubber Prices: Engle-Granger Causality Test*, In: Int. J. Econ. s Financ. Issues, 2017, 7, 6, 33–40
- [15] Tulasombat, S., Bunchapattanasakda, C., Ratanakomut, S., *The Effect of Exchange Rates on Agricultural Goods for Export: A Case of Thailand*, In: Inf. Manag. Bus. Rev., 2015, 7, 1, 1–11
- [16] Kumar, K.A. Pinto, P., Hawaldar, I.T., Spulbar, C.M., Birau, F.R., *Crude oil futures to manage the price risk of natural rubber: empirical evidence from India*, In: Agric. Econ. – Czech, 2021, 67, 10, 423–434
- [17] Kumar, K.A., Spulbar, C., Pinto, P., Hawaldar, I.T., Birau, R., Joisa, J., *Using Econometric Models to Manage the Price Risk of Cocoa Beans: A Case from India*, In: Risks, 2022, 10, 115, 1–18
- [18] Sakan, I., *Forecasting the price of natural rubber in Malaysia*, California State University, Sacramento, 2012
- [19] Khin, A.A., Chiew E, F.C., Shamsudin, M.N., Mohamed, Z.A., *Natural rubber price forecasting in the world market*, In: Agriculture Sustainability Through Participative Global Extension, 2008, June, 4–14
- [20] Ohlyver, M., Pudjihastuti, H., *Arima Model for Forecasting the Price of Medium Quality Rice to Anticipate Price Fluctuations*, In: Procedia Comput. Sci., 2018, 135, 3, 707–711
- [21] Mishra, M.K., Sisodia, B.V.S., Rai, V.N., *Forecasting technique of price of potato of Uttar Pradesh*, In: J. Pharmacogn. Phytochem., 2019, 8, 3, 60–62
- [22] Shil, S., Acharya, G.C., Jose, C.T., Muralidharan, K., Sit, A.K., Thomas, G.V., *Forecasting of areca nut market price in north eastern India: ARIMA modelling approach*, In: J. Plant. Crop., 2013, 41, June, 330–337
- [23] Darekar, A., Reddy, A.A., *Cotton Price Forecasting in Major Producing States*, In: Econ. Aff., 2017, 62, 3, 373–378
- [24] Sukiyono, K., Nabiu, M., Sumantri, B., Novanda, R.R., *Selecting an Accurate Cacao Price Forecasting Model*, In: J. Phys. Conf. Ser., 2018, 1114, 1–6
- [25] Abonazel, M.R., Abd-elftah, A.I., *Forecasting Egyptian GDP Using ARIMA Models*, In: Reports Econ. Financ., 2019, 5, 1, 35–47
- [26] Shathir, A., Mohammed Saleh, L.A., Al-Din Majeed, S., *Forecasting Monthly Maximum Temperatures in Kerbala Using Seasonal ARIMA Models*, In: J. Univ. Babylon Eng. Sci., 2019, 27, June, 223–231
- [27] Jakaša, T., Andročec, I., Sprčić, P., *Electricity price forecasting – ARIMA model approach*, In: International Conference on the European Energy Market, 2011, May, 222–225
- [28] Nochai, R., Tiltida, N., *ARIMA Model for Forecasting Oil*, In: Regional Conference on Mathematics, Statistics and Applications-University Sains Malaysia, 2006, June, 1–7
- [29] Chin, L., Fan, G., *Autoregressive analysis of Singapore 's private residential prices*, In: Emerald insights, 2005, 23, 4, 257–270
- [30] Tse, R.Y.C., *An application of the ARIMA model to real-estate prices in Hong Kong*, In: J. Prop. Financ., 1997, 8, 2, 152–163
- [31] Cortez, C.A.T., Saydam, S., Coulton, J., Sammut, C., *Alternative techniques for forecasting mineral commodity prices*, In: Int. J. Min. Sci. Technol., 2018, 28, 2, 309–322
- [32] Fattah, J., Ezzine, L., Aman, Z., El Moussami, H., Lachhab, A., *Forecasting of demand using ARIMA model*, In: Int. J. Eng. Bus. Manag., 2018, 10, 1–9
- [33] Shathir, A.K., Mohammed Saleh, L.A., *Best ARIMA Models For Forecasting Inflow of Hit Station*, In: Basrah J. Eng. Sci., 2016, 16, 1, 62–71
- [34] Farooqi, A., *ARIMA Model Building and Forecasting on Imports and Exports of Pakistan*, In: Pak.j.stat.oper.res, 2014, 10, 2, 157–168
- [35] Mondal, P., Shit, L., Goswami, S., *Study of Effectiveness of Time Series Modeling (ARIMA) in Forecasting Stock prices*, In: Int. J. Comput. Sci. Eng. Appl., 2014, 4, April, 13–29
- [36] Adebisi, A.A., Adewumi, A.O., Ayo, C.K., *Stock Price Prediction Using the ARIMA Model*, In: International Conference on Computer Modelling and Simulation, 2014, 105–111
- [37] Lappas, I., Matiatos, I., *Modelling of Rainfall Data Using Stochastic Methods (Seasonal ARIMA)*, In: Bull. Geol. Soc. Greece, 2013, 7, September, 1–11
- [38] Abdullah, L., *ARIMA Model for Gold Bullion Coin Selling Prices Forecasting*, In: Int. J. Adv. Appl. Sci., 2012, 1, 4, 153–158
- [39] Meeker, W.Q., *Graphical Tools for Exploring and Analyzing Data From ARIMA Time Series Models*, Ames: Iowa State University, 2001

- [40] Mohanasundaram, S., Narasimhan, B., Kumar, G.S., *The Significance of Autocorrelation and Partial Autocorrelation on Univariate Groundwater Level Rise (Recharge) Time Series Modeling*, In: JGWR Publ. by AGGS, India, 2013, 2, June, 131–142
- [41] Gujarati, D.N., Porter, D.C., Gunasekar, S., *Basic Econometrics*, 5th ed. Mc Graw Hill Education, 2009
- [42] Rawlings, J.O., Pantula, S.G., Dickey, D.A., *Applied Regression Analysis: A Research Tool*, 2nd ed. Springer Texts in Statistics, 1998
- [43] Brooks, C., *Econometrics Introduction*, Second. New York: Cambridge University Press, 2008
- [44] Stanton, J.M., *Galton, Pearson, and the Peas: A Brief History of Linear Regression for Statistics Instructors*, 2017, 1898
- [45] Brooks, C., *Stata Guide to Accompany Introductory Econometrics for Finance*, Cambridge University Press, 2014
- [46] Fabozzi, F.J., Focardi, S., Rachev, S.T., Arshanapalli, B.G., *The Basics of Financial Econometrics*, New Jersey: John Wiley & Sons, 2014

Authors:

KEPULAJE ABHAYA KUMAR¹, PRAKASH PINTO², CRISTI SPULBAR³, RAMONA BIRAU⁴,
IQBAL THONSE HAWALDAR⁵, SAMARTHA VISHAL⁶, IULIANA CARMEN BĂRBĂCIORU⁷

¹Department of Business Administration, Mangalore Institute of Technology & Engineering, Moodabidri, India
e-mail: abhaya.kepulaje@gmail.com

²Department of Business Administration, St. Joseph Engineering College, Vamanjoor, Mangalore, India
e-mail: prakashpinto74@gmail.com

³Faculty of Economics and Business Administration, University of Craiova, Romania
e-mail: cristi_spulbar@yahoo.com

⁴“Constantin Brâncuși” University of Târgu Jiu, Faculty of Economic Science, Tg-Jiu, Gorj, Romania

⁵Department of Accounting & Finance, College of Business Administration, Kingdom University, Sanad, Bahrain
e-mail: thiqbal34@gmail.com

⁶Department of MBA, Sahyadri College of Engineering & Management, Mangaluru, India
e-mail: director.mba@sahyadri.edu.in

⁷“Constantin Brâncuși” University of Târgu Jiu, Faculty of Engineering, Tg-Jiu, Gorj, Romania
e-mail: cbarbacioru@gmail.com

Corresponding author:

RAMONA BIRAU
e-mail: ramona.f.birau@gmail.com

Textile structures for the treatment of burn wounds – characterization of elastic and antibacterial properties

DOI: 10.35530/IT.074.02.2022108

EMILIA VISILEANU
ALEXANDRA ENE

CARMEN MIHAI
ALINA VLADU

ABSTRACT – REZUMAT

Textile structures for the treatment of burn wounds – characterization of elastic and antibacterial properties

The paper shows the elastic and antibacterial features of the textile structures (Layer I and III) which make up a three-layer composite material with well-defined features, aimed at the treatment of human burns. The textile structures obtained through weaving (5 variants) and interweaving (3 variants) were further treated with active substances: collagen, colloidal silver, CMC, clay, hyaluronic acid, polyurethane, etc. By using specialized software, fundamental statistical indicators were calculated for the modulus of elasticity and anisotropy variables: mean, dispersion and standard deviation, median and quartiles, skewness, and kurtosis for asymmetry and highlighting the cases in which interventions should be carried out. The histograms and box-plot graphs of the modulus of elasticity and anisotropy variables were obtained. For the functionalized textile structures, with different levels of anisotropy, the antibacterial activity was evaluated on Gram-positive microorganisms (*Staphylococcus aureus* ATCC 6538) and Gram-negative (*Escherichia coli* ATCC 8739) and *Candida albicans*, variety ATCC 10231 by determining the logarithmic and percentage reduction of microorganism populations. The hemocompatibility was determined by evaluating the hemolytic index (ASTM F756-13). The results obtained led to the definition of the combinations of structures of the multilayer matrix.

Keywords: elasticity, anisotropy, statistics, antimicrobial, microorganism, haemolytic

Structuri textile pentru tratarea plăgilor cauzate de arsuri – caracterizarea proprietăților elastice și antibacteriene

Lucrarea prezintă caracteristicile elastice și antibacteriene ale structurilor textile (Stratul I și III) care alcătuiesc un material compozit cu trei straturi cu proprietăți bine definite, care vizează tratarea arsurilor umane. Structurile textile obținute prin țesere (5 variante) și interțesere (3 variante) au fost tratate cu substanțe active: colagen, argint coloidal, CMC, argilă, acid hialuronic, poliuretan etc. Prin utilizarea unui software specializat s-au calculat indicatori statistici fundamentali pentru modulul de elasticitate și variabilele de anizotropie: medie, dispersie și abatere standard, mediană și quartile, asimetrie și coeficientul Kurt pentru asimetrie și evidențierea cazurilor în care ar trebui efectuate intervenții. Au fost obținute histogramele și graficele box-plot ale variabilelor modulului de elasticitate și anizotropiei. Pentru structurile textile funcționalizate, cu diferite niveluri de anizotropie, activitatea antibacteriană a fost evaluată pe microorganismele Gram-pozitive (*Staphylococcus aureus* ATCC 6538) și Gram-negative (*Escherichia coli* ATCC 8739) și *Candida albicans*, tulpina ATCC 10231 prin determinarea logaritmică și reducerea procentuală a populațiilor de microorganisme. Hemocompatibilitatea a fost determinată prin evaluarea indicelui hemolitic (ASTM F756-13). Rezultatele obținute au condus la definirea combinațiilor de structuri ale matricei multistrat.

Cuvinte-cheie: elasticitate, anizotropie, statistică, antimicrobial, microorganism, hemolitic

INTRODUCTION

Wounds are complex and there is no universal single dressing to treat all types of wounds [1]. The selection of the most adequate wound dressing for a specific wound requires specialist knowledge and clinical assessment; however, the most fitting dressing for wound management depends not only on the type of wound but also on the stage of the healing process. Wound dressings are costly to many developed countries' total annual healthcare budgets. The market potential for healthcare and medical textiles is considerably increasing. It has been predicted that there would be substantial market potential for advanced wound dressings. Some of the major requirements related to a wound dressing are: to alleviate pain, absorb exudates, prevent infection and

contaminant contact with the wound, sustain non-toxicity, have a moist environment, optimum gaseous permeability, temperature, and pH. A great number of desirable properties are also expected from a modern wound dressing, including biodegradability, bio-absorbability, and ease of application, to be flexible, comfortable, and impermeable to bacteria.

The antibacterial property is one of the most frequently desired properties from a wound dressing, as the growth of microorganisms is controlled/eliminated by the presence of antimicrobial agents that are embedded into the fibre structure.

Wound dressing materials can play a vital role in wound healing management. An ideal wound dressing not only acts as a physical barrier for a wound against mechanical trauma but also speeds up the healing process and prevents bacterial infection. In

this regard, the development of wound dressings can be discussed taking into consideration traditional and modern (advanced, smart) dressings.

The treatment of burn wounds is complex and involves many components [2].

Recent developments in dressing and bioengineering technology have introduced dressings and gels containing naturally occurring glycosaminoglycan and chitin [3–6], with the incorporation of growth factors into gel [7, 8]. These dressings have been reported to prevent early extension of burns [9] express antimicrobial properties [10, 11] and promote fibroblast proliferation, angiogenesis, and wound healing [12].

It is known that the diameter of the fibres, the hydrophilicity, the roughness and the stiffness of the surfaces are factors directly correlated with the ability of bacteria to attach and proliferate on the surface and in the section of the networks. On the other hand, simulations (CAD-FEM) of the behaviour of multilayer matrices in contact with the wounds have shown that the excess fluid causes both the movement of the yarns in the textile structure and its deformation [13], which is in close correlation with the elastic properties (figure 1).

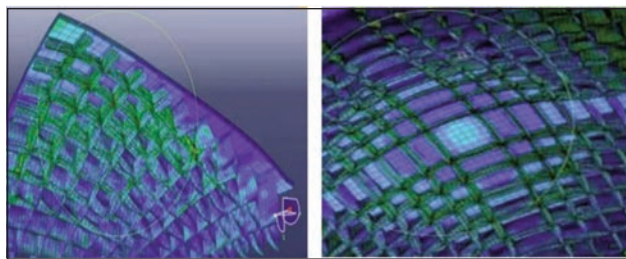


Fig. 1. Deformation of the structure

The paper shows the relation between the elastic properties on antimicrobial features of the textile structures (Layers I and III) treated with active substances, which make up a three-layer composite material with well-defined features, aimed at the treatment of burn wounds. The elastic characteristics were studied by applying descriptive statistics methods and antibacterial activity was evaluated on Gram-positive microorganisms (*Staphylococcus aureus* ATCC 6538) and Gram-negative (*Escherichia coli* ATCC 8739) and *Candida albicans*, variety ATCC 10231 by determining the logarithmic and percentage reduction of microorganism populations. The hemocompatibility was determined by evaluating the hemolytic index (ASTM F756-13) and the coagulation kinetics. The results obtained led to the definition of the combinations of structures of the multilayer matrix.

METHODS

To obtain the first layer, 5 types of woven textile structures were used, differentiated by: the nature of the raw material, the linear density of weft yarns, weft thickness, the structure type, for which the technological flows, installation and adjustment parameters, programming schemes were established. For Layer III, 3 variants of planar structures made by non-conventional techniques were selected, differentiated by the nature of the raw material. To increase the level of biocompatibility and the wound healing rate, the textile structures used for Layers I and III were functionalized by padding or spraying, with antibiotics and active substances, recognized for their antibacterial properties: colloidal silver (V1), hyaluronic acid (V2), clay (V3), CMC (V4), collagen (V5), polyurethane (6),

Table 1

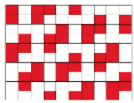
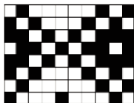

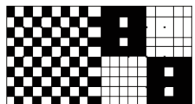
MAIN DESIGN PARAMETERS OF WOVEN STRUCTURES						
Woven textile code	Design parameters					Structure type
	Fibre composition (%)		Linear density (Tex/Nm)		The density of warp (yarn/10 cm)	
	Warp	Weft	Warp	Weft		
BZNT1	100% Cotton	80% Cotton/20% ZnO fibres	20×2(50/2)	14.7×2(68/2)	240	 Satin
BBT1	100% Cotton	100% Bamboo	20×2(50/2)	29.4×1(34/1)	250	 Honeycomb
BLT1	100% Cotton	100% Lenpur	20×2(50/2)	29.4×1(34/1)	200	
BAT1	100% Cotton	100% Tencel®	20×2(50/2)	130 dtex	350	 Honeycomb
BBT2	100% Cotton	100% Cotton	20×2(50/2)	16.6×2(60/2)	255	 Combined pattern

Table 2

PHYSICAL-MECHANICAL CHARACTERISTICS OF WOVEN STRUCTURES						
No.	Characteristics	UM	BZNT1	BBT1	BAT1	BBT2
1	Mass on the surface unit	g/sqm	177	170	137	170
2	Thickness	mm	0.546	0.520	0.448	0.624
3	Water vapours permeability	%	40.9	41.9	41.9	43.2
4	Air permeability	100 Pa, l/sqm/s	292.2	323.4	316.6	460.6
		200 Pa, l/sqm/s	533.6	590.4	583.0	792.4

Table 3

PHYSICAL-MECHANICAL CHARACTERISTICS OF NON-WOVEN STRUCTURES					
Feature	Variant	UM	Non-woven textile code		
			100HS	50HS	20HS
Fibre composition		%	100% Chitosan	50/50% Chitosan/Tencel®	20/80% Chitosan/Tencel®
Mass		g/m ²	108.16	54.68	43.12
Thickness		mm	1.38	0.3	0.23
Long./transv. Breaking strength,		N	35.39/44.07	33.37/45.64	57.42/70.70
Long./transv. Breaking elongation		%	54.37/45.37	33.05/43.34	29.19/44.2
Long./transv. tearing strength		N	9.1/9.11	4.29/4.43	6.96/7.49

treated with Ringer's solution (S). The physical-mechanical characteristics were determined: mass (g/m²), thickness (mm), breaking strength (N), breaking elongation (%), air permeability (l/m²/s), etc. antimicrobial activity, and hemolytic potential. Table 1 presents the main design parameters of woven structures. Tables 2 and 3 present the physical-mechanical characteristics of woven structures and non-woven structures, respectively.

To determine the elastic properties, the elastic modulus and the anisotropy of the functionalized textile structures designed for Layer I and Layer III of the composite structure were calculated (table 4).

Specific methods of descriptive statistics were used to characterize populations of variables, elasticity modulus, and anisotropy of plane structures from the point of view of the elastic features, used for Layers I

Table 4

ELASTIC PROPERTIES OF THE COMPOSITE STRUCTURE									
No.	Variants	Strength (N)	Lo (cm)	L1 (cm)	ΔL (cm)	A (sqcm)	G (mm)	Elasticity (N/cm ²)	Anisotropy
1	BBT2-5-weft	30	5	5.2615	0.2615	204.67	0.934	2.8026275	-0.04455969
	BBT2-5-warp	52.5	20	21.652	1.652	204.67	0.934	3.1054538	
2	BAT1-3-weft	80	5	5.206	0.206	203.2	0.6	9.5289552	1.230
	BAT1-3-warp	12.5	20	22.19	2.192	203.2	0.65	0.561054	
4	BAT1-5-weft	80	5	5.177	0.177	202.9	0.58	11.10437	1.189
	BAT1-5-warp	17.5	20	22.4	2.4	202.9	0.58	0.718603	
5	BBT1- 6 weft	20	5	5.2305	0.2305	203.26	0.652	2.1344066	-0.72346913
	BBT1-6-warp	70	20	20.61	0.61	203.26	0.652	11.291361	
9	BZNT1-6-weft	30	5	5.288	0.288	203.4	0.68	2.5606359	-0.310173375
10	BZNT1-6-warp	45	20	20.846	0.846	203.4	0.68	5.2302349	
11	100HS-6 Long.	11.25	5	5.067	0.067	203.33	0.666	4.1290132	0.331533051
12	100HS-6 Trans.	4.5	20	20.23	0.23	203.33	0.666	1.9244792	
13	50HS-S Long.	10.4	5	5.923	0.293	203.3	0.66	0.2771177	0.003169157
14	50HS-S Trans.	10.0	20	23.57	3.576	203.3	0.66	0.2751029	
15	20HS -5Long.	15.2	5	5.265	0.2565	202.22	0.444	1.4652176	-0.009226377
16	20HS-5Trans.	16.97	20	23.576	3.576	202.22	0.444	0.4693429	

and III of the multilayered matrix. Thus, a special software program made it possible to describe the distributions as a result of the tests performed. The following fundamental statistical indicators of variables, elasticity modulus, and anisotropy, were calculated for the values of the warp/weft elasticity (woven) and longitudinal/transversal (non-woven) modules, and anisotropy: mean, dispersion and standard deviation, median and quartiles, skewness and kurtosis for asymmetry and the cases where interventions should be performed were highlighted.

Testing the antimicrobial effect involved measuring the ability of some microorganisms to survive under the effect of an antimicrobial agent, or in the presence of a compound/material with antimicrobial potential, at an imposed or determined concentration and for a prescribed period. The antimicrobial activity of textile structures was evaluated concerning Gram-positive microorganisms – *Staphylococcus aureus* ATCC 653 and Gram-negative – *Escherichia coli* ATCC 8739 and *Candida albicans*, variety ATCC 10231 by calculating the percentage and logarithmic reduction of the populations of microorganisms.

The hemolytic potential of the materials was investigated according to the ASTM F756-13 standard: Standard practice for assessment of hemolytic properties of materials. The materials were conditioned in 10 mL saline solution 0.9% NaCl and incubated for 30 min at 37°C; then, 200 µl of diluted ACD blood (collected in a vacutainer over an anticoagulant mixture consisting of trisodium citrate, citric acid, and dextrose) was added, and the mixture was incubated for 60 minutes at 37°C. A separate sample of 100% hemolysis induced by 10 ml of deionized water was used as a positive control, and the sample for 0% hemolysis consisted of 0.9% NaCl saline solution, without material, used as a negative control. After incubation, all samples were centrifuged at 2000 rpm for 5 minutes, and the absorbance of the supernatant was determined at 545 nm. The percentage of hemolysis was calculated as follows:

$$\text{Hemolysis (\%)} = [(A_{\text{sample}} - A_{\text{negative}}) / (A_{\text{positive}} - A_{\text{negative}})] \cdot 100 \quad (1)$$

where A_{sample} is the absorbance value of the sample, A_{negative} – the absorbance value of the hemolysis produced by the saline solution (0.9% NaCl) and A_{positive} – the absorbance value of hemolysis produced by deionized water. The hemolysis results are the average of three determinations.

RESULTS AND DISCUSSIONS

The module of elasticity

The analysis of the results obtained for the elasticity modulus highlights the following:

- the textile structures aimed for Layer I and Layer III, which display a high modulus of elasticity in a certain direction or both directions, which is characterized by low elongation value, offering a strong mechanical reinforcement of multilayer structures,

but with the cost of increasing shear forces between layers. Of the textile structures designed for layer I, about 95% fall into this category, and of the textile structures designed for layer III, about 15%.

- textile structures aimed for Layer I and Layer III with a lower elasticity modulus on both warp/ weft or longitudinal/transversal direction, which do not generate high shearing forces, but have a higher degree of deformation. Among the textile structures aimed for Layer I, around 5% fall in this category, whereas from the textile structures aimed for Layer III, around 85%.

Anisotropy

The anisotropy of the textile structures aimed for Layer I has values within the $-0.30 \div 1.23$ range, whereas that of the textile structures aimed for Layer III, within the $-0.03 \div 0.49$ interval, these ensuring adequate environments to use in the multilayered structure of the polyurethane hydrogel.

Descriptive statistical analysis – Layer I

Table 5 shows the main statistical indicators for the modulus of elasticity, whereas table 6 shows the anisotropy of the textile structures aimed for Layer I. Figure 2, a and respectively figure 2, b show the histograms of the warp and the weft elasticity modulus, respectively. Figure 2, c shows the histogram for the anisotropy variable. Figure 3, a weft and figure 3, b warp show the box-plot graphs for the modulus of elasticity variables, whereas figure 3, c shows the anisotropy, box-plot graphs.

Table 5

STATISTICS FOR THE MODULUS OF ELASTICITY – LAYER I			
Indicators		Weft	Warp
N	Valid	17	22
	Missing	5	0
Mean		8.1088	4.2111
Std. Error of Mean		2.99750	0.87209
Median		4.2750	1.9500
Mode		2.56*	1.81*
Std. Deviation		12.35900	4.09045
Variance		152.745	16.732
Skewness		3.665	1.110
Std. Error of Skewness		0.550	0.491
Kurtosis		14.251	-0.206
Std. Error of Kurtosis		1.063	0.953
Range		52.34	12.73
Minimum		2.03	0.43
Maximum		54.37	13.16
Sum		137.85	92.65
Percentiles	25	2.6800	1.4278
	50	4.2750	1.9500
	75	9.8740	6.3250

Note: * Multiple modes exist. The smallest value is shown.

Table 6

STATISTICS FOR THE ANISOTROPY – LAYER I		
Indicators		Value
N	Valid	28
	Missing	56
Mean		0.2456
Std. Error of Mean		0.11280
Median		0.1976
Mode		-0.72*
Std. Deviation		0.59688
Variance		0.356
Skewness		0.291
Std. Error of Skewness		0.441
Kurtosis		-0.902
Std. Error of Kurtosis		0.858
Range		1.95
Minimum		-0.72
Maximum		1.23
Sum		6.88
Percentiles	25	-0.3031
	50	0.1976
	75	0.5056

Note: * Multiple modes exist. The smallest value is shown.

Layer I: statistical analysis result interpretation

1. The variable's modulus of elasticity in the weft/warp and the anisotropy do not present a high variability of results for any of the variants included in

the-study. The value with code 12 – value 9.5 N/cm² for the BAT1-3 variant (100% cotton in warp and 100% acetate in the weft), functionalized with clay, the variable modulus of elasticity in the horizontal direction, is located at a distance of more than 3 lengths of the box and must be excluded from the series of determinations.

2. The variable modulus of elasticity in the weft and the variable anisotropy shows the distribution of 50% of the values directed to the left, the median being directed to the bottom edge of the box, so small values are predominant. For the variable modulus of elasticity in the warp, the median is directed towards the upper edge of the box, so it can be stated that the distribution is directed to the right, and large values are predominant.

3. Distribution shape indicators:

- for the modulus of elasticity in the weft: 50% of the values are under 4.27 N/cm², 25% are under the 4.27 ÷ 9.87 N/cm² range, whereas 25% over 9.87 N/cm²;
- for the modulus of elasticity in the warp: 50% of the values are under 1.95 N/cm², 25% of the values are within the 1.42 ÷ 1.95 N/cm² range, whereas 25% of the values are over 1.95 N/cm²;
- for the anisotropy: 50% of the values are under 0.19, whereas 25% of the values are within the -0.3 ÷ 0.19 limits and 25% of the values go over 0.19.

4. Skewness indicators have the following values: 3.66 for the modulus of elasticity in the weft, 1.11 for the modulus of elasticity in the warp, and 0.291 for

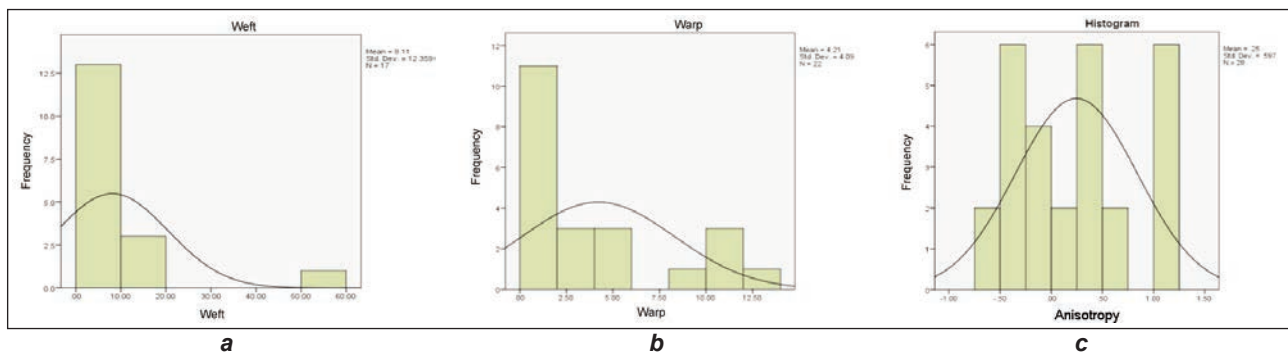


Fig. 2. Layer I histograms: a – weft elasticity; b – warp elasticity; c – anisotropy

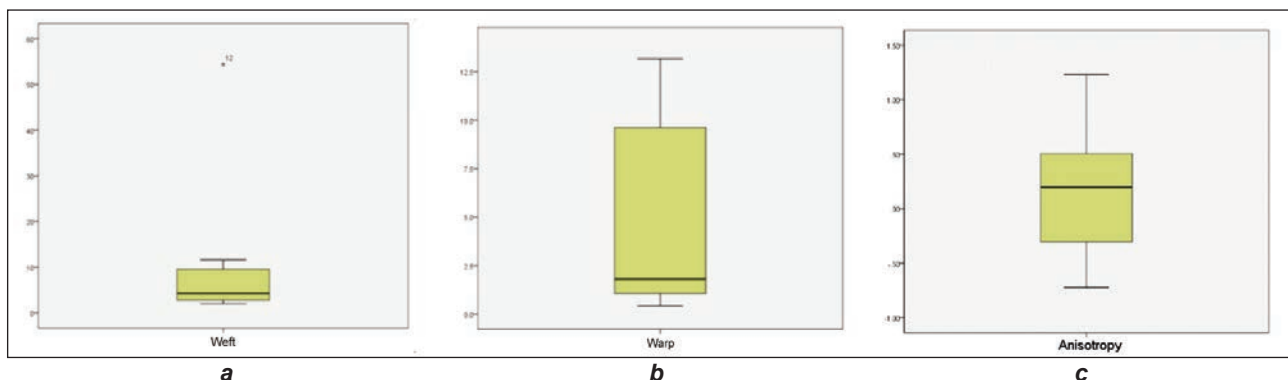


Fig. 3. Layer I box-plot graphs: a – weft elasticity; b – warp elasticity; c – anisotropy

the anisotropy, which highlights the extent to which the mean departs from the median and, as a result, the normal distribution curves depart from the middle, going to the right.

5. Kurtosis indicators have a positive value, of 14.25 for the modulus of elasticity in the weft – the curve is leptokurtic, whereas the modulus of elasticity in the warp and the anisotropy have negative values of -0.206 and -0.902 , respectively, and the curves are platykurtic.

Descriptive statistical analysis – Layer III

Table 7 shows the main statistical indicators for the modulus of elasticity, whereas table 8 for the anisotropy of the textile structures aimed for Layer III. The histograms of the variable modulus of elasticity in the horizontal direction and modulus of elasticity in the vertical direction are presented in figure 4, a and figure 4, b, respectively. The histogram for the anisotropy variable is presented in figure 4, c. The

box-plot graphs for the modulus of the elasticity variable are presented in figure 5, a longitudinal direction and figure 5, b transversal direction and for anisotropy in figure 5, c.

Layer III – interpretation, results, statistical analysis

1. The variables modulus of elasticity and anisotropy does not show high variability of results with any of the studied variants.
2. The values with code 11 – value 0.275 N/cm^2 , variable modulus of elasticity in the longitudinal direction, and code 11, modulus of elasticity in the transversal direction, with a value of 1.074 N/cm^2 for the 50HS variant, is located at a distance of 1–3 box lengths and must not be excluded from the series of determinations. The value with code 2, value 5.071 N/cm^2 for the 20 HS-1 variant, made up of 20% Chitosan/80%

Table 7

STATISTICS FOR THE MODULUS OF ELASTICITY – LAYER III			
Indicators		Weft	Warp
N	Valid	11	11
	Missing	0	0
Mean		0.9427	1.0873
Median		0.4680	0.5550
Mode		0.03*	0.47*
Std. Deviation		1.18806	1.40126
Variance		1.411	1.964
Skewness		2.221	2.744
Std. Error of Skewness		0.661	0.661
Kurtosis		5.519	7.898
Std. Error of Kurtosis		1.279	1.279
Range		4.10	4.80
Sum		10.37	11.96
Percentiles	25	0.2770	0.4350
	50	0.4680	0.5550
	75	1.4650	1.1180

Note: * Multiple modes exist. The smallest value is shown.

Table 8

STATISTICS FOR THE ANISOTROPY – LAYER III		
Indicators		Value
N	Valid	11
	Missing	12
Mean		0.694
Std. Error of Mean		0.9043
Median		-0.0038
Mode		-0.49^*
Std. Deviation		0.29992
Variance		0.090
Skewness		-0.071
Std. Error of Skewness		0.661
Kurtosis		-0.259
Std. Error of Kurtosis		1.279
Range		0.98
Minimum		-0.49
Maximum		0.49
Sum		0.76
Percentiles	25	-0.0826
	50	-0.0038
	75	0.3315

Note: * Multiple modes exist. The smallest value is shown.

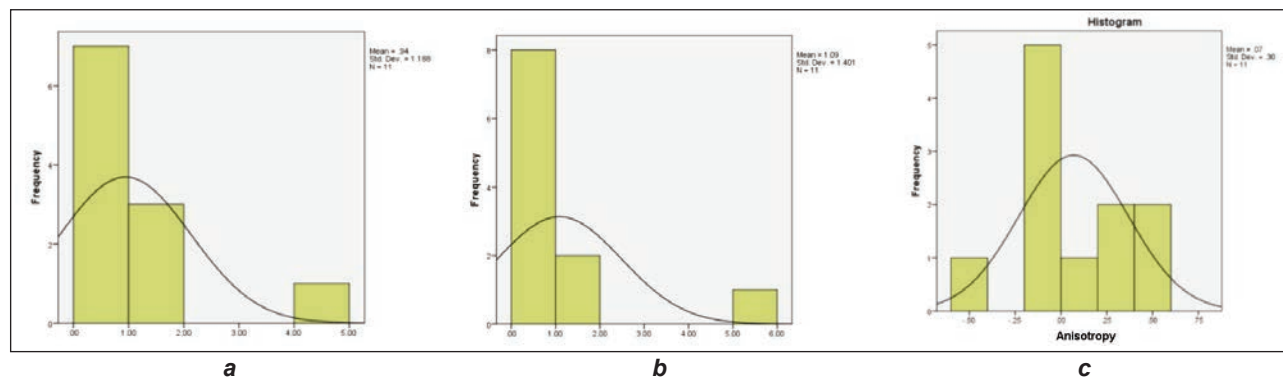


Fig. 4. Layer III histograms: a – elasticity-longitudinal; b – elasticity-transversal; c – anisotropy

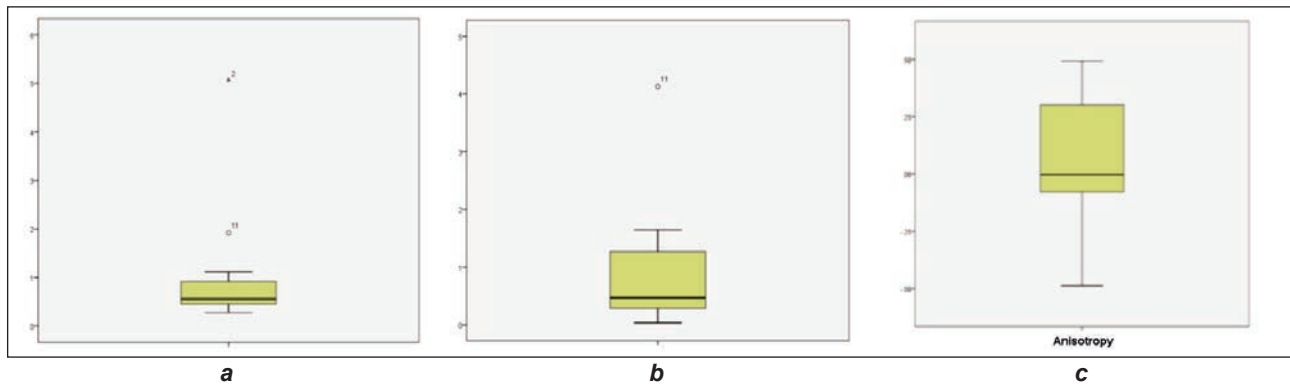


Fig. 5. Layer III box plot graphs: *a* – elasticity-longitudinal; *b* – elasticity-transversal; *c* – anisotropy

viscose, treated with colloidal silver, variable modulus of elasticity in the transversal direction is situated at a distance of more than 3 box lengths and must be excluded from the series of determinations.

3. The variable modulus of elasticity in the longitudinal direction and the transversal direction and the variable anisotropy show the distribution of 50% of the values directed to the left, the median being directed to the bottom edge of the box, so small values are predominant.

4. Distribution shape indicators:

- for the modulus of elasticity in the longitudinal direction: 50% of the values are below the value of 0.468 N/cm², 25% being within the 0.468 ÷ 1.46 N/cm² range, whereas 25% over 1.46 N/cm²;
- for the modulus of elasticity in the transversal direction: 50% of the values are under 0.55 N/cm², 25% of the values are within the 0.55 ÷ 1.11 N/cm² range, whereas 25% of the values over 1.11 N/cm²;
- for anisotropy: 50% of the values are below the value of –0.038 and 25% of the values are within the limits of –0.038 ÷ –0.33, and 25% of the values are above 0.33.

5. Skewness indicators have the following values: 2.221 for the modulus of elasticity in the longitudinal direction, 2.744 for the modulus of elasticity in the

transversal direction, which highlights the extent to which the average departs from the median and implicitly the normal distribution curves depart from the middle, these moving to the right and –0.071 for anisotropy, which highlights the extent to which the average moves away from the median and implicitly the normal distribution curves also move away from the middle, moving to the left.

6. The kurtosis indicators have positive values, of 5.519 for the modulus of elasticity in the longitudinal direction and 7.898 for the modulus of elasticity in the transversal direction – the curves being leptokurtic and negative values for anisotropy: –0.259, the curve being platykurtic

Woven textile structures have a higher modulus of elasticity in one direction (95%) compared to non-woven structures, which present a low value of modulus of elasticity in both directions (85%). The anisotropy of woven structures is higher compared to non-woven structures (–0.3 ÷ 1.23 against –0.03 ÷ 0.49). Woven structures are more rigid compared to non-woven ones.

Antimicrobial activity

The graphic expressions of the logarithmic reduction and the percentage reduction of the population of *Staphylococcus aureus* are presented in figure 6, *a* and figure 6, *b*.

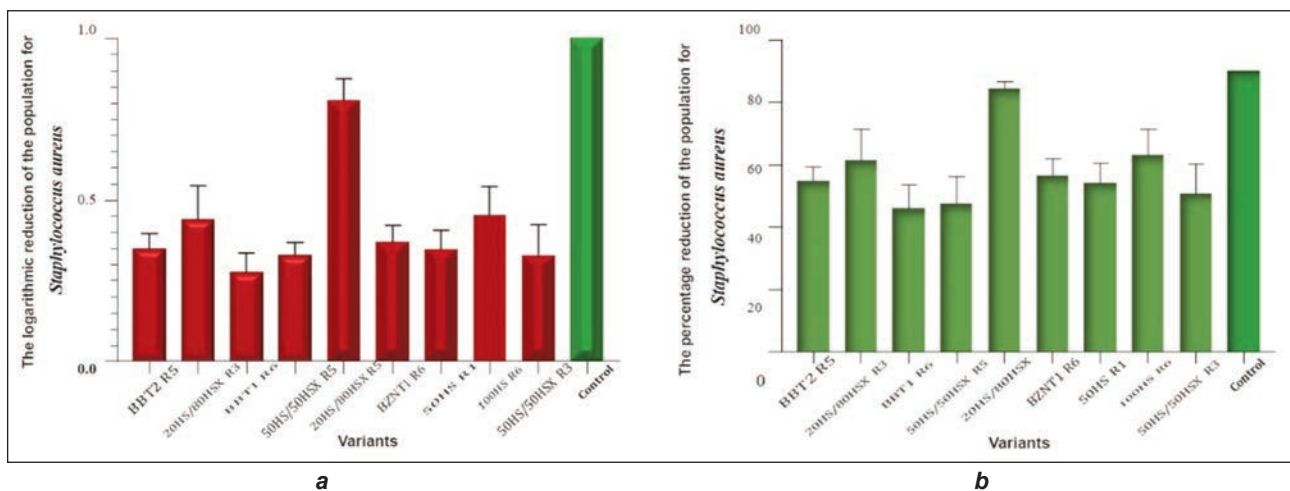


Fig. 6. Reduction of *Staphylococcus aureus* population: *a* – logarithmic; *b* – percentage

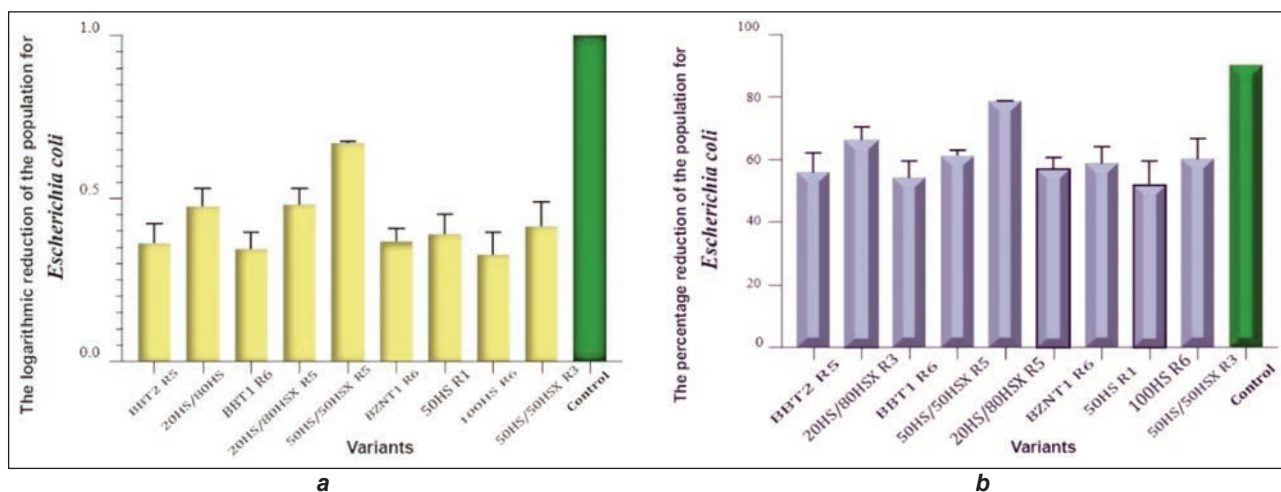


Fig. 7. Reduction of the *Escherichia coli* population: a – logarithmic; b – percentage

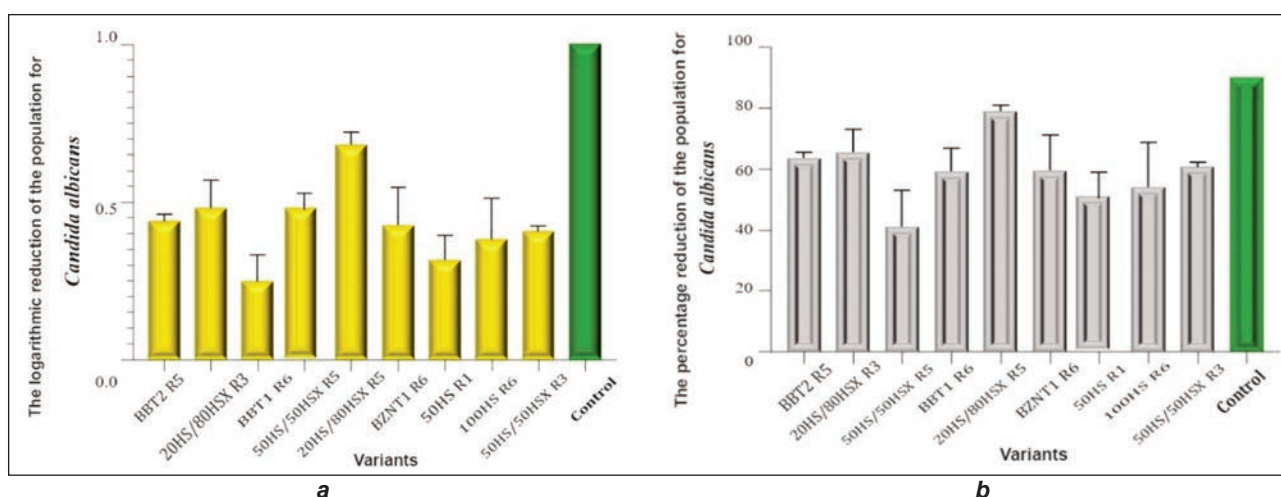


Fig. 8. Reduction of *Candida albicans* population: a – logarithmic; b – percentage

For the control sample (noted: Control), the logarithmic reduction has the default value of 1, a value corresponding to a 90% efficiency in reducing microbial populations.

For the tested samples, logarithmic reductions between 0.2759 and 0.8089 were obtained. The textile samples that provide the most effective antibacterial effect are those that include chitosan (50HS and 20HS). These non-woven structures have a low level of anisotropy (0.003 and -0.009) but the presence of Tencel® fibre together with that of chitosan enhances the antibacterial effect of the mixture, ensuring a percentage reduction in the population of *Staphylococcus aureus* close to 90%, a value considered as a reference in the inhibition of bacterial cultures.

Figures 7, a and 7, b show the graphical expressions of the logarithmic reduction and respectively of the percentage reduction of the *Escherichia coli* population.

For the tested samples, logarithmic reductions between 0.3269 and 0.6663 were obtained. The textile samples that ensure the most effective antibacterial effect are those that include chitosan, along with

Tencel fibres, treated with Collagen(R5), which ensure percentage reductions in the population of *Escherichia coli* (Gram-negative bacteria) of about 78%, lower than those against *Staphylococcus aureus* (Gram-positive bacteria), for which the percentage reduction was almost 90%. The woven structure with the highest percentage reduction (58%) is BZNT1 (R6) treated with Polyurethan, with the module of elasticity very low in both directions (warp: 0.052 N/cm^2 , weft: 0.025 N/cm^2) and anisotropy with a value 0.3.

In figures 8, a and 8, b, the graphical expressions of the logarithmic reduction and respectively of the percentage reduction of the population of *Candida albicans* are presented.

The logarithmic reductions obtained are between 0.2468 and 0.6805, and the percentage reductions are between 41% and 78%. Also in the case of inhibiting the development of *Candida albicans*, the mixture of Chitosan/Tencel 20/80% fibres, treated with Collagen (R5) is the most effective in reducing fungal populations.

Hemolytic potential

The hemolytic potential was evaluated based on the degree of erythrocytes and haemoglobin dissociation induced by the materials put in contact with ram blood.

The degrees of hemolysis of the samples with values lower than 5% are under international regulations regarding the hemocompatibility of medical devices (according to ASTM F756-00, Standard Practice for Assessment of Hemolytic Properties of Materials). Thus, the materials BBT2 R5 ($5.89 \pm 0.58\%$), 100HS R6 ($9.42 \pm 0.68\%$) and BZNT 1-R6 ($10.38 \pm 1.12\%$) are hemolytic. The materials with the lowest hemolytic indices are: BBT1-R6 ($0.16 \pm 0.09\%$), 20HS/80HSX-R5 ($0.59 \pm 0.17\%$), 50HS/50HSX-R5 ($0.64 \pm 0.17\%$) and 50HS-R1 ($0.71 \pm 0.17\%$).

According to the obtained results, it can be stated that the 100% chitosan textile (100HS) sample and the sample containing ZnO (BZNT1) are strongly hemolytic. In the case of non-hemolytic samples, it was observed that by spraying with clay dispersion, the hemolytic index increases. It is recommended to use textile materials that were not sprayed with clay dispersion.

CONCLUSIONS

- The elasticity module and anisotropy for textile functionalized structures (woven and non-woven) were calculated whereas to characterize statistical populations, descriptive statistics-specific methods were used. The distributions as a result of the tests performed were described.
- The analyzed textile structures are adequate from the point of view of the elastic features to be used in the multilayered composite material structure aimed for the treatment of burn wounds, as they achieve a balance between the shearing and the deformation potentials.
- The study of inhibiting the development of microorganisms and evaluating their ability to adhere to the

surface of textile materials showed for all the strains tested, that the best results were obtained for the sample of 20HS (20/80% chitosan – Tencel®) treated with Collagen (R5). The efficiency of this type of material could be because the surface of the fibres does not favour the retention of bacterial cells. Thus, a synergistic effect of Tencel fibres with chitosan could reduce the effect of low anisotropy (-0.009).

- The antimicrobial activity of all textile samples is moderate, however, bacterial growth is sufficiently inhibited to be able to respond to the specific applications of medical devices used as a wound dressing able to ensure a hemostatic effect. It is mentioned that the antimicrobial properties are only necessary until the systemic treatment with antibiotics starts (maximum 4–5 hours from the moment of application wound dressing application).
- The content of active substances in textile structures (ZnO, chitosan, polyurethane, etc.) compensates for their lower rigidity and is characterized by very small anisotropies (<1.0), which favour the development of microorganism cultures. In this way, it is possible to obtain appropriate levels of the reduction of microorganism populations and use them as medical devices.
- The textile structures from 100HS (100% chitosan) treated with Collagen and BNZT1 (containing ZnO) treated with Polylysine are strongly hemolytic.
- Three combinations of structures were selected to create layers I and III of the multilayer matrix: BZNT1/BZNTI, BZNTI/20HS, and 20HS/20HS.

ACKNOWLEDGEMENTS

This scientific paper is funded by the UEFISCDI within PNCDI III, Program 2 – Increasing the competitiveness of the Romanian economy through research, development, and innovation, Subprogram 2.1. Competitiveness through research, development, and innovation – Experimental – demonstrative project, Contract no. 496PED/2020.

REFERENCES

- [1] Uzun, M., *A review of wound management materials*, In: Journal Textile Engineering & Fashion Technology, eISSN: 2574-8114, 4, 1, 218
- [2] Liu, H-F., Zhang, F., Lineaweaver, W. C., *History and Advancement of Burn Treatments*, In: Annals of Plastic Surgery, 2017, 78, Supplement 1, 82-88
- [3] Alsarra, I.A., *Chitosan topical gel formulation in the management of burn wounding*, In: J. Biol. Macromol., 2009, 45, 16–21
- [4] Singh, R., Chacharkar, M. P., Mathur, A. K., *Chitin membrane for wound dressing application—preparation, characterization, and toxicological evaluation*, In: Int. Wound. J., 2008, 5, 665–673
- [5] Ribeiro, M.P., Espiga, A., Silva, D., et al., *Development of a new chitosan hydrogel for wound dressing*, In: Wound Repair Regen., 2009, 17, 817–824
- [6] Boucard, N., Viton, C., Agay, D., et al., *The use of physical hydrogels of chitosan for skin regeneration following third-degree burns*, In: Biomaterials, 2007, 28, 3478–3488
- [7] Travis, T.E., Mauskar, N.A., Mino, M.J., et al., *Commercially available topical platelet-derived growth factor as a novel agent to accelerate burn-related wound healing*, In: J. Burn Care Res., 2014, 35, e321–e329
- [8] Alemdaroğlu, C., Değim, Z., Celebi, N., et al., *An investigation on burn wound healing in rats with chitosan gel formulation containing epidermal growth factor*, In: Burns, 2006, 32, 319–327
- [9] Jin, Y., Ling, P. X., He, Y. L., et al., *Effects of chitosan and heparin on early extension of burns*, In: Burns, 207, 33, 1027–1031

- [10] Dai, T., Tegos, G.P., Burkatovskaya, M., et al., *Chitosan acetate bandage as a topical antimicrobial dressing for infected burns*, In: Antimicrob Agents Chemother, 2009, 53, 393–400
- [11] Dai, T., Tanaka, M., Huang, Y.Y., et al., *Chitosan preparations for wounds and burns: antimicrobial and wound-healing effects*, In: Expert Rev. Anti. Infect. Ther., 2011, 9, 857–879
- [12] Nascimento, E.G., Sampaio, T.B., Medeiros, A.C., et al., *Evaluation of chitosan gel with 1% silver sulfadiazine as an alternative for burn wound treatment in rats*, In: Acta Cir. Bras., 2009, 24, 460–465
- [13] Project: *Innovative medical device for emergency and operational medicine*, CELLMATRIX, Contract nr. 496PED/2020, PN-III-P2-2.1-PED-2019, Phase II: Experimental design of multilayer matrix for haemostasis and connective tissue regeneration following burns and gunshot wounds
-

Authors:

EMILIA VISILEANU, ALEXANDRA ENE, CARMEN MIHAI, ALINA VLADU

National Research and Development Institute for Textiles and Leather,
16, Lucretiu Patrascanu Street, sector 3, 030508, Bucharest, Romania
e-mail: office@incdtp.ro

Corresponding author:

EMILIA VISILEANU
e-mail: e.visileanu@incdtp.ro

Industria Textila magazine is an international peer-reviewed journal published by the National Research & Development Institute for Textiles and Leather – Bucharest, in print editions.

Aims and Scope: *Industria Textila* journal is addressed to university and research specialists, to companies active in the textiles and clothing sector and to the related sectors users of textile products with a technical purpose.

Submission of Manuscripts

Please read the guidelines below then visit the Journal's submission site manuscriptmanager.net/it or the button **Submit manuscript** to upload your manuscript. Please note that manuscripts not conforming to these guidelines may be returned.

Copyright Transfer Agreement must be signed and returned to our Editorial Office by mail, as soon as possible, after the preliminary acceptance of the manuscript. By signing this agreement, the authors warrant that the entire work is original and unpublished, it is submitted only to this Journal and all the text, data, Figures and Tables included in this work are original and unpublished, and have not been previously published or submitted elsewhere in any form. Please note that the reviewing process begins as soon as we receive this document. In the case when the paper has already been presented at a conference, it can be published in our journal only if it has not been published in a generally available conference materials; in such case, it is necessary to give an appropriate statement placed in Editorial Notes at the end of the article.

Manuscripts submitted are checked against plagiarism with **Anti-plagiarism System**. Manuscripts of the following types are accepted:

Research Papers – An original research document which reports results of major value to the Textile Community

Book Reviews – A brief critical and unbiased evaluation of the current book, normally invited by the Editor.

Manuscripts shall be submitted in English in single-spaced typing, A4 paper, Arial, margins 2 cm on all sides, under electronic version in Word for Windows format.

The volume of the submitted papers shall not exceed pages (including the bibliography, abstract and key words), typescript pages including tables, figures and photographs.

All articles received are reviewed by minimum two reviewers, renowned scientist and considered expert in the subject the article concerns, which is appointed by the editorial board. After the article has been accepted, with the completions and the modifications required by the reviewers or by the editorial staff, it will be published.

The submission of the above-mentioned papers is by all means the proof that the manuscript has not been published previously and is not currently under consideration for publication elsewhere in the country or abroad.

There may also be published papers that have been presented at national or international scientific events, which have not been published in volume, including the specification related to the respective event.

The articles assessed as inappropriate by the reviewer or by the editorial staff, concerning the subject matter or level, shall not be published.

The manuscript shall be headed by a concise title, which should represent in an exact, definite and complete way the paper content.

The manuscript shall also be headed by complete information about the author(s): titles, name and forename(s), the full name of their affiliation (university, institute, company), department, city and state, as well as the complete mailing address (street, number, postal code, city, country, e-mail, fax, telephone).

Tables and figures (diagrams, schemes, and photographs) shall be clear and color, where possible.

The photographs shall be sent in original format (their soft), or in JPEG or TIF format, having a resolution of at least **300 dpi**.

All tables and figures shall have a title and shall be numbered with Arabic numerals, consecutively throughout the paper and referred by the number in the text.

Generally, symbols and abbreviations shall be used according to ISO 31: Specifications for quantities, units and symbols. SI units must be used, or at least given comprehensive explanations or their equivalent.

Cited references shall be listed at the end of the paper in order of quotation and contain: **for a paper in a periodical** – the initials and surname of the author(s), title of journal and of the article, year and number of issue, number of volume and page numbers; **for a book** – the initial and surname of the author(s), full name of the book, publisher, issue, place and year of publishing, and the pages cited; **for patents** – the initial and surname of the author(s), the title, the country, patent number and year. It is preferable not to use sites as references.

[1] Hong, Y., Bruniaux, P., Zhang, J., Liu, K., Dong, M., Chen, Y., *Application of 3D-to-2D garment design for atypical morphology: a design case for physically disabled people with scoliosis*, In: *Industria Textila*, 2018, 69, 1, 59–64, <http://doi.org/10.35530/IT.069.01.1377>

Authors are requested to send an abstract of the paper, preferably no longer than 250 words and a list of 5–6 key words (preferably simple, not compound words, in alphabetical order).